UNIVERSITAT POLITÈCNICA DE CATALUNYA

Doctoral Programme:

AUTOMATIC CONTROL, ROBOTICS AND COMPUTER VISION

Doctoral Dissertation

Predictive Control with Dynamic Constraints for Closure and Opening Operations of Irrigation Canals

Eduard Galvis Restrepo

Supervisors: José Rodellar Benedé

Manuel Gómez Valentín

November, 2015

Abstract

Water delivery systems usually work in continuous way based on some prescribed flow conditions and user's needs. However there are situations in which abrupt changes in the operating conditions must be carried on. Typical examples are the alternative closing of a canal system during the non-demand periods to save water for other purposes as energy production, and the closure of a canal due the danger of water pollution in the supplier river. Closure of a canal means setting zero flow conditions by closing the gates along the canal, while maintaining specific water levels under the maximum allowed value. The closure operation requires a progressive and well planned set of actions to avoid overtopping and cracking in the canal lining, which can involve both economic and environmental issues. The opening operation involves restarting the canal to its normal operating condition from zero flow condition.

This thesis is devoted to develop a supervised decentralized predictive control strategy for solving the problems related to the closure and opening operations of canal systems. The evaluation is fulfilled by means of numerical simulation on two cases of study in a variety of operating scenarios. The strategy is also experimentally validated through real-time implementation in a laboratory canal available in the Technical University of Catalonia (canal PAC-UPC).

The control strategy has been developed in a two-level architecture: (i) a set of individual decentralized downstream water level predictive controllers, which are formulated via an optimal control problem under dynamic constraints and implemented by upstream local gates; and (ii) a supervising level to achieve the compromise of fast execution with smooth gate trajectories and water level regulation, even in the presence of disturbances.

The simulation and real-time implementation scenarios have demonstrated that the proposed strategy is convenient for closure and opening of irrigation canals. Problems presented when the canal closure operations are not managed properly, such as overtopping, have been avoided in all the scenarios.

Resumen

Los canales de riego usualmente trabajan en forma continua bajo unas condiciones de flujo prescritas y acorde a las necesidades de agua de los usuarios. Sin embargo hay situaciones en las cuales se presentan cambios abruptos en las condiciones de operación. Un típico ejemplo es la alternativa de cierre durante los periodos de inactividad de los regantes. Dicho cierre tiene por objeto el ahorro de agua para otros propósitos, como puede ser la produccion de energía. Otro ejemplo es la necesidad de cierre de un canal ante la presencia de un vertido de contaminantes aguas arriba en la fuente abastecedora de agua. El cierre de un canal requiere cerrar de forma progresiva y suave las compuertas de todo el canal, evitando desbordamientos y manteniendo unos calados de seguridad en los diferentes tramos del canal hasta llegar a una condición de caudal cero. La violación de los calados máximos puede producir inundaciones y pérdidas de agua innecesarias. La reducción de los niveles de agua por debajo de los calados mínimos permitidos puede causar daños en la estructura física del canal.

Esta tesis se centra en el desarrollo de una estrategia de control predictivo descentralizado supervisado para gestionar de forma automática las operaciones de cierre y apertura de canales de riego. La evaluación de la estrategia se lleva a cabo mediante la simulación numérica en dos casos de estudio. Dicha evaluación se completa mediante experimentos en tiempo real realizados en un canal de laboratorio existente en la Universitat Politècnica de Catalunya (canal PAC-UPC).

La estrategia de control se ha desarrollado con una arquitectura de dos niveles: (i) un conjunto de controladores individuales descentralizados para el control de niveles de aguas abajo, cuya formulación se plantea como un problema de control óptimo con restricciones dinámicas; y (ii) un nivel de supervisión encargado de alcanzar el compromiso de una ejecución rápida del proceso de cierre (o apertura) con movimientos suaves de compuerta y de una regulación de los niveles de agua dentro de los márgenes de consigna, incluso en presencia de perturbaciones.

Tanto los escenarios de simulación como los de implementación en tiempo real, han demostrado que la estrategia propuesta en esta tesis es satisfactoria para operaciones de cierre y apertura de canales de riego. En efecto, la estrategia de control ha sido capaz de evitar problemas, como por ejemplo el desbordamiento, que se presentan cuando la operación de cierre de un canal no se realiza adecuadamente.

Contents

List of figures

List of Tables

List of abbreviations and Acronyms

ASCE	American Society of Civil Engineers
ADEX	Adaptive predictive expert control
ARX	Auto-Regressive with eXogenous input
Fo	Froude number
GPC	Generalized Predictive Control
ID	Integrator Delay model
IDZ	Integrator Delay Zero
ERLB	Ebro River Left Bank canal
LTI	linear time invariant
LQ	Linear Quadratic regulator
LQG	Linear Quadratic Gaussian optimal controller
MAVE	maximum allowed values estimates,
MPC	Model Predictive Control
OM	Operating Mode
PC	Predictive Control
PCI	Peripheral Component Interconnect
RTU	remote terminal unit
S	Laplace parameter
SDPC	Supervised Decentralized Predictive control with dynamic constraints

SCADA	The Supervisory Control and Data acquisition,
DCPC	Dynamically-Constrained Predictive Control
QP	Quadratic programming
WUA	water users' association

Nomenclature

A	wetted cross sectional area
a	slope of the sigmoidal curve
B	width of the weir
B_{pz}	width of the permitted zone during a close/opening operation
C_{df}	gate coefficient
e_j	signal error
g	gravity acceleration
H_e	head over the weir
J	cost function
k	present sampling instant
L	gate opening
q	shift operator
Q	discharge
Q_i	input discharge
Q_{i+1}	output discharge
Q_m	maximum discharge
Q_{wi}	lateral discharge
R	weighting factor matrix

R_w tuning parameter for the desired closed-loop performance

S_0 bottom slope

S_f friction slope

SP set point

T_s sampling time

$u(k)$ control variable

V volume of the pool,

$w(k)$ disturbance signal

x_{m_i} state vector of the *i-th* pool

y_{sp} water level setpoint.

$y(k)$ output variable

y_r reference trajectory

y_k measured output at instant k.

y_i^* desired final value of variable y_i

y_{sp} water level setpoint.

Ψ weighting factor matrix

λ prediction horizon

τ_i delay time

Δu incremental control variable

$\Delta\hat{y}$ predicted output

$\Delta\hat{y}$ predicted incremental output.

Chapter 1

Introduction

1.1 Motivation

Current environmental and economic challenges require real commitment with the modernization of the irrigation canals facilities. Crop irrigation demands 70% of all freshwater worldwide and if current trends continue it is estimated that two out of three people will be affected by the lack of freshwater sources by 2025 (UN, 2006). Many irrigation projects throughout the world built decades ago are inefficient in terms of water and energy use and they are in urgent need of modernization (Hervé, 2002).

A need exists for improving the operational efficiency and flexibility in the water supply. Efficiency means increasing the volume ratio of water used on crops with respect to the volume of water removed from fresh water sources (e.g. rivers, streams, lakes, reservoirs). Flexibility is related to deliver water to users in time, frequency and duration as required. There are three main delivery concepts in water conveyance systems (Buyalski et al., 1991):

- Rotation: users share a constant water supply, while cooperating with other water users to establish the time and quantity of delivery.
- Scheduled: a notification of delivery time and quantity is required in advance, whereby water users are limited to contractual water allotment on a daily, monthly and yearly basis.
- Demand: unrestricted use of the available water supply with limitations only on maximum flow rate and total allotment.

Water conveyance system is constructed to convey water from one place to another to accomplish functions such as irrigate agricultural land, municipal/industrial expansion or for energy production (Buyalski et al., 1991). Water conveyance systems are mainly composed by a main canal, secondary canals, reservoirs, check structures, canal pumping plants, weirs and turnouts, among others. A single canal is usually divided into pools, whose boundaries are defined by the presence of gates.

Traditionally, check structures used on irrigation canals are operated manually based on the canal staff skills and experience. This type of canal management has several drawbacks:

- Low efficiency in terms of delivered water versus water taken from the source (Litrico, 1999).
- No operator is able to manage the interaction between all the parameters of a complex system such as a canal divided into several pools. Measurements and readings may be imprecise or even falsified by operators (Goussard, 1993).
- Large waters losses (Rivas et al., 2007).
- Manual operation cannot react against unforeseen changes, for instance, when farmers start to take water or a rain event (Horváth, 2013).

On the other hand, apart from irrigation, there are other important and necessary operations in canal management such as the closure and the opening of a canal facility. These are challenging management tasks because they can cause problems such as overtopping and cracking in canal lining. Overtopping is produced when the water level exceeds the top of canal bank, caused by the transient waves that bounce back iteratively when gates are closed. Cracking or structural damage sometimes occurs by reason of the pressure that the concrete canal lining is subject due to the sub-pressure effect of outside water when either the canal is emptied or the water level decreases considerably.

In general, the following elements are required to design and implement a canal control system in the field:

- A control strategy that can cope with irrigation canal management problems and fulfill water level regulation requirements (Sepúlveda, 2008).
- A good dynamical model of the canal to design, analyze and simulate control strategies.
- A controller (e.g. Programmable Logic Controllers (PLC), embedded systems or even general-purpose computer systems).
- Instrumentation / data acquisition system to measure relevant variables and to operate gates. The instrumentation elements include sensors (water levels gauges and flow meters) and actuators (valves, servomotors, etc.), among others.

The design of a control system for canal regulation is a complex task with challenging problems. Canals are distributed over long distances with significant time delays. However, despite the complexity in the design and implementation of control algorithms, automation offers a solution to improve the water delivery service and get a better water conveyance efficiency (an estimated

30% to 60%) in the global management of irrigation canals. Some advantages of automatic canal compared to conventional method are (Buyalski et al., 1991):

- Achieve operational flexibility when simultaneous information on the entire system is known.
- Immediate response to sudden and unforeseen variances in canal side diversion or to storm runoff flooding into the canal.
- Flexibility to adjust discharges through the system on a daily or an hourly basis.
- Problems like overtopping can also be avoided.

From the automatic control point of view, controlled variables are usually water levels, discharges or water volumes. Control action variables are gate opening or discharges under gates (another algorithm transforms discharge into gate position). In order to achieve quality of service, water levels should be maintained at reference setpoints, calculated on the basis of demand. It is also important to avoid fluctuations from setpoints, which translate into flow fluctuations at turnout checkpoints (Cantoni et al., 2007). The disturbances in the system are mainly as a result of turnouts variations, which are located typically at downstream part of each pool.

During the last 30 years, the research community has focused on control methods to improve the operational management of water conveyance systems, ranging from early classical feedback and feedforward control structures (Burt, 1999), (Burt and Piao, 2002) and (Clemmens et al., 2005), to more recent implementations of advanced control methods like predictive control (van Overloop et al., 2010) and (Aguilar et al., 2012). While there is an extensive literature on automatic control of canals in standard operation scenarios (see Chapter 2 for a literature review), the problems of canal closure and opening, which imply abrupt changes between different operation regimes, have received much less attention. Some references on the subject are (De Bievre et al., 2003), (Ghumman et al., 2009) and (Soler et al., 2010), including the recent work of an optimal predictive open-loop control of a 15 km length-canal for an emergency closure operation in (Soler et al., 2014).

Irrigation systems usually work in a continuous way around some prescribed flow operating conditions and users needs. An operating regime is determined mainly by the discharge along the canal. Gate movements affect both upstream and downstream water levels (y_1 and y_2), as illustrated in Figure 1.1 for a heading gate in a canal section. The discharge under the gate (Q) affects the levels as follows:

$$Q = C_{df} B L \sqrt{2g(y_1 - y_2)} \tag{1.1}$$

where C_{df} is the gate coefficient, B is the width of the gate, L is the gate opening and g is the acceleration of gravity. In a multireach canal, gate movements induce couplings among the reaches and therefore changes in operating conditions require efficient control strategies. This requirement is particularly stringent in scenarios where abrupt changes in the operating conditions must be carried out.

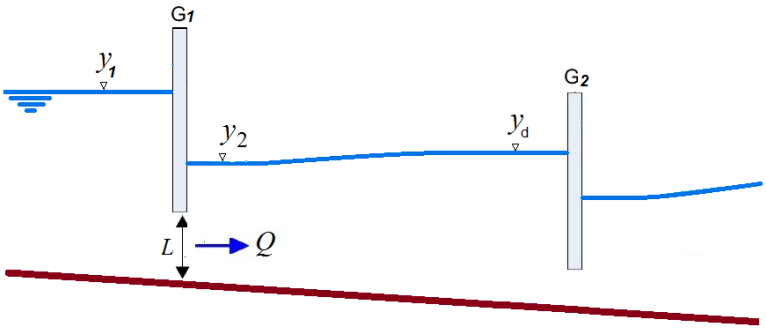

Figure 1.1 Sluice gate

Canal closure is a main example of such scenario, in which the operation must drive the canal from a baseline regime to setting zero discharge conditions by closing all the gates along the canal. Conversely, the opening operation means restarting the operating discharge from zero. Typical closures (and the corresponding reverse opening operations) may be required in circumstances such as: non-demand water periods; emergency situations in primary or secondary canals due to pollutants flowing along the supplier river; corrective or preventive maintenance of check structures or canal lining; and others.

Due to the couplings among canal pools, decreasing the discharge by means of closing the gates affects directly the controlled water levels in adjacent pools. Meanwhile, during the closure operation, water levels must keep within specified maximum and minimum values. Indeed, it is recommended to leave enough water level safeguards to avoid problems such as overtopping and cracking in canal lining by cause of subpressure effects. Consequently, a specific goal is to move the gates as smooth as possible. However, this goal is conflicting with the fact that feasibility of closure operation depends on the closing velocity. For instance, night closure must be as faster as possible to make it feasible and, clearly, emergency situations are particularly demanding.

In summary, these operational requirements are very challenging and almost impossible to achieve using local manual control methods for canal systems management. The literature on this topic is scarce and, to the best of our knowledge, there is no practical implementation of automatic controllers for closure operation to date.

The aim of this thesis is to contribute with new developments in canal automation to satisfy the requirements of the problem of closure and opening. Based on the strengths of predictive control and previous experiences of the research group, this methodology is adopted as the theoretical control background.

1.2 Thesis objectives

The overall objective is to develop a predictive control strategy with dynamic constraints for closure and opening operation of irrigation canals, which will be efficient in terms of designing feasible gate trajectories (compromise between smoothness of gate excursions and overall time for operation completion), while keeping water levels within prescribed bounds.

The following ***specific objectives*** are proposed to reach the overall goal and serve as roadmap in the developments:

- To define two case studies as benchmarks for numerical and experimental testing. One is an experimental facility, the laboratory canal PAC-UPC. New instrumentation and acquisition and control tools are designed in this work to facilitate closing and opening automatic operations. The other one is a main canal of the left bank of the river Ebro, which is numerically simulated via a state of art computational code.

- To perform a study about the problem of closing and opening the benchmark canals, considering different manual operations. The interest is twofold: (1) learning significant issues and difficulties that arise when check structures are required to get completely closed; and (2) getting practical inputs for the automatic control design.

- To develop a predictive control strategy for closure and opening of irrigation canals. The strategy includes optimization under dynamic constraints, a decentralized control architecture and a supervising scheme to achieve the compromise of fast execution with smooth gate trajectories and water level regulation even in the presence of disturbances.

- To validate the control methodology by means of numerical simulation on the two cases of study in a variety of operating scenarios. This includes comparisons of the performance with respect to the use of open-loop control of gate trajectories.

- To experimentally validate the methodology in the laboratory canal PAC-UPC.

1.3 Outline of the dissertation

The dissertation is organized in seven chapters, this Introduction being the first one, where motivation and objectives have been stated.

Chapter 2 reviews concepts related to irrigation canal management and control and presents a review on relevant literature.

Chapter 3 introduces the two case studies used to test the control strategy proposed in this dissertation, the experimental platform canal PAC-UPC and the main canal of the Ebro river left bank canal. Numerical simulation schemes are presented based on solving the Saint Venant equations and linear models are derived to serve as background in the formulation of the control strategy.

Chapter 4 discusses relevant hydraulic issues encountered in water conveyance canals under closure needs and presents the results of manual closures of the benchmark canals, which serve as motivation and learning prior to the automatic control design and implementation.

Chapter 5 develops the methodology to design a predictive control with dynamic constraints for irrigation canal automation, which is the core of this thesis.

Chapter 6 describes the assessment of the control methodology on both cases of study, first using the numerical simulation schemes. In a second step, experimental results are presented for the laboratory canal available in UPC.

Finally, Chapter 7 presents the conclusions, summarizes the main contributions and gives some suggestions for future research.

Chapter 2

Control of irrigation canals

2.1 Irrigation systems

A system of irrigation canals transports water from its source to the farmer fields. Irrigation is mainly used to assist the growing of agricultural crops during periods of inadequate rainfall. Typically, the system is a tree-shaped net of open canals and water flows downhill through the canals and enters the fields by gravity most of times. The main (or primary) canal taps water from the water source, which may be a river, a lake, a reservoir or groundwater. Water is then distributed by the smaller secondary canals to the tertiary canals which are even smaller. From these tertiary canals the water finally enters the fields where it will be used to irrigate a crop (Van den Bosch et al., 1992). Figure 2.1 shows a small dam on a river from which water is tapped and passes into the main canal. The water then passes into two smaller canals, and finally the fields are irrigated by siphons.

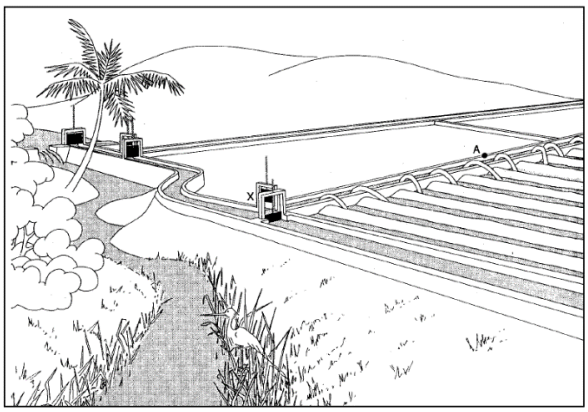

Figure 2.1 Part of a small irrigation system (taken from (Van den Bosch et al., 1992))

Canal system operation depends on check structures for depth and discharge management. An irrigation canal system is divided into pools and gates are usually the boundaries between canal pools, in this way the pools are located in a series configuration. From the hydraulics point of view, each pool has a unique response when the discharge through structures is changed. Physical parameters that influence the canal pool behavior are longitudinal bed slope, cross section size and shape, wall materials (surface roughness) and length (Clemmens, 2014). The check gates are the main control structure on an irrigation canal. Gates are mainly used to regulate water levels, to measure and control discharge, and to increase and regulate in-channel storage volumes (Buyalski et al., 1991).

There are several types of gates, such as undershot and overshot gates. The undershoot gates are movable gates allowing water to flow under the gates, meanwhile, the overshot gates are movable gates allowing water to flow over them. Sluice gates can be divided into two main different types, vertical rising and wall-mounted. Examples of undershot gates are radial, vertically hinged and sluice gates. A line weir is a typical example of overshot gates. Hydraulically, the overshot gate is a moveable weir. Meanwhile, the sluice gates are made of either wooden or metal plate, these gates may be vertical or curve. The sluice gates slide in grooves in the sides of the canal. In this dissertation only sluice gates are considered in the proposed case studies.

In the management of irrigation systems, one of the main goals is to guarantee the user's required discharge. Additionally, it is necessary to keep the water depths constant in checkpoints along the canal in order to avoid problems such as cracking in the canal lining. In order to describe the hydraulics in the canal, a set of variables can be used such as water depth (downstream or upstream), volume of water in a pool or discharge through a structure. The water depth (or water level) is the vertical distance from the lower point of the canal section to the free surface. The manipulated variables may be either discharge or gate openings. The disturbances in the system are mainly caused by turnout variations (offtakes), infiltration from the canal or rainfall (intakes). The turnouts are located typically at downstream part of canal pools. Meanwhile, a strong rainfall into the canal can result in higher rates of water level changes. The system operational constraints are mainly related either to maximum/minimum available discharges or related to check gate limits.

2.2 Concepts related to the automation of irrigation systems

Automatic control can improve the performance of the irrigation water delivery systems. The improvements are mainly related to the efficiency and the operational flexibility in the canal operation. The efficiency is the ratio of water volumes used in the irrigated fields to volume of water extracted from the available source. The flexibility is related to the capacity to give to the user the required discharge in time and quantity, with flexibility rather than restrictions over the time of water intake. Automation incorporates to the irrigation system, a control system that upgrades the conventional method of canal system operation. The control system is able to automatically operate check structures based on feedback information from the current state of the

hydraulics variables in the canal. The next subsections are devoted to describe some concepts related to automation of irrigation systems.

2.2.1 Control system architecture

In order to control water levels in a canal, the control system may be composed by several control loops and the system architecture is shaped as a cascade topology. For a model-based control, there are two global approaches that may be used (Sepúlveda, 2008):

a) To state a model where water levels depend on gate openings, a system architecture in this way is depicted in Figure 2.2 (left).

b) To state a model where water levels depend on gate discharges. With this approach, the gate discharge controller is an operating block that converts the desired discharge into gate openings by inverting the gate discharge equation proposed in (Chow, 1988). A system architecture related to this approach is depicted in Figure 2.2 (right). The control problem with this strategy is easier to solve than the approach stated in subparagraph a, it is due to the actuator nonlinearities are not considered in the design process when the model output (water level) depend on gate discharge.

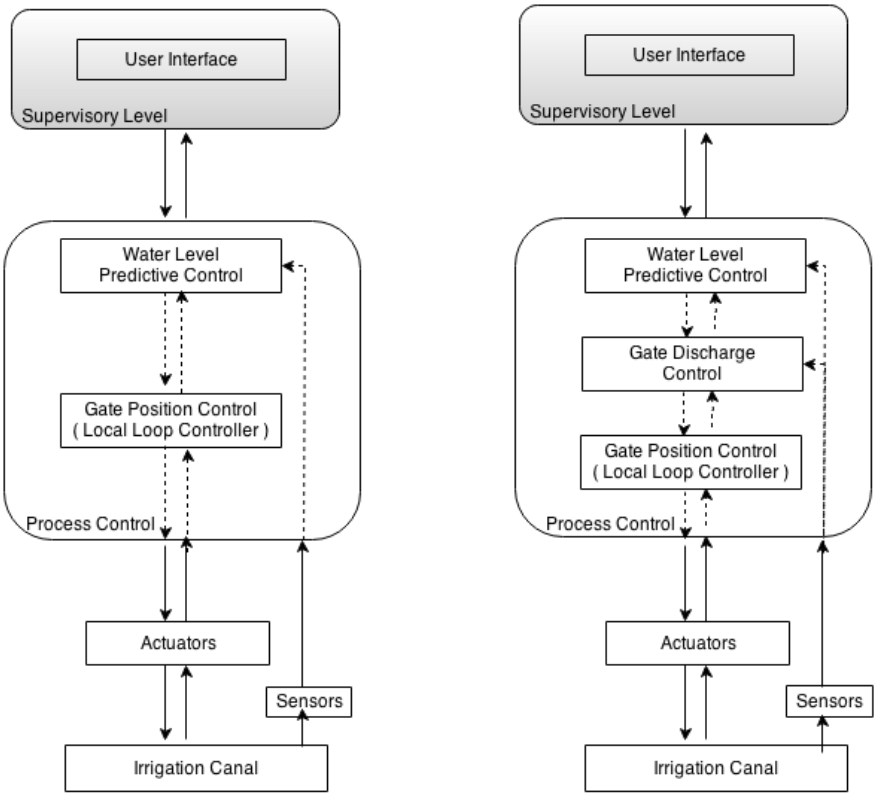

Figure 2.2 Control system architectures

The dynamics of the control loops are different in the control system architecture. Whatever the strategy, the dynamics of the outer loop (process control in Figure 2.2) changes slower than the

dynamics of the inner loops (gate position control and discharge control). The gate position controller is a feedback control that converts the desired gate openings into actuator movements (see Figure 2.3). The water level control reads and processes the feedback signals from water level sensors and updates the control variable every sampling time according to the control algorithm.

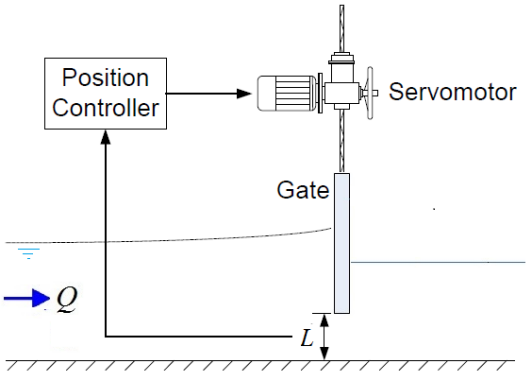

Figure 2.3 Gate Position Control (taken from (Sepúlveda, 2008))

Control system components may be grouped in two categories mainly: control center devices and remote site devices. The control center devices in the supervisory level are located in the system control center called headquarter or master station (Buyalski et al., 1991). Control center devices include human-machine interface (HMI), DAQ cards, computers, and so on. At supervisory level, the watermaster may fix the setpoints, and monitors/controls the irrigation canal using the HMI. The remote site devices are located in the field and they interact directly with the dynamics of the canal. Remote site devices include water level sensors, flowmeters, remote terminal units (RTUs), programmable logic controllers (PLC), check gates, servomotors, electrical relays and motor drivers.

2.2.2 Open-loop and closed-loop control

There are two common types of canal control system, open-loop system and closed-loop control systems.

- In the *open-loop control*, (or feedforward control) the output (control variable) is generated based only on inputs, such as, the dynamics of the system, the setpoint and the estimation of disturbances. The open-loop control can compensate the inherent system delay by anticipating user's needs but the system needs information that has to be approximated from climatic, agronomic, sociological data and records of the water consumption (Malaterre et al., 1998). The open-loop control performance is deteriorated by the presence of model errors and more especially by the presence of unknown disturbances.

- In the *closed-loop control* (or feedback control), the output is generated considering the measured error between the actual controlled variable and the setpoint. Disturbances are considered indirectly, since they affect the system output. Closed-loop can be applied to all controlled variables. As an example, Figure 2.4 depicts a water level feedback control for a single pool configuration canal.

The control strategy proposed in this dissertation only focuses on closed-loop control. There are two types of closed-loops in water level control: upstream control and downstream control. The following subsection presents the two main types of closed-loop control.

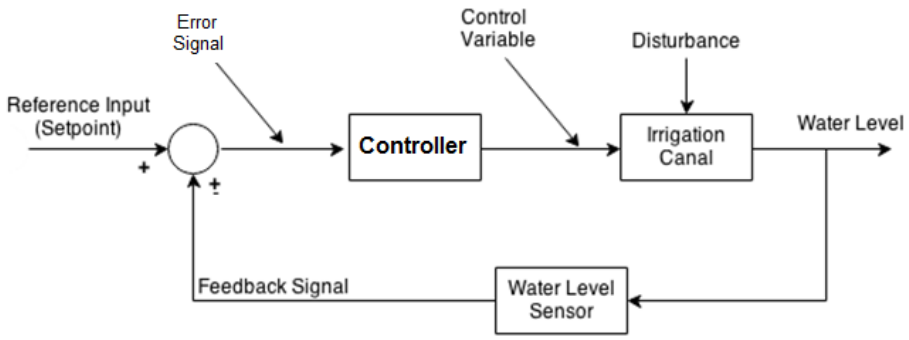

Figure 2.4 Closed-loop control

2.2.3 Canal control concepts: Upstream control vs. Downstream control

Depending on where the controlled variable is located in the control system, canal control concepts may generally be categorized into upstream and downstream:

- **Upstream control**: The adjustment of the check structures is based on the feedback information measured by sensors located upstream (Buyalski et al., 1991). The disadvantage is that only levels or volumes can be controlled with this approach when flow condition is subcritical although most canals operate in subcritical flow conditions. In this way the upstream water supply is transferred downstream to the points of diversion, and it allows a supply-oriented delivery in the water conveyance system (Horváth, 2013).

- **Downstream control:** The adjustment of the structures is based on the feedback information from measured by sensors located downstream. The controlled variables are located downstream of the control variables, for instance, the downstream water level in a canal pool is controlled by a sluice gate located at the upstream part of the pool (Horváth, 2013). All variables can be controlled by the downstream control. The canal operation with downstream control turns the downstream demands to the upstream source and hence it is compatible with the demand-oriented delivery concepts in the water conveyance system.

2.2.4 Centralized and decentralized control

Depending on where the control decision is made in the canal pool, control strategies can be categorized into centralized and decentralized.

- The *centralized control* strategy considers globally all the objectives that have to be fulfilled for all pools in the irrigation system. The control law is obtained for the whole system. The controller is designed using global information of canal state. The most effective control performance may be obtained with this strategy, however, it is

computationally burden and the infrastructure investment is high to implement in actual canals. The implementation cost increases due to the strategy needs a relatively complex communication system between control structures and a central control unit (van Overloop et al., 2010).

- In *decentralized control* (or local control) there are separate control units designed for each pool. This strategy divides the whole system into subsystems (Gómez et al., 2002). There are as many subsystems as pools in the irrigation system. Each controller receives information from its downstream or upstream neighbor pool. This strategy is normally based on simpler control methods than the centralized one. The hydraulics transmission of information no requires additional equipment, so in this way the implementation and maintenance of this approach is considerably cheaper and less complex than the centralized one.

2.3 Literature review

In the last three decades, significant research and development efforts have been reported in the literature concerning the design of automatic controllers for irrigation canals. A detailed classification of control algorithms that had been developed till 1998 is given in (Malaterre et al., 1998),while some unifying essentials in the formulation of control algorithms are discussed in (Rogers et al., 1998). The state of the art in canal automation is summarized in several works such as (Malaterre et al., 1998), (Rogers & Goussard, 1998), (Mareels et al., 2005), (Rivas Pérez et al., 2008), (Sepúlveda, 2008), (Bastin et al., 2009), (Malaterre, 2011) and (Horváth, 2013). The following subsection presents various types of automatic control algorithms that have been applied either in simulation or real-time control of irrigation canals.

2.3.1 Types of Automatic control applied on irrigation canals

2.3.1.1 Proportional-Integral-Derivative (PID) Control

The PID control is a feedback control strategy widely used in industrial control, including the hydraulics processes. In PID approach, the control variable is obtained based on the measured error which is the difference between the controlled variable and the desired setpoint. In the control of irrigation canals, and especially in downstream water level control, the time delay has very high values. This time delay makes that the positive effect of the derivative action on phase and gain margins minimal, and therefore, the derivative action is usually not implemented (Aguilar et al., 2012).

Some examples of PID control implemented on irrigation canals can be found in the literature. For instance, (Schuurmans et al., 1999) proposed a controller that has a master-slave structure where

every pool is controlled by its upstream discharge under gate. The master controller consists of a PI-based controller for feedback and a decoupler with feedforward capability. The decoupling is based on the inversion of a simple dynamic model of the canal system. The tuning procedure of the controller is based on the Integrator Delay model, and a filter is also used to minimize the effect of the canal inherent resonance. The applicability of the controller is tested in field experiments. Meanwhile, (Litrico & Georges, 1999) implements a PID controller for a dam-river system and the simulation results indicated that the controller responds quickly to unpredicted disturbances, but with oscillations. In (Ratinho et al., 2002), a Proportional-Integral (PI) upstream water level control is developed and tested experimentally in a prototype canal. (Litrico et al., 2005) tuned the PI controller parameters using frequency response of each pool. Making use of the gain margin obtained for different discharge conditions, a series of robust controllers were calculated. The downstream control tested in a laboratory canal showed a satisfactory behaviour. In (Montazar et al., 2005), a downstream water level controller is presented for the first nine pools of the Narmada main canal in India. The control system consists of a downstream PI feedforward controller.

On the other hand, (van Overloop et al., 2005) addressed the problem of controller tuning from the perspective of multiple models based optimization. The authors propose an optimization function and its gradient to obtain the variation of the gains of decentralized PI controllers considering the minimization of a cost function which penalizes the deviation of error against the control outputs. Adjustment of controller parameters for various values of the flow rate operation had resulted in performance improvement, better disturbance rejection and smoother gate movements. The goal of the author was expanding the operating range while maintaining a good performance. The validation of the controller is done at simulation using the channel model Umatilla Stanfield Branch Furnish (USBF) located in Oregon. Meanwhile, (Rijo & Arranja, 2010) presents a supervisory control system, which used an optimization method in order to determinate the globally optimal tuning parameters of the PI upstream controllers for the entire canal. Finally, (Aguilar et al., 2009) implements a decentralized PI control in the Canal de Lodosa, Spain. The model describing the dynamic behavior includes experimental identification with positive performance.

2.3.1.2 Fuzzy Logic

The fuzzy logic control is a kind of nonlinear control which is based on a knowledge database consisting of the so-called fuzzy IF-THEN rules. A fuzzy IF-THEN rule is a statement (not an equation) in which some words are characterized by continuous membership functions (Wang, 1997). The control algorithm is transparent and intuitive, the tuning procedure is easier than classical controllers such as PI controller, and no linearization of the governing equations are involved. The disadvantage of the algorithm is reduced precision in its outputs due to the approximation inherent in the fuzzy logic (Gopakumar & Mujumdar, 2009). A study developed by (Lobbrecht et al., 2005) has demonstrated the applicability of the fuzzy logic technology for management and control of an irrigation system.

Two examples of fuzzy control developed for irrigation canals control can be found in (Gopakumar & Mujumdar, 2009) and (Begovich, Martinez, et al., 2007). In (Gopakumar & Mujumdar, 2009), simulations results of centralized control for downstream discharge and water level of the ASCE

test canal 2 are presented. The algorithm is based on the Saint-Venant equations, where the momentum equation is replaced by a fuzzy rule based model, while retaining the continuity equation in its complete form. The authors came to the conclusion that the main limitation of the fuzzy algorithm relates to the non-applicability in those situations where very significant backwater effects exist. Meanwhile, (Begovich et al., 2005) and (Begovich, Martinez, et al., 2007) present a decentralized fuzzy gain scheduling controller for the downstream water levels of an irrigation canal prototype. Each local control is a gain scheduling controller composed by a Linear Quadratic Gaussian (LQG) regulators and the switching among controllers is fulfilled using fuzzy logic.

2.3.1.3 Optimal control

In optimal control, the control law for a given system is found based on the optimization of a certain optimality criterion. In (Malaterre, 2008), a linear quadratic optimal controller is applied to control an eight-pool irrigation canal. The model used to design the controller is derived from the Saint-Venant equations discretized through the Preissmann implicit scheme. The MIMO structure of the controller exhibited big advantages to counteract the canal coupling and transport delay effects, however the method have three disadvantages. First, the large dimensions of vectors and matrices. Second, the model validation is assured only for subcritical flows. And third, the difficulty of Linear Quadratic (LQ) optimal control to include gate restrictions.

There are several examples of optimal control strategies used to control irrigation canals, such as (Sawadogo et al., 1995), which presents an application of optimal control theory to the automatic control of a single irrigation canal pool. (Durdu, 2005) used a Linear Quadratic Gaussian (LQG) optimal controller for a multipool irrigation canal in order to test different state observers. (Litrico & Fromion, 2006) presents experimental results on a real canal of a mixed controller designed into the H_∞ optimization framework. The controller considers a compromise between the water resource management and the performance in terms of rejecting unmeasured perturbations. Meanwhile, (Weyer, 2006) presents a LQ water levels control of an irrigation canal using overshot gates located along the channel. The results demonstrated that the designed controller has very positive performance in field tests on a fully operation channel, the multivariable centralized LQ controller attenuated disturbances as they travelled upstream and had better error propagation characteristics than decentralized PI controllers. A drawback is that LQ control requires further design effort than decentralized PI control, but the author suggests to use optimal control provided that performance improvements justify the additional effort.

2.3.1.4 Predictive control

The application of predictive control for water systems has been investigated mainly since the 90s. One of the first numerical evidence of a predictive controller was on channel-West Maricopa (Arizona, U.S.) published by (Ruiz & Ramirez, 1998). The analytically linear time-invariant state

space prediction model was derived from Saint Venant equations. According to results, the generalized predictive control was slightly sensitive to the magnitude and delay variation. In (Sawadogo et al., 1998) a centralized predictive control approach was used to control the automatic operation of gates of each pool in an irrigation canal; the designed controller considers explicitly the interactions among subsystems. Meanwhile, a predictive control with constraints was proposed by (Pages et al., 1998) for water management applications in France. On the other hand, (Akouz et al., 1998) showed simulation results about the centralized generalized predictive control (GPC) technique used to control the downstream water levels of the first three reaches of the ASCE canal test 2. The strategy demonstrated to compensate the time delay and to overcome the system nonlinearity.

Other examples of predictive control strategies to control of irrigation canals in the last two decades can be found in (Rodellar et al., 1989), (Pages et al., 1998), (Gómez et al., 2002), (Wahlin, 2004) (van Overloop, 2006), (Begovich, et al., 2007), (Sepúlveda, 2008), (Mantecon et al., 2010), (Delgoda et al., 2012), (Horváth, 2013), (Álvarez et al., 2013), (Horváth et al., 2014a), (van Overloop et al., 2014) and (Horváth et al., 2015).

Predictive control has demonstrated a positive performance when it has been implemented and tested in actual irrigation canals. An implementation of real-time control for eight-pools of the WM Canal at the Maricopa-Stanfield Irrigation and Drainage District (USA) was reported by (van Overloop et al., 2010). The results show that the water could be efficiently delivered to users with little deviations in the water level. However, the behavior of the system with known setpoint changes in water demand was not as effective as expected, thus the authors suggested to continue exploring in this area to take advantage of all the benefits of this control technique. Meanwhile, an implementation of adaptive predictive expert (ADEX) control of water levels in the Canal Imperial de Aragon, Spain was fulfilled by (Aguilar et al., 2012). The results showed that predictive control had a better performance than PI control in field tests related to both change in setpoint levels and disturbance rejection.

In addition to nonlinear predictive control, there are some variants of predictive control, the most popular being adaptive predictive control, distributed model predictive control and predictive control based on multiple models. The following paragraphs describe briefly the application of these variants of predictive control to irrigation canals control.

In adaptive predictive control, the predictive control is proposed within the framework of adaptive systems (Martín Sánchez & Rodellar, 1996). Adaptability plays an important role in practical applications such as control involving time delay or when the predictions made by the model are not satisfactory due to unmodeled dynamics. Examples of adaptive predictive control applied to irrigation canals can be found in (Cardona et al., 1997), (Sawadogo et al., 2000), (Aguilar et al., 2009), (Lemos et al., 2009) and (Aguilar et al., 2012).

Distributed control is a control structure that involves centralized and decentralized control in the same structure. In distributed control, each local controller communicates with neighbor controllers in order to find a cooperative solution for the overall control problem (Maestre et al., 2011). Examples of distributed predictive control for water systems can be found in (Dunbar,

2007), (Negenborn et al., 2009), (Zafra-Cabeza et al., 2011), (Alvarado et al., 2011) and (Lemos et al., 2013).

Although industrial processes are nonlinear, most predictive control applications are based on the use of linear models. However there are several examples of nonlinear predictive control applied to water systems such as (Igreja & Lemos, 2009), (Arnold et al., 1999) and (Georges, 2009). Meanwhile, (Xu et al., 2012) develops a comparison between linear and nonlinear schemes applied to control of open channel flow. The first scheme is based on a linearized Saint-Venant model and the second one is based on the discretization of the Saint-Venant equations and its formulation as linear time-varying state-space model. The performance is evaluated in terms of control accuracy and computational time. The authors came to the conclusion that both schemes can control the water system with positive performance, but the drawback of the schemes is that computational complexity of nonlinear predictive control is higher and the computational time longer than the linear one.

Predictive control based on multiple models is an extension of the standard predictive control framework that incorporates more than a single model in the predictive control formulation. The methodological approach was proposed by (Murray-Smith & Johansen, 1997). The main advantage of the multi-model strategy is that well known linear system theory can be used. The strategy is useful when there are different operating points, the approach is based on the 'divide-and-conquer' strategy, which develops local linear models corresponding to specific operating conditions. The global model is obtained by the integration of local linear models. Results obtained by both (Duviella et al., 2010) and (van Overloop et al., 2008) have shown the suitability to use this approach to improve the performance of controllers in canal systems.

2.3.2 Control of canals under large change in operating condition

Two examples of control strategies applied to irrigation canals under large change in operating conditions can be found in (Duviella et al., 2010) and (Charbonnaud et al., 2011). In (Duviella et al., 2010) two model-based gain scheduling controllers have been proposed for canals systems in order to deal with large operating condition. The first controller is based on representing the canal behavior as a Hayami linear parameter varying model that allows to consider the way that the parameters vary according to the operating point. The second control strategy is based on representing the canal behavior as a set of linear time-invariant models that can be obtained through a multi-modeling identification process. The supervision of the operating mode is fulfilled on-line and it is combined with a control accommodation method which switches to the best controller. Both controllers have given similar performances. In (Charbonnaud et al., 2011), a supervised robust predictive multi-controller strategy is proposed. The 'divide and conquer' strategy is used to divide the system operating range into four operating range discharges in order to control a canal under large changes in operating condition (from 0 m^3/s to 5 m^3/s). The overall controller follows a multi-controller approach, namely, from the identified discrete models, a bank of robust predictive controllers was designed. Every predictive controller corresponds with an identified discrete model.

It is noteworthy that, during the last 20 years, the research community has focused on control methods to improve the operational management of water conveyance systems. However, automatic canal closure operation has received much less attention in the literature of irrigation canals. A case study on night closure feasibility for water saving of the Upper Swat-Pehur High Level canal system in Pakistan is found in (Ghumman et al., 2009). The results show that where canal lengths are less than 5 km, the potential to save water in the irrigation system is quite positive. Reducing the discharges rate at night have demonstrated to save a significant amount of water in medium-sized canal networks (De Bievre et al., 2003). For instance, significant water savings were achieved through night-time closure of Shingrai Minor in Pakistan (Khan & Ghumman, 2008). In general, the feasibility of night-time closure depends on the speed of filling and emptying the canal each day, and the time required to meet full irrigation demand during the day.

An application of open-loop predictive control on automatic closure/opening operations of the Ebro River Left Bank canal in Spain is found in (Soler et al., 2010) and (Soler et al., 2014). The left bank canal usually works at its maximum capacity of 19 m^3/s. The objective of the closure operation is to isolate the irrigation system from a scenario considering a pollutant flowing in the supplier river. The closure operation is designed to be performed in three stages. The first stage carries the canal from the unknown initial state to a 15 m^3/s steady state by applying only one gate movement. The second stage is devoted to drive the canal from the 15 m^3/s steady state to another defined by 2 m^3/s. The third stage carries the canal to zero discharge with only one gate movement, in this way, the canal is isolated totally. Namely, in both first and third stage, the gates are moved in automatic manual operation, while in the second stage the optimal gate trajectories are obtained with open-loop predictive control in order to change the discharge from 15 m^3/s to 2 m^3/s as smooth as possible. Meanwhile, the opening operation is designed to be performed in two stages. In the first stage, the open-loop predictive strategy generates the gate opening trajectories in order to drive the canal from 0 m^3/s to a 15 m^3/s steady state in a smooth way. The second opening stage is devoted to raise all the gates above the water surface except the most upstream gate (Soler et al., 2014).

2.4 Predictive control essentials

This subsection is devoted to explain basic concepts related to predictive control, which is chosen in this dissertation as control strategy to manage irrigation canal operations involving abrupt changes in the operating conditions. Predictive control is known with several names in the literature, such as model predictive control, model-based predictive control or receding horizon control. Throughout this dissertation, only the name predictive control will be used.

Some of the advantages of predictive control that have received special interest from researches in both industrial and academic communities are (Maciejowski, 2002; Wang, 2009):

- Ability to handle constraints on the inputs, states and outputs of the controlled system and also with safety and equipment constraints.
- Completely multivariable framework.

- Predictive Control is more powerful than Proportional-Integral-Derivative (PID) control
- Ability to perform on-line optimization.

Based on a model of the process, predictive control makes the predicted process dynamic output equal to a desired dynamic output conveniently predefined (Martín Sánchez & Rodellar, 1996). Predictive control essentially relies on the use of a model able to predict the system output as a function of the system inputs on a moving horizon scenario. The model allows to compute the control sequence that makes the predicted output to follow a desired trajectory through the minimization of a performance criterion (also called cost function or objective function in technical literature). A predictive control problem has the framework of a finite horizon optimal control problem. One of the elements of the predictive controller is the optimizer, which computes at each sampling time, the optimal output based on the controlled variable error, the cost function, constraints and process disturbances. Figure 2.5 shows a block diagram of the predictive control strategy. Predictive control essentially solves a standard optimal control problem on-line (each sampling time) for the current state of the plant.

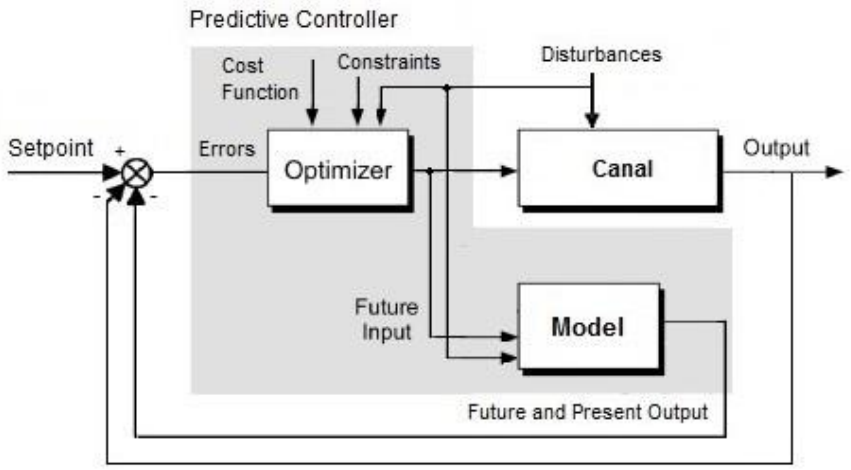

Figure 2.5 Predictive control block diagram.

An implementation of predictive control must consider the following requirements:

- An accurate model that captures the dynamic behavior to obtain a positive closed-loop performance. Besides, a control-oriented model must be also simple enough for allowing the on-line optimization. It is noteworthy that real systems often have problems as nonlinearity, strong coupling, uncertainty and wide operating range, which makes the synthesis of an appropriate model a challenging task.

- The optimization problem must be solved at each sampling time, which implies computationally demanding algorithms in terms of load (burden) in real-time implementation.

A great amount of survey papers may be found in the literature. For instance, (Henson, 1998), (Morari & Lee, 1999), (Mayne et al., 2000), (Qin & Badgwell, 2003), (Morari & Barić, 2006), (Camacho & Bordons, 2010), (Darby & Nikolaou, 2012), (Martín-Sánchez et al., 2012), (Xi et al.,

2013), (Christofides et al., 2013) and (Mayne, 2014), most of them highlighting developments and challenges proposed until their publication date. It is widely agreed that one of the most attractive feature of predictive control lies in the ability to explicitly handle constraints. In the last 30 years, predictive control has been successfully applied to complex industrial processes, showing its great potential of handling complex control problems. Currently a considerable number of industrial applications demand on-line optimization with constraints management in the control system design rather than only solving the traditional regulating problem (Xi et al., 2013).

The fundamentals of the predictive control developed in this dissertation follows the approach proposed by (Martín Sánchez & Rodellar, 1996). This approach has been used in the control of a canal with single pool configuration (Rodellar et al., 1993, 1989) and also in a multi-pool configuration in (Gómez et al., 2002) and (Aguilar et al., 2009, 2012).

The system is usually represented by a difference equation, which may be expressed as follows:

$$A(z^{-1})y(k) = B(z^{-1})u(k) + w(k) \tag{2.1}$$

where $y(k)$ is the output variable. $u(k)$ is the control variable and $w(k)$ is the disturbance signal. $A(z^{-1})$ and $B(z^{-1})$ are polynomials in the backward shift operator given by

$$B(z^{-1}) = b_1 z^{-1} + b_2 z^{-2} + \cdots\ b_m z^{-m} \tag{2.2}$$

$$A(z^{-1}) = 1 - a_1 z^{-1} + a_2 z^{-2} + \cdots\ a_n z^{-n} \tag{2.3}$$

In predictive control, in order to stablish the prediction, a time horizon $[k, k+\lambda]$ is considered, where k is the present instant and λ is the prediction horizon. The notation $\hat{u}(k+j|k)$ indicates the control variable for a future time instant $k+j$. Meanwhile, the future sequence of control actions

$$\widehat{U}(k) = [\hat{u}(k|k)\ \ \hat{u}(k+1|k) \ldots\ \hat{u}(k+\lambda-1|k)]^T$$

is optimized at each sampling time, by minimizing a cost function. The minimization may include penalties on deviations of the controlled variable of the desired reference and penalties on the requested control variable changes, namely:

$$\min_u J = \sum_{j=1}^{\lambda} \hat{e}_j\ (k+j|k)^T \Psi_j \hat{e}_j(k+j|k) + \sum_{j=0}^{\lambda-1} \hat{u}(k+j|k)^T R_j\, \hat{u}(k+j|k) \tag{2.4}$$

where $\hat{e}_j(k+j|k) = \hat{y}(k+j|k) - y_r(k+j|k)$ is the signal error and $y_r(k+j|k)$ is the reference trajectory. Ψ_j and R_j are weighting factors.

The prediction model may be linear as in (2.1), or nonlinear. Therefore, based on the type of model used in the optimization, predictive control can be categorized as linear or nonlinear. The theory of predictive control using linear models is more developed than the nonlinear one. Thus almost all commercial implementations are based on a linear prediction model (Álvarez et al., 2013). The nonlinear predictive control is applied when the process has severe nonlinearities or

when the processes operate in continuous transitions, namely with no operation around a stationary state, and therefore, linear modelling is not enough to model the main dynamic characteristics of the process.

In practice, virtually all systems operate under practical constraints. In many systems, control variables cannot be arbitrarily large and may have some magnitude limits. Actuators such as valves or gates have a limited operating range and limited slew rate (maximum rate of change). Even state variable values must be limited in many applications.

The problem of dealing with constraints is tackled systematically by using optimization. The constraints are presented as linear inequalities of the control variable. Since the cost function *J* is a quadratic function and the constraints are linear inequalities, the problem of finding the optimal predictive control can be stated as a standard quadratic programming problem. Therefore, the predictive control problem may be expressed as follows:

$$\min_{u} J = \frac{1}{2} u^T H\, u + u^T b \qquad (2.5)$$

$$\text{subject to:} \qquad Mu \leq \gamma$$

where u is the control variable and M is a matrix that collects the constraints. $H, b,$ and γ are compatible matrices and vectors. It is noteworthy that, it takes a longer time to calculate the constrained predictive control optimal value in comparison with the unconstrained one. Thus, the real-time implementation demands for either fast algorithms that require less computation time or high performance computing devices with small sampling time (Xi et al., 2013).

The feasibility is also an important issue in order to guarantee that the optimizer satisfies the constraints. Usually, the normal way of using a constrained predictive control algorithm is to compute $u(k)$ using (2.5) and apply it to the process. If $u(k)$ violates the constraint then $u(k)$ is saturated to its limits by either the predictive control algorithm or the actuator (Camacho & Bordons, 2004). However, in case of unfeasibility, there are methods dealing with the constraint management in order to try to recover the feasibility. Such methods act over the constraints in different ways, such as disconnection of the controller, a temporary elimination of constraints or a temporary relaxation of the constraints limits.

2.5 Final remarks

The control methodology developed in this thesis combines prediction issues as described above with constrained optimal control as described in (2.5), all of them within a supervised decentralized control scheme with a strategy to manage constraints in a time-varying manner.

Chapter 3

Description and modelling of case studies

3.1 Introduction

This chapter is devoted to present the case studies where the dynamically-constrained predictive control strategy will be tested. The first part of the chapter presents a general description of the case studies, the experimental platform canal PAC-UPC and the Ebro River Left Bank canal. The laboratory canal was specially designed to test irrigation canal control algorithms. The second case study is the canal where the motivational work fulfilled by (Soler et al., 2014) was developed. Secondly, some aspects about the implementation of the numerical model developed in SIC software are presented. Finally, the mathematical models used in the derivation of the proposed predictive control algorithms are described.

3.2 Laboratory canal PAC-UPC

Laboratory canals may be considered as an intermediate step between the numerical simulation and real-time implementation on the field. Although there are few laboratories for experimentation in irrigation canals in the world, these are very useful tools to test control algorithms. Canal PAC-UPC is the acronym of "Canal de Pruebas de Algoritmos de Control – Universitat Politècnica de

Catalunya. The canal was built in 2006 and it is located at the Laboratory of Physical Models of the Technical University of Catalonia, Barcelona, Spain.

The experimental facility has the following characteristics and instrumentation components:

- Length of 220 m in a serpentine shape (see Figure 3.1), this shape aims to minimize the space to be occupied by the canal.
- Bottom slope of 0 m/m in order to achieve the largest possible time delay (Horváth, 2013).
- Rectangular cross section with canal width of 0.44 m and deep of 1 m.
- Area of 22.5 m x 5.4 m.
- Manning's coefficient of 0.016.
- Maximum discharge of 150 l / s.
- A head reservoir.
- Three pools in series with length of 87, 90.2 and 43.5 m.
- Three sluices gates of 1m x 0.4 m (G_1, G_2 and G_3 in Figure 3.1). The gate velocities are 1.524 mm/s for G_2 and 3.125 mm/s for G_1 and G_3.
- Four rectangular weirs used for lateral offtakes. Weirs are at the end of each pool and another one at the end of the canal. The weirs consist of a wall of plastic specially designed to cover a broad range of weir heights.
- Three orifices connected to manual valves (see Figure 3.2b).
- Electromechanical devices. Each gate is controlled by a three-phase servomotor of 0.75 CV of power. The servomotors are located on top of the gates (see Figure 3.2c). Each servomotor has a motor driver which has been installed in a control box beside the canal. The control boxes allow either the local or the distant operation of the motorized gates.
- Ten water level sensors (LS in Figure 3.1). Sensors are located upstream and downstream of each gate and at every rectangular weir.
- Three PCI data acquisition cards made by Advantech, with analog output channels and single-ended analog inputs.

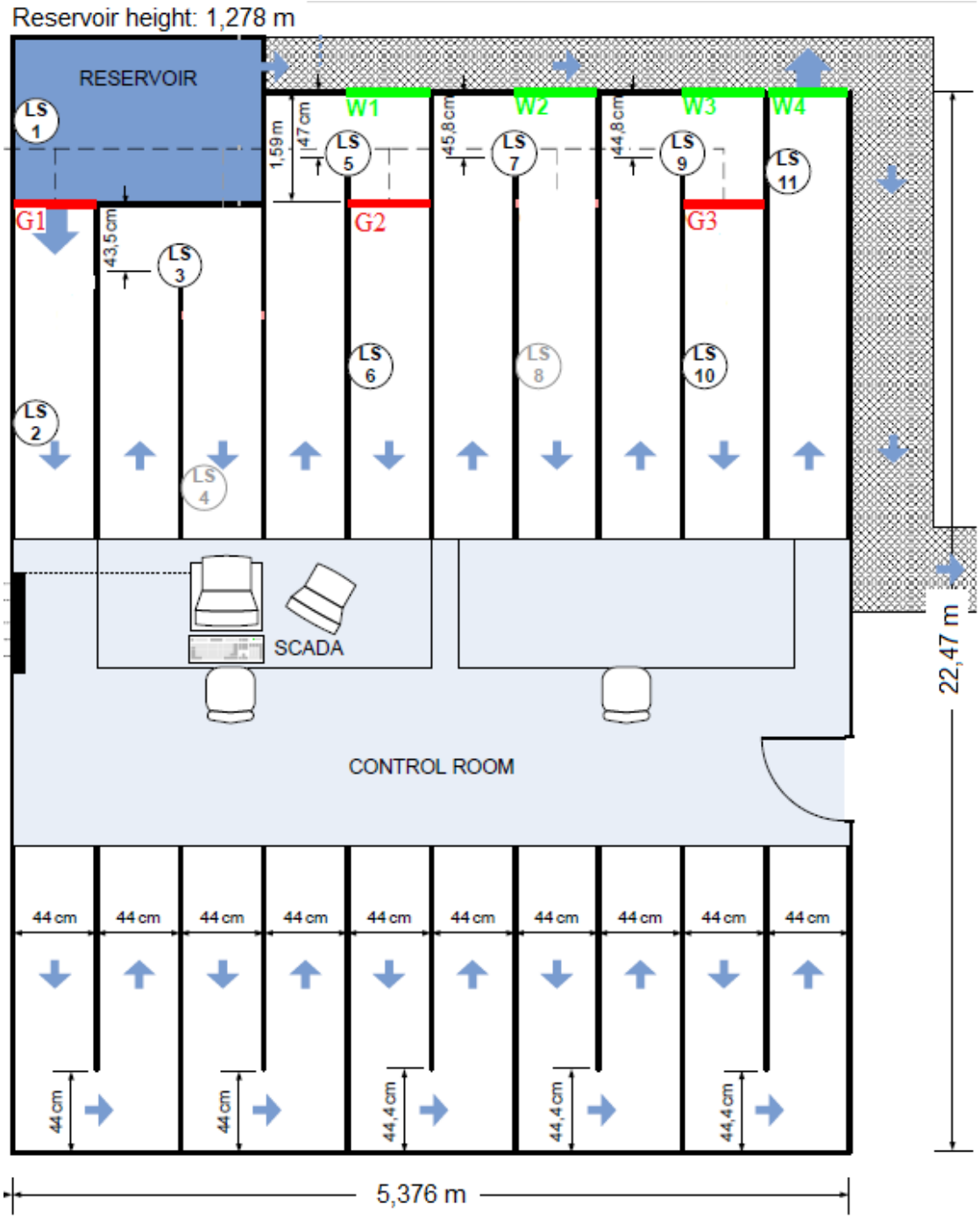

Figure 3.1 Schematic layout of the UPC PAC canal, from (Sepúlveda, 2008).

Figure 3.2 Experimental canal facility

A Simulink/Matlab-based SCADA system has been developed in order to manage the control system in the facility. The Supervisory Control and Data acquisition (SCADA) system provides both monitoring and control of remote sensors and actuators. The HMI (human-machine interface) implemented in the control room (see Figure 3.2d) has been developed in Matlab/Simulink environment (see Figure 6.43). The supervisory system is combined with a data acquisition system. In this way, the system receives as input signals the measurements of water levels from different points of the canal and also the three gate opening measures. The analog output signals are sent to the actuators (servomotors) which execute the control actions allowing gate movements. The 4-20 mA standard analog communication protocol is used for communicate sensors with the computer-based controller over a pair of conductors. In the standard protocol, the current signal range is 4 mA to 20 mA, this means 0% to 100% of measurement range, respectively. A flow path of sensor signals is depicted in Figure 3.3.

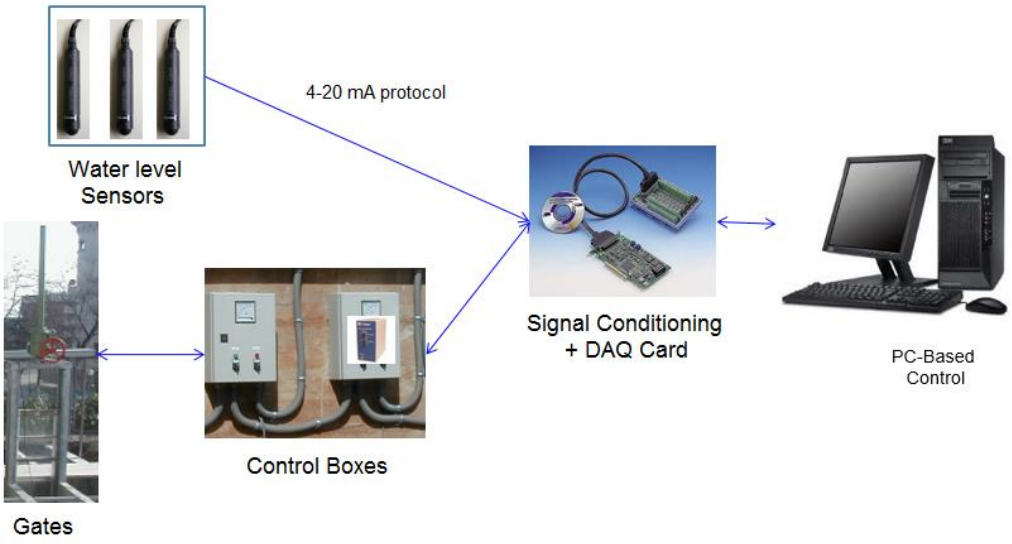

Figure 3.3 A flow path of the sensor signals in canal PAC-UPC

The canal, its software and hardware facilities have been documented in two PhD dissertations (Sepúlveda, 2008) and (Horváth, 2013). Subsequently it has been used for testing control algorithms in (Aguilar et al., 2009), (Horváth et al., 2014b) and (Horváth et al., 2015) and also for teaching purposes (Mantecon et al., 2010). The general maintenance tasks of the facility, the calibration procedure guidelines and some improvements of the SCADA system, including a more accurate and documented version of the gate position controller has been part of the work fulfilled during the development of the dissertation presented here.

Flow measures on gates and weirs discharge are calculated based on hydraulic relationships. Discharge under gates are obtained using water level measures in submerged flow conditions using (1.1). The rectangular weirs (see Figure 3.4) are used in the canal as control structures, weir discharge is calculated using the Kindsvater-Carter's equation (Herschy, 1995):

$$Q = C_{dw}\frac{2}{3}\sqrt{2g}(B_w + 0.003)(H_e + 0.001)^{3/2} \tag{3.1}$$

where

$$C_{dw} = 0.587\left(1 - 0.003\frac{W}{H_e}\right) \tag{3.2}$$

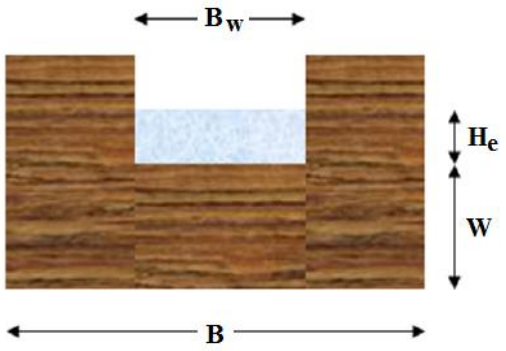

Figure 3.4 Rectangular weir (taken from (Horváth, 2013))

In the laboratory canal, undershot gates and rectangular weirs and their respective coefficients have been calibrated using experimental data in (Sepúlveda, 2008) and (Horváth, 2013). The accuracy in the gate position control is a big deal for the algorithms tested in the facility, consequently the hysteresis phenomenon is considered in order to calibrate the gates properly. Hysteresis refers to the dependence characteristic of the actuator on both current state and past inputs. In this way, for the position control, the calibration curve when motorized gate is moving up is different to the calibration curve when the motorized gate is moving down, as it is illustrated in Figure 3.5. Consequently, the gate position control algorithm is implemented with two calibration curves.

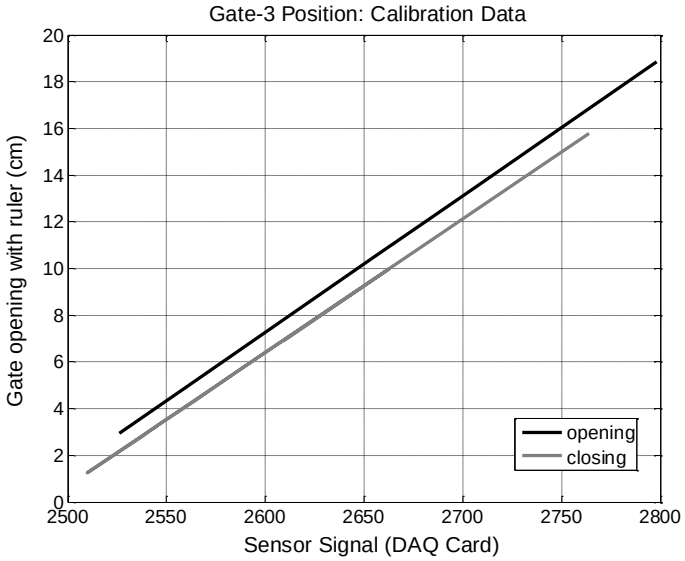

Figure 3.5 Calibration curves of Gate-3 Position Control

There are some physical and instrumentation limits in the facility, for instance, the minimum accurate gate movement is about 2 mm, the accepted water level measurement error is around 10 mm and the accepted discharge error is around 6 l/s. Meanwhile, the servomotors which move gates have a 4 mm-pitch, namely the minimum change in gate opening is 4 mm at every sampling time, and this gate opening is equivalent to 2 l/s approximately.

3.3 Ebro River Left Bank canal (ERLB Canal)

The cultivated area associated to the Ebro River Left Bank canal (ERLB canal hereafter) in Spain is mostly irrigated by surface flooding and its water delivery system is always operating to avoid seawater intrusion. The delivery system consists of a tree-shaped network of open canals. The ERLB canal inlet takes off water from the Ebro River at the Xerta weir and proceeds downstream parallel to the river until Tortosa, in Catalonia, Spain (see Figure 3.6). The main canal is 15 km in length, 3 m depth, it has a capacity of 19 m^3/s, and it has been designed with five pools separated by five check gates. Characteristics of the whole canal have been documented in (Soler et al., 2010, 2014).

Figure 3.6 The river Ebro delta, taken from ("Portal de CHEbro," 2015)

In the hydraulic model proposed by (Soler et al., 2014), the canal has been divided into 18 reaches. The model includes two types of sections, namely, trapezoidal with bank slope of 0.176327 m/m and rectangular with zero bank slope. The Manning coefficient is 0.016. The main characteristics of the pools are given in Table 3-1. The main characteristics of check gates are detailed in Table 3-2.

Reach	Elevation [m]	Length [m]	Depth [m]	Manning Coeff.	Bottom Width [m]	Bank slope
1	7.06	0	3	0.016	8	0
2	7.21	75	3	0.016	7.6	0.176327
3	6.98	1200	3	0.016	7.6	0.176327
4	6.83	1875	3	0.016	7.6	0.176327
5	6.78	2375	3	0.016	4	0
6	6.65	2475	3	0.016	4	0
7	6.01	3675	3	0.016	10	0.176327
8	5.89	5475	3	0.016	4	0
9	5.63	5825	3	0.016	8.2	0.176327
10	5.61	6150	3	0.016	10.5	0
11	5.63	6200	3	0.016	8	0.176327
12	5.55	6300	3	0.016	10.5	0.176327
13	5.3	9475	3	0.016	8.2	0.176327
14	5.22	10450	3	0.016	10.5	0.176327
15	5.12	11100	3	0.016	4	0
16	4.98	11350	3	0.016	10.5	0.176327
17	4.63	13025	3	0.016	4	0
18	3.89	13125	3	0.016	3.8	0
	3.29	14825	3			

Table 3-1 Canal pool characteristics

Gate	Upstream reach	Downst. reach	Width [m]	Discharge coefficient	Step [m]	Haul [m]
1	--	1	8	0.61	0	3
2	5	6	4	0.61	0.5	3
3	10	11	8	0.61	0	3
4	14	15	4	0.61	0	3
5	17	18	4	0.61	0.7	3

Table 3-2 Check gates characteristics

3.4 Models of irrigation canals

For the design of control systems, mathematical models are needed to describe adequately the dynamic behavior of the system. A concept map related to system models used in control and systems engineering is depicted in Figure 3.7. Models can be of many kinds (Soderstrom & Stoica, 1989):

- Mental, intuitive or verbal models.
- Graphs and tables. A Bode plot of a servo system is a typical example of a model in a graphical form. The step response, i.e. the output of a process excited with a step input, is another type of model in a graphical form.
- Physical models.
- Mathematical models.

The mathematical models may be described in several forms, such as differential equation, difference equations, transfer functions and state-space equations. The variables of the model are usually inputs, outputs, system variables and disturbances. In order to capture the most relevant dynamics of the canals, the model may have first, second or higher order. Mathematical modelling could be obtained by system identification or analytical approach. A widely used approach involves the construction of mathematical equations based on physical laws known to govern the behavior of the system (H. Garnier et al., 2008). Meanwhile, the system identification considers experimental data in order to model the system dynamic. In this dissertation, the mathematical models used in the predictive controller design are obtained by both analytic approach and system identification techniques.

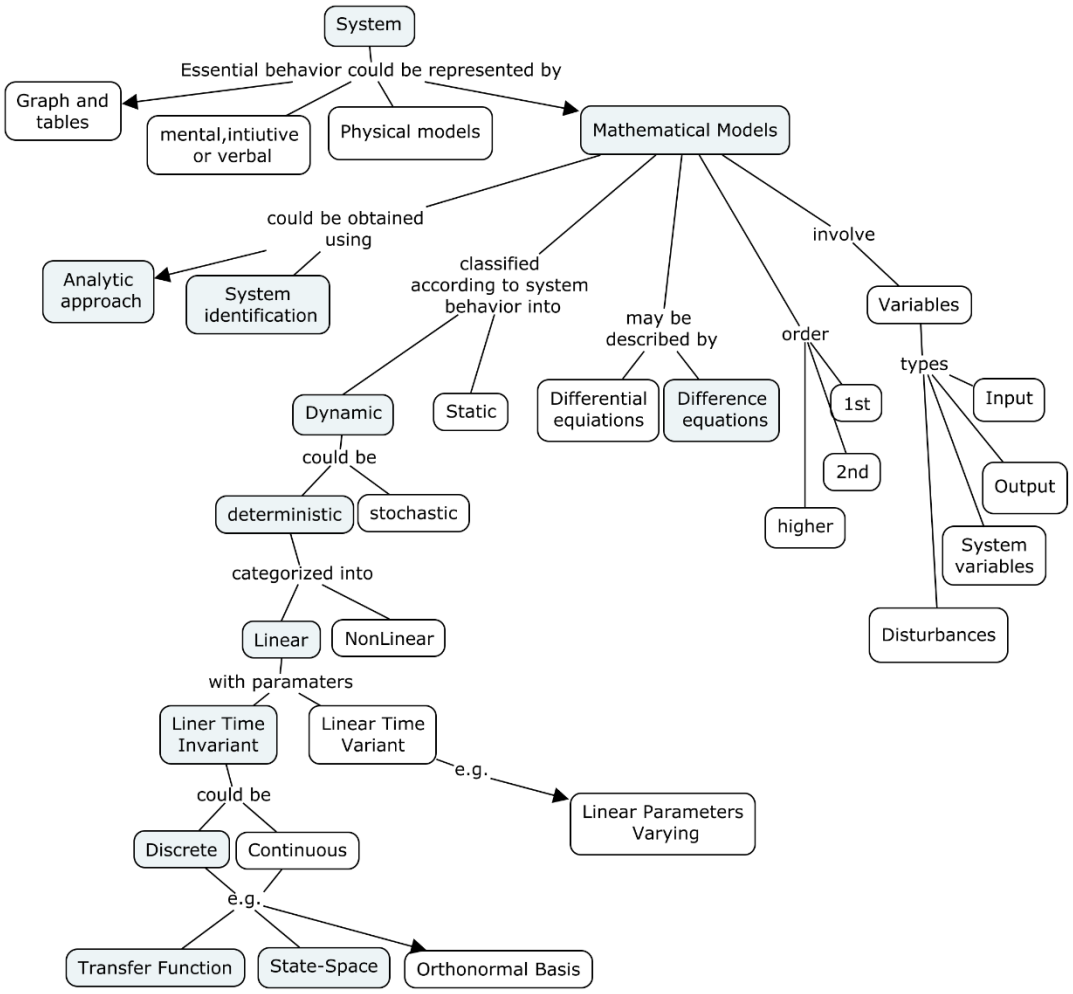

Figure 3.7 Concept map related to models of systems

Currently, the most accepted analytic approach to model open channels are the Saint Venants (SV) equations, which contain the following mass and momentum conservation equations (Chow, 1988):

$$\frac{\partial A}{\partial t} + \frac{\partial Q}{\partial x} = Q_{wi} \tag{3.3}$$

$$\frac{\partial Q}{\partial t} + \frac{\partial}{\partial x}\left[\frac{Q^2}{A}\right] + gA\frac{\partial y}{\partial x} + gA(S_f - S_0) = 0 \tag{3.4}$$

where A is the wetted cross sectional area [m^2], x is the longitudinal coordinate in the flow direction, t is time, $y = y(x,t)$ is the water level, $Q = Q(x,t)$ is the discharge [m^3/s], Q_{wi} is the lateral discharge (see Figure 3.8), S_f is the friction slope [m/m], S_0 is the bottom slope [m/m], and g is the gravity acceleration [m^2/s]. It is noteworthy that A depends explicitly on both the water level and the canal cross section shape.

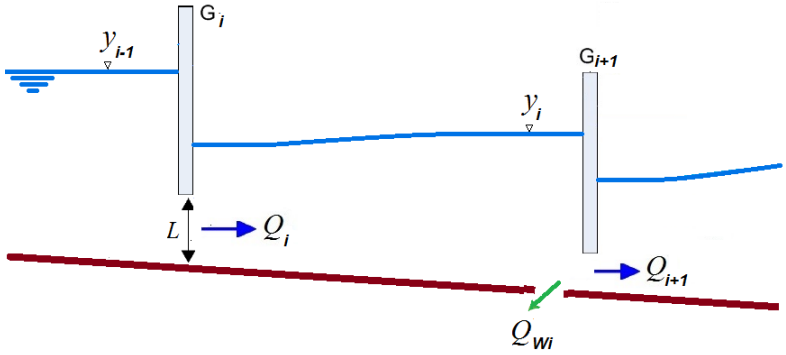

Figure 3.8 Simplified representation of a canal pool

The SV equations are nonlinear hyperbolic partial differential equations that do not have analytic solutions in most cases. Consequently, given a problem (defined by its initial and boundary conditions), numerical methods are needed to solve the equations. The method of characteristics of Abbott (Abbott, 1966) and the implicit difference method (Preissmann, 1961) are classical methods in the one dimensional case. As simulation tools, these numerical solutions can be quite accurate but require enormous computational burden that make them inadequate models as a basis for designing control systems (Aguilar et al., 2011). A concept map of how the Saint Venant equations are usually addressed is shown in Figure 3.9.

For control design purposes, methods involving simplified linearized models are preferred over complex models. Linearized models such as black box and white box models are widely used for control purposes. The black box models are obtained by system identification. The white box models are based on linearized SV equations around an operating point (Litrico & Fromion, 2004a). The preference of linearized models is mainly due to that the pair of partial differential SV equations has no analytic solution for an arbitrary geometry as it was mentioned in former paragraph. An analysis of behavior of linearized SV equations is fulfilled by (Malaterre et al., 1998).

The linearized deterministic model is categorized as linear whether the model obey the superposition principle, otherwise the model is a nonlinear one. Linear Time-Invariant (LTI) models are models whose parameters do not change over the time. An example of Linear Time Variant (LTV) model is the linear parameters varying. An LPV model is essentially a parameterized family of LTI models. A common identification strategy used to obtain LPV models is to define range of operating points, and then collect enough data to identify LTI models with different coefficients around specific operating points (Bolea et al., 2014). The identified LTI coefficients then can be used as interpolation points to find the coefficients as polynomial functions. Meanwhile, the state-space model is a descriptive form which considers input, output and state variables. A explanation about how to obtain the linearized SV model can be found in (Litrico & Fromion, 2004b). A detailed discretization of the Saint-Venant equations and the formulation as linear time-varying state space model is proposed by (Xu et al., 2012).

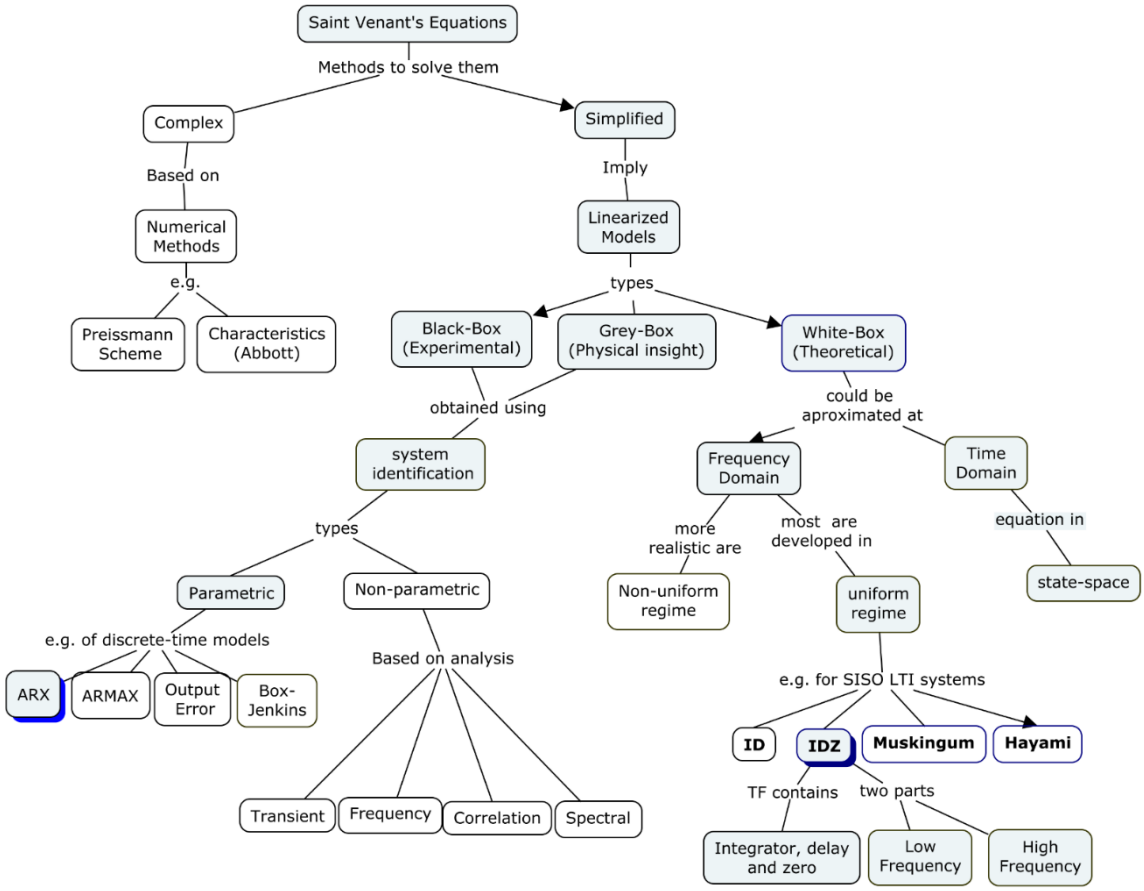

Figure 3.9 Concept map of solution of Saint Venant equations

3.5 Numerical models of the case studies

3.5.1 Numerical model of the canal PAC UPC

Simulations of case studies in this thesis are fulfilled by the SIC (Simulation and Integration of Control for Canals) modeling software developed by IRSTEA France, which is a one dimensional hydrodynamic software based on the Preissmann Scheme (Malaterre, 2012). This scheme belongs to the category of implicit finite differences. The SIC software permits simulating the hydraulic behavior of the irrigation canals under steady and unsteady flow conditions. A model in SIC is composed by three main units. The first unit is used to describe the canal geometry. Unit 2 is devoted to steady flow calculation and unit 3 is used for the unsteady flow calculation. The software was especially developed for simulation of automatic control of irrigation canals, and there are several possibilities to model different hydraulic structures, such as gates and weirs. Some of the most common control algorithms, such as PID control, are incorporated in a regulation module. An advantage of SIC software is that it is possible to evaluate any control algorithm written in Matlab® (see Figure 3.11).

The canal PAC-UPC has been modelled in SIC using 6 nodes and 5 reaches (a reach is a part of the canal bounded by nodes). This configuration is depicted in Figure 3.10 . The last node is located in the end of the canal, in the place of weir 4 (see Figure 3.14). The three gates G_1, G_2 and G_3 are placed in nodes *Nd2*, *Nd3* and *Nd5* respectively. The discharge over weir W_4 as a function of the water level is included as a system boundary condition. The validation of the model using experimental data has been fulfilled in (Horváth, 2013).

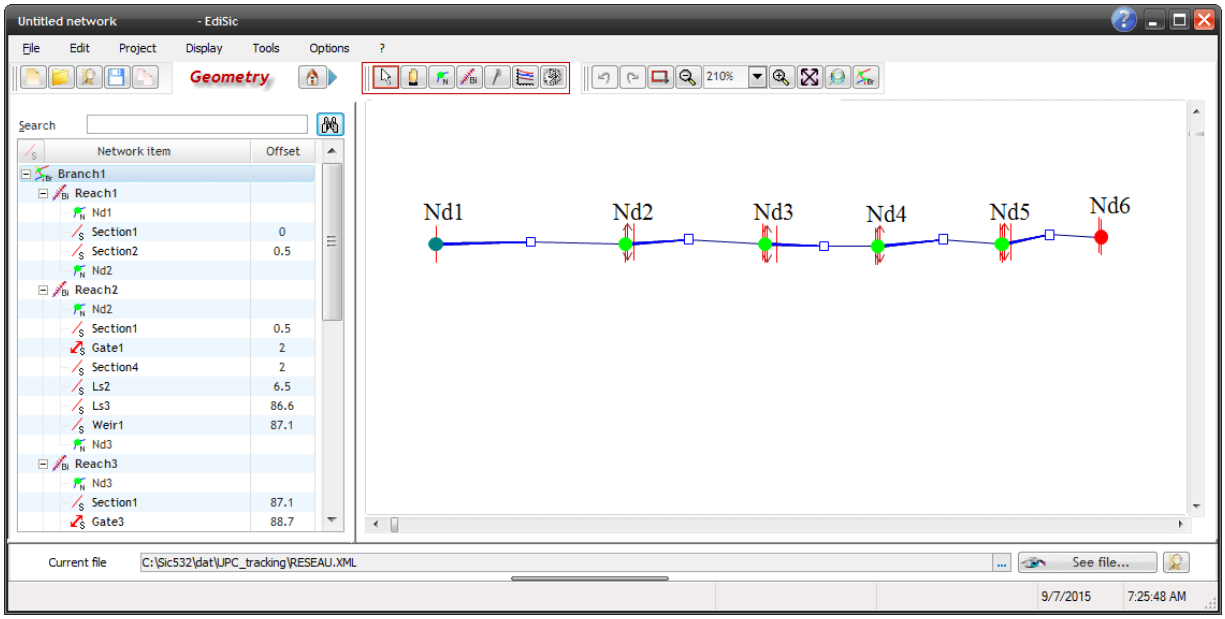

Figure 3.10 SIC window with the canal PAC-UPC geometry.

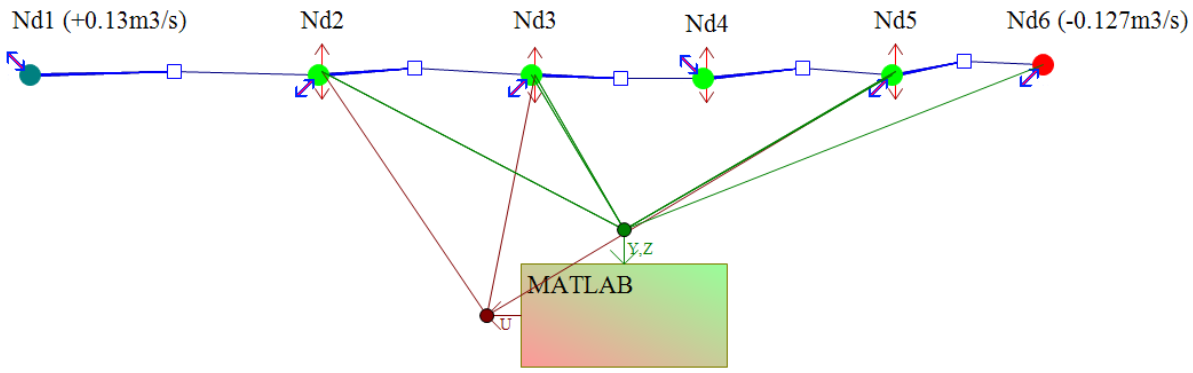

Figure 3.11 The regulation module of SIC software.

3.5.2 Numerical model of the Ebro River Left Bank canal

The Ebro River Left Bank canal, has been modelled in SIC using 19 nodes ($N_1, \ldots, N_{19}$) and 18 reaches as is depicted in Figure 3.12. The water level of 4.5 m is the upstream boundary condition in order to obtain water surface profile of the initial steady state. The discharge over spillway

located at the canal end is included as downstream boundary condition. The model simulation results were validated by comparison with results obtained by (Soler et al., 2014).

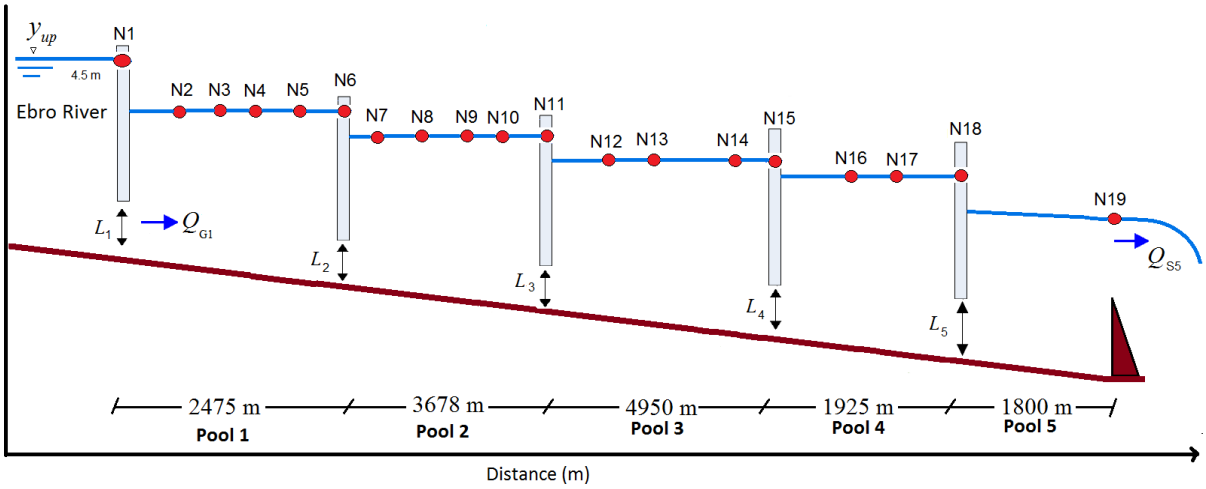

Figure 3.12 Sketch of the ERLB canal for simulation purposes

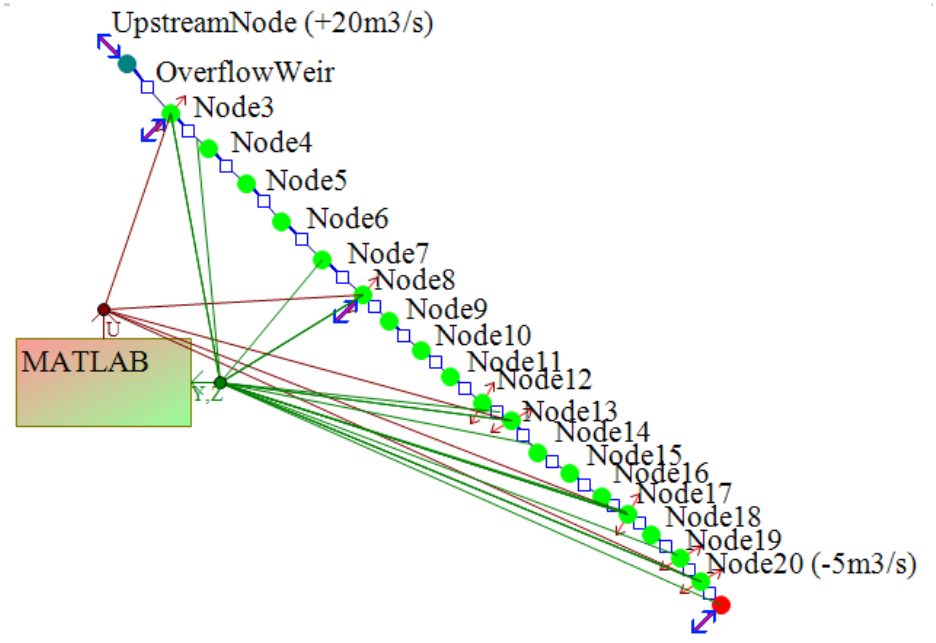

Figure 3.13 Simulation of the ERLB canal including a regulation module in SIC

3.6 Model of canals for control purposes

In canal control, models may be categorized as “flow-flow” and “flow-water level" models according to the control and controlled variable which are chosen to represent inputs and system outputs. The flow-water level mathematical model gives the information about the behaviour of the water level based on the upstream flow that the predictive controller needs in order to predict

the future output of the system. Along the canal there are offtakes to farms and secondary canals. Offtakes are usually treated as disturbances (Weyer, 2003). In a single pool configuration, such as it is depicted in Figure 3.8, a basic mass balance gives:

$$\frac{dV(t)}{dt} = Q_i(t) - Q_{i+1}(t) - Q_{wi}(t) \tag{3.5}$$

where V is the volume of the pool, Q_i is the input discharge, Q_{wi} is the lateral offtake, and Q_{i+1} is the output discharge. A mathematical model that considers the water level y_i as output variable, may be described as function of the discharge along the canal. A simple description is possible assuming that the volume in a pool is proportional to the water level.

Particularly, in downstream water level control, the task of the controller is to move an upstream gate in order to achieve the required downstream water level. One of the difficulties that makes this task a challenging one, it is the time delay, which is the time taken for the water to arrive from upstream to downstream. Therefore the model must consider the time delay explicitly. Subsections 3.5.1 and 3.5.2 present the discrete-time models used in the controller design in this dissertation.

3.6.1 Parametric model of the canal PAC UPC

A transfer function model is used to describe the first case study of this dissertation. The transfer function is expressed as a difference equation based on a multivariable Auto-Regressive with eXogenous input (ARX) model. This black-box model has been obtained by parametric identification by (Sepúlveda, 2008). The model is a relationship between the downstream water level and the upstream flow in the canal pool. The difference equation consider in this model only has constant coefficients. The canal was already introduced in Section 3.2 and its scheme is illustrated in Figure 3.14. In this sketch, y_1, y_2 and y_3 are the controlled downstream water levels; Q_{G1}, Q_{G2} and Q_{G3} are the discharge under gates; Q_{W4} is the weir discharge at the end of the canal. Q_{w1} and Q_{W2} are the lateral weir discharges. The model parameters were obtained using a sampling time of 10 s.

The model for the three pool configuration of the laboratory canal has the following form:

$$\begin{bmatrix} y_1(k) \\ y_2(k) \\ y_3(k) \end{bmatrix} = \begin{bmatrix} 1 - A_{p1}(q) & 0 & 0 \\ 0 & 1 - A_{p2}(q) & 0 \\ 0 & 0 & 1 - A_{p3}(q) \end{bmatrix} \begin{bmatrix} y_1(k-1) \\ y_2(k-1) \\ y_3(k-1) \end{bmatrix} + \begin{bmatrix} B_{11}(q) & B_{12}(q) & 0 \\ 0 & B_{22}(q) & B_{23}(q) \\ 0 & 0 & B_{33}(q) \end{bmatrix} \begin{bmatrix} Q_{G1}(k-1) \\ Q_{G2}(k-1) \\ Q_{G3}(k-1) \end{bmatrix} + \begin{bmatrix} B_{12}(q) & 0 \\ 0 & B_{23}(q) \\ 0 & 0 \end{bmatrix} \begin{bmatrix} Q_{w1}(k-1) \\ Q_{w2}(k-1) \end{bmatrix} \tag{3.6}$$

where q is the shift operator: $qf(k) = f(k+1),\ q^{-1}f(k) = f(k-1)$

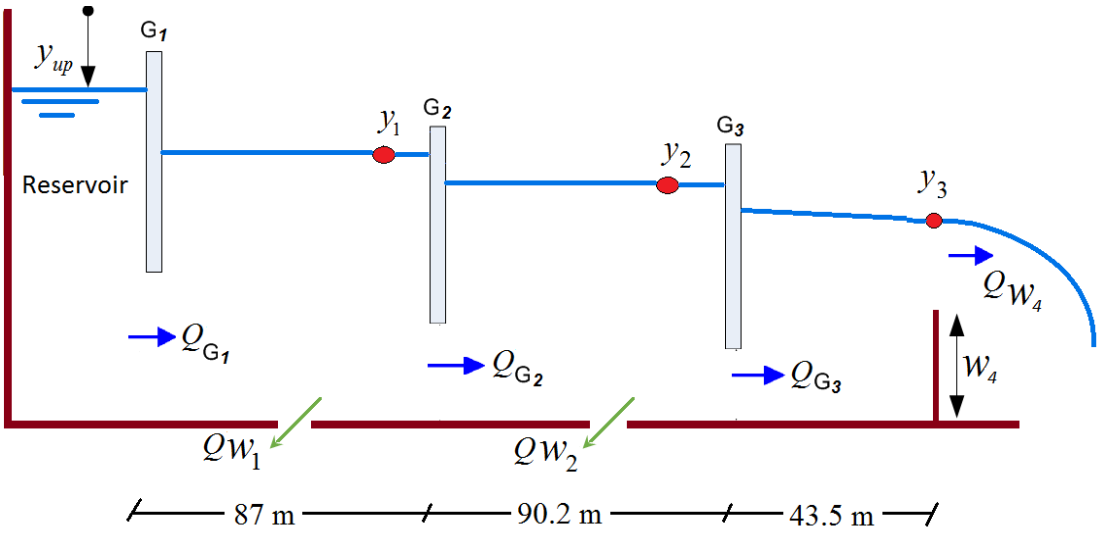

Figure 3.14 Scheme of the Canal PAC

The ARX model for the first pool is

$$A_{p1}(z)y_1(k) = B_{11}Q_{G1}(k-1) + B_{21}(Q_{G2}(k-1) + Q_{w1}(k-1)) \tag{3.7}$$

where

$$A_{p1}(z) = 1 - 0.6918z^{-1} + 0.091z^{-2} + 0.07062z^{-3} + 0.1638z^{-4} + 0.2801z^{-5} + 0.213z^{-6}$$

$$B_{11} = z^{-3} - 0.2895z^{-4}$$

$$B_{12} = -1.154z^{-1} + 0.4729z^{-2} - 0.0675z^{-3} + 0.4496z^{-4} - 0.4899z^{-5}$$

The ARX model for the second pool is

$$A_{p2}(z)y_2(k) = B_{22}Q_{G2}(k) + B_{23}(Q_{G3}(k) + Q_{w1}(k-1)) \tag{3.8}$$

where

$$A_{p2}(z) = 1 - 0.0.4315z^{-1} - 0.1178z^{-2} - 0.0393z^{-3} + 0.03022z^{-4} - 0.1962z^{-5} + 0.05333z^{-6} - 0.3033z^{-7} - 0.3838z^{-8}$$

$$B_{22} = 0.1644z^{-4}$$

$$B_{23} = -1.994z^{-1} + 0.4728z^{-2} - 0.1484z^{-3} + 0.6077z^{-4} - 0.4835z^{-5}$$

And the ARX model for the third pool is

$$A_{p3}(z)y_3(k) = B_{33}Q_{G3}(k-1) \tag{3.9}$$

where

$$A_{p3}(z) = 1 - 0.6495z^{-1} - 0.2344z^{-2} + 0.142z^{-3} - 0.3175z^{-4} - 0.2122z^{-5}$$

$$B_{13} = 0.1422z^{-2} - 0.9872z^{-3}$$

There is a need to convert the calculated discharge into gate opening, since the control variable is discharge and the actuators are check gates. This problem is addressed in (Litrico et al., 2008) and (Sepúlveda, 2008). The gate openings are calculated using the desired discharge, the water level measurements and the inverse non-linear gate equation (Ferro & Ansar, 2001). If the gate opening is physically unfeasible, for instance it is higher that the canal bank, the maximum allowed gate opening is fixed in the actuator.

The validation of the ARX model using experimental data have been fulfilled by (Sepúlveda, 2008). Meanwhile, Figure 3.15 and Figure 3.16 show the numerical results of the response of the ARX models in comparison with the response of SV model simulated by the SIC software. The ARX model step responses were simulated by Simulink® with the same data input. The validation in the time-domain is illustrated in Figure 3.15 and Figure 3.16, the test was performed producing a step discharge (dotted line) in the upstream gate, while keeping the downstream discharge constant. The system output are the water levels (solid lines). The test results in Figure 3.15 are related to the first pool of the canal PAC-UPC only, and the results show that the step response for both positive change (left) and negative input discharge are quite similar for the ARX model in comparison with the SV model. In order to quantify the similitude of step responses in every canal pool, the square of the correlation coefficients are $R_{c1}^2 = 0.9998$ for pool 1, $R_{c2}^2 = 0.9996$ for pool 2 and $R_{c3}^2 = 0.961$ for pool 3.

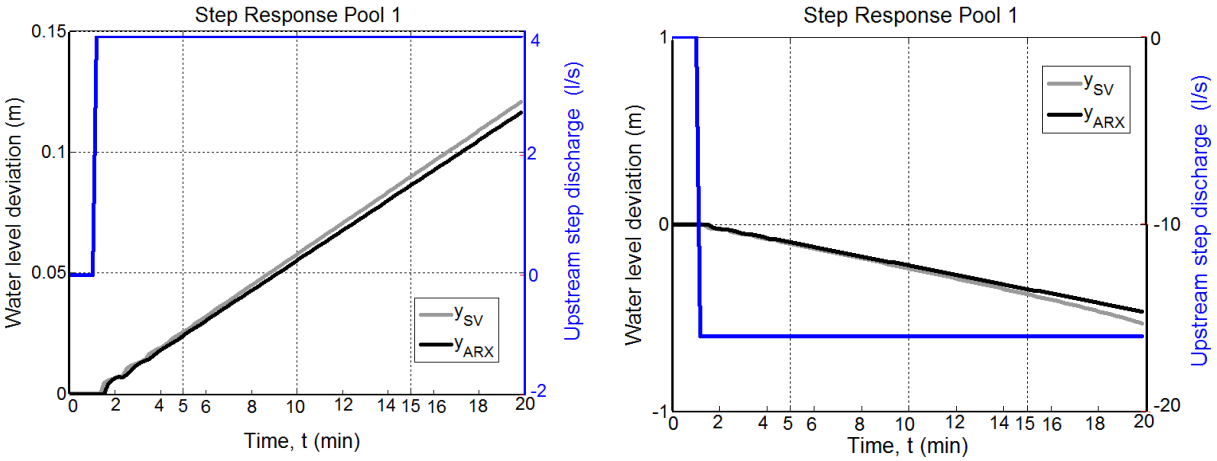

Figure 3.15 Step responses of the ARX model of pool 1.

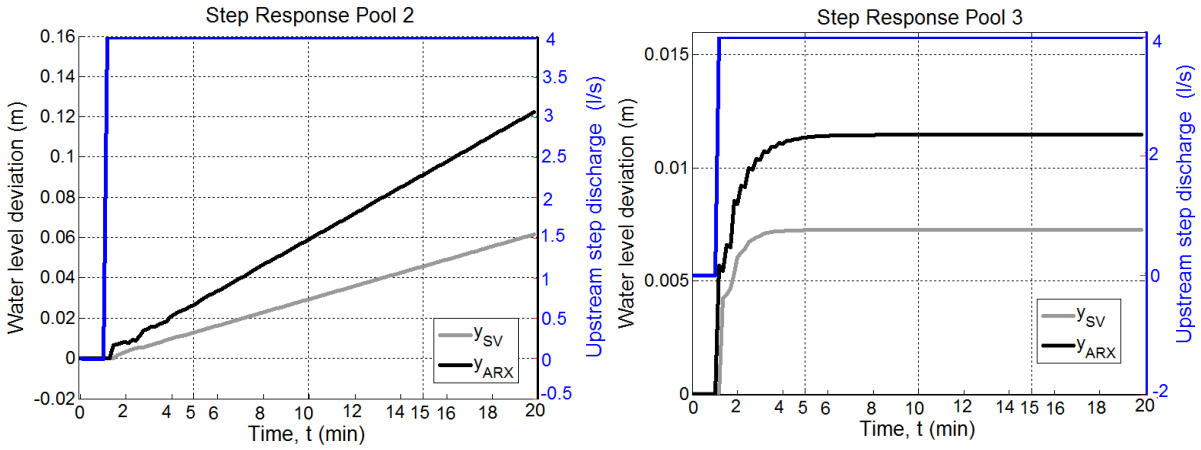

Figure 3.16 Step responses of the ARX models of pool 2 and 3.

Another way to validate the model is considering the frequency domain. For instance, a comparison between the SV model and the ARX model for the first pool is depicted in Figure 3.17. Results indicate that the Bode magnitude and phase plots for both models are almost equal in the low frequency area and the first resonance peak is located in the same frequency in both models. A validation in frequency domain for the rest of the canal pools is illustrated in (Sepúlveda, 2008).

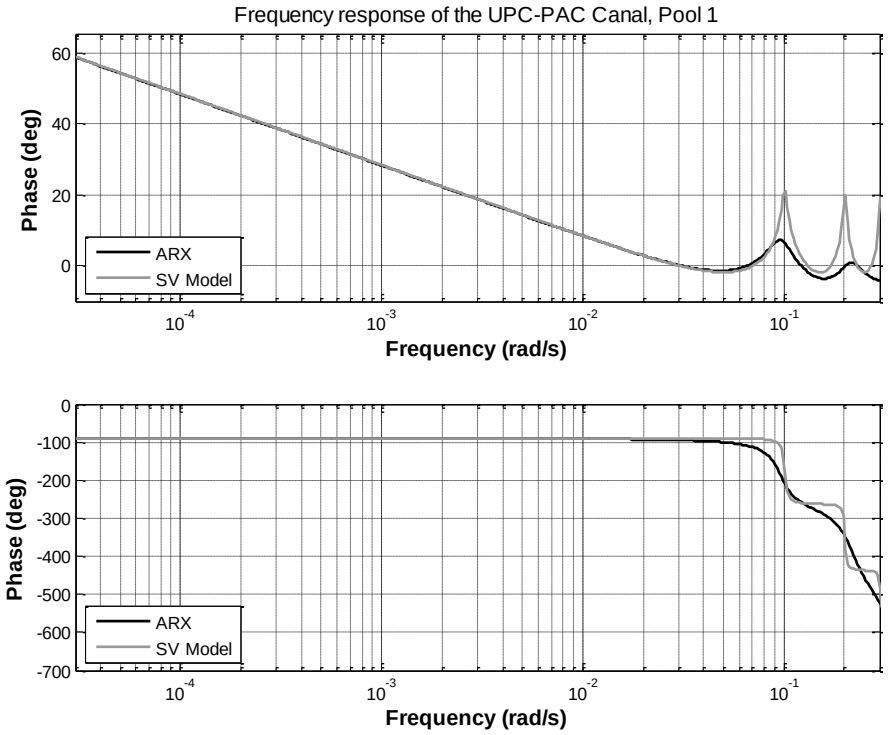

Figure 3.17 . Bode plot diagrams of SV model and ARX model for Pool1

3.6.2 State-space model of the canal PAC UPC

In order to get a model for the whole canal, the linear model of each pool may be transformed into a state-space model described by

$$x_{m_i}(k+1) = A_{m_i}x_{m_i}(k) + B_{m_i}u_i(k) + B_d w_i(k) \tag{3.10}$$

$$y_i(k) = C_{m_i}x_{m_i}(k) \tag{3.11}$$

where $x_{m_i}(k+1)$ is the *n*-dimensional state vector of the *i-th* pool containing the water levels and the discharges under gates in previous sampling times, *u(k)* is the control variable containing the discharge under gate, w_i is the input disturbance, y_i is the controlled variable (water level), A_{m_i}, B_{m_i}, and C_{m_i} are matrices of proper dimension.

The model may be stated to use system input and output variables as its state variables. The space-state variable for the first pool $x_{m1}(k)$, for instance, considers the downstream discharge Q_{G2} and Q_{w1} as the measurable disturbances for a decentralized control scheme. In this way, based on the ARX model, the state-space variable for the first pool may be written as follows:

$$x_{m1}(k) = [y_1(k)\, y_1(k-1)\, y_1(k-2) \ldots\ y_1(k-5)\ \ u_1(k-1)\ \ u_1(k-2)\ \ u_1(k-3)]^T$$

where $u_1(k) = Q_{G1}(k)\ \ [\frac{m^3}{s}]$, $n_1 = 9$, $A_{m_1} \in \Re^{n_1 x n_1}$, $B_{m_1} \in \Re^{n_1 x 1}$, $C_{m_1} \in \Re^{1 x n_1}$

$$A_{m_1} = \begin{bmatrix} A_{11} & A_{12} & A_{13} & A_{14} & A_{15} & A_{16} & A_{17} & A_{18} & A_{19} \\ 1 & 0 & 0 & 0 & 0 & 0 & 0 & 0 & 0 \\ 0 & 1 & 0 & 0 & 0 & 0 & 0 & 0 & 0 \\ 0 & 0 & 1 & 0 & 0 & 0 & 0 & 0 & 0 \\ 0 & 0 & 0 & 1 & 0 & 0 & 0 & 0 & 0 \\ 0 & 0 & 0 & 0 & 1 & 0 & 0 & 0 & 0 \\ 0 & 0 & 0 & 0 & 0 & 0 & 0 & 0 & 0 \\ 0 & 0 & 0 & 0 & 0 & 0 & 1 & 0 & 0 \\ 0 & 0 & 0 & 0 & 0 & 0 & 0 & 1 & 0 \end{bmatrix} \tag{3.12}$$

$$B_{m_1} = [0 \quad 0 \quad 0 \quad 0 \quad 0 \quad 0 \quad 1 \quad 0 \quad 0]^T$$

$$C_{m_1} = [1 \quad 0 \quad 0 \quad 0 \quad 0 \quad 0 \quad 0 \quad 0 \quad 0]$$

where *A_{11}=0.6819, A_{12}=-0.091, A_{13}=0.07, A_{14}=-0.1638, A_{15}=0.2801, A_{16}=0.213, A_{17}=0, A_{18}=1, A_{19}=-0.289*

For the second pool, the space-state variable $x_{m2}(k)$, considers the downstream discharge Q_{G3} and Q_{w2} as the measurable disturbances. Meanwhile, based on the ARX model, the state-space variable may be written as follows:

$$x_{m2}(k) = [y_2(k)\ \ y_2(k-1) \ldots\ y_2(k-7)\, u_2(k-1)\ \ u_2(k-2)\ \ u_2(k-3)]^T$$

Other parameters of the state-space model for the second pool are:

$$u_2(k) = Q_{G2}(k) \ [\frac{m^3}{s}],\ n_2 = 10,\ A_{m_2} \in \Re^{n_2 x n_2},\quad B_{m_2} \in \Re^{n_2 x 1},\ C_{m_2} \in \Re^{1 x n_2}$$

where

$$A_{m2=}\begin{bmatrix} A_{11} & A_{12} & A_{13} & A_{14} & A_{15} & A_{16} & A_{17} & A_{18} & A_{19} & A_{1A} & A_{1B} \\ 1 & 0 & 0 & 0 & 0 & 0 & 0 & 0 & 0 & 0 & 0 \\ 0 & 1 & 0 & 0 & 0 & 0 & 0 & 0 & 0 & 0 & 0 \\ 0 & 0 & 1 & 0 & 0 & 0 & 0 & 0 & 0 & 0 & 0 \\ 0 & 0 & 0 & 1 & 0 & 0 & 0 & 0 & 0 & 0 & 0 \\ 0 & 0 & 0 & 0 & 1 & 0 & 0 & 0 & 0 & 0 & 0 \\ 0 & 0 & 0 & 0 & 0 & 1 & 0 & 0 & 0 & 0 & 0 \\ 0 & 0 & 0 & 0 & 0 & 0 & 1 & 0 & 0 & 0 & 0 \\ 0 & 0 & 0 & 0 & 0 & 0 & 0 & 0 & 0 & 0 & 0 \\ 0 & 0 & 0 & 0 & 0 & 0 & 0 & 0 & 1 & 0 & 0 \\ 0 & 0 & 0 & 0 & 0 & 0 & 0 & 0 & 0 & 1 & 0 \end{bmatrix}$$

with *A_{11}=0.04315, A_{12}=0.1178, A_{13}=0.0393, A_{14}=-0.030, A_{15}=0.1962, A_{16}=-0.053, A_{17}=0.3033, A_{18}=0.3838, A_{19}=0, A_{1A}=0, A_{1B}=1.644*

and

$$B_{m_2} = [0 \quad 0 \quad 0 \quad 0 \quad 0 \quad 0 \quad 0 \quad 0 \quad 1 \quad 0 \quad 0]^T$$

$$C_{m_2} = [1 \quad 0 \quad 0 \quad 0 \quad 0 \quad 0 \quad 0 \quad 0 \quad 0 \quad 0 \quad 0]$$

Finally, for the third pool, based on the ARX model, the state-space variable may be written as follows:

$$x_{m3}(k) = [y_3(k)\ y_3(k-1)\ y_3(k-2)\ y_3(k-3)\ y_3(k-4)\ u_3(k-1)\ u_3(k-2)\ u_3(k-3)]^T$$

Other parameters of the state-space model for the third pool are:

$$u_3(k) = Q_{G3}(k) \ [\frac{m^3}{s}],\ n_3 = 7,\ A_{m_3} \in \Re^{n_3 x n_3},\quad B_{m_3} \in \Re^{n_3 x 1},\ C_{m_3} \in \Re^{1 x n_3}$$

where

$$A_{m3} = \begin{bmatrix} 0.6495 & 0.2344 & -0.142 & 0.3175 & -0.2112 & 1.422 & -0.9872 \\ 1 & 0 & 0 & 0 & 0 & 0 & 0 \\ 0 & 1 & 0 & 0 & 0 & 0 & 0 \\ 0 & 0 & 1 & 0 & 0 & 0 & 0 \\ 0 & 0 & 0 & 1 & 0 & 0 & 0 \\ 0 & 0 & 0 & 0 & 0 & 0 & 0 \\ 0 & 0 & 0 & 0 & 0 & 1 & 0 \end{bmatrix}$$

$$B_{m_3} = [0 \quad 0 \quad 0 \quad 0 \quad 0 \quad 1 \quad 0\ ]^T$$

$$C_{m_3} = [1 \quad 0 \quad 0 \quad 0 \quad 0 \quad 0 \quad 0\ ]$$

3.6.3 IDZ model of the Ebro River Left Bank canal

The model used in this dissertation to describe the second case of study is based on the Integrator Delay Zero (IDZ) model proposed by (Litrico & Fromion, 2004b). The integrator delay zero (IDZ) model is an expansion of the ID model that incorporates a zero in the transfer function. The integrator delay (ID) model assumes that the canal consists of two parts: a downstream part (characterized by backwater) and an upstream part (characterized by uniform flow). In the part affected by backwater, a simple reservoir model is used, and the parts with uniform flow are approximated by the kinematic wave model. The two models are connected in the ID model. Meanwhile, the IDZ model is able to represent the canal behavior in low and high frequencies; the integrator delay accounts for low frequencies, whereas the zero represents the direct influence of the discharge on the water level in high frequencies and the delay is related to the system delay.

The transfer function of the IDZ model describes the ratio of the downstream water level and the upstream discharge under gate in the Laplace domain**.** In a single pool configuration (see Figure 3.8), the IDZ model is written as follows:

$$G_{IDZ_i}(s) = \frac{y_i(s)}{Q_{Gi}(s)} = \frac{K_{1_i}s + 1}{A_{e_i}s}\,\mathrm{e}^{-\tau_i s} \tag{3.13}$$

where K_{1i} is a parameter calculated from the canal properties, τ_i is the delay time and A_{e_i} is the integrator/backwater approximation. The downstream water level considering the downstream discharge may be expressed as (Litrico & Fromion, 2004b):

$$Y(s) = \frac{K_i s + 1}{A_i s}\,e^{-T_i}Q_i(s) - \frac{K_2 s + 1}{A_i s}\,Q_{i+1}(\mathrm{s}) \tag{3.14}$$

The Ebro River Left Bank canal was already introduced in Section 3.3, and a scheme of this canal is illustrated in Figure 3.18.

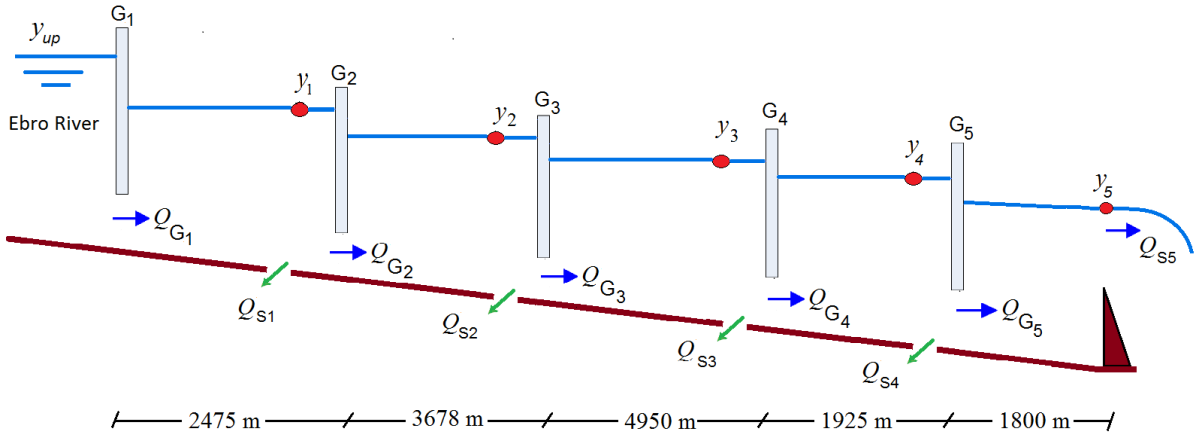

Figure 3.18 Scheme of the ERLB canal

The model parameters of each pool for different operating points (Q_{op}) are given in Table 3-3.

Pool	Q_{op} [m³/s]	K_i	A_i [m²]	T_i [s]	K_2
1	15	353.50	18959.07	433.55	513.92
2	15	210.03	26212.79	635.32	741.62
3	15	451.98	49153.04	880.94	989.85
4	15	103.63	20623.44	380.74	462.19
5	15	213.47	5614.43	243.55	299.70
1	2	16.38	20460.94	501.74	522.22
2	2	0.08	29041.42	747.75	778.35
3	2	3.13	53151.90	993.58	1023.32
4	2	0.00	21467.16	425.71	439.80
5	2	39.11	6426.29	329.30	355.24
1	8.5	288.39	19877.15	466.48	530.02
2	8.5	101.91	27788.81	690.26	781.22
3	8.5	305.40	51581.19	937.40	1028.76
4	8.5	28.02	21181.13	402.60	456.21
5	8.5	203.80	5849.50	282.11	338.49
1	19	360.60	18476.69	415.08	500.08
2	19	213.99	25519.02	607.51	748.05
3	19	481.55	47881.54	847.64	958.51
4	19	142.66	20212.77	368.15	460.86
5	19	216.83	5763.97	223.13	274.36

Table 3-3 parameters of the IDZ models of ERLB canal

The discretized model with five downstream controlled water levels has the following form:

$$\begin{bmatrix} y_1(k) \\ y_2(k) \\ y_3(k) \\ y_4(k) \\ y_5(k) \end{bmatrix} = \begin{bmatrix} 1-A_{p1}(q) & 0 & 0 & 0 & 0 \\ 0 & 1-A_{p2}(q) & 0 & 0 & 0 \\ 0 & 0 & 1-A_{p3}(q) & 0 & 0 \\ 0 & 0 & 0 & 1-A_{p4}(q) & 0 \\ 0 & 0 & 0 & 0 & 1-A_{p5}(q) \end{bmatrix} \begin{bmatrix} y_1(k-1) \\ y_2(k-1) \\ y_3(k-1) \\ y_4(k-1) \\ y_5(k-1) \end{bmatrix}$$
$$+ \begin{bmatrix} B_{11}(q) & B_{12}(q) & 0 & 0 & 0 \\ 0 & B_{22}(q) & B_{23}(q) & 0 & 0 \\ 0 & 0 & B_{33}(q) & B_{34}(q) & 0 \\ 0 & 0 & 0 & B_{44}(q) & B_{45}(q) \\ 0 & 0 & 0 & 0 & B_{55}(q) \end{bmatrix} \begin{bmatrix} Q_{G1}(k-1) \\ Q_{G2}(k-1) \\ Q_{G3}(k-1) \\ Q_{G4}(k-1) \\ Q_{G5}(k-1) \end{bmatrix}$$
$$+ \begin{bmatrix} B_{12}(q) & 0 & 0 & 0 \\ 0 & B_{23}(q) & 0 & 0 \\ 0 & 0 & B_{34}(q) & 0 \\ 0 & 0 & 0 & B_{45}(q) \\ 0 & 0 & 0 & 0 \end{bmatrix} \begin{bmatrix} Q_{S1}(k-1) \\ Q_{S2}(k-1) \\ Q_{S3}(k-1) \\ Q_{S4}(k-1) \end{bmatrix}$$

In order to validate the models in time-domain, the open-loop discharge step response of each pool has been tested. The numerical results are shown in Figure 3.19. The tests were performed producing a step discharge (dotted line in Figure 3.19) in the upstream gate, while keeping the downstream discharge constant. The system output are the water levels (solid lines). The step response of the IDZ models is compared numerically with the response of SV model obtained by the SIC software. The IDZ model step responses were simulated by Simulink® (see Figure 3.20) with the same data input generated by SIC. In order to quantify the similitude of step responses in every canal pool, the square of the correlation coefficients are: $R_{c1}^2 = 0.9889$ for pool-1 model, $R_{c2}^2 = 0.9986$ for pool 2, $R_{c3}^2 = 0.9964$ for pool 3, $R_{c4}^2 = 0.9964$ for pool 4 and $R_{c5}^2 = 0.9444$ for pool 5 model.

3.7 Final remarks

As a summary, this chapter has described the two case studies that will be further used to validate the control developments. Numerical schemes solving the SV equations have been presented for simulation purposes. And linearized models have been derived, which will be used for the control design.

The following chapter is devoted to illustrate some common canal operations involving abrupt changes in the operating conditions. Abrupt changes are tested using the SV models presented in this Chapter 3. It is expected that the numerical simulation results highlight some problems that

arise when the canal operations are not managed properly, and motivate the need for automatic control.

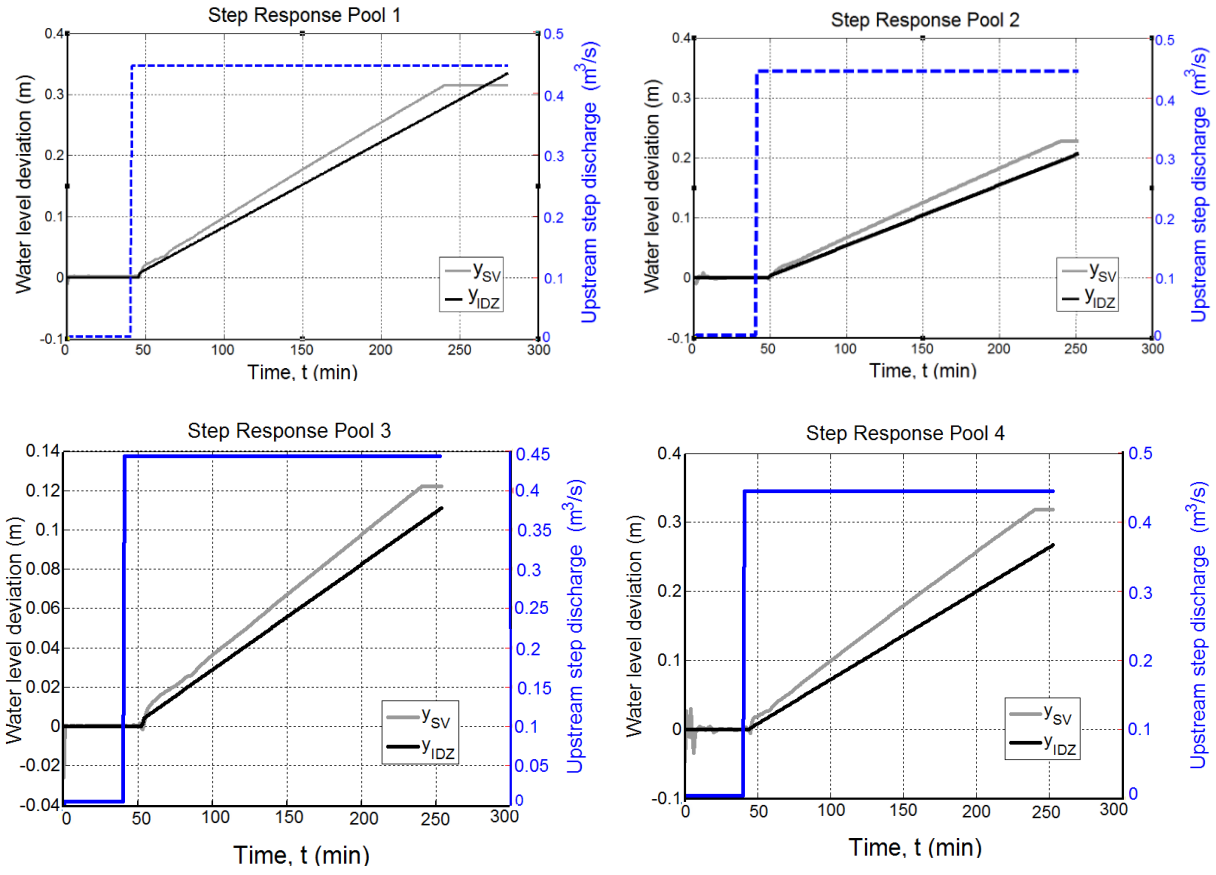

Figure 3.19 Comparison of the IDZ models and the 1D-Saint-Venant equations

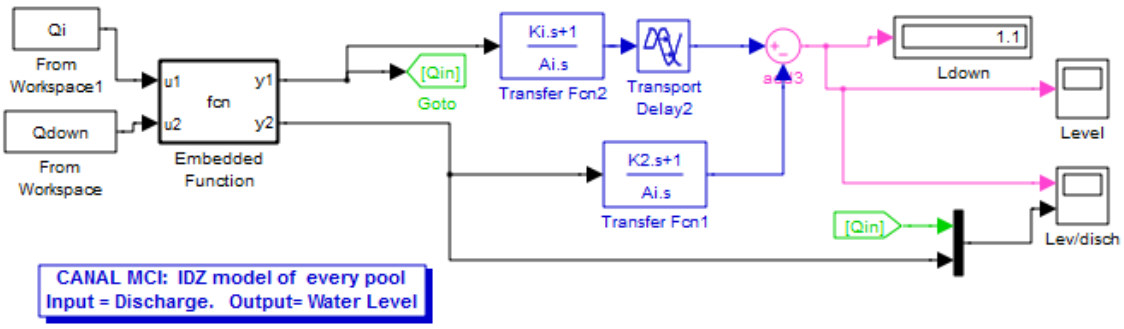

Figure 3.20 Simulink block diagram for IDZ model validation

Chapter 4

Management practices involving canal closure and opening operations

4.1 Introduction

Modern management policies for irrigation canals aim to delivery water on demand, thus allowing the users to handle their irrigation needs with flexibility instead of receiving water under rigid scheduling. This means to ensure adequately water delivery at the turnouts with the actual requirements, taking into account timing and quantity of the particular crops served (Goussard, 1993). However, there are situations in which abrupt changes in the operating conditions must be managed. Typical examples are the canal closure during non-demand periods (e.g. to save water for other purposes as energy production), or the emergency closure of an open canal as a result of pollutants flowing along the supplier river, or when elements of the canal, such as canal lining or check structures, require corrective or preventive maintenance. Restarting a closed canal to its normal operating conditions is another problem in which abrupt changes in the operating conditions must be considered. This chapter is focused mainly on the closure operation problem, but opening involves similar issues.

Canal closure is a required operation in virtually all canal facilities. Typically, when irrigation season ends, canals are closed and emptied to clean sediments, repair structural damages and maintain electromechanical elements as gates, motors, cables and communication devices, among others (see Figure 4.1). However, there are situations in which canals must be closed but not

emptied, namely maintaining a prescribed water volume despite the zero flow condition. This dissertation refers to this type of canal closure.

Figure 4.1 empty canal (from http://www.gauthiere-engineering.com)

The main motivation for a canal closure operation is to save water, which can be used for several purposes such as drinking water resources or energy production. Turning the canal off (canal closure) means setting zero flow conditions by gradually closing the gates along the canal in a smooth way, while maintaining specific water levels between maximum and minimum critical values in order to avoid overtopping, drying up or canal fracture by sub-pressure effects, which could involve both economic and environmental issues.

The objective of this chapter is to discuss the main motivation and issues related to canal closure. It describes several management practices involving abrupt changes in operating conditions of canals and some of the related common issues encountered in water conveyance systems. The discussion is also illustrated with simulation results of closure operations using local manual control.

4.2 Management practices involving closing and opening operations

4.2.1 Night closure to save water

Night closure to save water can be used in both irrigation canals and canals used for hydraulic power generation. In irrigation canals, there are cases in which farmers do not irrigate over the night in order to save water, and gates are consequently closed reach zero flow through the canal. Namely, these canals operate at maximum discharge at daytime only. Meanwhile, in canals used for hydraulic power generation, the power output in the hydro-plant depends on the volume of water travelling through the canal. In this way, when night falls and when the power consumption decreases considerably, the gates may be closed in order to save water. In these canals, an opening operation is fulfilled next day early in the morning to produce electricity again.

4.2.2 Night closure in rotational delivery systems

When farmers practice a rotational delivery system, night irrigation is done only during times of peak crop water demand (some reasons to do this are personal safety, cold and darkness). So, as a result water does not flow continuously, and a large proportion is saved in medium-sized canal networks (Ghumman et al., 2009). A typical strategy developed in a tree-shaped net of open canals is day and night opening of main canal but night closure of secondary canals (see the layout depicted in Figure 4.2).

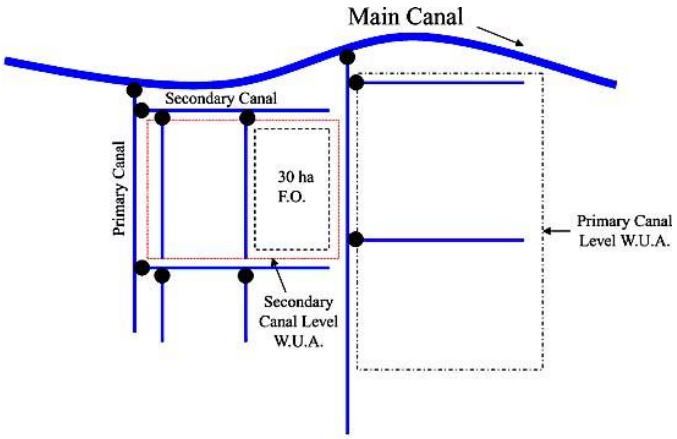

Figure 4.2 A typical irrigation scheme (from (Van den Bosch et al., 1992)).

4.2.3 Canal closure on weekends

When a canal decreases the irrigation on weekends, it is advisable to close it in order to reduce operational labor and energy and subsequently save water, money and manpower.

4.2.4 Emergency plan

Another motivation for closing a canal is the danger of contamination of water due to a pollutant flowing in the supplier river. Once any pollutant flowing down the river is detected in the upstream main canal, some authorities decide to call for an emergency plan in order to avoid pollutants travel downstream the canal. Typically, in those situations a warning signal is sent to the canal management staff who must then initiate the emergency procedure. The procedure starts closing the upstream pool in order to isolate the overall system. Subsequently, the gates can be closed as quickly as the water delivery system allows, while maintaining the water level between prescribed allowed maximum and minimum operating levels. The aim is to prevent damages in the canal lining (Soler et al., 2014).

The polluted water takes time to travel along the canal pools, and this time is a function of the geometry and the canal flow. For instance, in the Ebro River left bank canal in Spain, the pollutant

takes approximately 7.3 h traveling 40 km downstream from a gauging station to the canal inlet. The gauging station is in charge to detect whether any pollutant is flowing downriver and emits an emergency warning. Namely, the 15 km-long canal system has a period of time of 7.3 h in which it has to be isolated (Soler et al., 2014). Therefore, the challenge for the emergency plan is to design a strategy able to close the canal as quickly as possible considering physical characteristics that impose some constraints to the control possibilities. Some characteristics are maximum capacity, amount of depth fluctuations and amount of storage, among others.

4.2.5 On demand partial closure

Canals must irrigate agricultural crops in some periods of short rainfall, however in specific periods of time, irrigation is not required, although canal must remain filled -with less amount of flow but filled- to supply freshwater for nearby population. That means that the canal acts as source or reservoir of potable water for human consumption.

On demand operation, a lot of farmers choose not irrigate their crops overnight, namely, the canal management operators need to slow down the discharge in order to save water. This operation involves to change a large percentage of the operating point but without driving the canal to zero flow.

4.2.6 Opening operation

Opening a previously closed canal means restoring a non-zero operating flow without altering the prescribed water levels. The goal is to move gradually the gates from zero flow condition to a nominal flow value. The upstream gates movement will generate naturally a waving effect in the canal, however there are two main objectives to ensure during the opening operation. The first objective is to maintain specific water levels between maximum and minimum critical values in order to avoid problems, such as, canal overtopping. The second objective is to execute the opening operation as quick as possible. In some canals, finally all the gates will be completely open.

Consequently, restarting the canal on (canal opening) requires a progressive and well planned set of actions to achieve a prescribed flow condition maintaining water levels between the permitted values under normal operating conditions. The opening operation must be done as quickly as possible but considering that to lead the system to a desired steady state, some variables such as water levels, gate opening, and flow at the end of the canal will have a transient behavior until the water demand is reached. Since restarting the canal to the previously steady state implies to supply an extra water volume to compensate water losses during the time that the canal has been closed, the opening operation is expected to be longer than the closing operation.

4.3 Drawbacks associated to closure operation

An operating point change within a wide range, as in closure operations, must not imply water level changes in the same proportion. Whatever the reason to change drastically the operating point in the system, the experience indicates to leave enough canal freeboard to avoid some hydraulic issues like cracking in the canal lining and overtopping. For instance, in the Ebro river left bank canal, which has 3 m of canal depth, it is recommended around 1 m-freeboard in several checkpoints in order to protect the canal lining (Soler et al., 2014).

4.3.1 Cracking in the canal lining

A common problem related to canal closure is the transient wave phenomenon originated when the gates are suddenly closed along the canal, which usually leads to the risk of exceeding the minimum/maximum safety levels required on the canal. Particularly, if the water level decreases below the minimum safety level, it can lead to structural damage or cracking (see Figure 4.3). Cracking in the canal lining arises by reason of the pressure that the concrete canal lining are subject to the effect of outside water by sub-pressure effects. Namely, cracking occurs when the equilibrium between the subsurface water pressure and that of water in the canal is broken, and the pressure difference generates over tension on the canal lining. The cracked concrete canal lining may result in a significant loss of water and money. Leakage often starts on a small scale, but the moment when water finds a way through a canal embankment, a hole will develop through which water will leak. Serious leakage can be avoided when the canal system is inspected frequently and when repairs are carried out immediately. The longer a hole or crack is left, the larger it will become (Van den Bosch et al., 1992).

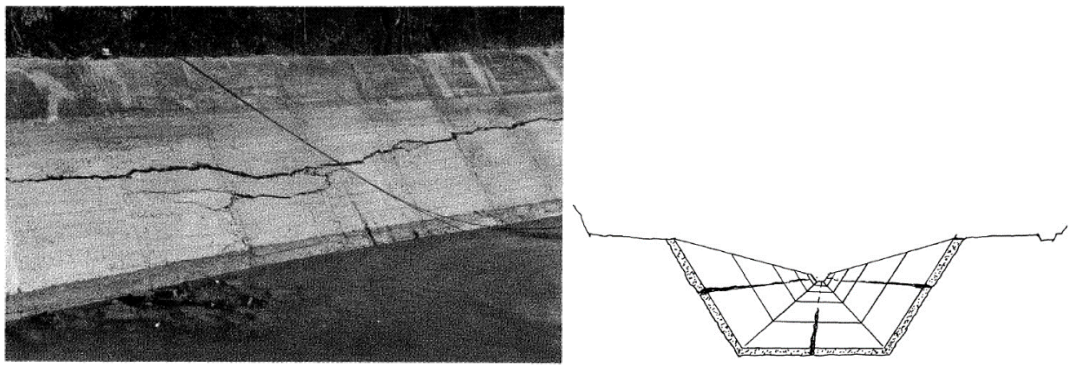

Figure 4.3 Photo and schematic of longitudinal cracking (taken from (Moreno, 1986))

4.3.2 Overtopping

Another important issue to bear in mind in both closure and opening operations is the transient wave phenomena originated when the gates are suddenly closed/open along the canal. The wave travels in downstream direction and it arrives at the downstream end and bounces back iteratively. Exceeding the maximum safety level may lead to the water exceeds the top of canal bank with negative consequences (Figure 4.4). Overtopping is a problem because it causes erosion of the canal banks and may lead to serious breaches (Van den Bosch et al., 1992). Overtopping of a canal section is induced by an exaggerated discharge in a particular section exceeding the actual canal capacity. Moreover, canal banks that are frequently overtopped are very probably eroded and lowered, and thus the actual capacity will be less than the original one for which the canal has been designed.

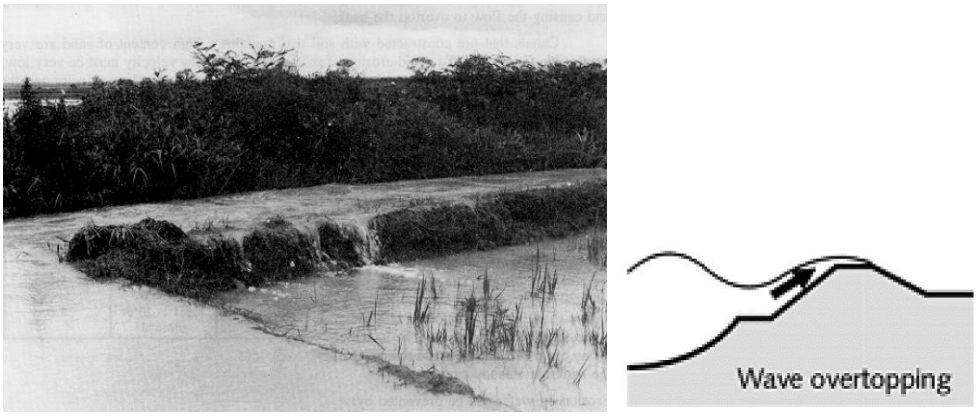

Figure 4.4 Photo and schematic of overtopping (from (Van den Bosch et al., 1992))

4.4 Feasibility of closure operation

Depending on the reason to closing a canal, the feasibility of closure operation must be analyzed from two points of view mainly. First, when the closure operation has the objective to save water. Secondly, when the closure operation has the objective to isolating a canal in the presence of pollutant flowing in the supplier river.

Feasibility of closure operation to save water

The feasibility of closure operation with the objective to save water, considers night-closure, closure on weekends and night-closure in rotational delivery systems. Particularly, canals can be closed at nights provided that the closure operation is fast enough to make it feasible. To determine feasibility of closure, some aspects have to be assessed, such as time taken to achieve a new steady

state, and time required to meet full crop water demand in the service (Ghumman et al., 2009). These aspects are analyzed below.

- *Time taken to achieve steady state hydraulic conditions after the canal is opened in the morning*. Canal physical characteristics determine both the time taken to achieve steady state hydraulic conditions after the canal is opened in the morning and the minimum time required to perform the closure operation. A case study of feasibility of night closure of the Upper Swat-Pehur canal (USC) system in Pakistan is found in (Ghumman et al., 2009). Based on hydrodynamic simulation models, the results show that where canal lengths are less than 5 km, there is good potential to make savings. In the particular case of Dagai Distributary (3.2 km long), it attained a steady state within 2 hours of canal opening, and later took 60 min to drain (with discharge 0.16 m^3/s). Namely, mainly values of both time filling and emptying make suitable the night-time closure.

- *Time required to meet full crop water demand in the service area*. Required time to meet full crop water demand in the service during the day due to crop water demand varies through a season. The management of an irrigation system must offer flexible service in order to deliver the required amount of water at an appropriate time to meet the farmers' needs. The goal is deliver optimal water supply at peak demand and reduce the amount at early growth stage of crops (Ghumman et al., 2009).

Feasibility of closure operation due to an emergency plan

The feasibility of closure operation with the objective to isolate the canal in the presence of pollutant flowing in the supplier river is mainly evaluated by the time taken for discharges to go from a baseline to zero in a downstream checkpoint of the canal. This time is evaluated in both closure and opening operations. A detailed study on the closure as a result of pollutant flowing in the supplier river is found in (Soler et al., 2014). In the event of a pollutant discharge, the water users' association have decided to design an emergency plan in order to isolate the system for the protection of the main canal lining. In thus study, the pollutant takes approximately 7.3 h traveling 40 km downstream from a gauging station to the canal inlet in the Ebro River left bank canal. The gauging station is in charge to detect whether any pollutant is flowing downriver and emits an emergency warning. Therefore, the system has the period of time of 7.3h as the maximum value in which system must be isolated.

In summary, the feasibility and usefulness of a closure operation is mainly determined by comparing the time required to achieve the objective (i.e. closing the canal before the pollutant arrival to specific checkpoints) and the minimum time required to perform the closure operation, which relies on the canal geometry, flow conditions and velocity of check structures.

4.5 Manual closure simulation results in the cases of study

The aim of this section is to illustrate, by simulation results, several scenarios of closure operation using local manual control. Simulations are fulfilled in SIC (Simulation of Irrigation Canals) modeling software. In particular, it is expected that some scenarios reveal evidence of the previously discussed problems and motivates the need of automatic control systems. The closure simulations suppose idealized motorized gates, whose velocities can be changed manually. Simulation results include three variables, downstream water levels, discharges under gates and gate openings.

Five scenarios have been designed to check the transient response after closing gates of cases of study under manual local control. Scenarios depending on the gates velocities. The first scenario is devoted to test the downstream water levels closing all gates at the same velocity. In the second scenario, all gates are closed at the same velocity but with a value lower than the first scenario. In the third scenario, gates are closed with different velocities and the velocity of most upstream gate is higher than the rest of the gates. In the fourth scenario, gates are closed with different velocities and the velocity of most upstream gate is lower than the rest of the gates. The fifth scenario simulates a closure operation when only the most upstream gate is closed. Disturbances are not considered in these scenarios.

4.5.1 Manual closure of the canal PAC-UPC

The laboratory canal is a zero-slope rectangular one, having 220 m length, 44 cm width, 1m depth and a Manning's coefficient of 0.016. The maximum affordable inflow is around 150 l/s. The maximum and minimum operating levels recommended for accuracy and safety purposes are 97 cm and 63 cm respectively (Subsection 3.2 contains more information related to characteristics of the canal).

To fulfill simulations, a three pool configuration has been used (Figure 4.5). There is a rectangular weir, W_4 at the end of the canal. In Figure 4.5, L_1, L_2 and L_3 are openings of gates G_1, G_2 and G_3 respectively; y_1, y_2 and y_3 are downstream water surface elevations; y_{up} is the reservoir water level; Q_1, Q_2 and Q_3 are discharges under gates; Q_{W1}, Q_{W2} are lateral offtakes (site of turnouts); and Q_{W4} is the flow-rate through the rectangular weir W_4.

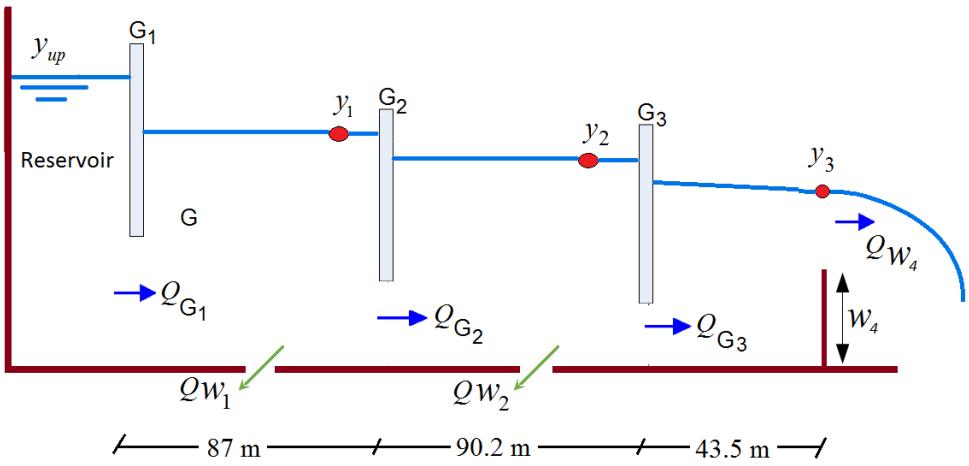

Figure 4.5 Illustration of canal PAC-UPC in three pool configuration

Scenarios

Simulation results include three variables: downstream water levels, discharges under gates and gate openings. The scenarios are the following:

- Scenario 1: Closing all gates at the same velocity with $V_{g1} = V_{g2} = V_{g3} = 3.125$ mm/s
- Scenario 2: Closing all gates at the same velocity with $V_{g1} = V_{g2} = V_{g3} = 1.5$ mm/s
- Scenario 3: Closing all gates with different velocity, $V_{g1} = 3.125$; $V_{g2} = V_{g3} = 1.5$ mm/s
- Scenario 4: Closing all gates with different velocity, $V_{g1} = 1.5$; $V_{g2} = 3.125$; $V_{g3} = 3.125$ mm/s
- Scenario 5: closure of gate G_1 only with velocity $V_{g1} = 1.5$ mm/s. The rest of the gates remain in the same position along the time of simulation.

For each scenario, two operating steady state flows are considered:

- Low flow (52 l/s)
- High flow (121 l/s)

Canal closure at low flow

Figures 4.6 to 4.8 show results for the low flow cases. In Figure 4.6, simulation starts with an operating point around a steady state of 52 l/s, then after 5 seconds all the gates close simultaneously. In the first scenario, all gates closed at 3.125 mm/s in left part of Figure 4.6. Simulation results of Scenario 2 are illustrated in the right part of Figure 4.6 .

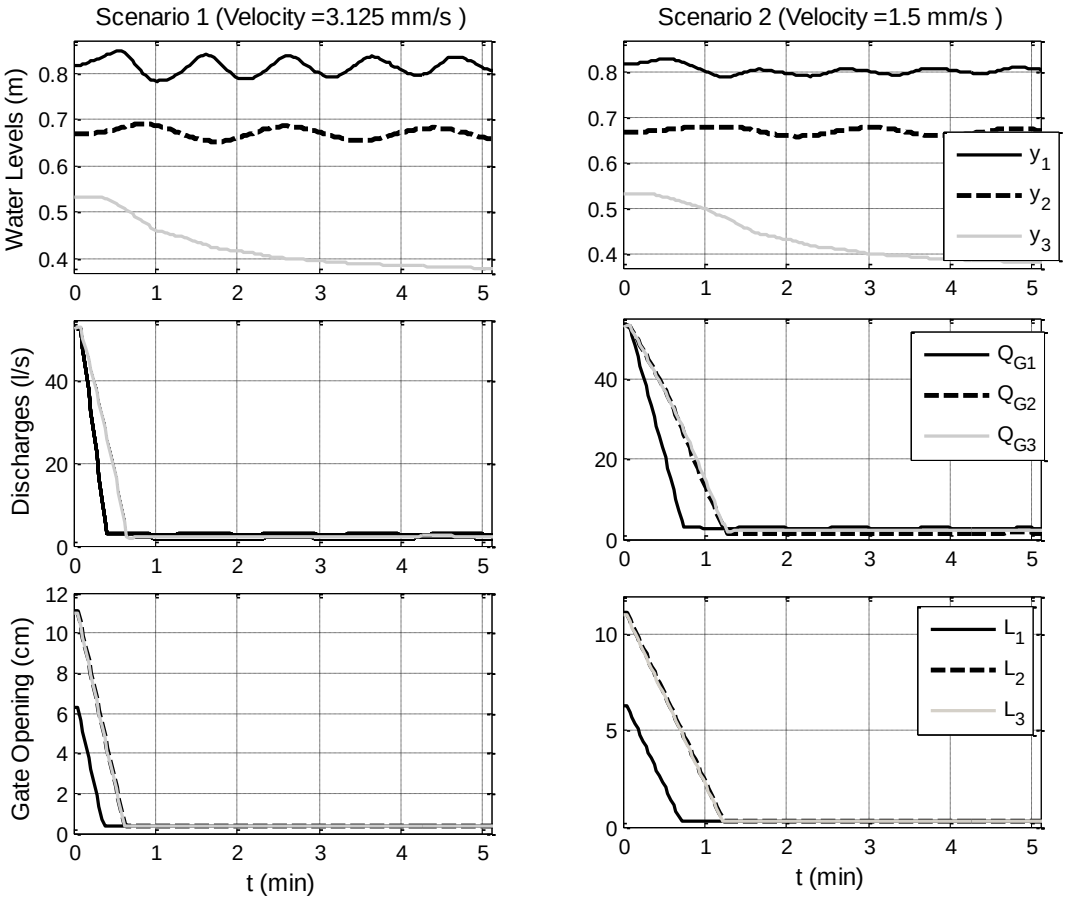

Figure 4.6 Simultaneous closing of all gates with the same velocity at low flow

As it can be noted, starting from a relatively low flow (52 l/s), closing can be done in less than 1.5 minutes maintaining water levels y_1 and y_2 inside the safety band prescribed for this canal. Meanwhile, water level in the third pool decays exponentially as a result of the presence of the weir at the end of the canal. The wave phenomenon still remain for a period of time even after all the gates have been closed. Open loop responses show a relatively low maximum error: 2.71 cm for first pool and 1.9 cm for second pool at 3.125 mm/s and 0.91 cm for the 87 m-long pool and 1 cm for second pool at 1.524 mm/s, it indicates that, water levels in two first pools have less variation closing at 1.524 mm/s than closing at 3.125 mm/s.

Simulation results using different velocities in the closure operation are illustrated in Figure 4.7. In both scenarios, there are no overtopping despite wave phenomenon. However, in the fourth scenario, the velocity of G_1 slower than G_3 and G_2, produces a higher ripple in the transient response of water level y_1.

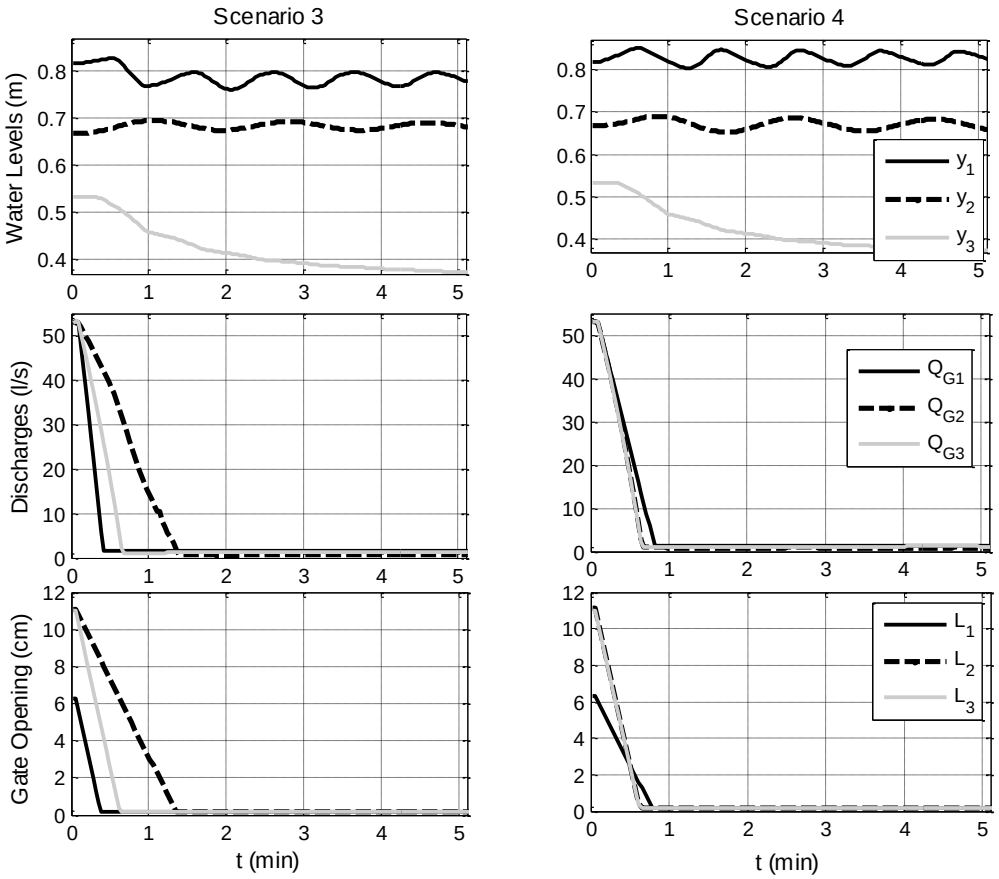

Figure 4.7 Closing scenarios 3 and 4 at low flow (different velocities)

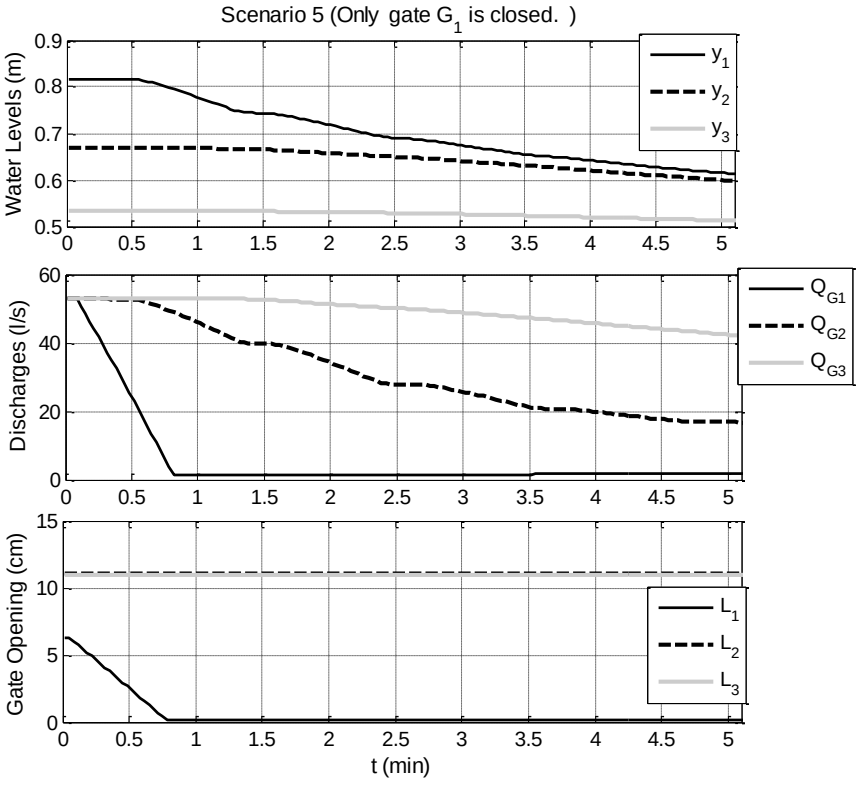

Figure 4.8 Scenario 5 at low flow

The fifth scenario aims to isolate quickly the downstream pools from the water source (reservoir) by only closing the upstream pool. This operation results in water levels that go further below the minimum allowed values, as is depicted in Figure 4.8.

Canal closure at high flow

When the input flow increases, the operation scenarios get more complicated and problems could arise. Simulation results of both scenarios 1 and 2 starting from a steady state of 121 l/s are shown in Figure 4.9. Initial water levels y_1, y_2 and y_3 are 93.3, 80.8, and 66.5 cm respectively and the initial gate openings are 17.4, 30 and 26.1 cm for G_1, G_2 and G_3 respectively. The gate velocities are 3.125 mm/s in the left plot and 1.524 mm/s in the right plot. When the gates are all closed simultaneously following a straight line trajectory, the resulting water profiles decrease their amplitude in the deepest value around 6.88% at 3.125 mm/s and 10.9% at 1.524 mm/s. Percentage-wise, the first pool water level has decreased further with respect to the operating point of 52 l/s.

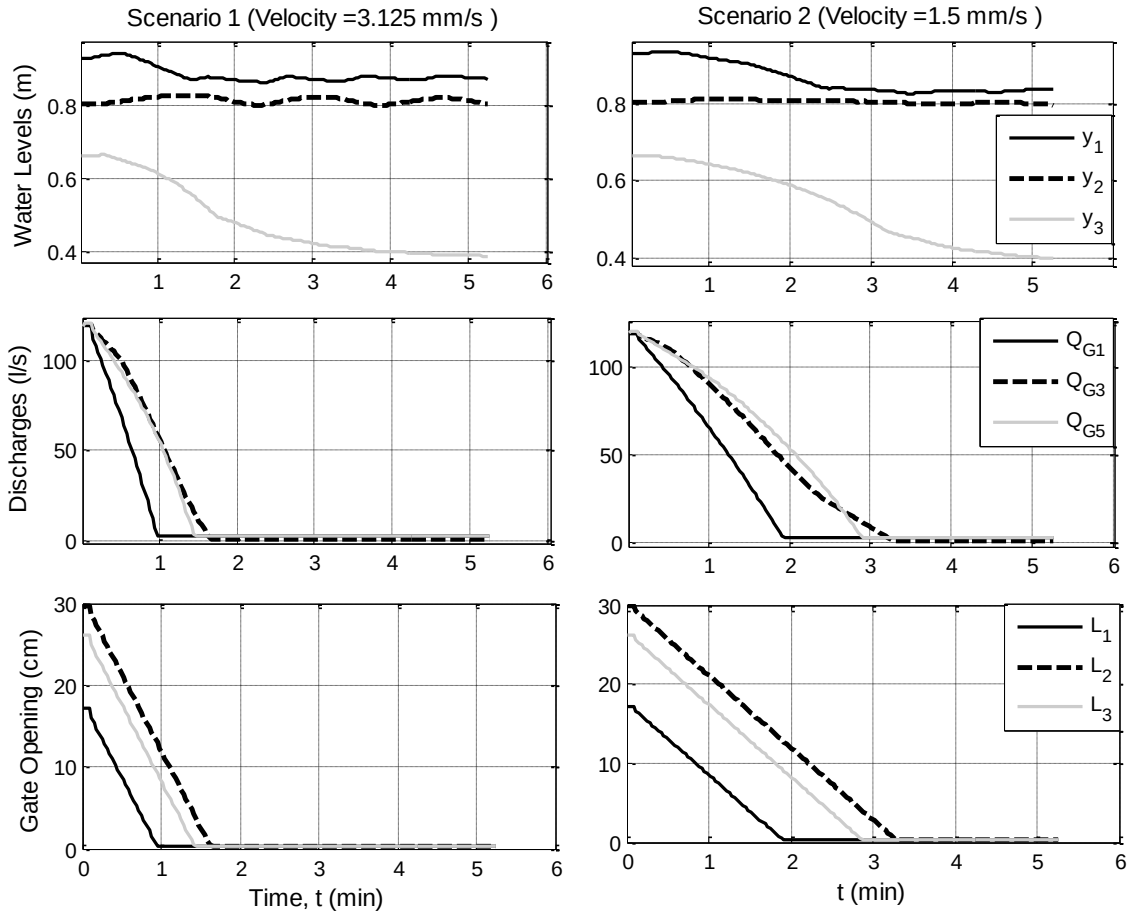

Figure 4.9 Simultaneous closing of all gates at high flow

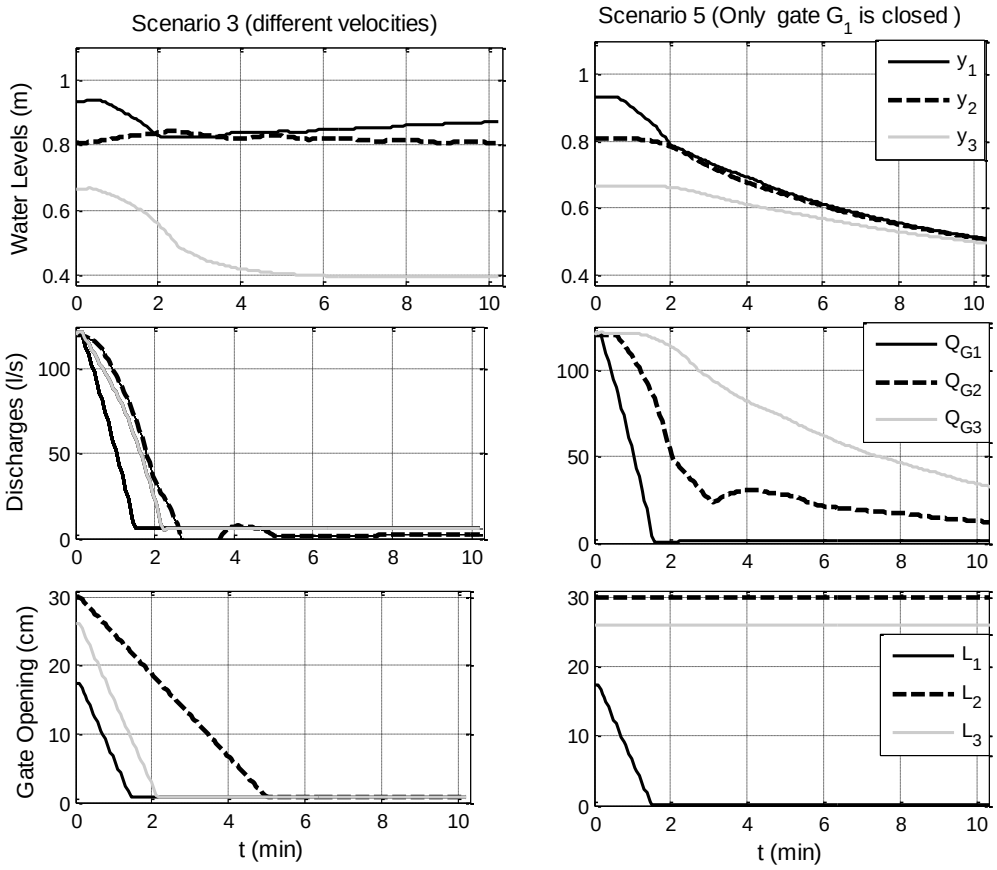

Figure 4.10 Scenarios 3 and 5 at high flow (different velocities)

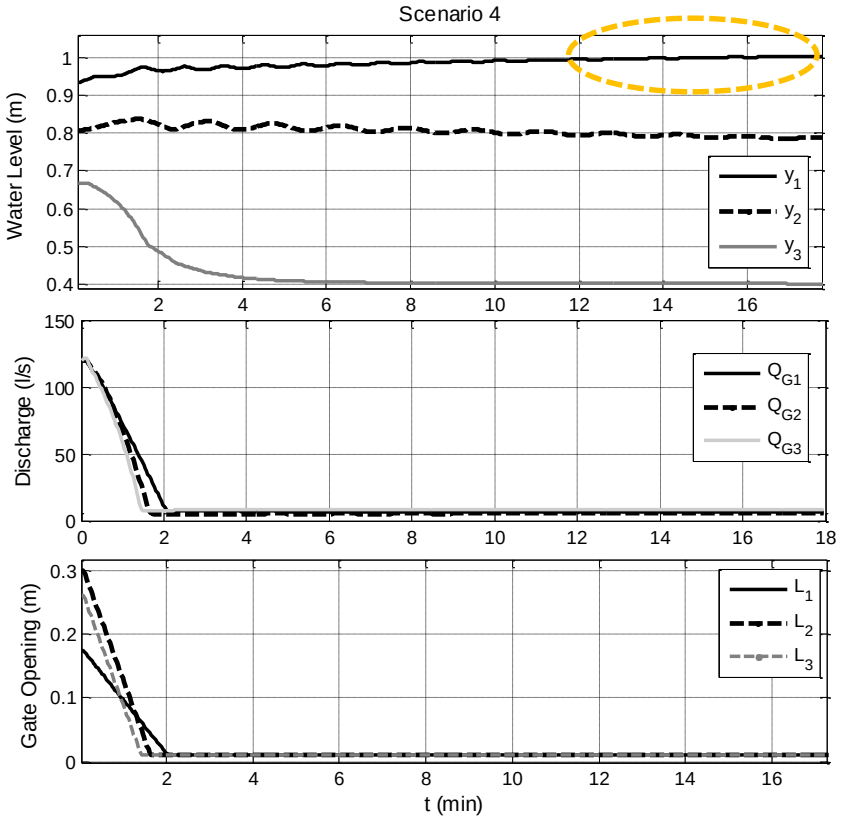

Figure 4.11 Scenario 4 at high flow (leading to overtopping)

In the scenarios 3, 4 and 5 where gate movements have two different velocities, the transient behavior gets worse in the upstream pool. Scenarios 3 and 5 are shown in Figure 4.10. The simulation of the Scenario 4 is shown in Figure 4.11, where the system starts from a steady state of 121 l/s and water levels y_1, y_2 and y_3 of 93.3, 80.8 and 66.5 cm respectively. When all the gates are closed simultaneously following a straight line trajectory, the resulting water profiles exhibit an unaffordable amplitude leading to overtopping in the first canal pool.

4.5.2 Manual closure of the Ebro River left bank canal

The Ebro River left bank canal in Spain has been designed with five pools separated by five sluice gates. The maximum operating level for safety purposes is 2.99 m. Depending on the water level of the river, the aquifer affects the canal lining by creating external pressure. In this way a minimum operating level of 2 m is recommended to avoid problems of cracking in the canal lining. To fulfill simulations, the configuration depicted in Figure 4.12 has been used. In this sketch, $y_1, \ldots, y_5$ are downstream water levels; $Q_{S1}, \ldots, Q_{S4}$ are turnouts in the lateral spillways and Q_{W5} is the discharge in the spillway S_5.

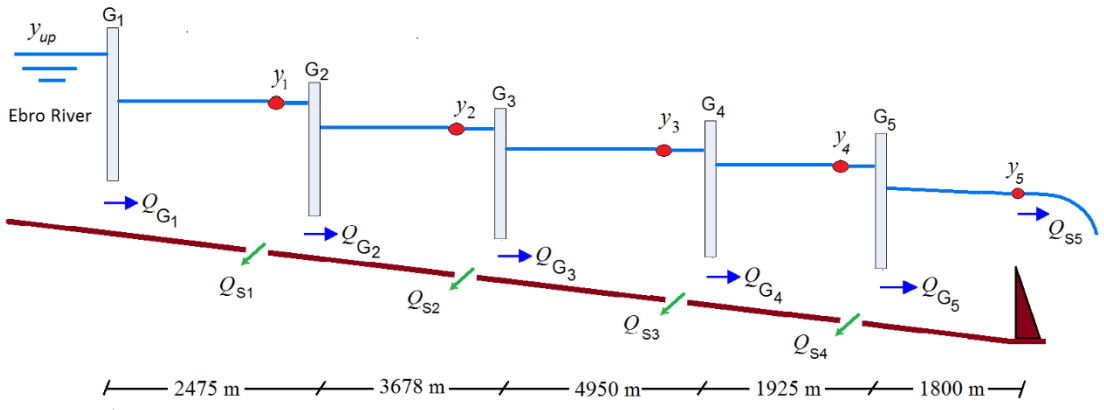

Figure 4.12 Sketch of the ERLB canal

Scenarios

Simulation results include three variables: downstream water levels, discharges under gates and gate openings. The scenarios, depending on the gate velocities, are the following:

- Scenario 1: Closing all the gates at the same velocity,
  $V_{g1} = V_{g2} = V_{g3} = V_{g4} = V_{g5} = 3.125 \frac{\text{mm}}{\text{s}} = 18 \frac{\text{cm}}{\text{min}}$
- Scenario 2: Closing gates at the same velocity,
  $V_{g1} = V_{g2} = V_{g3} = V_{g4} = V_{g5} = 0.5 \frac{\text{mm}}{\text{s}} = 3 \frac{\text{cm}}{\text{min}}$
- Scenario 3: Closing at different velocities,
  $V_{g1} = 3.125 \frac{\text{mm}}{\text{s}}$; $V_{g2} = V_{g3} = V_{g4} = V_{g5} = 1.5 \frac{\text{mm}}{\text{s}} = 9 \frac{\text{cm}}{\text{min}}$
- Scenario 4: Closing gates at different velocities,
  $V_{g1} = 1.5$; $V_{g2} = V_{g3} = V_{g4} = V_{g5} = 3.125 \frac{\text{mm}}{\text{s}}$

- Scenario 5: closure of gate G_1 only with velocity of $V_{g1} = 3.125\ \frac{\text{mm}}{\text{s}}$. The rest of the gates remain in the same position along the time of simulation.

To simulate the manual closure operation, each scenario starts from an operating point around 15.29 m^3/s. At time $t = 0$, gate openings are $L_1 = 0.456, L_2 = 2.737, L_3 = 1.325,\ L_4 = 1.749$ = and $L_5 = 2.109$ m. The initial water levels are $y_1 = 2.78, y_2 = 2.22, y_3 = 2.73,\ y_4 = 2.3$ = and $y_5 = 2.5$ m. The minimum gate opening is 0.008 m, this means less than 2% of the initial operating point in each discharge under gate.

In the first scenario (Figure 4.13), after 30 seconds all the gates close simultaneously. This scenario assumes that all gates are equal and it attempts to resemble a situation of panic in which the water master decides to close simultaneously all the gates. As can be noted, the resulting water profile of y_3 reaches an unaffordable amplitude leading to overtopping in less than 9 minutes.

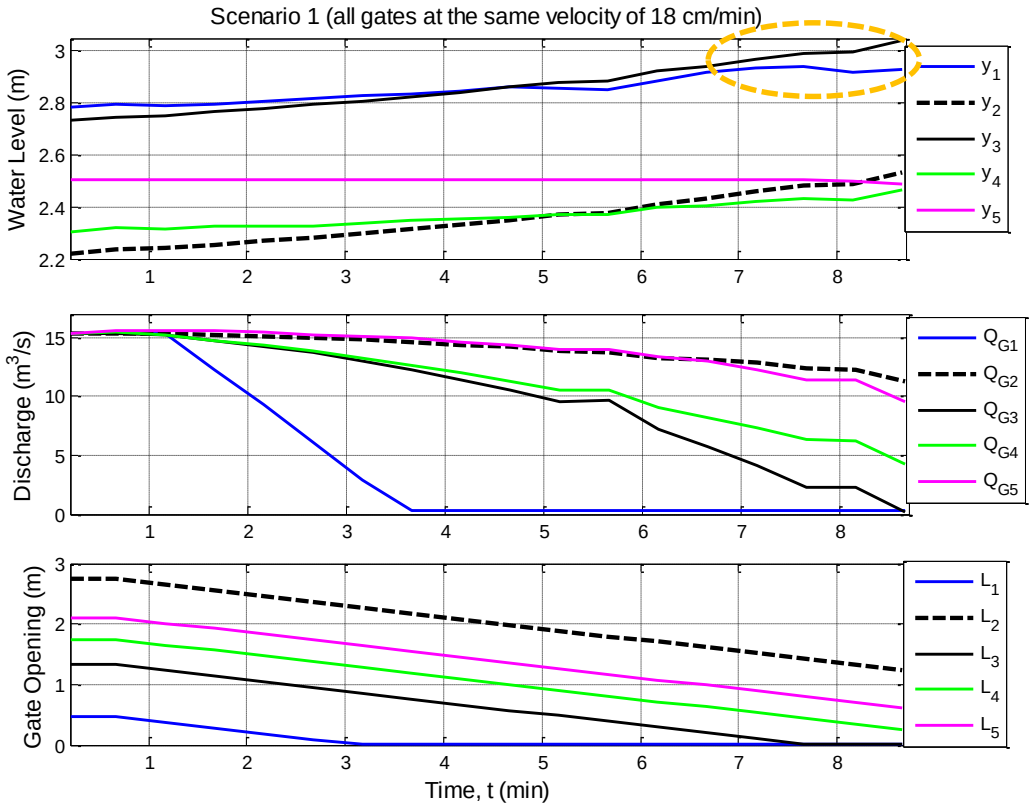

Figure 4.13 Simulation results of Scenario 1, illustrating overtopping.

Simulation results of Scenario 2 are illustrated in Figure 4.14. In this scenario, the closure operation starts at the same initial steady state of 15.29 m^3/s. In this scenario gates are closed simultaneously but at lower gate velocity than in Scenario 1. As can be noted, after 45 minutes of simulation there is no to overtopping in any pool (the maximum value is y_3 = 2.9 m), however water level y_1 has decreased to 1.35m (51% of its initial value). This water level is lower than the 2m-minimum recommended safeguard, which is not admissible.

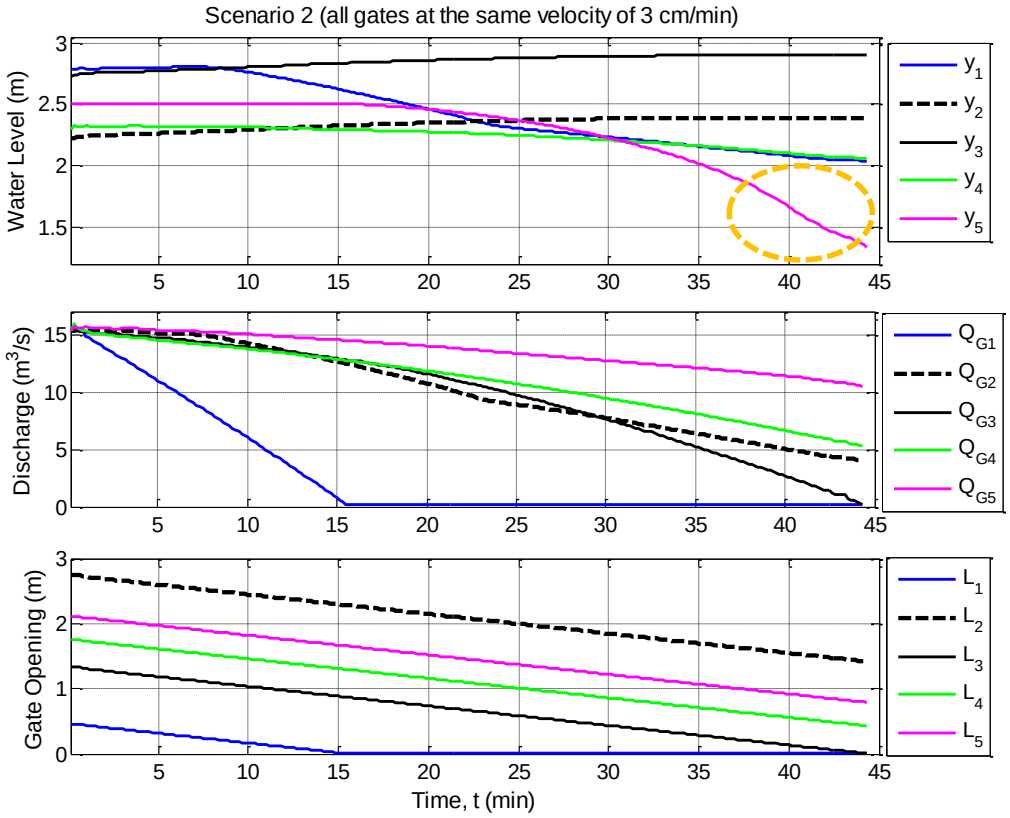

Figure 4.14 Simulation results of Scenario 2

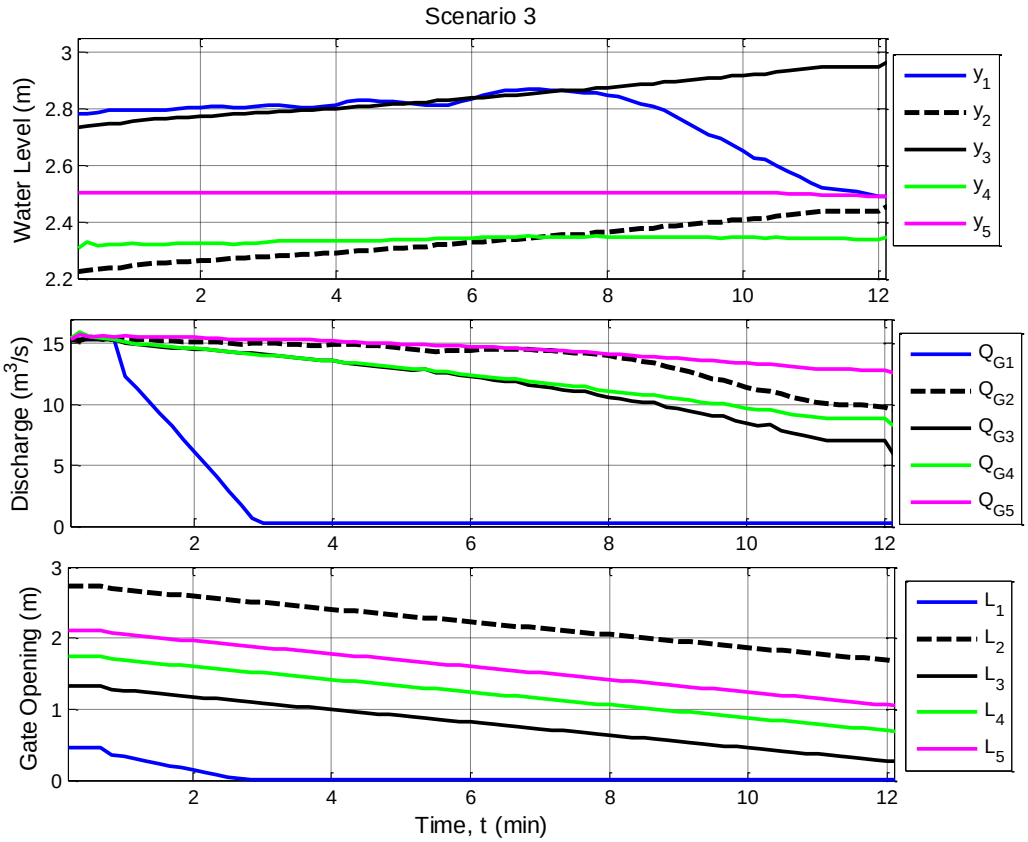

Figure 4.15 Simulation results of Scenario 3

Simulation results of scenarios 3 and 4 are illustrated in Figure 4.15 and Figure 4.16 respectively. In both scenarios gates movements have two different velocities. In the scenario 3, water level y_1 has decreased around 30 cm in 12 minutes. In Scenario 4 there is overtopping of water level y_3 in less than 8 minutes.

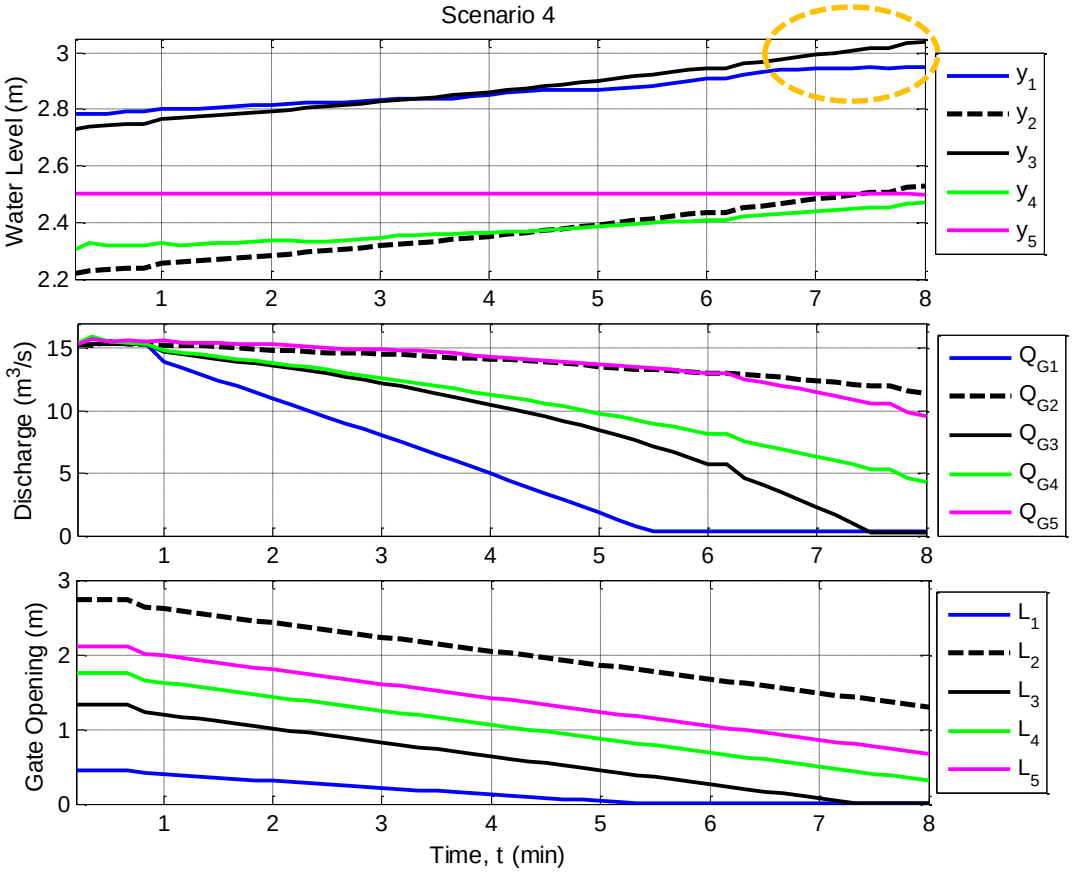

Figure 4.16 Simulation results of Scenario 4 (leading to overtopping)

Simulation results of Scenario 5 are shown in Figure 4.17. This scenario attempts to resemble a situation where the water master decides to close only the most upstream gate. As a result, most of the water levels are lower than the 2m-minimum recommended safeguard in less than 2.6 hours.

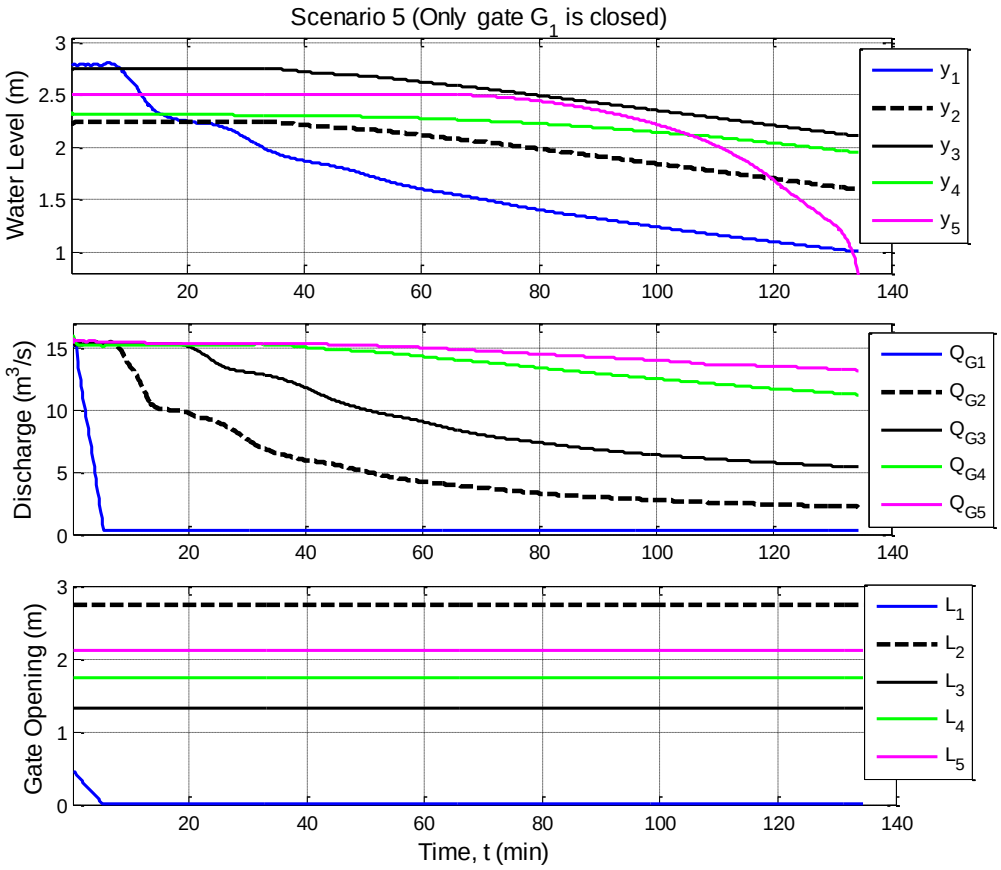

Figure 4.17 Simulation results of Scenario 5

4.5.3 Discussion of the simulation results

The quality of the closure operation is determined by aspects, such as closing velocity, water levels inside the minimum/maximum safety levels required on the canal, and to keep the water levels as close as possible to the setpoint. Using different gate closing velocities in the canal closure operation produces meaningful changes in the amplitude, peak, trough (valley) and wavelength of both upstream and downstream water levels. Wave phenomenon occurs regardless which are the initial conditions or which are the motor velocities. Oscillatory behavior is a result of reflections, gate movements and disturbances in pools. A canal system to be closed is affected by upstream and downstream disturbances. Therefore, the controller to manage closure and opening operations must avoid the risk of exceeding the minimum/maximum safety levels required on the canal.

Operating the canal gates sequentially, progressing either downstream or upstream, is a technique commonly used to change canal system flow. On conventionally operated canals, the basic procedure is to initiate a discharge change in the headwork and progress in the downstream direction (Buyalski et al., 1991). Based on the results on (Soler et al., 2014) and on the simulation and real-time experiment carried out on during the development of this thesis, have demonstrated that overtopping risk can be reduced by closing the gates sequentially from upstream to downstream with some time delay between a gate and the next one. The results have been obtained by imposing a trajectory to each gate in an open-loop control system. In this sense, a simulation

of manual closure operation using the strategy of sequential gate movements in the laboratory canal PAC-UPC is illustrated in Figure 4.18. For comparison purposes, this simulation starts from the same steady state that illustrated in Figure 4.11 (scenario 4) but closing the gates sequentially from upstream to downstream and imposing a smooth trajectory to each gate. As it can be observed, with this strategy, water levels in pools 1 and 2 are lower than those in Figure 4.11. Nevertheless, maintaining the levels in each pool inside the safety band prescribed for the canal is not guaranteed. Moreover, amplitude variations of levels y_1 and y_2 from its original positions are higher than 3 cm (lower than the case depicted in Figure 4.9). Therefore, there is an improvement in that there is no overtopping, however the problem of closure is not completely solved because the open loop-control system does not consider neither the influence of the output variable (water levels) in the control action nor the disturbances that may occur during the closure and opening operations.

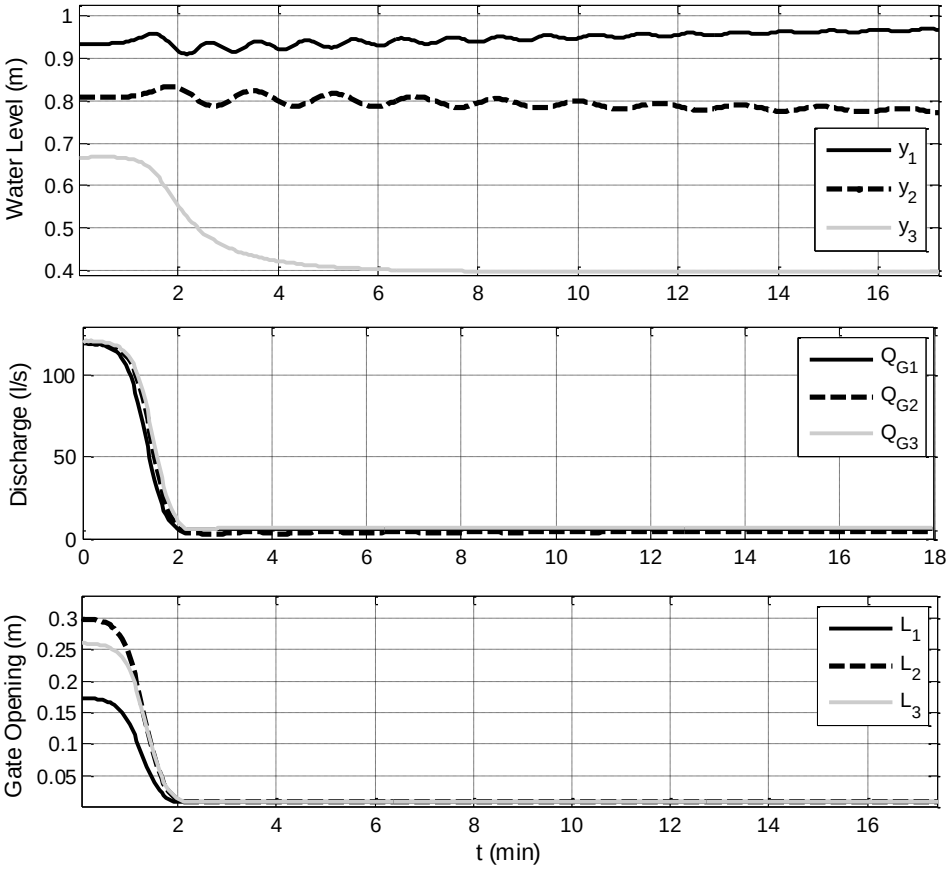

Figure 4.18 Sequential closure of all gates with no overtopping in Canal PAC-UPC

4.6 Conclusion

Based on the issues described in this chapter, a proper closure operation of a given canal system must consider the following operation requirements:

- To drive any canal pool from its initial steady state to another state with a minimum discharge, the closure operation must be as smooth as possible by way of moving the gates in a progressive and smooth manner.

- The water levels on the canal pools must be settled to given set-points between the minimum and maximum safety water levels for each pool during the closure/opening operations.

- The gates along the canal must be closed subsequently from upstream to downstream to avoid as much as possible both the oscillatory behavior of the water profiles and the potential overtopping.

- The closure/opening operations must be done as soon and quick as possible. The minimum allowed time is determined by the geometry of the canal, the flow conditions, the velocity of the check structures and the final objective pursued with the closure operation.

The closure operation is a very challenging task whose primary goal is to save water. The operational requirements of the closure operation are almost impossible to achieve using local manual control methods. In this dissertation, an automatic control strategy is proposed to guarantee the users' water demands while keeping the water levels within specified maximum and minimum values in order to prevent damages to the canal.

Chapter 5

Predictive control with dynamic constraints in canal automation

5.1 Introduction

This chapter develops the control strategy and the formulation to carry out the closing operation with the aim of minimizing the problems discussed in Chapter 4. Due to its advantages and results highlighted in the literature review subsection, predictive control has been chosen in this dissertation as the control methodology in order to deal with abrupt changes in operating conditions of irrigation canal systems.

A key aspect of predictive control is the use of a model explicitly in the design methodology. The model is used as part of the control algorithm and hence its performance is influenced by the accuracy of the model. In control engineering, the suitable process models should be accurate enough to represent the most important dynamics of the process and simple enough to make the real-time implementation feasible when online optimization is required.

The dynamics of a canal may be approximated around a given operating point with linear time-invariant (LTI) models in order to use linear control design tools, as it is usual in control engineering practice (Duviella et al., 2010). However, in the canal control context, when the operating point changes within a wide range, it results in changes of LTI model parameters and in the time delay. These changes represent a problem for predictive control, as well as others model-based control techniques (a related concept map is depicted in Figure 5.1), where the linearized

model obtained around a particular operating point considers a positive performance only over a small interval of discharges. Therefore, this problem is an extra challenge to face in the controller design. The main control strategies to tackle the problem when parameters change in time are robust control, adaptive control and predictive control. There are four approaches to deal with this problem when using predictive control (PC): adaptive PC (Martín Sánchez & Rodellar, 1996), multimodel PC (van Overloop et al., 2008), nonlinear PC (Allgower et al., 2004) and multiobjective PC (Bemporad & Muñoz de la Peña, 2009). For instance, in the multimodel PC approach, when the operating conditions are too wide, the dynamic relationship between input and output is approximated using decomposition into a set of operating regimes (each of them associated to a local model).

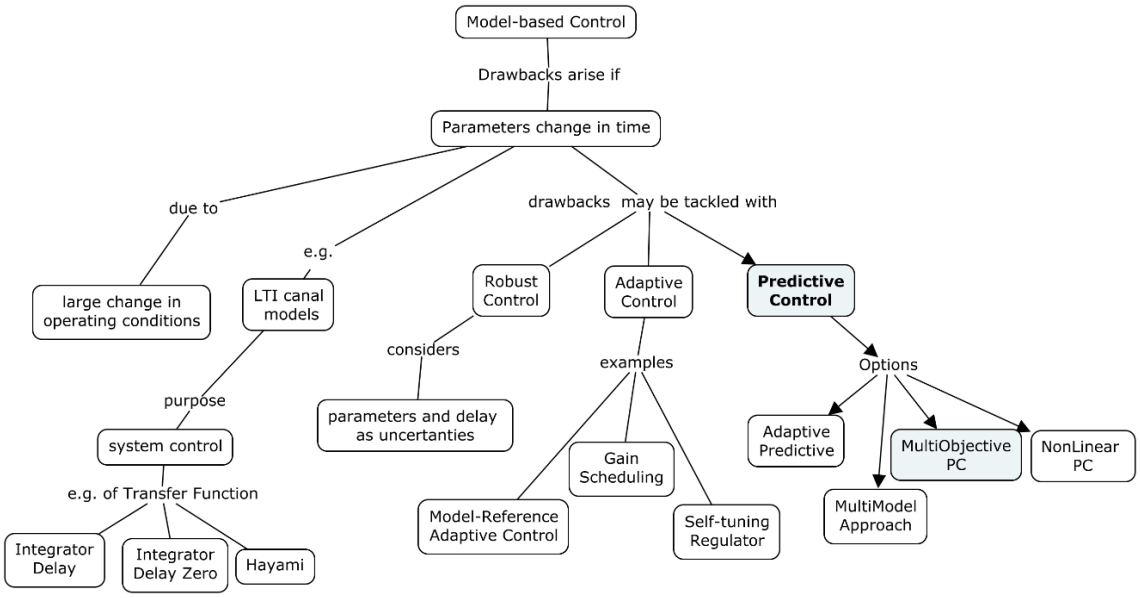

Figure 5.1 Concept map related to the model-based control

This thesis focuses on designing controllers for irrigation canal systems involving abrupt changes in operating condition such as closure and opening operation. These abrupt changes lead to models used for control purposes that should change along the time. To deal with those problems, this dissertation proposes a new strategy called *supervised decentralized predictive control with dynamic constraints* (SDPC) from now on. Within this approach, the overall canal is decomposed into a number of pools connected by controllable gates in a local manner. Every local controller observes the downstream pool behavior to control its local subsystem, considering the interaction between pools as a measurable disturbance. Each controller also considers the external disturbances such as the interacting flow caused by downstream lateral offtake/intake variation. In an upper hierachical level, a supervisor is designed, which coordinates a sequential operation of the local controllers, manages the tuning of the control parameters depending on the operating mode and dinamically updates constraints on the control gates depending on the presence and magnitude of abrupt changes.

The chapter is organized as follows. Section 5.2 describes the overall supervised control strategy. Section 5.3 presents the formulation of the local predictive controllers and two ways to obtain the optimal solution (unconstrained and constrained). Section 5.3.3 introduces the idea of dynamic constraints in the canal closure operation, while Section 5.5 turns this idea into a component within the supervised control scheme. Finally, Section 5.6 focuses on some issues concerning the

implementation of the developed control scheme, prior to the numerical assessment that will be presented in Chapter 6.

5.2 Overall control strategy

5.2.1 Basic objective

As it was mentioned in Chapter 4, closing a canal means changing form an operating flow condition to an almost zero discharge steady state while maintaining the prescribed water levels in all the canal pools. There are two main objectives involved in the problem of automatic closure/opening in canals. The first objective is to regulate the water levels in order to keep them as close as possible of the setpoint (constant reference). The second objective is to regulate the discharge passing through the check gates, in order to change the operating discharge within a wide range. The purpose of the control system is to manipulate the upstream discharge in order to maintain the downstream water level within specified maximum and minimum values to avoid the related problems mentioned in Section 4.2. Namely, in order to make the closure operation feasible, once the closure operation has started, the gate openings must decrease as faster as possible but avoiding overtopping, and other problems related to surpassing the safety band for the water levels.

A schematic of a feedback control in a one-pool configuration irrigation system is illustrated in Figure 5.2 to control the downstream water level. Water level is used as feedback signal for the computer-based controller, which sends the control variables to the position controller through a data acquisition card (DAQ card). The computer takes the downstream water level to calculate the control variable at each sampling time. The position controller is an inner control loop that converts the desired gate openings into actual gate movements. The system considered herein can be an isolated pool or it may also be a controlled pool within a multi-pool irrigation network, such as it is considered in this thesis.

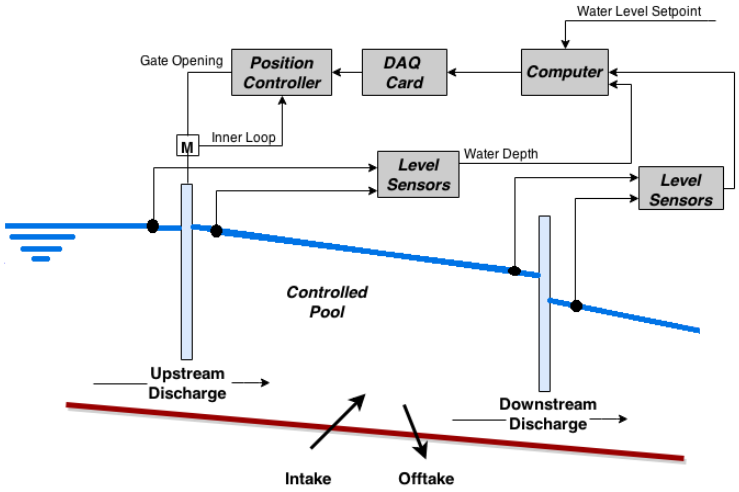

Figure 5.2 Illustration of the control problem for a decentralized operation (taken from (Rodellar et al., 1993))

5.2.2 Controller architecture: supervised control

The problems that arise in a closure operation when all the gates in a canal are simultaneously closed (see Subsection 4.3) and the improvements obtained when the gates are sequentially closed, suggest the convenience of an agent (supervisor) in the control system determining the right moment to move the different gates in the canal. Operating the canal gates sequentially, progressing either downstream or upstream, is a technique commonly used to change the canal system flow. On conventionally operated canals, the basic procedure is to initiate a discharge change in the headwork and progress in the downstream direction (Buyalski et al., 1991).

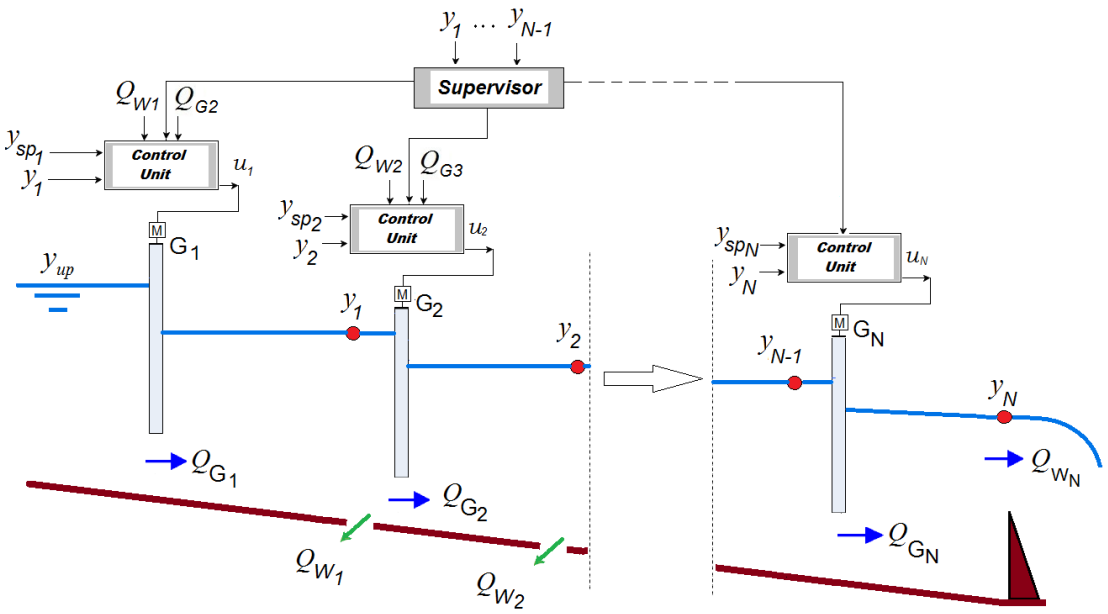

Figure 5.3 Supervised decentralized downstream control system

In supervised decentralized control, the global scheme is composed by a set of gates operating along a series of pools as depicted in Figure 5.3. The cyclic sequential movement of the gates is the responsibility of the supervisor. Each pool is seen as a system controlled by its upstream gate (Gómez et al., 2002). Every individual gate moves as a result of the computation of the control law on its corresponding decentralized controller, which may facilitate the real time operation. Hence, the overall system is decomposed into a set of coupled subsystems (controlled pools) and the design effort is placed in deriving decentralized controllers for each subsystem. Therefore, for a *N*-pool configuration, the controller architecture is composed by *N* decentralized controllers and a global supervisor, which commands the convenient order of closing the gates. Each local control unit or local controller (see Figure 5.4) is responsible for closing its motorized gate following a smooth trajectory able to maintain the water level in the pool inside the allowed safety band.

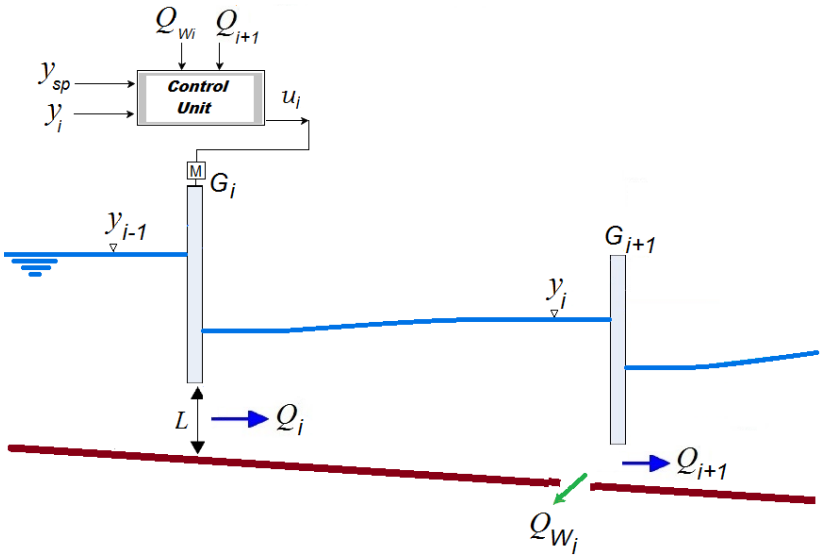

Figure 5.4 Decentralized control of a single-pool configuration

The predictive local controllers designed in this dissertation consider the interactions between adjacent pools. Check structures, such as gates and offtakes are located along the canal and strongly interact with the canal dynamics. Thus, the whole canal has to be regarded as a complex dynamic system with high number of variables related to states, inputs and outputs. (Gómez et al., 2002). In this way, an upstream gate movement affects directly the controlled water levels of its controlled pool but also the water level in neighbor pools, namely the interactions occur between input and output of adjacent pools in the system. Consequently, disturbances occur both downstream and upstream. There are two unknown disturbances considered in the proposed controller, first the downstream disturbances caused by the downstream gate opening and second, the lateral offtakes/intakes. Therefore, each controller includes in its control law the control actions computed by its neighbors as a measurable disturbance (feedforward input).

Three operating modes at supervisory level are proposed:

- Normal
- Closure
- Opening

The operating mode (OM) is determined manually by the water manager depending on the operation that the facility requires to fulfill. In normal operating mode, the main goal of the control system is to keep the water levels as close as possible to the setpoints, this goal is enough to judge the controller's ability to deliver the needed offtakes discharges (Clemmens et al., 1998). There is no abrupt changes in the operating conditions under normal operation. The closure operation mode means change from a baseline operating regime to setting zero discharge conditions by closing all the gates along the canal. The discharge decreasing tendency is imposed once the supervisory level decides to close the canal. In the opening operation mode, the gates are moved in order to restarting the operating discharge from zero.

The supervisory level in the controller is the monitoring structure responsible for the following tasks:

- Coordinating the sequential operation of each local controller. For closure mode without disturbances, the sequence initiates with a discharge change in the headwork and progress in the downstream direction, then the sequence repeats itself till to reach zero flow in all the pools. Meanwhile, on opening operation without disturbances, the sequence of operation is to initiate a discharge change in the headwork and progress in the downstream direction, then the sequence repeats itself till to reach the new steady state with a baseline flow in all the pools.

- Scheduling the controller parameters according to the OM. The predictive controller parameters, prediction horizon, constraints, and weighting factor, are different for each operating mode. Tuning of each controller must be done offline and separately. In the normal operating mode, for instance, the plant model and constraints are time-invariant because the operation is assumed to be around a particular operating point. In the closure (or opening) operating mode, the supervisor changes the parameters of the dynamic constraints that determines the maximum discharge of each controlled pool in the presence of unknown disturbances. Namely, the constraints are dynamic because change over the time (see Subsection 5.3.3).

- Locating disturbances. In the presence of an unexpectedly large disturbance, the supervisor must detect the location where a sudden raise of water level has occurred and then to decide which is the next controller to operate during the closure operation. For instance, in case of an unexpectedly large intake Q_{W1} (see Figure 5.3) during a closure operation, the supervisor sends an enable signal to the local controllers in order to restart the sequence with a change in the position of gate G_2 first. Meanwhile, in case of an unexpectedly intake Q_{W2}, the supervisor decides to restart the sequence changing the position of G_3 first, in order to reduce the effect of the disturbance.

5.3 Local water level predictive controllers

In this section, a generic control law is formulated using predictive control. In a first step, the control is derived assuming no constraints; a further step introduces constraints in the control variable.

5.3.1 Unconstrained Predictive Control

Predictive control essentially relies on the use of a model able to predict the system output as a function of the system inputs on a moving horizon scenario. The model allows to compute the control sequence that makes the predicted output to track the setpoint through the minimization of

the cost function. The model is usually given as a difference equation. In this work it is assumed that the process is described by the following discrete transfer function:

$$y(z) = \frac{B(z^{-1})}{A(z^{-1})}[u(z) + w(z)] \tag{5.1}$$

where $y(z)$ is the output variable with the Z-transform applied to $y(k)$, $u(z)$ is the control action or input and $w(z)$ is the measurable disturbance. $A(z^{-1})$ and $B(z^{-1})$ are the polynomials:

$$B(z^{-1}) = b_1 z^{-1} + b_2 z^{-2} + \cdots b_m z^{-m} \tag{5.2}$$

$$A(z^{-1}) = 1 - a_1 z^{-1} + a_2 z^{-2} + \cdots a_n z^{-n} \tag{5.3}$$

The next step in the design process is to compute the future control signal sequence that will make the predicted output equal to a conveniently selected output trajectory along the prediction horizon. Incremental formulation of the predictive model is used in this dissertation because it introduces some practical advantages in the real time implementation. One of the advantage is that the incremental formulation is able to handle potential steady state deviations from the setpoint due to load disturbances (Martín Sánchez & Rodellar, 1996). Taking a difference operation at instant *k*, the control action $u(k)$ and the predicted output $y(k)$ can be written as

$$\Delta u(k) = u(k) - u(k-1)$$

$$\Delta y(k) = y(k) - y(k-1)$$

where Δu is the incremental control variable, and Δy is the incremental output.

A predictive model is used to predict the sequence of incremental outputs $\Delta\hat{y}(k+j|k)$ as a function of an incremental control sequence $\Delta\hat{u}(k+j-1|k)$ over the entire interval $[k, k+\lambda]$ at the present sampling instant k, namely

$$\Delta\hat{y}(k+j|k) = \sum_{i=1}^{\hat{n}} \hat{a}_i \Delta\hat{y}(k+j-i|k) + + \sum_{i=1}^{\hat{m}} \hat{b}_i \Delta\hat{u}(k+j-i|k) + \sum_{i=1}^{\hat{p}} \hat{c}_i \Delta\hat{w}(k+j-i|k) \tag{5.4}$$

$$j = 1,2, \ldots \lambda$$

Where
$$\hat{y}(k+1-i|k) = y(k+1-i) \qquad i = 1, \ldots, \hat{n} \tag{5.5}$$

$$\hat{w}(k+1-i|k) = w(k+1-i) \qquad i = 1, \ldots, \hat{p}$$

$$\hat{u}(k+1-i|k) = u(k+1-i) \qquad i = 1, \ldots, \hat{m}$$

where $y(k+1-i)$ and $u(k+1-i)$ are the measured output and inputs already applied at instant k. $w(k+1-i)$ is the measureable disturbance at the present time k. This extended prediction thus includes the specific case of λ=1. In problems where disturbances are known in advance, the disturbances may be added to the controller in order to introduce feedforward

capability, which allows both tracking setpoint changes and overcoming the unmeasured disturbances that are usually present in the canal.

The controller proposed in this dissertation is based on a decentralized control strategy, therefore the predictive model (5.4) describes a single-input, single-output (SISO) process. Hereinafter, the formulations of the local controller are based on the model (5.4). At every sampling time, the future sequence of control actions is optimized over the prediction horizon. The optimization is fulfilled by minimizing an objective function with penalties on deviations from setpoint and penalties on requested control signal changes. The objective function used in this dissertation is the following linear quadratic function:

$$J = \sum_{j=1}^{\lambda} \Psi_j (\hat{y}(k+j|k) - y_r(k+j|k))^2 + \sum_{j=0}^{\lambda-1} R_j \Delta\hat{u}(k+j|k)^2 \tag{5.6}$$

where $y_r(k+j|k)$ is a reference trajectory. Ψ_j and R_j are weighting factors defined for each future time $k+j$. For simplicity, they can be constant (Ψ, R) along the whole prediction horizon.

The next step is to express the predictive model (5.4) as a function of the information of the process inputs and outputs at instant k, as well as the predicted control input, $\Delta\hat{u}$. In this way, by using the initial condition (5.5) recursively, the predictive model (5.4) may be written as follows:

$$\begin{aligned} \Delta\hat{y}(k+j|k) = & \sum_{i=1}^{\hat{n}} \hat{e}_i^{(j)} \Delta y(k+1-i) \\ & + \sum_{i=2}^{\hat{m}} \hat{g}_i^{(j)} \Delta u(k+1-i) + \sum_{i=2}^{\hat{p}} \hat{d}_i^{(j)} \Delta w(k+1-i) \\ & + \sum_{i=0}^{j-1} \hat{g}_1^{(j-i)} \Delta\hat{u}(k+i|k) \\ & + \sum_{i=0}^{j-1} \hat{d}_1^{(j-i)} \Delta\hat{w}(k+i|k) \qquad (j = 1,2,\dots,\lambda) \end{aligned} \tag{5.7}$$

Assuming that future disturbances $\hat{w}(k+i|k)$ for $j > 0$ remain unchanged and constant, then the values $\Delta\hat{w}(k+i|k) = 0$, and equation (5.7) may be simplified as follows:

$$\begin{aligned} \Delta\hat{y}(k+j|k) = & \sum_{i=1}^{\hat{n}} \hat{e}_i^{(j)} \Delta y(k+1-i) \\ & + \sum_{i=2}^{\hat{m}} \hat{g}_i^{(j)} \Delta u(k+1-i) + \sum_{i=1}^{\hat{p}} \hat{d}_i^{(j)} \Delta w(k+1-i|k) \\ & + \sum_{i=0}^{j-1} \hat{g}_1^{(j-i)} \Delta\hat{u}(k+i|k) \qquad (j = 1,2,\dots,\lambda) \end{aligned} \tag{5.8}$$

where $\hat{e}_i^{(j)}$, $\hat{d}_i^{(j)}$and $\hat{g}_i^{(j)}$ are coefficients obtained from the parameters $\hat{a}_i$ and $\hat{b}$ of the predictive model by means of the following recursive algorithm (Martín Sánchez & Rodellar, 1996):

$$\hat{e}_i^{(j)} = \hat{e}_i^{(j-1)}\hat{a}_i + \hat{e}_{i+1}^{(j-1)}\ ; \quad \text{i} = 1, \dots, \hat{n}; \quad \text{j} = 2, \dots, \lambda \tag{5.9}$$

$$\hat{d}_i^{(j)} = \hat{e}_i^{(j-1)}\hat{c}_i + \hat{d}_{i+1}^{(j-1)}\ ; \quad \text{i} = 1, \dots, \hat{p}; \quad \text{j} = 2, \dots, \lambda$$

$$\hat{g}_i^{(j)} = \hat{e}_i^{(j-1)}\hat{b}_i + \hat{g}_{i+1}^{(j-1)}\ ; \quad \text{i} = 1, \dots, \hat{m}; \quad \text{j} = 2, \dots, \lambda$$

with

$$\hat{e}_i^{(1)} = \hat{a}_i\ ; \qquad \text{i} = 1, \dots, \hat{n}$$

$$\hat{g}_i^{(1)} = \hat{b}_i\ ; \qquad \text{i} = 1, \dots, \hat{m}$$

$$\hat{d}_i^{(1)} = \hat{c}_i\ ; \qquad \text{i} = 1, \dots, \hat{p}$$

$$\hat{e}_{\hat{n}+1}^{(j-1)} = 0\ ; \quad \text{j} = 2, \dots, \lambda$$

$$\hat{g}_{\hat{m}+1}^{(j-1)} = 0\ ; \quad \text{j} = 2, \dots, \lambda$$

$$\hat{d}_{\hat{p}+1}^{(j-1)} = 0\ ; \quad \text{j} = 2, \dots, \lambda$$

In a compact matrix-vector form, the predicted output in (5.8) may be expressed as follows:

$$\Delta\hat{Y} = E\Delta Y + G\Delta U + P\Delta W + G_0\Delta\hat{U} \tag{5.10}$$

where

$$\Delta\hat{Y} = [\Delta\hat{y}(k+1|k), \Delta\,\hat{y}(k+2|k), \dots, \Delta\hat{y}(k+\lambda|k)]^T$$

$$\Delta\hat{U} = [\Delta\hat{u}(k|k), \Delta\,\hat{u}(k+1|k), \dots, \Delta\hat{u}(k+\lambda-1|k)]^T$$

$$\Delta Y = [\Delta y(k), \Delta y(k-1), \dots, \Delta y(k-\hat{n}+1)]^T$$

$$\Delta U = [\Delta u(k-1), \Delta u(k-2), \dots, \Delta u(k-\hat{m}+1)]^T$$

$$\Delta W = [\Delta w(k), \Delta w(k-1), \dots, \Delta w(k-\hat{p}+1)]^T$$

Superscript ^{T} indicates matrix transpose, $\Delta\hat{Y}$ and $\Delta\hat{U}$ are vectors of λ length, and matrices $E \in \mathbb{R}^{\lambda\, x\, \hat{n}}$, $G \in \mathbb{R}^{\lambda\, x\, (\hat{m}-1)}$, $P \in \mathbb{R}^{\lambda\, x\, (\hat{p}-1)}$ and $G_0 \in \mathbb{R}^{\lambda x \lambda}$.

Matrices E, G, P and G_0 are calculated offline just once, they are computed as follows:

$$E = \begin{bmatrix} \hat{e}_1^{(1)} & \hat{e}_2^{(1)} & \dots & \hat{e}_{\hat{n}}^{(1)} \\ \hat{e}_1^{(2)} & \hat{e}_2^{(2)} & \dots & \hat{e}_{\hat{n}}^{(2)} \\ \vdots & \vdots & \ddots & \vdots \\ \hat{e}_1^{(\lambda)} & \hat{e}_2^{(\lambda)} & \dots & \hat{e}_{\hat{n}}^{(\lambda)} \end{bmatrix}; \qquad G = \begin{bmatrix} \hat{g}_2^{(1)} & \hat{g}_3^{(1)} & \dots & \hat{g}_{\hat{m}}^{(1)} \\ \hat{g}_2^{(2)} & \hat{g}_3^{(2)} & \dots & \hat{g}_{\hat{m}}^{(2)} \\ \vdots & \vdots & \ddots & \vdots \\ \hat{g}_2^{(\lambda)} & \hat{g}_3^{(\lambda)} & \dots & \hat{g}_{\hat{m}}^{(\lambda)} \end{bmatrix}$$

$$P = \begin{bmatrix} \hat{d}_2^{(1)} & \hat{d}_3^{(1)} & \dots & \hat{d}_{\hat{p}}^{(1)} \\ \hat{d}_2^{(2)} & \hat{d}_3^{(2)} & \dots & \hat{d}_{\hat{p}}^{(2)} \\ \vdots & \vdots & \ddots & \vdots \\ \hat{d}_2^{(\lambda)} & \hat{d}_3^{(\lambda)} & \dots & \hat{d}_{\hat{p}}^{(\lambda)} \end{bmatrix}; \quad G_0 = \begin{bmatrix} \hat{g}_1^{(1)} & 0 & 0 & \dots & 0 \\ \hat{g}_1^{(2)} & \hat{g}_1^{(2)} & 0 & \dots & 0 \\ \vdots & \vdots & \vdots & \ddots & \vdots \\ \hat{g}_1^{(\lambda)} & \hat{g}_1^{(\lambda-1)} & \hat{g}_1^{(\lambda-2)} & \dots & \hat{g}_1^{(1)} \end{bmatrix}$$

The objective function (5.6) may be represented in matrix form as follows:

$$J = \left[Y_r - \hat{Y}\right]^T \Psi \left[Y_r - \hat{Y}\right] + \Delta\hat{U}^T R \Delta\hat{U} \tag{5.11}$$

The error, e is

$$e = Y_r - \hat{Y} \tag{5.12}$$

where Y_r is the reference trajectory, and $\hat{Y}$ is the predicted output:

$$Y_r = [y_r(k+1|k), y_r(k+2|k), \dots, y_r(k+\lambda|k)]^T$$

$$\hat{Y} = [\hat{y}(k+1|k), \hat{y}(k+2|k), \dots, \hat{y}(k+\lambda|k)]^T$$

The prediction horizon, λ is chosen greater than the delay time. The weighting matrices Ψ and R are chosen in this work by setting $\Psi = I_{\lambda x \lambda}$ and $R = R_C I_{\lambda x \lambda}$ $(R_C > 0)$. $I_{\lambda x \lambda}$ means λ-by-λ identity matrix. This means that a single weighting factor is to be tuned, which penalizes the changes in the control variable ($\Delta\hat{U}$) in a relative way with respect the error $Y_r - \hat{Y}$.

The value for R_C may be calculated by normalizing the objective function (5.11) with maximum allowed values estimate (MAVE). The MAVE captures the estimation of how much an input or output may vary (van Overloop, 2006). In this dissertation, $\Delta\hat{U}$ is the discharge under gate and the error, e is related to the water level deviation, thus, a calculated maximum discharge change has the same penalty as a maximum water level deviation that need to be corrected. For instance, the maximum allowed water level error is chosen to be 0.03 m, therefore, the maximum allowed value estimated of the water level, e_{MAVE} is equal to 0.03 m.

Since in the objective function (5.11), $\Delta\hat{U}$ is penalized with the weighing factor , and Ψ has been chosen equal to the identity matrix, the sub-objectives in the objective function are normalized. In this way, equation (5.11) may be written as follows:

$$J = \left[Y_r - \hat{Y}\right]^T \frac{1}{(e_{MAVE})^2} \left[Y_r - \hat{Y}\right] + \Delta\hat{U}^T \frac{1}{(\Delta u_{MAVE})^2} \Delta\hat{U} \tag{5.13}$$

where Δu_{MAVE} is the maximum allowed value estimated of the change in discharge. R_C is calculated with the reciprocal of the square of the Δu_{MAVE}, namely

$$R_C = \frac{1}{(\Delta u_{MAVE})^2} \tag{5.14}$$

In order to obtain a value for R_C, the equation (5.14) must be multiplied by $(e_{MAVE})^2$ due to the normalization, namely:

$$R_C(\text{normalized}) = \frac{1}{(\Delta u_{MAVE})^2} \cdot (e_{MAVE})^2 \tag{5.15}$$

On the other hand, note that equations (5.8) and (5.10) give the predictions of the incremental outputs $\Delta\hat{Y}$ over the interval $[k, k+\lambda]$, as function of the increments of the measured outputs ΔY available at the current time k , the previous applied control ΔU, the previous disturbance ΔW, as well as a function of the future controls included in the vector $\Delta\hat{U}$. Within this scheme, a relation between the absolute predicted output vector $\hat{Y}$ and the corresponding incremental vector $\Delta\hat{Y}$ is obtained below.

The outputs predicted at the subsequent time instants over the predictions interval can be expressed in the form

$$\hat{y}(k+1|k) = y(k) + \Delta\hat{y}(k+1|k)$$

$$\hat{y}(k+2|k) = y(k) + \Delta\hat{y}(k+1|k) + \Delta\hat{y}(k+2|k)$$

$$\vdots$$

$$\hat{y}(k+\lambda|k) = y(k) + \Delta\hat{y}(k+1|k) + \ \ldots\ + \Delta\hat{y}(k+\lambda|k)$$

Therefore, $\hat{Y}$ may be written as follows:

$$\hat{Y} = Z\Delta\hat{Y} + Y_k \tag{5.16}$$

where Z is the λ-by-λ matrix.

$$Z = \begin{bmatrix} 1 & 0 & 0\ldots & 0 \\ 1 & 1 & 0\ldots & 0 \\ \vdots & \vdots & \vdots\ddots & \vdots \\ 1 & 1 & 1\ \ldots & 1 \end{bmatrix}$$

and Y_k is a vector with λ elements defined by $Y_k = \ y(k) \cdot \ [1\ 1\ \ \ldots\ \ 1]^{\,T}$

By replacing (5.16) in (5.11) , the objective function is written as follows:

$$J = \left[Y_r - Z\Delta\hat{Y} - Y_k\right]^T \Psi \left[Y_r - Z\Delta\hat{Y} - Y_k\right] + \Delta\hat{U}^T R\Delta\hat{U} \tag{5.17}$$

Substituting (5.10) into (5.17) , the cost function may be expressed as follows:

$$\begin{aligned} J = \left[Y_r - Z(E\Delta Y - G\Delta U - P\Delta W) - Y_k - ZG_0\Delta\hat{U}\right]^T \Psi \left[Y_r - Z(E\Delta Y - G\Delta U - P\Delta W)\right. \\ \left. - Y_k - ZG_0\Delta\hat{U}\right] + \Delta\hat{U}^T R\Delta\hat{U} \end{aligned} \tag{5.18}$$

The unconstrained optimal solution $\Delta\widehat{U}$ is obtained by minimizing the cost function (5.18) in a finite horizon involving λ unknowns $\Delta\hat{u}(k|k), \Delta\hat{u}(k+1|k), \ldots \Delta\hat{u}(k+\lambda-1|k)$. The necessary condition of the minimum J is obtained by

$$\frac{\partial J}{\partial \Delta\widehat{U}} = 0$$

Taking the first derivative of the cost function (5.18) , it gives

$$\frac{\partial J}{\partial \Delta\widehat{U}} = -2Z^T {G_0}^T \Psi\left[Y_r - Z(E\Delta Y - G\Delta U - P\Delta W) - Y_k - ZG_0\Delta\widehat{U}\right] + 2R\Delta\widehat{U} = 0$$

Hence, the unconstrained optimal solution $\Delta\widehat{U}$ may be expressed as follows:

$$\Delta\widehat{U} = \left[{G_0}^T Z^T \Psi Z G_0 + R\right]^{-1} {G_0}^T \Psi[Y_r - Z(E\Delta Y - G\Delta U - P\Delta W) - Y_k] \qquad (5.19)$$

Predictive control use the receding horizon control principle, consequently despite the optimal parameter vector $\Delta\widehat{U}$ contains the controls $\Delta\hat{u}(k|k), \Delta\,\hat{u}(k+1|k), \ldots, \Delta\hat{u}(k+\lambda-1|k)$, the controller only implements the first sample of this sequence, while the rest of the sequence is neglected. This procedure is repeated iteratively every sampling time.

From Equation (5.19), the control law (unconstrained) may be written as follows:

$$\Delta\widehat{U}(k|k) = K_{pc}(E\Delta Y - G\Delta U - P\Delta W - Y_k) \qquad (5.20)$$

where K_{pc} is the first row of matrix $\left[{G_0}^T Z^T \Psi Z G_0 + R\right]^{-1} {G_0}^T \Psi$. The matrix$\left[{G_0}^T Z^T \Psi Z G_0 + R\right]$ is assumed to be positive definite.

5.3.2 Predictive control with constraints

In process control, there are four types of operational constraints that are frequently observed: control variable slew rates, control variable ranges, constraints on the state variable and constraints on the controlled variable. This dissertation considers the first two types of constraints:

1. Constraints related to the control variable slew rate (maximum rate of change). The values for these constraints are determined by the slew rate of the actuators. These constraints are independent of time. The constraints are defined for the increment of the control signal as follows:

$$\Delta u_{min} \leq \Delta u(k) \leq \Delta u_{max} \qquad (5.21)$$

where Δu_{min} is the lower limit and Δu_{max} is the upper limit. The value of Δu_{min} is determined by the actuator nonlinearities because gates in general exhibit a dead zone. In the experimental canal PAC-UPC, for instance, the servomotors which move gates have a 4 mm-pitch, namely the minimum change in gate opening is 4 mm in a sampling time. This gate opening is equivalent to $\Delta u_{min} = 2$ l/s approximately. The value Δu_{max} is directly related to the maximum rate of change

of the gate opening, in such a way that gates can move only a percentage of the operating range in a sampling time.

It is noteworthy that the constraints are imposed over the whole control variable vector $\Delta\widehat{U}$. However, since the predictive controller only implements the first sample of the $\Delta\widehat{U}$ sequence, in order to simplify the computation burden and considering that the controller only implements the first sample of this sequence, the constraints are imposed only on the first element of $\Delta\widehat{U}$. Therefore, $\Delta u(k)$ is used instead of $\Delta\widehat{U}$ hereinafter in this section to simplify the discussion.

In order to solve the predictive control optimization problem, all these inequalities need to be translated into inequalities regarding the control variable, $\Delta u(k)$ (Maciejowski, 2002). The operational constraints related to discharge slew rate permit to the control variable $\Delta u(k)$ increase in a magnitude less than Δu_{max} every sampling time, and decrease in a magnitude less than Δu_{min} every sampling time. Thus, the control variable slew rate constraints (5.21) may be formulated by two inequalities:

$$-\Delta u(k) \leq -\Delta u_{min} \tag{5.23}$$

$$\Delta u(k) \leq \Delta u_{max}$$

The inequalities may be expressed in a matrix form as follows:

$$\begin{bmatrix} -1 \\ 1 \end{bmatrix} \Delta u(k) \leq \begin{bmatrix} -\Delta u_{min} \\ \Delta u_{max} \end{bmatrix} \tag{5.22}$$

2. Constraints related to the control variable range. In DCPC control, these constraints are used in order to consider the amplitude of discharge which must decrease along the closure operation. The constraints may be formulated as follows:

$$U_{min} \leq u(k) \leq U_{max} \tag{5.24}$$

Equation (5.24) must be expressed in incremental form due to the predictive control has been formulated in incremental form. Therefore, $u(k)$ is replaced by its incremental value, $\Delta u(k) = u(k) - u(k-1)$, namely:

$$U_{min} \leq u(k-1) + \Delta u(k) \leq U_{max}$$

$$U_{min} - u(k-1) \leq \Delta u(k) \leq U_{max} - u(k-1) \tag{5.25}$$

This constraint may be formulated by two inequalities:

$$-\Delta u(k) \leq -U_{min} + u(k-1) \tag{5.26}$$

$$\Delta u(k) \leq U_{max} - u(k-1)$$

The inequalities may be expressed in a matrix form as follows:

$$\begin{bmatrix} -1 \\ 1 \end{bmatrix} \Delta u(k) \leq \begin{bmatrix} -U_{min} + u(k-1) \\ U_{max} - u(k-1) \end{bmatrix} \tag{5.27}$$

Due to the requirements of the canal operating modes, some constraints are imposed in the control signal in order to achieve the control objectives. To consider measurable constraints and actuator dead zone, it is necessary to formulate the predictive control problem as a standard optimization problem to solve it at every sampling time. The predictive control problem focuses on obtaining the optimal solution $\Delta\widehat{U}$ by minimizing the cost function (5.18) in a prediction horizon. Then, the predictive control problem is formulated considering the related constraints (5.21) and (5.24) in the context of the optimization problem (2.5). Therefore, the new problem may be expressed as follows:

$$\begin{aligned} \min_{\Delta\widehat{U}} J = \left[Y_r - Z(E\Delta Y - G\Delta U - P\Delta W) - Y_k - ZG_0\Delta\widehat{U}\right]^T \Psi \left[Y_r - Z(E\Delta Y - G\Delta U\right. \\ \left. - P\Delta W) - Y_k - ZG_0\Delta\widehat{U}\right] + \Delta\widehat{U}^T R\Delta\widehat{U} \end{aligned} \tag{5.28}$$

$$\text{Subject to:} \quad -\Delta u(k) \leq -\Delta u_{min}$$

$$\Delta u(k) \leq \Delta u_{max}$$

$$\Delta u(k) \leq U_{max} - u(k-1)$$

$$-\Delta u(k) \leq -U_{min} + u(k-1)$$

In this study, the controlled variable is water level and the control variable is the discharge under gates. Therefore, in the canal closure (or opening) operation context, U_{min} and U_{max} are the minimum and maximum available discharge respectively.

The next step is to express the problem (5.28) as the following standard quadratic programming problem

$$\min_u \ \frac{1}{2} u^T H\, u + u^T b \tag{5.29}$$

$$\text{subject to:} \quad Mu \leq \gamma$$

To do this in a simple manner, the following variable change may be considered:

$$\theta = Y_r - Z(E\Delta Y - G\Delta U - P\Delta W) - Y_k \tag{5.30}$$

It is noteworthy that θ does not depend on $\Delta\widehat{U}$.

Replacing (5.30) into equation (5.18), allows to write the objective function as follows:

$$J = \left[\theta - ZG_0\Delta\widehat{U}\right]^T \Psi \left[\theta - ZG_0\Delta\widehat{U}\right] + \Delta\widehat{U}^T R\Delta\widehat{U} \tag{5.31}$$

Now, properties of transpose matrices are applied to (5.31) to develop the cost function as follows:

$$J = \left[\theta^T - \Delta\widehat{U}^T {G_0}^T Z^T\right]\Psi\left[\theta - ZG_0\Delta\widehat{U}\right] + \Delta\widehat{U}^T R\Delta\widehat{U}$$

$$J = \theta^T\Psi\theta - \theta^T\Psi ZG_0\Delta\widehat{U} + \Delta\widehat{U}^T {G_0}^T Z^T\Psi ZG_0\Delta\widehat{U} - \Delta\widehat{U}^T {G_0}^T Z^T\Psi\theta + \Delta\widehat{U}^T R\Delta\widehat{U}$$

Grouping the elements with common factor:

$$J = \theta^T\Psi\theta - 2\Delta\widehat{U}^T {G_0}^T Z^T\Psi\theta + \Delta\widehat{U}^T\left[{G_0}^T Z^T\Psi ZG_0 + R\right]\Delta\widehat{U} \tag{5.32}$$

Finally, replacing (5.30) into (5.32) leads to

$$\begin{aligned} J = {} & [Y_r - Z(E\Delta Y - G\Delta U - P\Delta W) - Y_k]^T\Psi[Y_r - Z(E\Delta Y - G\Delta U - P\Delta W) - Y_k] \\ & - 2\Delta\widehat{U}^T {G_0}^T Z^T\Psi[Y_r - Z(E\Delta Y - G\Delta U - P\Delta W) - Y_k] \\ & + \Delta\widehat{U}^T\left[{G_0}^T Z^T\Psi ZG_0 + R\right]\Delta\widehat{U} \end{aligned} \tag{5.33}$$

Due to the first factor of (5.33) does not depend on $\Delta\widehat{U}$, the optimization problem (5.28) may be reformulated considering (5.33) as follows:

$$\begin{aligned} \min_{\Delta\widehat{U}} J = {} & -2\Delta\widehat{U}^T {G_0}^T Z^T\Psi[Y_r - Z(E\Delta Y - G\Delta U - P\Delta W) - Y_k] \\ & + \Delta\widehat{U}^T\left[{G_0}^T Z^T\Psi ZG_0 + R\right]\Delta\widehat{U} \end{aligned} \tag{5.34}$$

$$\text{Subject to:} \quad -\Delta u(k) \le -\Delta u_{min}$$

$$\Delta u(k) \le \Delta u_{max}$$

$$\Delta u(k) \le U_{max} - u(k-1)$$

$$-\Delta u(k) \le -U_{min} + u(k-1)$$

In order to formulate the problem (5.34) as (5.29) comparing factors, let us consider:

$$u = \Delta\widehat{U}$$

$$J = \frac{1}{2}u^T Hu + u^T b$$

where

$$H = {G_0}^T Z^T\Psi ZG_0 + R \tag{5.35}$$

$$b = -2{G_0}^T Z^T\Psi[Y_r - Z(E\Delta Y - G\Delta U - P\Delta W) - Y_k] \tag{5.36}$$

Meanwhile, the inequalities in (5.34) may be expressed in a matrix form as follows:

$$\gamma = \begin{bmatrix} \Delta u_{max} \\ \Delta u_{min} \\ U_{max} - u(k-1) \\ -U_{min} + u(k-1) \end{bmatrix} \tag{5.37}$$

Due to the predictive controller only implements the first sample of the $\Delta\widehat{U}$ sequence, the matrix M in (5.29) may be considered as follows:

$$M = \underbrace{\begin{bmatrix} 1 & 0 & 0 \dots & 0 \\ -1 & 0 & 0 & \dots 0 \\ 1 & 0 & 0 \dots & 0 \\ -1 & 0 & 0 \dots & 0 \end{bmatrix}}_{\lambda} \tag{5.38}$$

where $M \in \mathbb{R}^{4x\lambda}$.

Finally, within the optimization framework, the complete constrained predictive control problem (5.28) is reformulated as follows:

$$\min_{\Delta \widehat{U}} \frac{1}{2}\Delta \widehat{U}^T \left[{G_0}^T Z^T \Psi Z G_0 + R\right]\Delta \widehat{U} - \Delta \widehat{U}^T {G_0}^T Z^T \Psi \left[Y_r - Z(E\Delta Y - G\Delta U - P\Delta W) - Y_k\right] \tag{5.39}$$

$$s.t.: \quad M\Delta \widehat{U} \leq \begin{bmatrix} \Delta u_{max} \\ \Delta u_{min} \\ U_{max} - u(k-1) \\ -U_{min} + u(k-1) \end{bmatrix}$$

Downstream water level control

As was mentioned in Section 5.2, the irrigation canal control stated in this dissertation defines the discharge as control variable and the water level as controlled variable. The discharge is used as control variable in order to state the control problem as linear, the use of gate opening directly would lead to a nonlinear control problem (Sepúlveda, 2008).

The optimal solution of (5.39) gives the values of the incremental control action at instant *k* for the canal in a normal operating mode. In normal operation the main goal is achieve a water level error equal to zero. In the decentralized operation, the control algorithm computes the required gate discharge at every pool as follows:

$$\hat{Q}(k) = \widehat{U}(k) = \Delta \widehat{U}(k) + \widehat{U}(k-1) \tag{5.40}$$

Finally, a gate discharge controller (see Figure 5.4) converts the required discharge into gate opening (L) in the real-time algorithm by inverting the gate discharge equation (Chow, 1988) as follows:

$$L(k) = \frac{\hat{Q}(k)}{C_{df} B L \sqrt{2g(y_1(k) - y_2(k))}} \tag{5.41}$$

5.3.3 Predictive control with dynamic constraints

The control scheme derived in Section 5.3.2 presumes that the canal is operating in a normal mode. Two objectives are involved in the optimal predictive control: minimizing the error ($e = Yr - \hat{Y}$) between the controlled water level and the reference trajectory related to the setpoint, while keeping the control variable within "small" enough values and increments, as prescribed by the following cost function subject to specified constraints:

$$J = \left[Yr - \hat{Y}\right]^T \Psi \left[Yr - \hat{Y}\right] + \Delta\hat{U}^T R \Delta\hat{U} \tag{5.42}$$

In a canal closure operation, a third control objective needs to be addressed, which is conflicting with the objectives in the normal mode operation: it is the fact that the control variable has to decrease throughout time since the goal is that the gate openings decrease to get closed.

The closure operation of a canal by manipulating the discharges under gates is not an easy task. Decreasing the discharge by means of closing an upstream gate affects directly two controlled water levels (y_1 and y_d) in adjacent pools as it is illustrated in Figure 5.5 and described by the following relation:

$$Q = C_{df} B L \sqrt{2g(y_1 - y_2)} \tag{5.43}$$

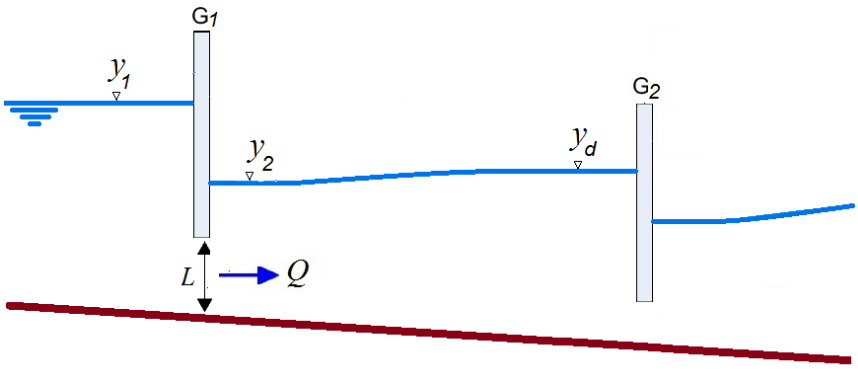

Figure 5.5 One pool configuration canal

On the other hand, during the closure operation, the control must keep the water level within specified maximum and minimum safety levels to avoid problems in the canal as it has been mentioned in the Subsection 4.3.1. There are two natural reactions in case of a closing warning. The first natural reaction is to consider closing all the gates in the canal at maximum velocity, however this reaction may result on overtopping as has been illustrated in some scenarios in Subsections 4.5.1 and 4.5.2. The second reaction is to move the gates slowly and as smooth as possible during the closure operation. However, this reaction is conflicting with the fact that feasibility of closure operation depends on the closing velocity. For instance, night closure must be as fast as possible to make it feasible, as it has been discussed in Section 4.4.

Consequently, minimizing the cost function (5.42) as an attempt to minimize the error during the closure operation is not enough to solve the challenging problem in closing/opening operating modes. Then, the optimization problem with only one cost function is not feasible because two control objectives cannot be achieved simultaneously. Therefore the predictive control problem must be reformulated in a multiobjective way. Another contribution of this thesis is related to handling a predictive control problem that cannot be solved optimizing the typical cost function (5.42) even considering time-invariant constraints. The problem is tackled with a versatile strategy

called dynamically-constrained predictive control (DCPC), which keeps the constrained predictive control formulation presented in previous section, but introducing dynamic constraints to help to drive the closure operation smoothly with the maximum discharge changes, while keeping the water level under the control objectives.

The physical idea is to restrict the control variable inside a moving interval that makes the gates to follow a smooth trajectory along the time. A significant number of simulation and experimental results executed in the cases of study proposed in this dissertation, have led to the evidence that a very convenient shape for a smooth gate trajectory that drastically reduces the amplitude peak value of the resulting water profile oscillation is the trajectory given by a sigmoid function.

The sigmoid function, also called the sigmoidal curve, is a bounded differentiable real function. The curve has a pair of horizontal asymptotes as $t \to \pm\infty$. In the DCPC context applied to irrigation canal control, the sigmoid function may be expressed as follows:

$$U_{max}(t) = \frac{Q_m}{1 + e^{-a(t-c)}} \tag{5.44}$$

where a is the slope of the curve, Q_m is the maximum amplitude (discharge), the parameter c determines the time where value U_{max} is half of Q_m and t is the time. Depending of the sign of the parameter a, the function is inherently open to right or to the left. Values less than zero are useful for closure operations and greater than zero for opening operations. Whether the discharge under gate follows an imposed sigmoidal function, the velocity of the closure of each gate in a multiple-pool canal may be managed just varying the parameters, a and c. Figure 5.6 (left) illustrates an example of sigmoidal function with values of *c=100* min, $Q_m = 15.06$ m^3/s and $a = -0.0011$. Figure 5.6 (right) illustrates an example of sigmoidal function with values of *c=100* min, $Q_m = 15.06$ m^3/s and $a = 0.0011$.

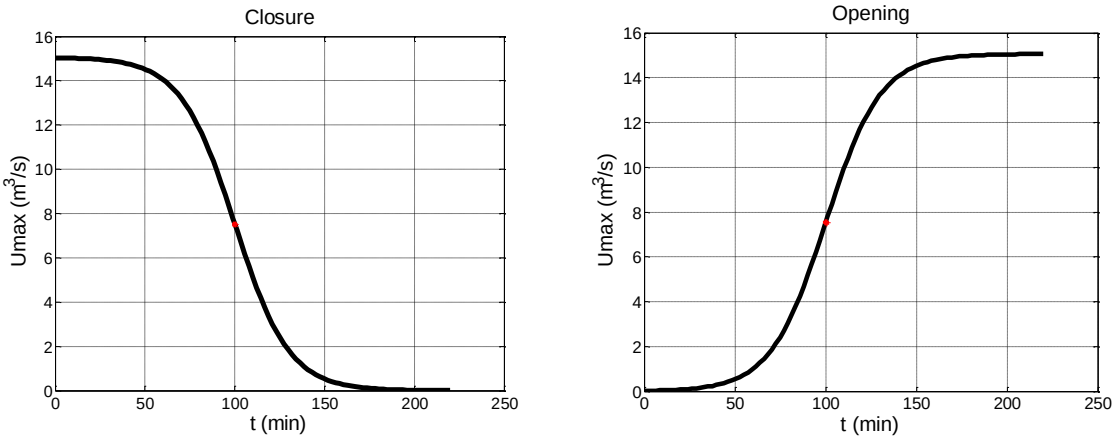

Figure 5.6 Examples of sigmoidal functions used as dynamic constraints.

In the proposed DCPC strategy, each local predictive controller considers two constraints. The first constraint is the time-invariant constraint related to discharge slew rate (5.21). The second one, is the time-variant constraint related to the discharge range (5.24).

At each control instant *k*, the optimal control problem (5.39) is solved to obtain the discharge control under the gate, where constraints are imposed on the increment (Δu_{max}) and the absolute value (U_{max}). In the case of a closure operation (similarly for opening), when the water master decides to initiate the operation, the sigmoidal function is used in the solution of the control problem (5.39). Time *t=0* in Figure 5.6 is the initial time and, for subsequent control instants *k*, the constraint on the discharge amplitude is made time-varying ($U_{max}(k)$) and it is determined by the sigmoidal function (5.44) with $t = kT_s$ (T_s is the sampling time). Therefore, the sigmoidal function is used in the DCPC control as a dynamic constraint imposed to the controller in order to allow the discharge under gates change along the time in a smooth way in the direction of closing or opening, depending on the operation mode.

5.4 Supervised decentralized predictive control (SDPC)

The result of Section 5.3 is a control scheme able to govern the upstream gate of a single pool through the solution of the optimal predictive control (5.39) at each control instant *k*, including the dynamic constraints in the closure and opening modes. When the objective is to control a multi-pool canal, the individual controllers are assembled to set up the overall supervised decentralized predictive control (SDPC) scheme outlined in Section 5.2.2 and illustrated in Figure 5.3

The supervisor is responsible for managing a cyclic sequential movement of each motorized gate that delimits the pool of the entire irrigation canal. The supervisor may be located at headquarter (master station). Each subsystem corresponds with a controlled pool. Each decentralized control (control unit) is a local automatic water level controller. Each control unit requires the current state of its controlled pool and information of neighbor pools. For the practical implementation, the proposed control system requires a remote terminal unit (RTU). The RTU monitors the water levels and equipment status, and transmit these data to the supervisor.

The supervisor is also responsible for scheduling the parameters of the controllers depending on the operating mode. Particularly important is the management of the constraints in the closure and opening modes, which becomes fundamental in the presence of unexpectedly large disturbances.

In a well (a priori) defined operation scenario (a closure, for instance) the supervisor may tune the sigmoidal curve to state reasonable dynamic constraints according to the maximum allowed discharge for each controlled pool. However, during a closure operation, the presence of an unexpectedly large disturbance may force the control variable outside its limits. Therefore, the optimizer cannot find a practical value to introduce the control variable into its feasible region. In these circumstances, the constraints become temporarily incompatible (Camacho & Bordons, 2004) and the predictive control problem can become infeasible, because the region defined for the control variable by the set of constraints is empty.

In the proposed DCPC control scheme, a large disturbance may occur under two situations. The first situation is a sudden discharge change more than 10% of the operating discharge with regard to the previous discharge. The second situation is a sudden change in water level greater than 5% of the set point with regard to the previous measured water level.

The solution proposed in this thesis to tackle the unexpectedly large disturbance problem, is a supervised automatic control that reshapes systematically the sigmoidal function through the constraints relaxation. The relaxation or softening is present throughout the disturbance. As a result of relaxation, constraints related to the control variable range are treated as soft constraints in the optimization problem statement. In the literature of quadratic programming, constraints which cannot violated are referred to as hard constraints, while those which can be violated are known as soft constraints (Camacho & Bordons, 2004).

In order to include the soft constraints, the general form of constraints are expressed as follows:

$$M\Delta u \leq \gamma + V\mathrm{z} \tag{5.45}$$

In this inequality, matrix *M*, vectors γ and V depend on both process parameters and signal limits. *M*, and γ are calculated before starting an operation that involve an abrupt change in the operating condition. Matrix *M* and hard constraints related to discharge slew rate do not change throughout the closure/opening operations. Meanwhile, *z* depends on the process state that changes every sampling time, and it is recomputed accordingly to the disturbances along the canal. For instance, in the presence of a positive disturbance caused by a strong runoff or a storm that add water to a pool during a closure operation, constraints relax by increasing its value.

With soft constraints, the optimization problem (5.29) is modified to

$$\begin{aligned} \min_{u} \quad & \frac{1}{2}u^T H\, u + u^T b \\ s.t.: \quad & Mu \leq \gamma + V\mathrm{z} \end{aligned} \tag{5.46}$$

Consequently, the complete optimization problem (5.39) may be expressed as follows:

$$\begin{aligned} \min_{\Delta\widehat{U}} \ & \frac{1}{2}\Delta\widehat{U}^T\left[{G_0}^T Z^T \Psi Z G_0 + R\right]\Delta\widehat{U} \\ & - \Delta\widehat{U}^T {G_0}^T Z^T \Psi[Y_r - Z(E\Delta Y - G\Delta U - P\Delta W) - Y_k] \end{aligned} \tag{5.47}$$

$$s.t.: \quad M\Delta\widehat{U} \leq \begin{bmatrix} \Delta u_{max} \\ \Delta u_{min} \\ U_{max}(k) - \widehat{U}(k-1) \\ -U_{min}(k) + \widehat{U}(k-1) \end{bmatrix} + \begin{bmatrix} 0 \\ 0 \\ 1 \\ 1 \end{bmatrix} [Qw_i(k)] \tag{5.48}$$

where the U_{max} value is computed at any control instant, k according to the sigmoidal function (5.44), $U_{min} = U_{max} - B_{pz}$, where B_{pz} is a scalar that determines the width of the permitted zone during a close/opening operation and Qw_i is the disturbance of *i-th* pool of the canal (lateral offtake/intake).

When this control problem is integrated to the overall decentralized control scheme, the supervisor plays two important roles in: a) locating the pool where the large disturbance Qw_i occurs, and b) re-tuning the sigmoidal trajectory to adapt to the new discharge conditions. Practical details illustrating these issues are made clear in chapter 6, in different scenarios involving large disturbances.

5.5 Computational implementation

There is not an explicit analytic solution of the optimization problem (5.46) as it exists in the case without constraints. Subsequently, the predictive control problem may be solved minimizing the quadratic cost function and the linear constraints recursively (Camacho & Bordons, 2004). The predictive control solves the optimal control problem, this is performed on-line for the current state of the plant at each control instant *k* considering the moving prediction horizon. The initial state is the current state of the system being controlled. There are several techniques to solve the quadratic programming problem. (Camacho & Bordons, 2004) shows a revision of the main algorithms used in predictive control. This section is not intended to describe in detail an optimization technique, merely to highlight some relevant aspects of the algorithm used in this dissertation.

To obtain the numerical solution of the constrained optimization problem, the Hildreth's quadratic programming algorithm (Luenberger, 1969), (Wismer & Chattergy, 1978) has been used in this dissertation. The Hildreth's procedure solves the optimization problem (5.46). All the required information about the algorithm can be found in (Wang, 2009). To deal with inequality constraints, the Hildreth's procedure reduces the problem to an equality constraint problem using Lagrange multipliers. In this way, the procedure solves the following dual problem:

$$\max_{\lambda \geq 0} \min_{u} \left[\frac{1}{2} u^T H u + u^T b + \lambda^T (Mx - \gamma) \right] \tag{5.49}$$

The problem (5.49) considers the so-called Lagrange expression, which is expressed as the objective function

$$J_L = \frac{1}{2} u^T H u + u^T b + \lambda^T (Mx - \gamma) \tag{5.50}$$

The minimization of the Lagrange expression, gives the optimal λ and *u* taking the first partial derivatives and then equating these derivatives to zero (Wang, 2009):

$$\frac{\partial J_L}{\partial u} = Hu + b + M^T \lambda = 0 \tag{5.51}$$

$$\frac{\partial J_L}{\partial \lambda} = Mx - \gamma = 0 \tag{5.52}$$

Both equations (5.51) and (5.52) contain $n+m$ variables *u* and λ, where *n* is the dimension of *u* and *m* is the dimension of λ. The variables *u* and λ are the necessary conditions for minimizing the Lagrange expression with equality constraints. The Lagrange multipliers are the elements of vector λ.

Isolating *u* from (5.51) and then replacing it into (5.52) leads to

$$u = -H^{-1}(M^T \lambda + b) \tag{5.53}$$

$$\lambda = -(MH^{-1}M^{T})^{-1}\,(\gamma + MH^{-1}b) \tag{5.54}$$

The optimal solution of (5.46) using a simple and effective algorithm implemented with the Hildreth's procedure gives the values of the incremental control action at instant k of the supervised decentralized predictive control with dynamic constraints. The implementation of the algorithm in Matlab (Mathworks, 2008) is shown in appendix A.

5.6 Concluding remarks

The main outcome of this chapter is a supervised decentralized predictive control strategy for the automatic operation of a multi-pool irrigation canal. Local controllers are derived based on the on-line computational solution of optimal control problems with time-varying constraints. A supervisor is used to manage the sequential operation of the local controller and the tuning of the constraints, particularly in the closure/opening scenarios in the presence of large unknown disturbances. Practical details related to the implementation and the performance are presented and discussed in the next chapter.

Chapter 6

Simulation and real-time results

6.1 Introduction

The aim of this chapter is to illustrate, by both simulation and experimental results, the performance of the supervised decentralized predictive control (SDPC) with dynamic constraints developed in Chapter 5, as a convenient strategy for the automatic closure and opening of irrigation canal systems. The simulations results in the two cases of study have been obtained using the SIC software. The SDPC is tested in real time in the experimental facility of the Technical University of Catalonia. This chapter also shows some practical aspects related to the real-time implementation in the laboratory canal to allow doing experiments involving abrupt changes in the canal operating points.

6.2 Simulation results in the case studies

The simulations of this subsection are mainly focus on the unsteady flow calculation. Simulation experiments are stablished to test scenarios that involve abrupt changes in the operating regime. All simulation experiments start from a steady state conditions. All the algorithms have been implemented using Matlab/Simulink environment (Mathworks, 2008). The interaction between the control algorithms and the hydraulic scenarios implemented in SIC is achieved using the *regulation module* available in SIC.

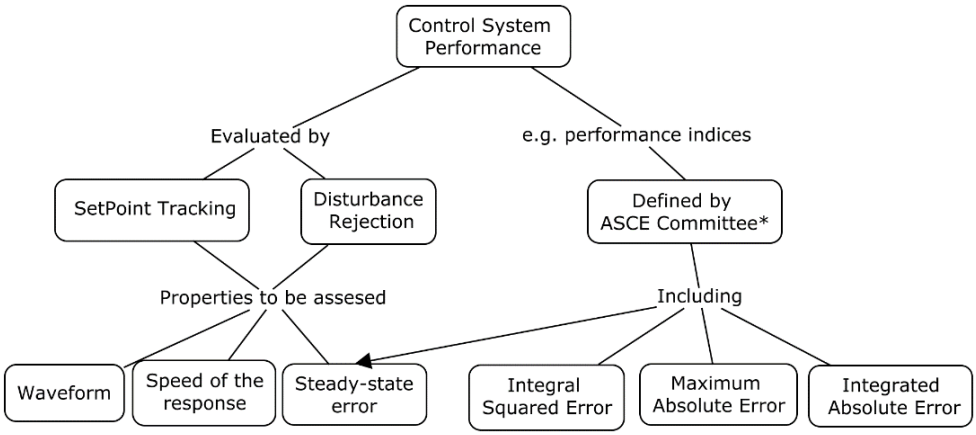

Figure 6.1 Performance evaluation indexes

In order to evaluate the perfomance of the control system in irrigation canals, test experiments as setpoint tracking and disturbance rejection are fulfilled. Some performances indexes suggested by the American Society of Civil Engineers (ASCE) committee are considered to evaluate the performance. The strength of the control system against modeling error and disturbances is also assessed (see the concept map depicted in Figure 6.1).

The evaluation of the waveform is related to the oscillatory nature of the response of the water levels. This oscillatory behavior prevents the controlled variable to reach the setpoint value quickly. If the oscillations increase, water level becomes considerably larger than the setpoint. This situation might lead to harmful effects on the canal as was depicted in Subsection 4.3. A performance index such as maximum absolute overshoot is included in the properties of the waveform.

In order to evaluate the quality of the controlled responses, the following error based performance indexes proposed by (Clemmens et al., 1998) are used in this dissertation:

RMSE: Root Mean Squared Error
MAPE: Mean Absolute Percentage Error
ISE: Integral Squared Error
IAE: Integral Absolute Error
MAO: Maximum Absolute Overshoot
SSE: Steady State Error

The performance indexes are defined as follows:

$$RMSE = \sqrt{\frac{1}{N}\sum_{k=1}^{N}\left(Y_k - \hat{Y}_k\right)^2}$$

$$MAPE = \frac{100}{N}\sqrt{\sum_{i=1}^{N}\left|\frac{Y_k - \hat{Y}_k}{Y_i}\right|}$$

$$ISE = \sum_{k=1}^{N} \left(Y_k - \hat{Y}_k\right)^2$$

$$IAE = \frac{T_s}{T} \sum_{k=1}^{T} \left|Y_k - \hat{Y}_k\right|$$

where $Y_k - \hat{Y}_k$ is the error related to the difference between the controlled water level and the setpoint (target water level). The controlled water level, Y_k is the observed water level at time *k*. *N* is the number of samples in the test. $T = N * T_s$ is the time period for the test.

The RMSE is a measure related to the standard deviation of the difference between the setpoint and the measured value. Meanwhile, the MAPE is an index used to express the accuracy as a percentage. The *ISE* is a measure of error that integrates the square of the error over time. The ISE penalizes large errors more than smaller ones and the IAE integrates the absolute error over time.

Practical performance indexes useful in control system are the maximum absolute overshoot (MAO) and the steady state error (SSE). The MAO is a quantity applied to both disturbance rejection and setpoint tracking responses. The MAO is estimated with the maximum peak of the water level waveform. The SSE is the difference between the setpoint and the actual water level when a canal reach a new steady state.

6.3 Simulation of water level control at canal PAC-UPC

This section is devoted to show the numerical simulation of both closure and opening operations on the canal PAC-UPC. The automatic control system uses the predictive controller with dynamic constraints presented in Chapter 5. The tests have been done on the three pools configuration depicted in Figure 6.2. Water is drawn at two points along the length of the canal, as it is illustrated in Figure 6.2. The lateral discharges are lateral offtakes, which are equivalent to the disturbances for the control system. The gate discharge coefficients are 0.63, 0.65 and 0.69 for G_1, G_2 and G_3 respectively.

6.3.1 Control objective and operating scenarios

The overall control objective is to drive the system to an equilibrium state for which the water levels are equal to the setpoint (constant reference), meanwhile the operating point is changed abruptly. The regulating task is evaluated by both setpoint tracking and disturbance rejection. The specific requirements to bear in mind for the proposed tests are:

- Canal freeboard of 8 cm.
- Manage the canal operation to drive the discharges from 120 l/s to 1.6 l/s in less than eight minutes. This mean an 8 min-settling time.

- The accepted steady state offset (error of the controlled water levels) is 2 cm (lower than 2%).
- The maximum absolute overshoot (ripple value) must be less than 5% of the setpoint for every controlled water level. It is expected less than 92 cm for the first pool, this value means a percentage overshoot lower than 8% of the top of the canal lining.

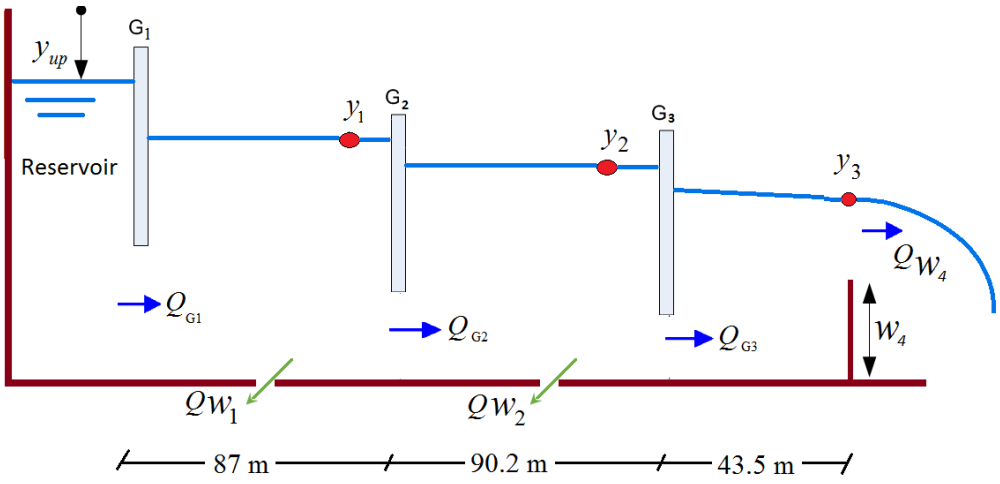

Figure 6.2 Scheme of the Canal PAC

Three scenarios have been simulated with the Saint Venant (SV) model of the laboratory canal in order to check the controller performance in presence of abrupt change in operating condition.

- Scenario 1: Automatic canal closure without disturbances. The initial operating flow is 113 l/s.
- Scenario 2: Automatic canal opening from 0 l/s to 113 l/s without disturbances. The opening time must be less than 12 minutes.
- Scenario 3: Automatic closure in the presence of a disturbance $\boldsymbol{Qw_1}$ of 42 l/s during $0 \leq t \leq 2$ min. After on, the disturbance changes suddenly to 0 l/s. The 42 l/s are equivalent to 31% of the operating discharge in the first pool of the canal.

6.3.2 Implementation issues

In order to implement the supervised decentralized predictive control (SDPC) for water level control in the canal PAC UPC, three local DCPC controllers were designed. The parametric models used in the control are described in Subsection 3.6. The incremental formulation of the predictive control has been used to control the downstream water levels. The control action implemented in each pool is determined by solving equations (5.47) and (5.48) at each sampling time, *k*. The supervisor is in charge of coordinating the overall work of the controllers and the dynamic constraints as described in Section 5.3.3. Particularly, in the presence of large unknown disturbances along the closure/opening scenarios, the supervisor is also responsible for redefining

(reshaping) the dynamic constraints. The maximum gate opening is determined by the water level value, because the undershot gates are not allowed to come out the water.

The general tuning parameters of each local controller are obtained considering the time delay and the dynamics of each pool. The prediction horizon (λ) is chosen greater than the time delay. The weighting parameter R_C is calculated by normalizing the objective function with maximum allowed values estimates. The maximum accepted water level error is chosen to be 3 cm, therefore, the maximum allowed value estimated of the water level, e_{MAVE} is equal to 0.03 m. The MAVE of the change in discharge, Δu_{MAVE} is chosen to be 0.01 m^3/s. These MAVE values were used with positive results in a previous experimental work by (Horváth, 2013). In this dissertation, several sets of tuning values were tested in simulation. For the prediction horizon (λ), it is recommended integer values over the entire interval [10, 20]. For the weighting factor, it is recommended $R_C > 10$. The chosen tuning parameters are detailed in Table 6-1. The sampling time has been fixed to 10 s.

Pool	λ	R_C
Pool 1	10	15
Pool 2	10	15
Pool 3	10	15

Table 6-1 Tuning parameters of local controllers at canal PAC UPC

6.3.3 Results

- *Scenario1*: This test is devoted to analyze a closure operation without changes in the lateral offtakes. This scenario starts from the steady state detailed in Table 6-2. The initial operating flow is 0.113 m^3/s and the height of the final weir (W_4) is 35 cm. The Backwater curve is illustrated in Figure 6.3.

Qop **[l/s]**	y_1 **[cm]**	y_2 **[cm]**	y_3 **[cm]**	L_1 **[cm]**	L_2 **[cm]**	L_3 **[cm]**	W_1 **[cm]**	W_2 **[cm]**	W_4 **[cm]**
113	88	77	65	15	29.8	26.1	90	90	35

Table 6-2 Initial steady state for Scenario 1

Simulation of the closure operation of the canal PAC-UPC using SDPC without any presence of disturbances is depicted in Figure 6.4. The test is detailed in Table 6-3. The water level setpoint (SP_1) is 88 cm for the first pool and SP_2 is 77 cm for the second pool. There are only two controlled water levels because of the presence of the sharp crested weir (W_4) at the downstream end of the canal. The final value of y_3, after a considerable time, is determined by the weir height. In this closing scenario, the flow through each canal pool decrease gradually from its initial value (113 l/s) to a zero discharge in a progressive and smooth manner in less than 7 minutes. The SDPC

control makes the gates operate sequentially progressing downstream till reach a zero gate opening.

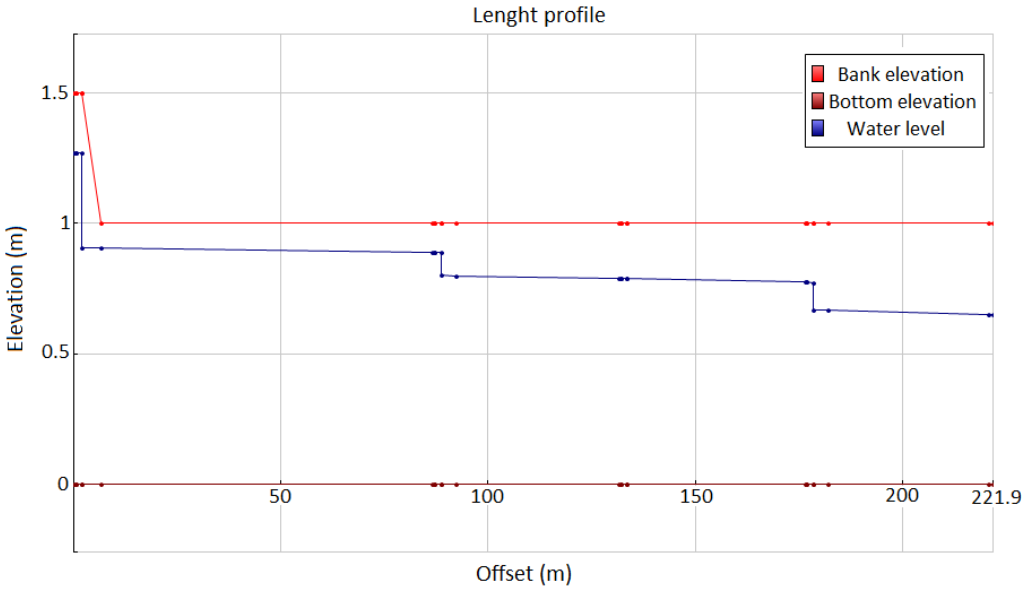

Figure 6.3 Backwater curve of the initial steady state of Canal PAC-UPC obtained by SIC

The controlled system exhibits a satisfactory behaviour based on performance requirements given in Subsection 6.3.1. The maximum absolute overshoots are 89.45 cm and 78.3 cm for y_1 and y_2 respectively (lower than 2 % of the setpoint for both cases). The steady state errors for y_1 and y_2 are 1.16 and 0.37 cm respectively, which represent values lower than 1.5 % of the setpoint for both cases.

Time [sec]	**Q_{op} [l/s]**	***SP_1* [cm]**	***SP_2* [cm]**	***SP_3* [cm]**	**W_1 [cm]**	**Q_{W1} [l/s]**	**W_2 [cm]**	**Q_{W2} [l/s]**	**W_4 [cm]**
0	113	88	77	65	90	0	90	0	35
5	113	88	77	--	90	0	90	0	35
480	0	88	77	--	90	0	90	0	35

Table 6-3 Test of closure operation without disturbances

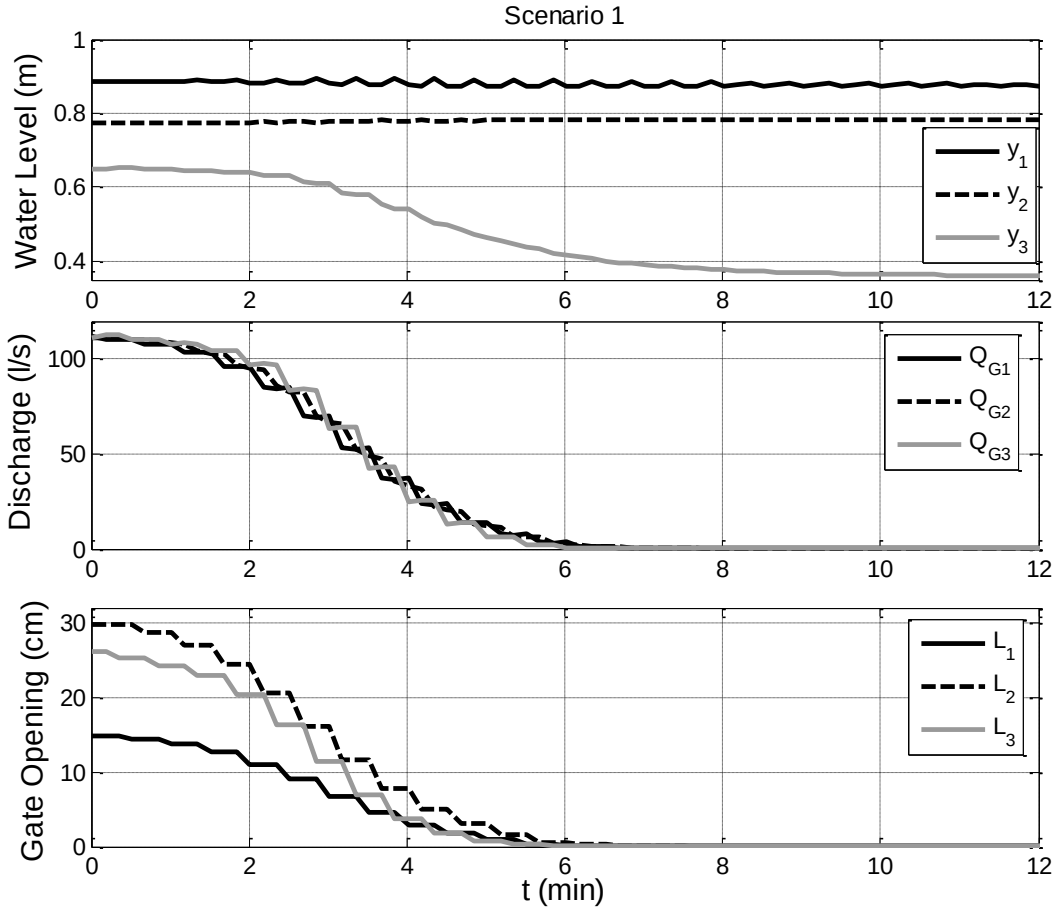

Figure 6.4 Simulation results of automatic closure of canal PAC-UPC under SDPC

- *Scenario 2*: This scenario is devoted to analyze the automatic canal opening from 0 l/s to 113 l/s without disturbances. This scenario starts from the steady state detailed in Table 6-4

Qop **[l/s]**	y_1 **[cm]**	y_2 **[cm]**	y_3 **[cm]**	L_1 **[cm]**	L_2 **[cm]**	L_3 **[cm]**	W_1 **[cm]**	W_2 **[cm]**	W_4 **[cm]**
0	88	77	36	0	0	0	90	90	35

Table 6-4 Initial Steady State for Scenario 2

The automatic opening operation using SDPC is depicted in Figure 6.5. The time taken to achieve a new steady state hydraulic condition after the canal has been opened is ten minutes long approximately. The three discharges change from 0 l/s to a baseline in a smooth way. The opening operation is longer than the closure one due to the system has to fill up the downstream pool whose water level was just determined by the downstream weir height W_4.

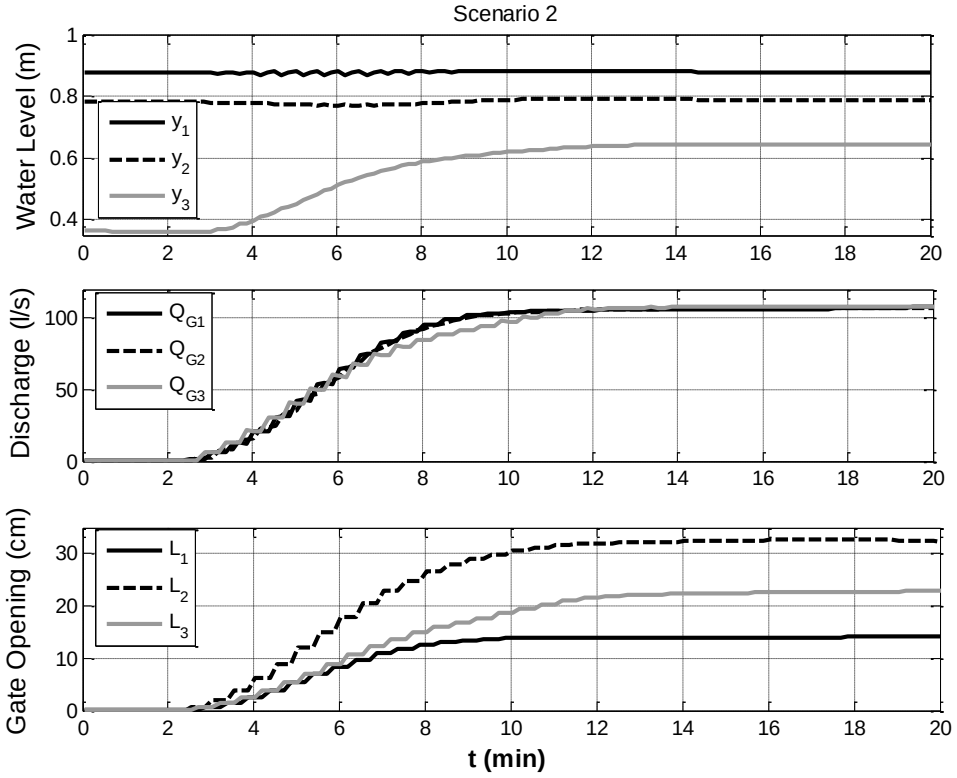

Figure 6.5 Simulation results of opening operation of canal PAC-UPC under SDPC

In this scenario there are three controlled water levels. It is noteworthy that the opening scenario assumes that a closure operation has been executed previously, which means that the volume of the third pool (and therefore its water level) has decreased after the closure operation due to the presence of the weir at the end of the canal. In this way, the water level setpoint in the first pool (SP_1) has been set to 88 cm and SP_2 has been set to 77 cm for the second pool. Meanwhile, for the third pool, a setpoint curve for water level y_3 ($SP_3(t)$) has been proposed as the reference trajectory in the formulation of the cost function (5.6). The goal of the reference trajectory is helping to fill up the third pool in a smooth way.

The reference trajectory SP_3 avoids large positive changes in the setpoint of the third pool. SP_3 also prevents from a significant overshooting in the water level y_3 because the gates are moving in such a way that they reduce the oscillations. In this way, the automatic control system leads the controlled variable to a desired value following a suitable sigmoidal function described by:

$$SP_3(t) = \frac{y_3^*}{1 + e^{-a(t-c)}} + y_3(0) \tag{6.1}$$

where y_3^* is the desired water level final value, $y_3(0)$ is the water level at time *t=0*, parameter *a* determines the slope of the curve, the value *c* is the half of the opening time and t is the time. Time *t=0* is the opening initial time and, for subsequent control instants *k*, the setpoint of the water level y_3 is made time-varying with $t = kT_s$, where T_s is a the sampling time. An example of the reference trajectory, $SP_3(t)$ is illustrated in Figure 6.6.

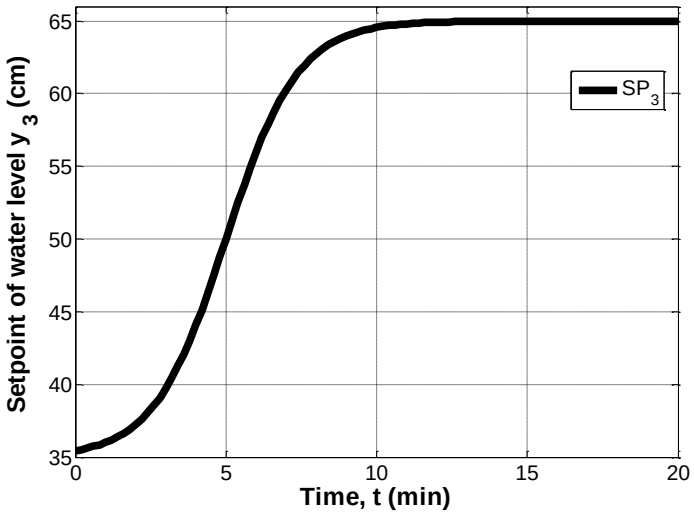

Figure 6.6 Sigmoidal function of SP_3, with $a = 0.014$, c=5 min, y_3^* =65 cm and $y_3(0)$=35 cm

The closed-loop automatic control exhibits a positive behaviour based on various performance indexes. The maximum absolute overshoots of both levels are lower than 2%. The MAO of $y_1$is 88.73 cm, which is equivalent to 0.83% of SP_1. The MAO of y_2 is 78.3 cm, which is equivalent to 1.72% of SP_2. The steady state errors are: 0.44 cm for y_1, 0.4 cm for y_2 and 0.45 cm for y_3. These values are lower than 1.5 % of every water level setpoint.

- *Scenario 3*: This scenario is devoted to analyze the automatic closure in the presence of a strong disturbance. The lateral offtake $\boldsymbol{Qw_1}$ of 41 l/s is present during $0 \leq t \leq 2$ min. After on, the disturbance changes suddenly to 0 l/s. The test is detailed in Table 6-5.

Time [sec]	$\boldsymbol{Q_{op}}$ **[l/s]**	$\boldsymbol{SP_1}$ **[cm]**	$\boldsymbol{SP_2}$ **[cm]**	$\boldsymbol{SP_3}$ **[cm]**	$\boldsymbol{W_1}$ **[cm]**	$\boldsymbol{Q_{W1}}$ **[l/s]**	$\boldsymbol{W_2}$ **[cm]**	$\boldsymbol{Q_{W2}}$ **[l/s]**	$\boldsymbol{W_4}$ **[cm]**
0	131	82	73	61.2	65	41	90	0	35
5	131	82	73	--	65	41	90	0	35
120	120	82	73	--	90	0	90	0	35
480	0	82	73	--	90	0	90	0	35

Table 6-5 Disturbance test in the Scenario 3.

The 41 l/s are equivalent to 31% of the operating discharge in the first pool of the canal. The purpose of this scenario is to resemble that, at the beginning of the simulation, there were a farmer irrigating his/her local crops during the closure operation. However, at time *t = 2* min, the farmer suddenly decided stop irrigation due to a warning of closure. In this scenario, only the appointed disturbance is considered, the lateral offtake $\boldsymbol{Qw_2}$ being equal to zero.

The closure operation of Scenario 3 under SDPC is depicted in Figure 6.7. The closing time is 7.5 minutes approximately. The process duration is longer than the closure operation without

disturbances due to that the supervisor redefines the dynamic constraints to deal with the strong disturbance (as it is explained in Subsection 6.3.4). The higher the disturbance, the longer the closing time.

The closed-loop automatic control exhibits a satisfactory behaviour even in presence of disturbance along the closure operation. The maximum absolute overshoots of both levels are lower than 7%. The MAO of $y_1$is 87.16 cm, which is equivalent to 6.3% of SP_1. The MAO of $y_2$is 73.6 cm, which is equivalent to 0.83% of SP_2. The SSE for y_1 and y_2 are 0.13 and 0.07 cm respectively, which represent values lower than 1 % of the setpoint for both cases.

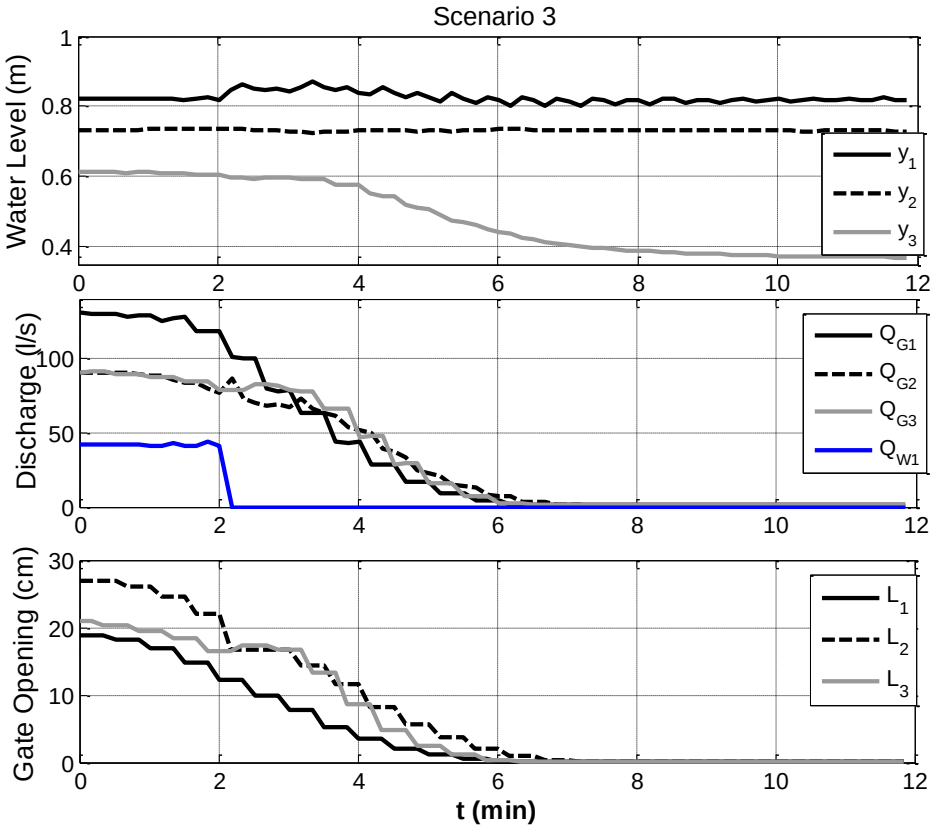

Figure 6.7 Simulation results of closure operation with disturbance test at canal PAC-UPC.

6.3.4 Discussion of results

In all the scenarios, water levels in each pool remain inside the safety band along both transient and steady response. As it can be noted in figures 6.4, 6.5 and 6.7 there is no overtopping neither in the closure nor in the opening operation. The closure operation performance has improved comparing to open-loop closure operations illustrated in the local manual closure at Section 4.5.1.

The laboratory canal is prismatic and the lengths of the first two pools are quite similar (87 m and 90.2 m respectively). As a consequence, the dynamic constraints for pools 1 and 2 are quite similar during a closure operation without disturbances, as it is illustrated in Figure 6.8 (left). The sigmoidal function that determines the constraint for discharge in the third pool, U_{max3}, has a little

bit higher slope because the length of pool 3 (45 m) is approximately a half of pools 2 and 1. As it has been observed from the experimental data, the time delay of pool 3 is lower than the first two pools in the laboratory canal.

In closure scenarios without disturbances, the gate openings decrease in a smooth way till reach the zero gate position. The supervisor set the parameters of the dynamic constraint that determines the maximum discharge of the *i-th* pool following the sigmoidal function (5.44).

On the other hand, if a sudden raise of the water level occurs, then the supervisor will reshape the dynamic constraints in the next sampling time. The supervisor is checking values of water levels at every sampling time and compares current values with previous values in order to determine higher rates of water level changes caused by a change in the lateral offtake/intake (disturbance). Consequently, the dynamic constraints (and therefore the gate openings) are different in the presence of disturbances, as it is illustrated in Figure 6.8 (Scenario 3).

As a consequence of the measurement of the higher rates of water level changes, the supervisor detects where the disturbance is located, and then it decides the way to operate the canal during the closure/opening operating mode. For instance, in the presence of a positive disturbance (intake) during a closure operation, the upstream local controller remains with the same constraint. However, the rest of downstream discharge constraints change their parameters to allow the transmission of the incorporated discharge to the canal. The gate openings change the negative slope as soon as a raise of water is detected (see Figure 6.8 and Figure 6.9 related to the Scenario 3). Assuming that Q_{w1} changes suddenly at time $k = k_d$, making the water level y_1 increase suddenly, then the dynamic constraint $U^1_{max}(k)$ does not change over the closing time (see Figure 6.8 related to the Scenario 1). However, the supervisor will change both constraints, $U^2_{max}(k)$ and $U^3_{max}(k)$, by means of updating their amplitude value Q^2_m and Q^3_m in proportion to the disturbance amplitude presented in the canal, namely:

$$Q^2_m(k^+_d) = Q^2_m(k^-_d) + Q_{w1}$$

$$Q^3_m(k^+_d) = Q^3_m(k^-_d) + Q_{w1}$$

where $Q^i_m(k^+_d)$ indicates the discharge value defined a sampling time after the change of Q_{w1} and k^-_d indicates a sampling time before the sudden change of Q_{w1}.

An additional way used by the supervisor to reshape the dynamic constraints in the presence of large disturbances, is by time shifting the original dynamic constraint to Δc. In this way, the original constraint given by (5.44) is modified to the following sigmoidal function:

$$U_{max}(t) = \frac{Q_m}{1 + e^{-a(t-(c+\Delta c)}} \tag{6.2}$$

where the parameter Δc shifts the function left or right according to its sign. Effectively, $U_{max}(t - \Delta c)$ equals what $U_{max}(t)$ was before as long as both parameters Q_m and a remain with the same value.

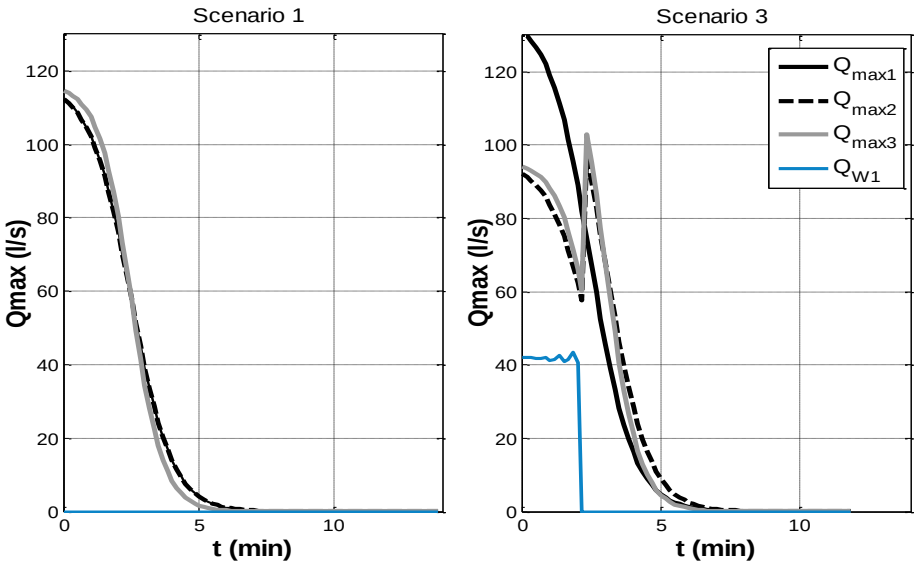

Figure 6.8 Sigmoidal functions of Scenarios 1 and 3

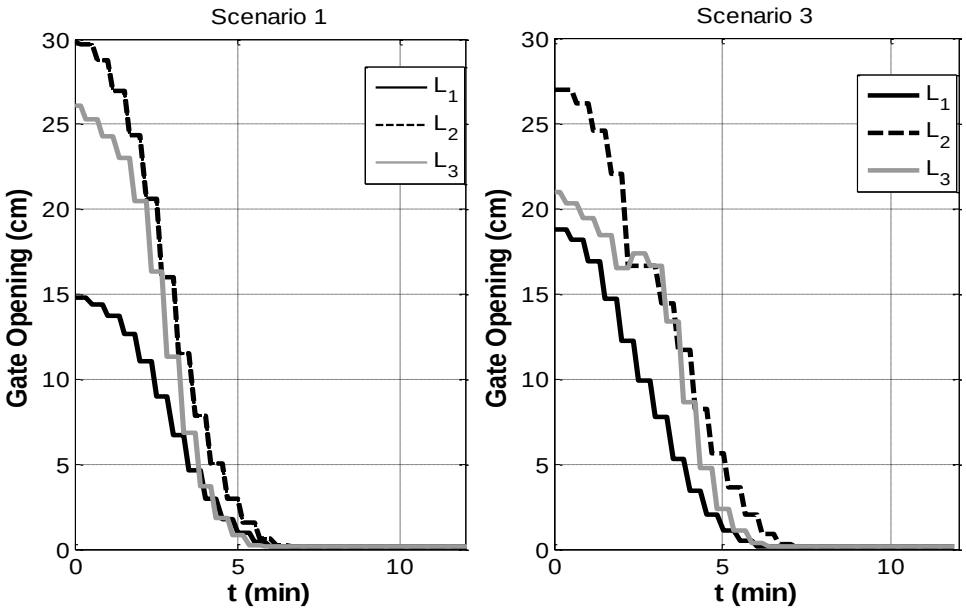

Figure 6.9 Gate openings of Scenarios 1 and 3

6.4 Simulation of water level control at Ebro River left bank (ERLB) canal

This subsection is devoted to the simulation of the downstream water level control of the ERLB canal. In order to conduct a series of simulations, the configuration depicted in Figure 6.10 has been used. Water may be drawn at four points along the length of the canal, as it is illustrated in Figure 6.10. The lateral discharges, Q_{S1}, Q_{S2}, Q_{S3} and Q_{S4} are the disturbances for the control system. The disturbances may be positive or negative. A positive disturbance or intake (a pumping for instance) is equivalent to impose a constant discharge as boundary condition at the

offtake in SIC. For the simulation, it is assumed that the pump has a flowmeter to measure the positive disturbance. Meanwhile, a negative disturbance is equivalent to a lateral offtake, which is a point of outflow. The negative disturbances are calculated using the formula of the discharge over a sharp crested weir (Horváth, 2013):

$$Q = \frac{2}{3}\sqrt{2g}C_{dw}BH_e^{3/2} \tag{6.3}$$

where H_e is the head over the weir, C_{dw} is the discharge coefficient and B is the width of the weir.

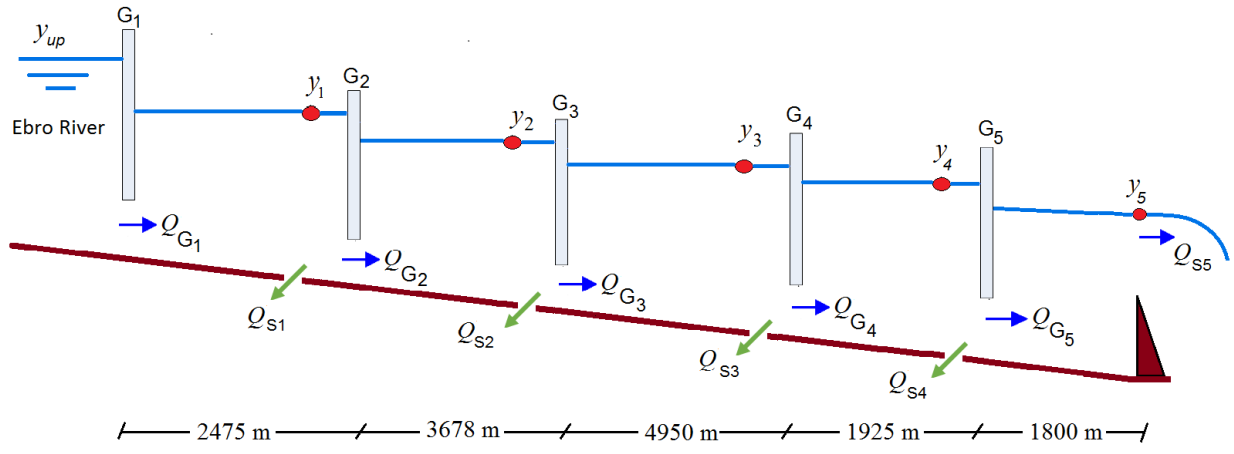

Figure 6.10 Sketch of the ERLB canal

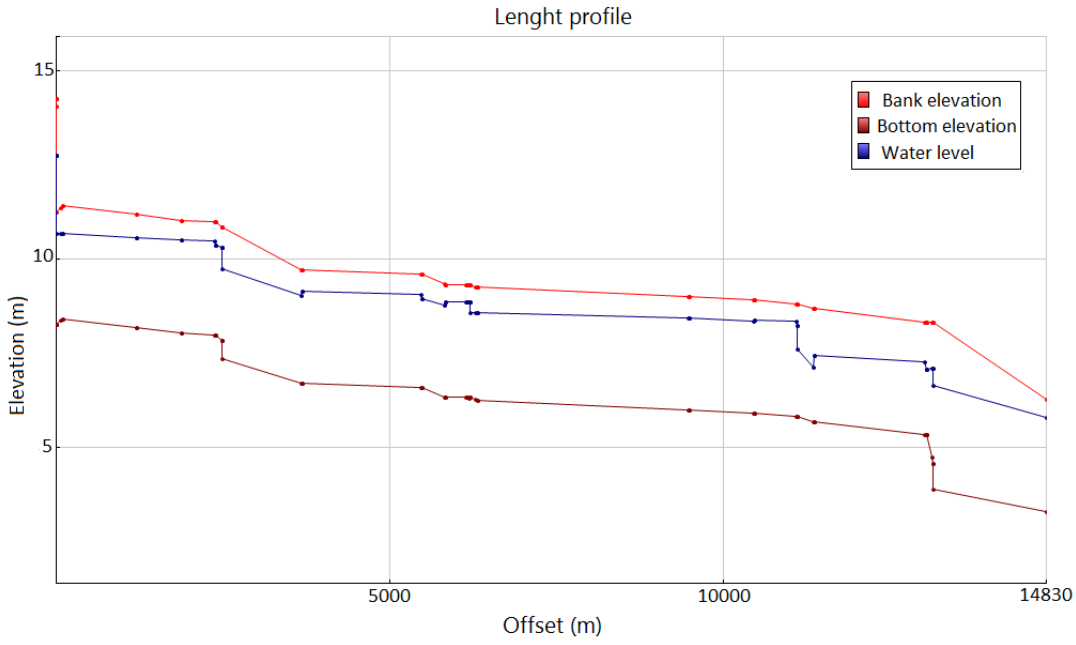

Figure 6.11 Water surface profile of initial steady state of ERLB canal obtained by SIC.

The simulation for closure operation starts with an operating point of 15 m^3/s. In order to obtain the initial state conditions, the gate openings are: $L_1 = 0.483, L_2 = 1.827, L_3 = 1.326, L_4 = 1.753$ and $L_5 = 2.109$ m. The steady state water levels are: $y_1 = 2.5, y_2 = 2.54, y_3 = 2.46,$

$y_4 = 2.51$ and $y_5 = 2.5$ m. These gate openings will remain the same along 79 min of simulation. After on, at $t = 80$ min, it is considered the beginning of the closure operation. The time $t = 250$ min is considered the end of the simulation for the canal closure operations. Figure 6.11 shows the backwater curves of steady state of the ERLB canal.

6.4.1 Control objective and operating scenarios

The overall control objective of the predictive control system is to regulate the downstream water level while the operating flow changes in a wide range. The specific requirements to bear in mind during the automatic closure and opening operations are:

- Once the closure (or opening) operation has started, the setpoints for all water levels is 2.5 m.
- Managing the canal operation in order to drive the discharges from 15 m^3/s to 2 m^3/s in less than 3 hours, namely a three hours-settling time. This time is also a requirement for the opening operation.
- The accepted steady state offset (error for the controlled water levels) is ±5 cm (2%).
- The maximum absolute overshoot is expected to be less than 2.7 m, namely a percentage overshoot lower than 8%. Large overshoots are undesirable because percentage overshoot exceeding 20% produces overtopping.

Nine scenarios have been designed to simulate the performance of the predictive control system with abrupt changes in the operating conditions in the canal. The first scenario is devoted to test a partial closure of the ERLB canal. Seven scenarios have been simulated in order to check the disturbance rejection during a closure operation. The eighth scenario simulates the closure operation and the ninth scenario simulates the opening operation. Simulation results include three variables, downstream water levels, discharges under gates and gate openings. In the scenarios only the appointed disturbance is considered, while the rest of the spillway discharges are equal to zero. The scenarios are the following:

- Scenario 1: Partial closure from 15 m^3/s to 2 m^3/s with no disturbances.
- Scenario 2: Partial closure with a positive disturbance (lateral intake) $\boldsymbol{Qs_1}$ of 5.8 m^3/s, for $100 \leq t \leq 140$ min.
- Scenario 3: Partial closure with a lateral intake of $\boldsymbol{Qs_1}$ of 6.8 m^3/s, for $100 \leq t \leq 162$ min.
- Scenario 4: Partial closure with a lateral intake of $\boldsymbol{Qs_2}$ of 5.8 m^3/s, for $100 \leq t \leq 140$ min.
- Scenario 5: Partial closure with a lateral intake of $\boldsymbol{Qs_3}$ of 5.8 m^3/s, for $100 \leq t \leq 150$ min.
- Scenario 6: Partial closure with a lateral offtake of $\boldsymbol{Qs_1}$ of -4.3 m^3/s, for $100 \leq t \leq 250$ min.
- Scenario 7: Partial closure with two lateral offtakes of $\boldsymbol{Qs_1}$ of -4.3 m^3/s, for $100 \leq t \leq 250$ min and $\boldsymbol{Qs_3}$ of -3.8 m^3/s, for $110 \leq t \leq 250$ min.
- Scenario 8: Total closure from 15 m^3/s to 0 m^3/s without disturbances.
- Scenario 9: Total opening from 0 m^3/s to 15 m^3/s without disturbances.

For the closure operation scenarios, 1 to 7, the downstream boundary condition at the end of the canal is determined by the scheduled hydrograph shown in Figure 6.12. The discharge starts at 15 m^3/s and it ends at 2 m^3/s. Changing from an operating point of 2 m^3/s to zero discharge could be done closing all the gates simultaneously at maximum velocity with no risk of overtopping as it is remarked by (Soler et al., 2014).

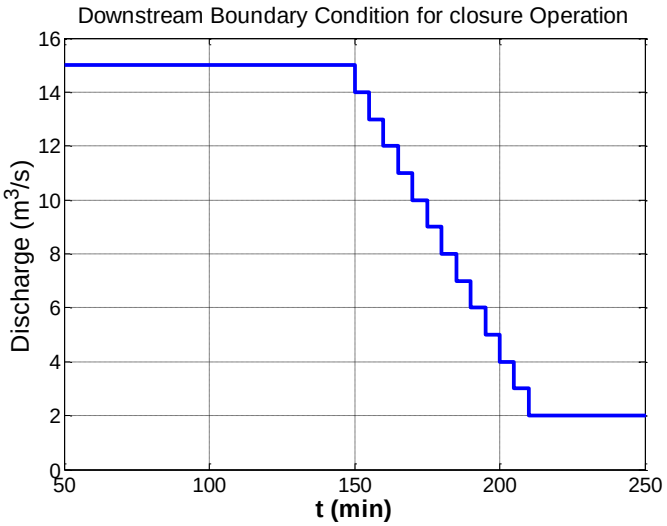

Figure 6.12 Downstream boundary condition for closure operation

6.4.2 Open-loop and closed-loop predictive control applied on the ERLB canal

A considerable number of scenarios have been tested to make a comparison between open-loop and closed-loop control. The open loop control is implemented using a predictive control algorithm so-called *GoRoSo* (Soler et al., 2012) and the closed loop control is implemented using the supervised decentralized predictive control (SDPC) control strategy developed in this dissertation. The open-loop control assumes that there are not disturbances along the closure operation. This implies that the same gate trajectories have been implemented for Scenario 1 and the rest of scenarios (2 to 7). On the other hand, the closed-loop control considers the disturbances, therefore the supervisor will manage the dynamic constraints to achieve a positive performance even in presence of disturbances.

Open-loop control

The *GoRoSo* algorithm may be categorized as *open-loop centralized predictive control*. It is a feedforward control algorithm for irrigation canals based on sequential quadratic programming (SQP). The SQP method is proposed by (Fletcher, 2013) and (Luenberger, 1969). With the *GoRoSo* algorithm, it is possible to compute the gate trajectories that smoothly carry the canal from the initial state to the final state by keeping the downstream water levels constant (Soler et al., 2014). The algorithm minimizes a linear quadratic objective function with penalties on water level deviations from setpoint as follows:

$$J = \frac{1}{2}\sum_{j=1}^{\lambda}\left(\hat{y}(k+j|k) - y_{sp}\right)^2 \tag{6.4}$$

where y_{sp} is the water level setpoint and $\hat{y}(k+j|k)$ denotes the future water levels.

The gate trajectories are calculated offline before the closure operation starts. The prediction horizon (λ) is 6-h long and it is discretized into 72 operation periods of 5 min each one. Each gate trajectory is defined by means of a piecewise time function divided into the same 72 pieces. In this way, each gate trajectory consists of 72 sequential gate openings, one for every sampling time. The implementation also considers functional constraints over the gate movements, such as the gate openings are lower than 15 cm of the previous position at every sampling time.

Closed-loop control

Within the SDPC strategy, the analytically obtained IDZ models described in Chapter 4 are used to make predictions of the behavior of the 5-pool configuration. The incremental formulation of the predictive control has been used to control the downstream water levels. The control action implemented in each pool is determined by equations (5.47) and (5.48) at every sampling time.

The SDPC algorithm has a functional constraint over the maximum gate opening. The maximum gate opening is determined by the water level. Increasing a gate opening over the water level is pointless. However, whether during a specific time an undershoot gate goes out of the water (it means neither submerged nor free flow), the SIC software applies the unidimensional Saint-Venant equations directly to calculate the discharge in this node. Namely, SIC automatically considers that there is no effective structure when a gate opening is greater than the water depth.

The decentralized controller considers the downstream disturbances caused by the change of both the output discharge and lateral offtake/intake. In the canal, pools are coupled to each other, therefore, a gate movement affects directly the controlled water levels in adjacent pools. In this way, disturbances occur both downstream and upstream. Namely, each decentralized controller considers the measured disturbances as the sum up of both the downstream discharge and the discharge change caused by the lateral disturbance.

For the tuning procedure, the maximum allowed water level error is chosen to be 10 cm, namely, the maximum allowed value estimated of the water level, e_{MAVE} is equal to 0.1m. The MAVE of the change in discharge, Δu_{MAVE} is chosen to be 0.1 m^3/s. For the closed-loop control system, several set of tuning values were tested in simulation. The chosen tuning parameters for the closure scenarios are detailed in Table 6-6. For the diagonal matrix of weighting factor (R), it is recommended $R_C < 2$ ($R = R_C I_{\lambda x \lambda}$). The sampling time for the supervisor has been fixed to 60 s. Meanwhile, the sampling time for the decentralized controllers is 300 s.

The supervisor is in charge of managing the dynamic constraints for each decentralized predictive controller in case of large disturbances, in a similar way as previously described in Section 6.3.4 for the canal PAC-UPC.

Pool	λ	R_C	a [x10^{-3}]	c [min]	ΔU_{max} [m^3/s]	ΔU_{min} [m^3/s]
Pool 1	15	1	1.1	150	0.5	0.5
Pool 2	21	1	1.2	157	0.5	0.5
Pool 3	23	1	1.5	166	0.5	0.5
Pool 4	12	1	2	178	0.5	0.5
Pool 5	9	1	2	181	0.5	0.5

Table 6-6 Parameters for each controlled pool for the closure scenarios

6.4.3 Results

- ***Scenario1*:** Partial closure from 15 m^3/s to 2 m^3/s without disturbances. In this scenario all the spillways are closed, the spillway height being at its maximum (3 m). Discharge is only over spillway 5, at the end of the canal.

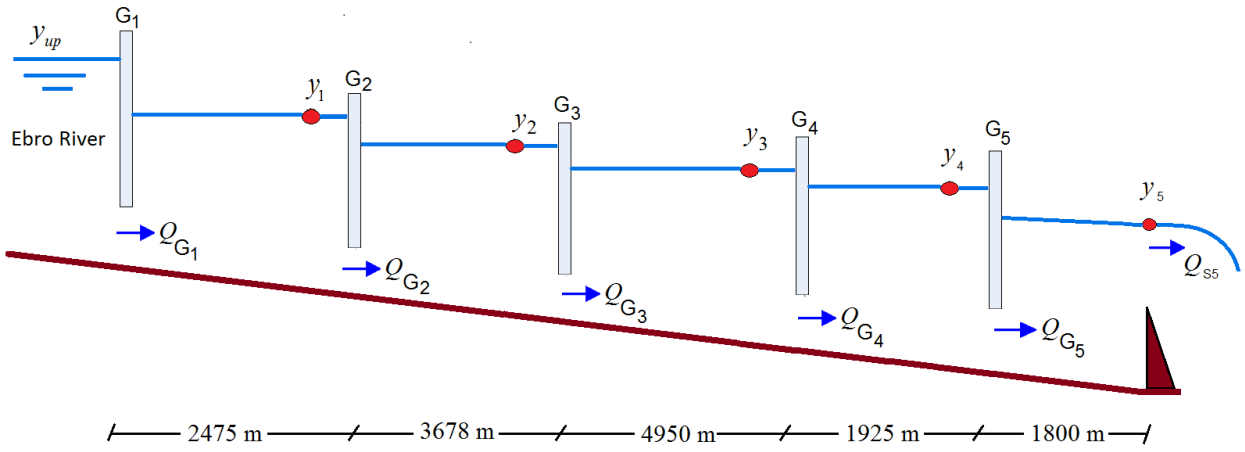

Figure 6.13. Sketch of the Scenario 1

The closure operation managed by the open-loop controller is depicted in Figure 6.14. The procedure is to initiate a discharge change in the most upstream gate and progress in the downstream direction. The optimal gates trajectories for the closure operation can be seen in the bottom part of Figure 6.14. As it can be observed the performance is really positive because the closure operation transient is short (lower than 3h). The oscillations have ripple values lower than 2.552 m and the water levels remain practically around the setpoint value of 2.5 m. The maximum water level decrease is 3 cm.

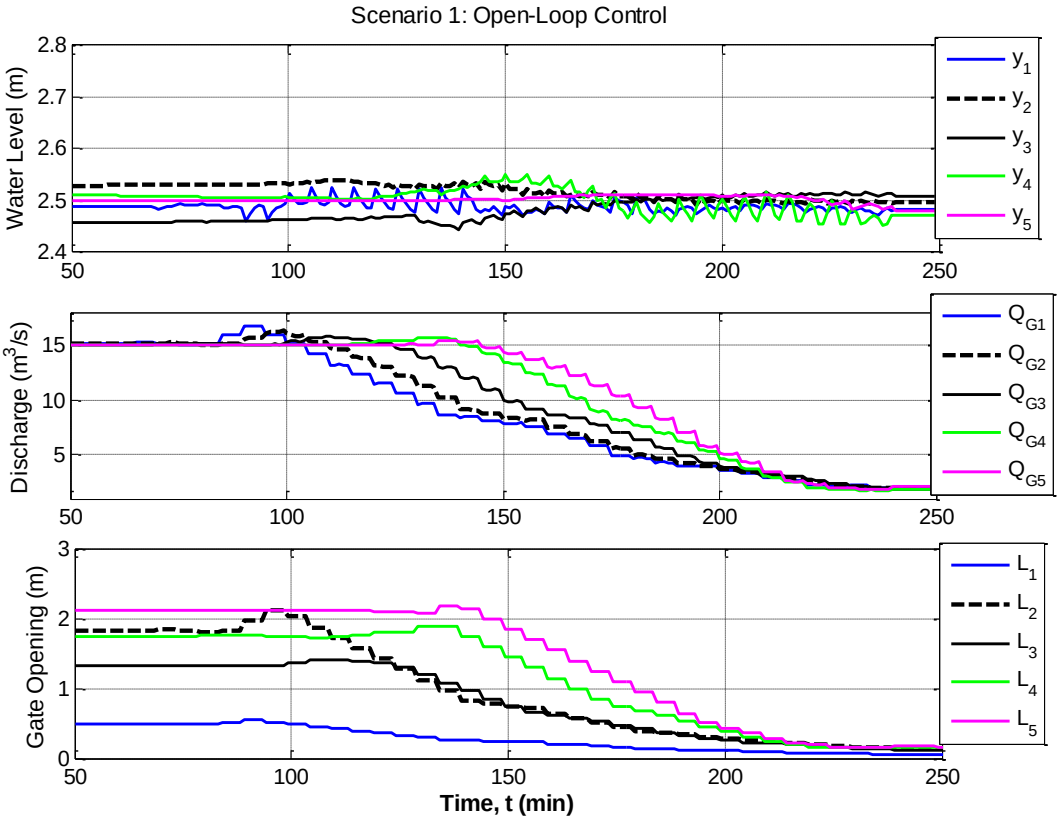

Figure 6.14 Simulation results of automatic closure of ERLB canal under open-loop control in Scenario 1

The closure operation managed by the SDPC controller is depicted in Figure 6.15 . The closed-loop control modifies the discharges under gates in a sequential order driven by the supervisor. The procedure is to initiate a discharge change in the most upstream gate and progress in the downstream direction. In the simulation results, the water depths remain practically around the setpoint value of 2.5 m. The steady state errors are lower than 2.2 cm. The closure operation generates a positive translational wave with a maximum height of 2.563 m.

The automatic closure operation under the SDPC control exhibits a satisfactory performance. The values of all performance indexes proposed in Section 6.2 are detailed in Table 6-7. According to results, both controllers (open and closed loop) present a positive performance with small oscillations, none of them presenting a clear better performance for all the performance indexes. The closure generates a positive translational wave that results into oscillations along all the pools. The highest values of MAO are presented at pool 4 (2.559 for open-loop control and 2.562 for closed-loop control).

The comparison of the evolution of water level error over the closing time is depicted in Figure 6.16. Given the larger prediction horizon used in the open-loop control (6 h), the gates are moved from the beginning of the closure operation, which generates small oscillations in the water levels. On the other hand, two situations, first the smaller prediction horizon of closed-loop controller, and second the almost zero slope in the sigmoidal function at the beginning of the closure operation produces small changes in gate openings and therefore, no oscillations in the water level are produced along the first 40 minutes.

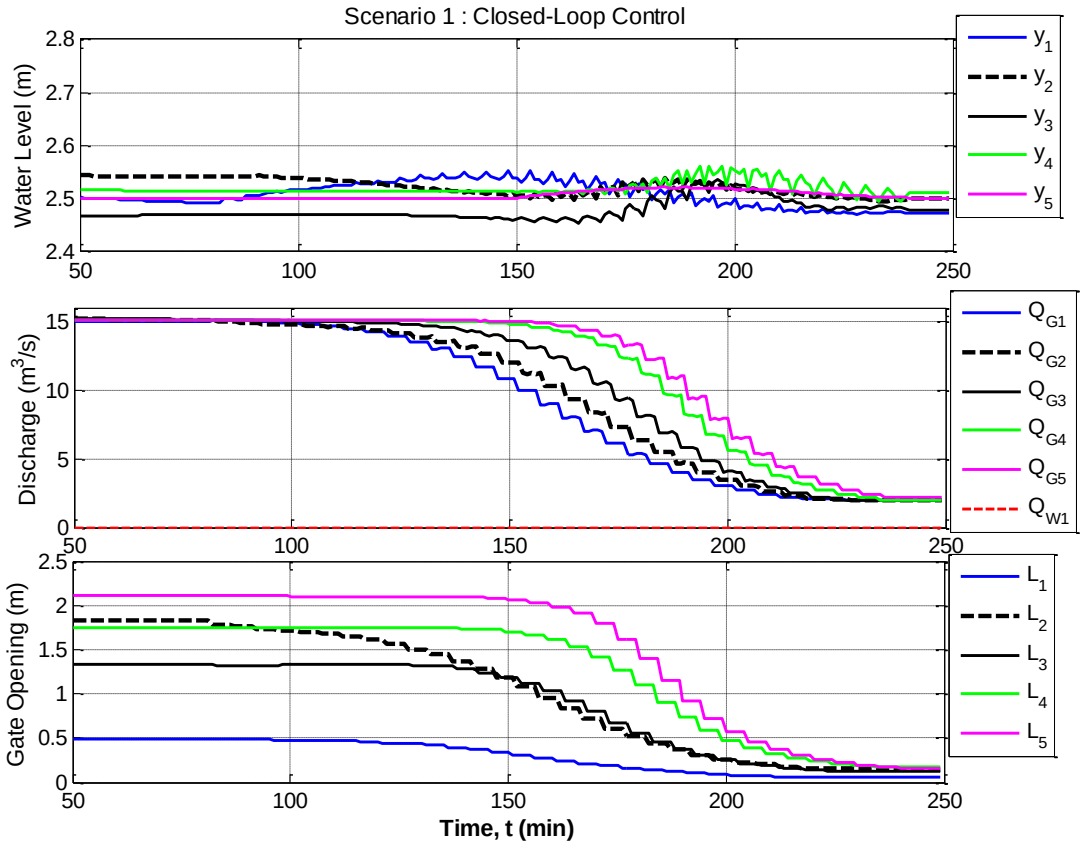

Figure 6.15 Simulation results of closure operation of ERLB canal under closed-loop control in scenario 1

Pool	Control	RMSE [m]	MAPE [%]	ISE [m]	IAE [m]	MAO [m]	SSE [m]
Pool 1	OL	0.0133	0.4436	0.0303	1.8856	2.533	0.0117
	CL	0.0270	0.96241	0.1244	4.0902	2.5526	0.0257
Pool 2	OL	0.0306	1.0075	0.1593	4.2818	2.552	-0.0051
	CL	0.0236	0.7607	0.0948	3.2329	2.5436	0
Pool 3	OL	0.0210	0.7721	0.07522	3.2815	2.5247	-0.018
	CL	0.0275	1.031	0.12935	4.3819	2.5352	0.022
Pool 4	OL	0.0261	0.9064	0.11625	3.8525	2.5591	0.0217
	CL	0.0243	0.8183	0.10076	3.4779	2.5622	-0.0130
Pool 5	OL	0.0085	0.2661	0.01253	1.1312	2.5127	0.0195
	CL	0.0107	0.3070	0.01970	1.3049	2.522	-0.0020

Table 6-7 Performance indexes of Scenario 1 (OL = Open-Loop, CL = Closed-loop)

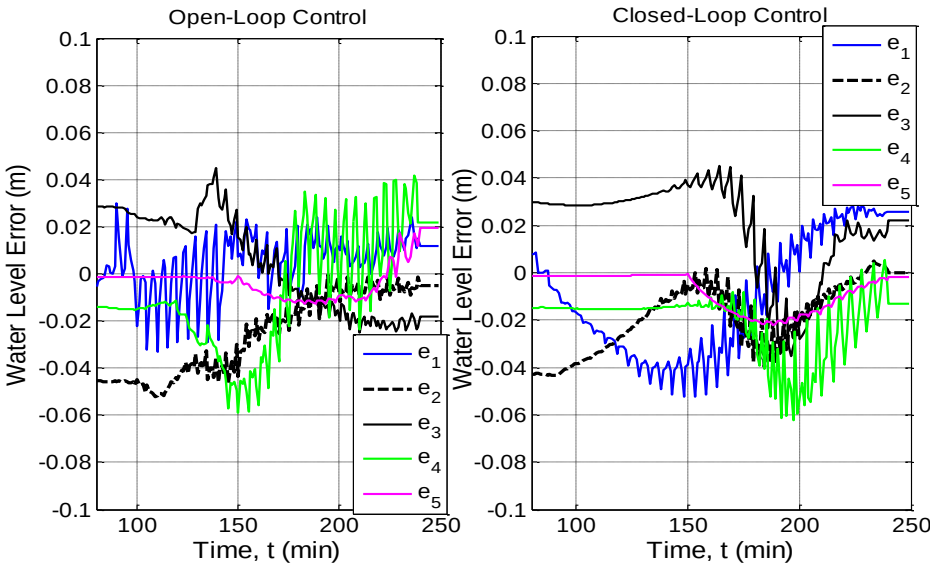

Figure 6.16 Water level error during the closure process (open loop vs. closed loop control)

- ***Scenario 2***: Partial closure from 15 m^3/s to 2 m^3/s with the presence of a large disturbances. The sketch of the Scenario 2 is depicted in Figure 6.17.

The automatic control has to deal with the disturbance discharge Qs_1 = 5.8 m^3/s along 40 minutes of the closure operation, and for the remaining time Qs_1 = 0 m^3/s. This value of Qs_1 is equivalent to 38.6 % of the operating point of 15 m^3/s. The purpose is to simulate a pumping station to resemble a rain event or a runoff flooding into the canal. To implement a positive disturbance (intake) at node 7 in SIC, an *imposed discharge (pump)* has been defined in the SIC software, as it is illustrated in Figure 6.18.

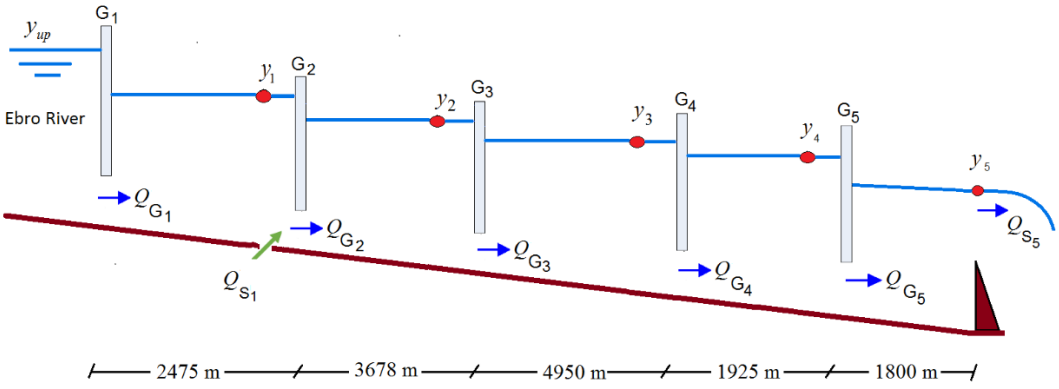

Figure 6.17 Sketch of the Scenario 2

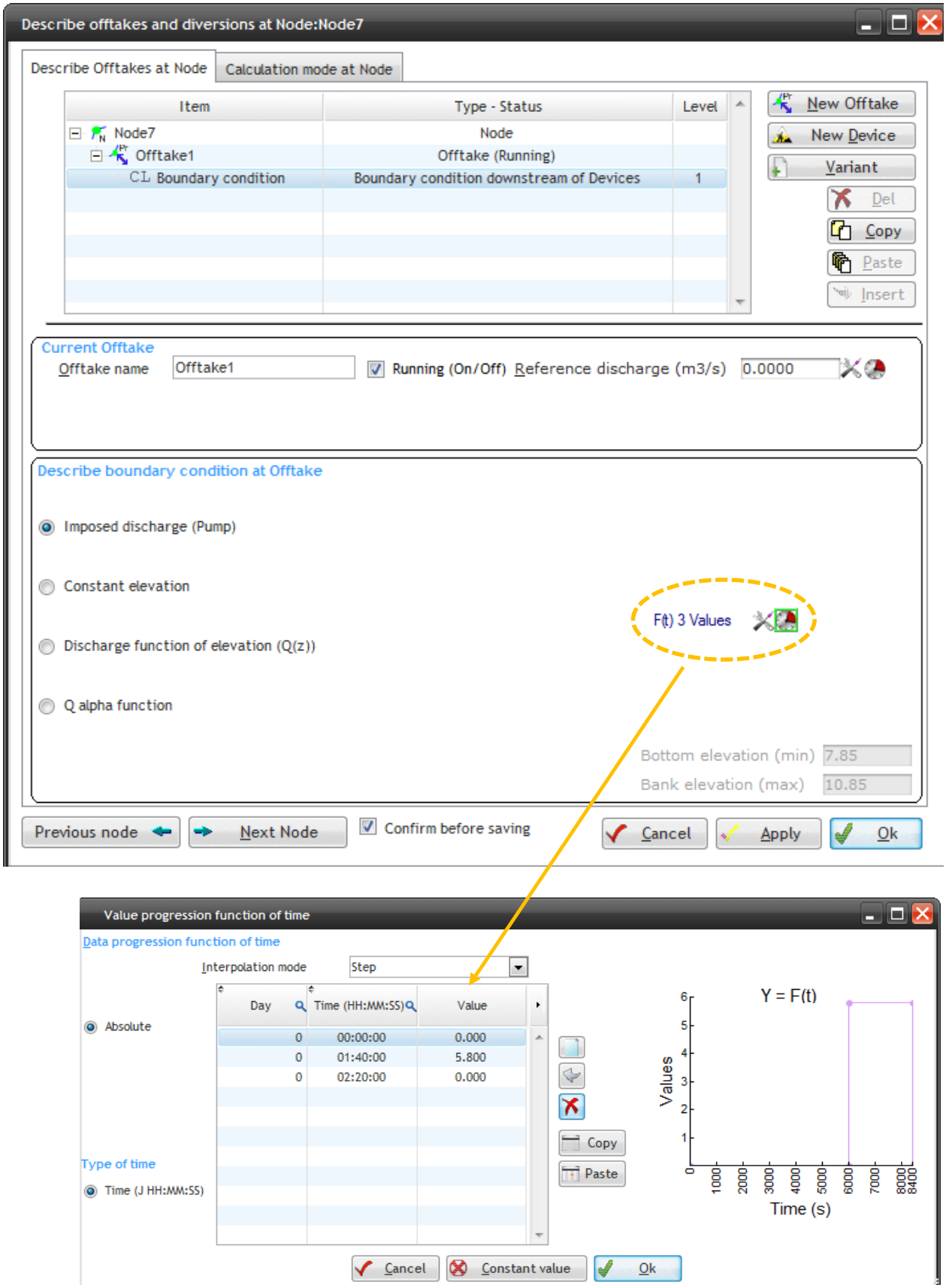

Figure 6.18 Implementation of positive disturbance in SIC

In the presence of a large disturbance along the closure operation, the fixed gate trajectories computed by the open-loop control may lead the canal to the problem of overtopping. In the case of Scenario 2, where results are shown in Figure 6.19, the overtopping occurs at time *t = 140* min.

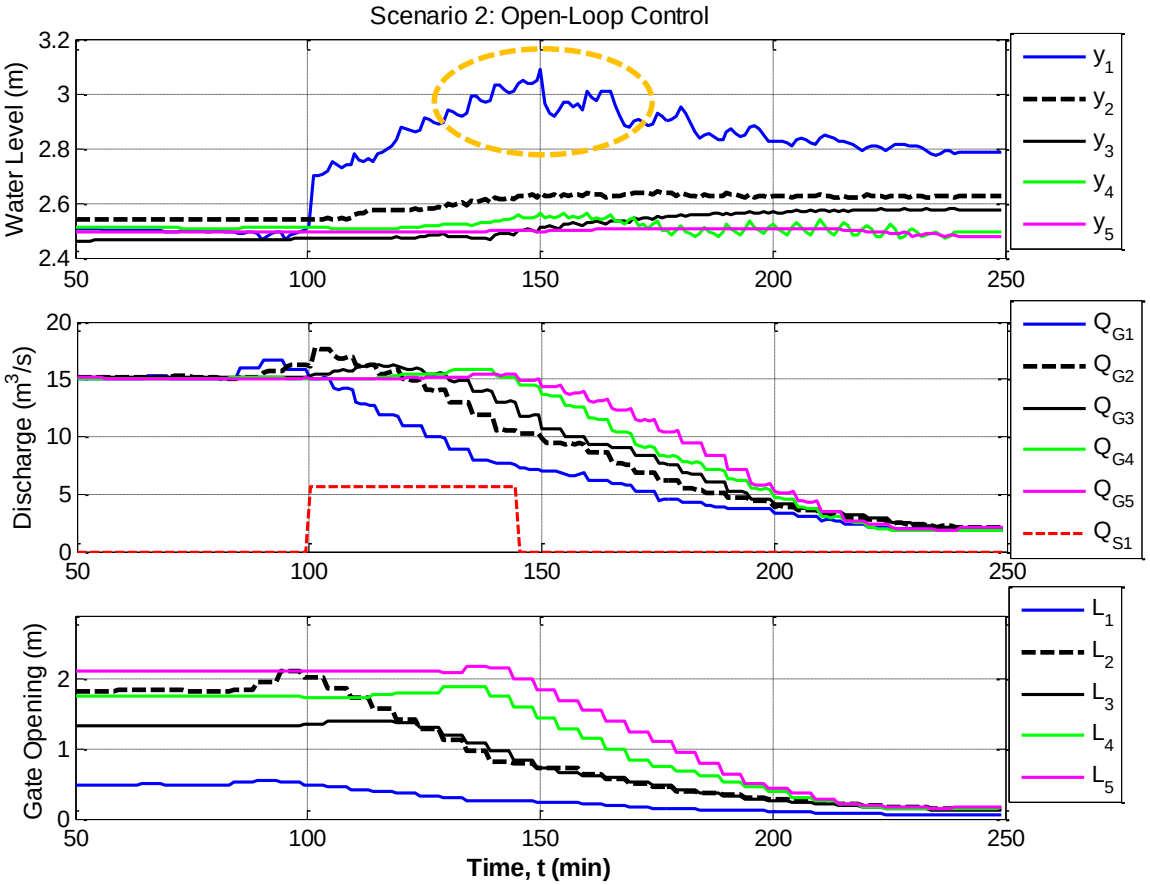

Figure 6.19 Simulation results of closure operation of ERLB canal under open-loop control in Scenario 2

The SDPC control considers the effect of the strong disturbance and it reconfigures the constraints of the decentralized controllers to reject the disturbance properly, in such a way that the sigmoidal functions that determine the maximum discharge along pools 2, 3, 4 and 5 are time shifted as described in (6.2). Figure 6.20 illustrates the advantages of closure operation under SDPC control over the operation managed by the open-loop control depicted in Figure 6.19. In this scenario, the SDPC avoids the overtopping in the canal, and all the water levels remain with steady state errors lower than 5 cm.

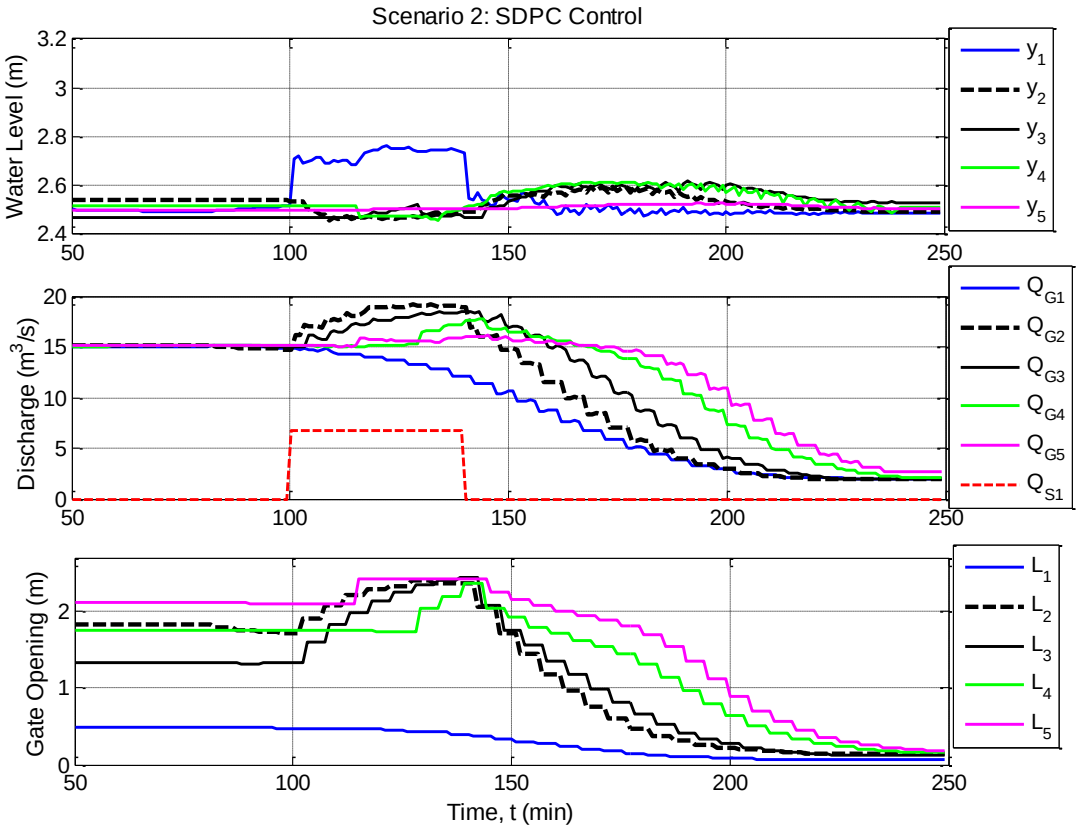

Figure 6.20. Simulation results of automatic closure of ERLB canal under SDPC control in Scenario 2

- ***Scenario 3***: Partial closure from 15 m^3/s to 2 m^3/s with the presence of a strong disturbance Qs_1 of 6.8 m^3/s for $100 \leq t \leq 162$ min. For the remaining time, $Qs_1 = 0$ m^3/s.

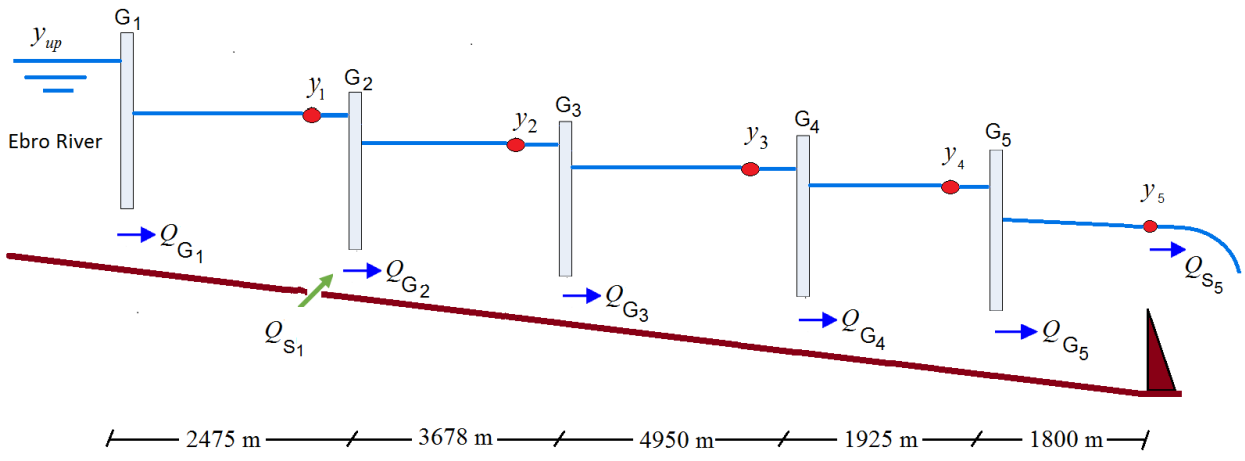

Figure 6.21. Sketch of the Scenario 3

In this case, the disturbance in the first pool is both longer and higher than in the Scenario 2, as it is illustrated in Figure 6.22. In this scenario, the open-loop control leads the canal to the problem of overtopping after longer time in comparison with the Scenario 2. On the other hand, the closed-loop control avoids the overtopping, as it is illustrated in Figure 6.24. With the results presented

in Table 6-8, it is clear that the closed-loop control performed better than the open-loop control for most of the performance indexes in all pools.

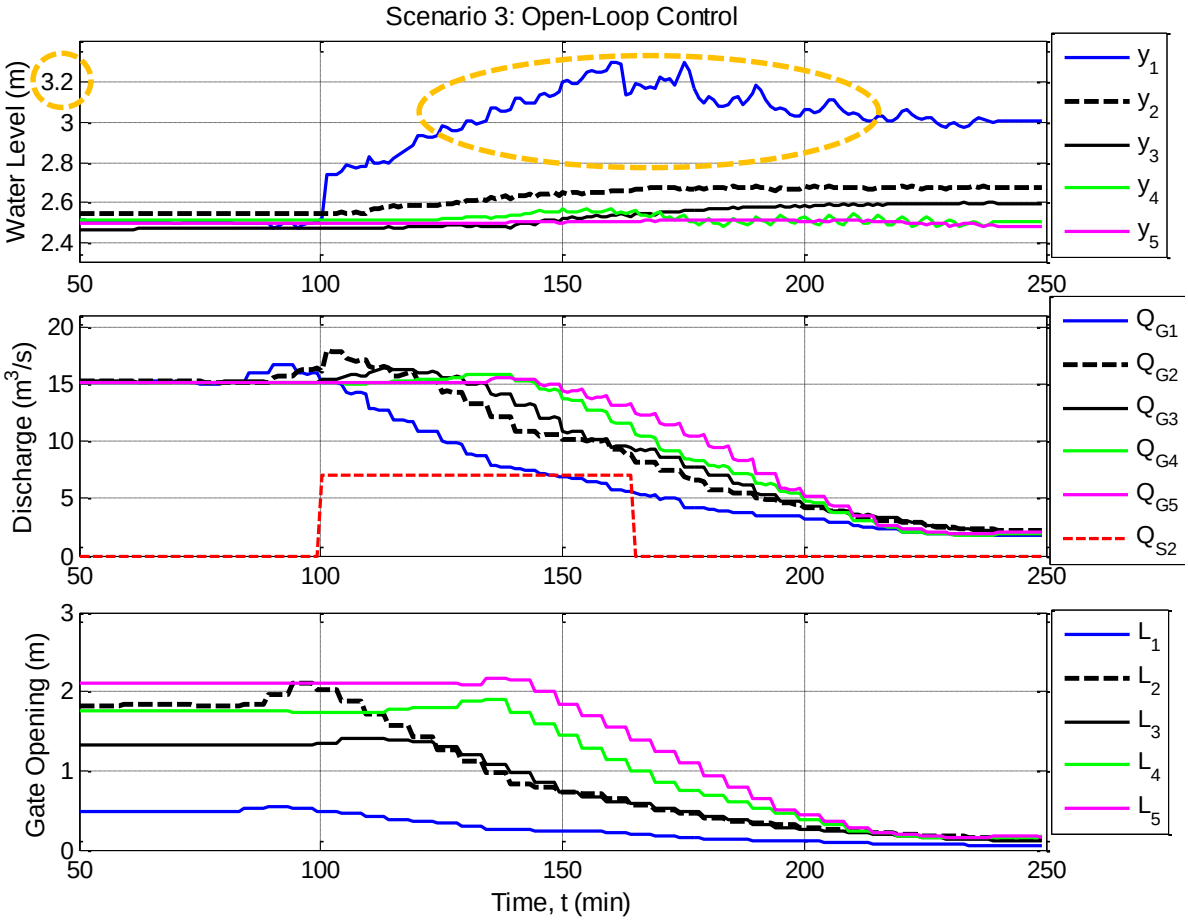

Figure 6.22 Simulation results of closure operation of ERLB canal under open-loop control in Scenario 3

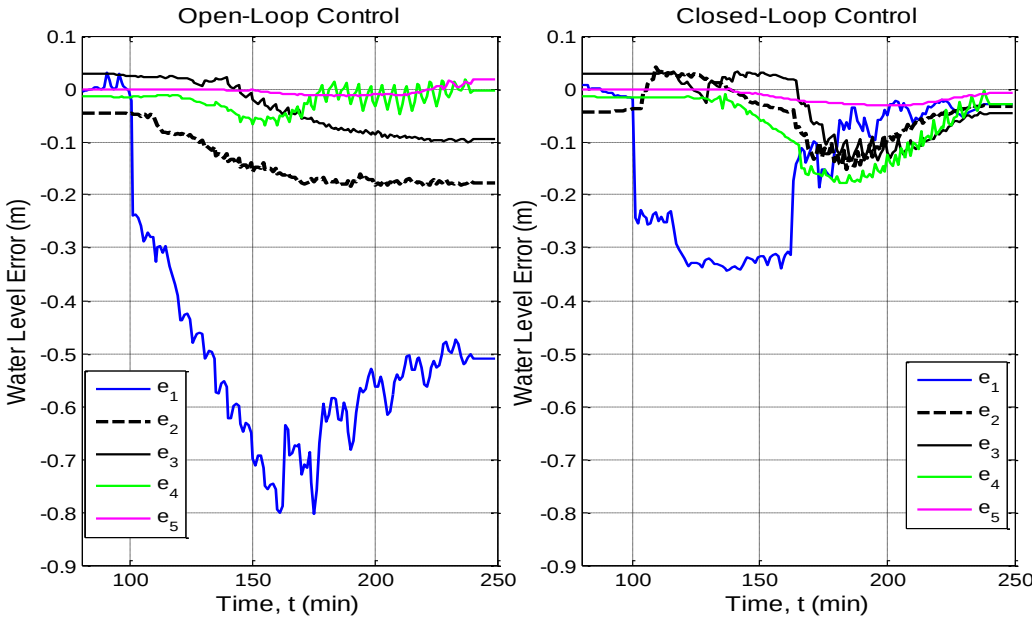

Figure 6.23 Water level error during the closure process in Scenario 3

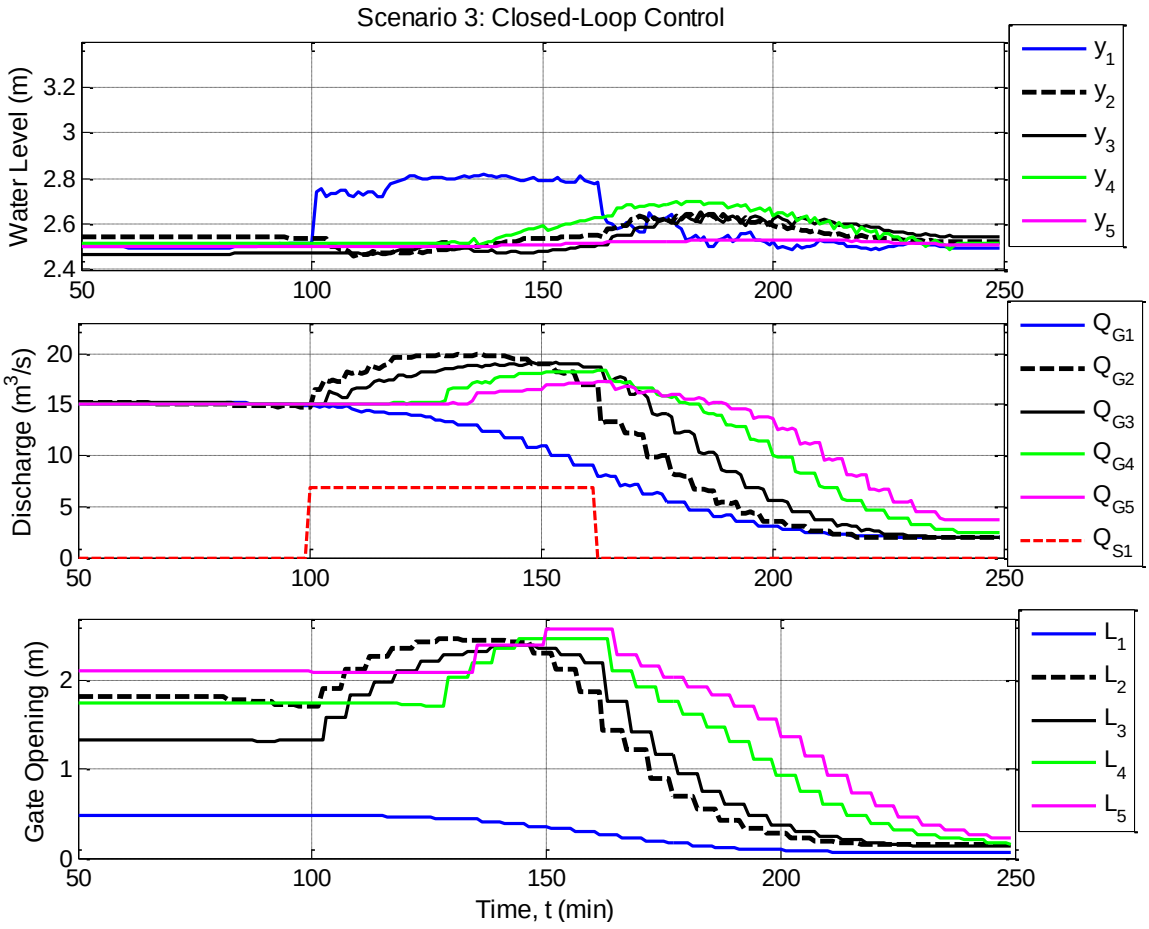

Figure 6.24. Simulation results of automatic closure of ERLB canal under closed-loop control

Pool	Control	RMSE [m]	MAPE [%]	ISE [m]	IAE [m]	MAO [m]	SSE [m]
Pool 1	OL	0.52444	19.157	46.756	81.417	3.3023	-0.5089
	CL	0.17577	4.8579	5.2519	20.646	2.8187	0.0035
Pool 2	OL	0.14388	5.3867	3.5192	22.893	2.6845	-0.1767
	CL	0.06553	2.1181	0.7301	9.002	2.65	-0.0259
Pool 3	OL	0.06210	2.1084	0.6557	8.961	2.6015	-0.0954
	CL	0.06936	2.2084	0.81798	9.386	2.6437	-0.0464
Pool 4	OL	0.02829	0.8926	0.1361	3.7937	2.5696	-0.0035
	CL	0.09981	2.9816	1.6938	12.672	2.6977	-0.0157
Pool 5	OL	0.00822	0.2595	0.0114	1.1029	2.513	0.01703
	CL	0.01809	0.5555	0.0556	2.361	2.5328	-0.0097

Table 6-8 Performance indexes of Scenario 3 (OL = Open-Loop, CL = Closed-loop)

- ***Scenario 4:*** Partial closure from 15 m^3/s to 2 m^3/s with an imposed disturbance intake of Qs_2 of 5.8 m^3/s. In this scenario, the intake adds water to the canal for $100 \leq t \leq 140$ min. For the remaining time of simulation Qs_2 = 0 m^3/s.

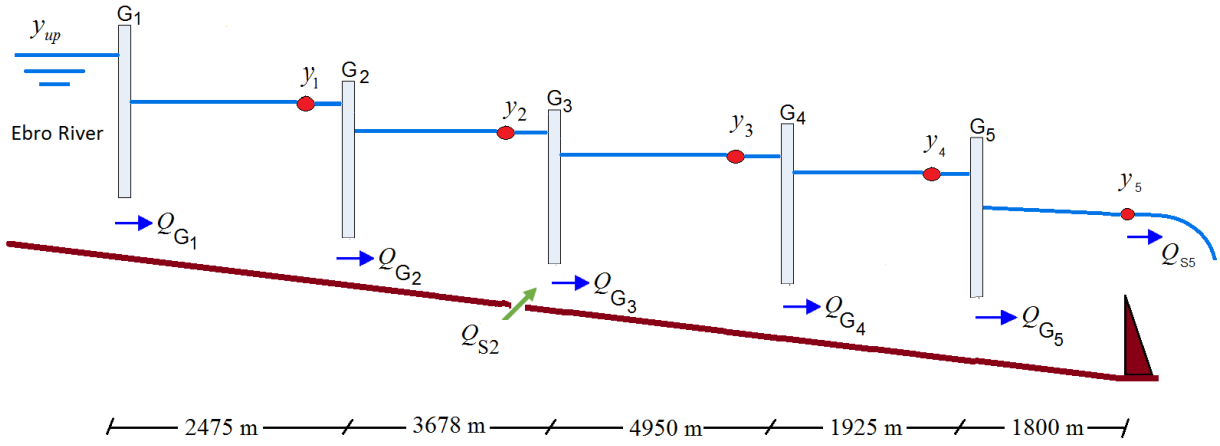

Figure 6.25. Sketch of the Scenario 4

In this scenario, the open-loop control approach leads the water levels y_2 and y_3 outside the accepted steady state error band, as it is illustrated in Figure 6.26. On the other hand, the scenario tackled with SDPC control leads the system to a final steady state where all water level errors are lower than 5 cm, as it is shown in Figure 6.27, namely inside the safety water level band.

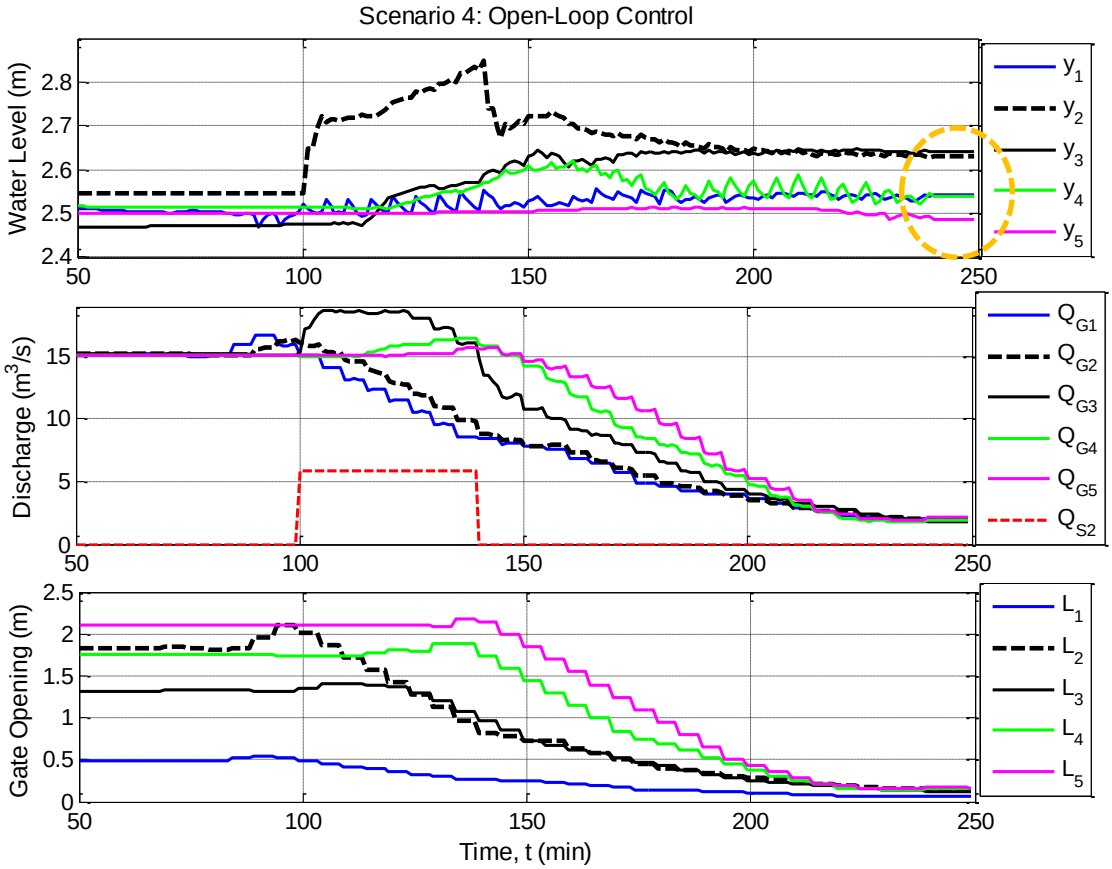

Figure 6.26 Simulation results of automatic closure of ERLB canal under open-loop control in scenario 4

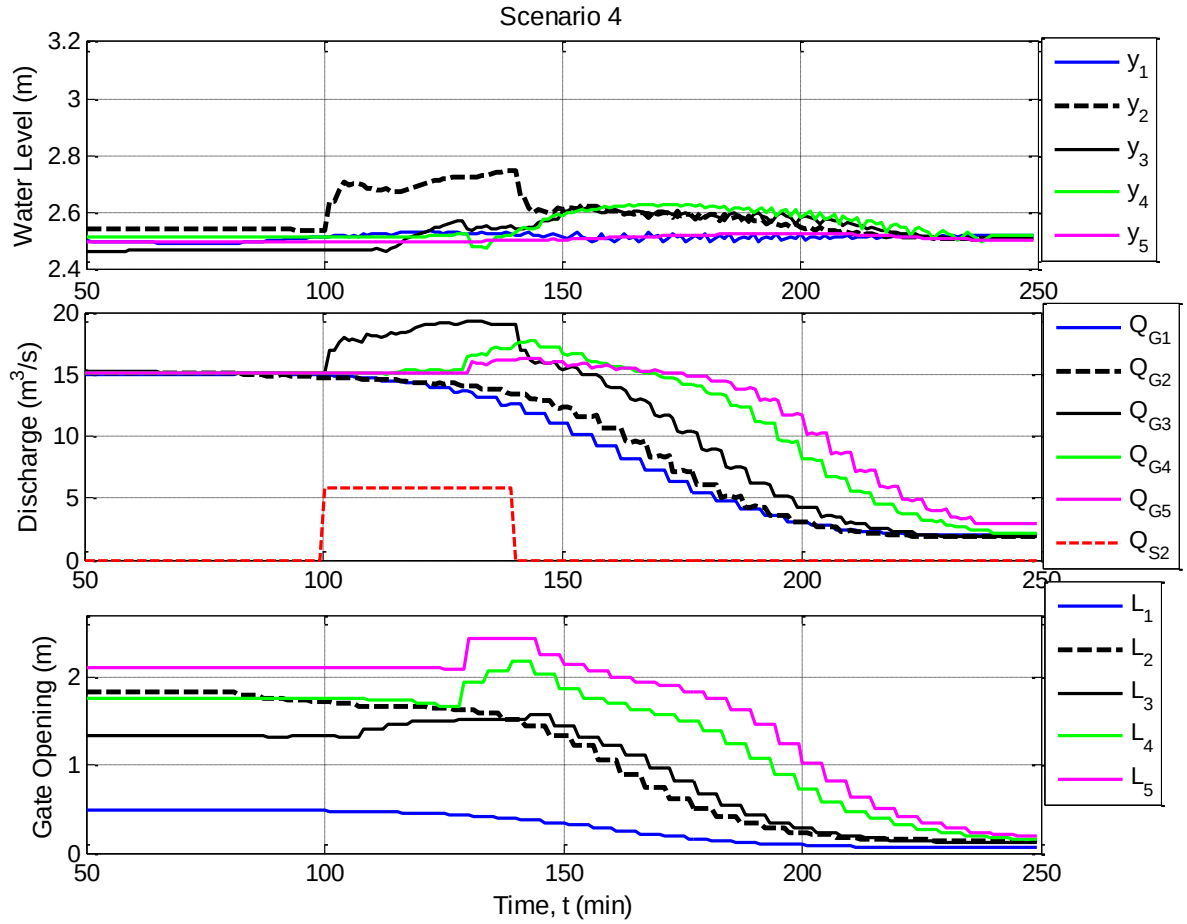

Figure 6.27. Simulation results of closure operation of ERLB canal under SDPC control in scenario 4

- ***Scenario 5***: Partial closure from 15 m^3/s to 2 $m^3/$ with the presence of the disturbance Qs_3 of 5.8 m^3/s, $100 \leq t \leq 150$ min. For the remaining time, $Qs_3 = 0$ m^3/s.

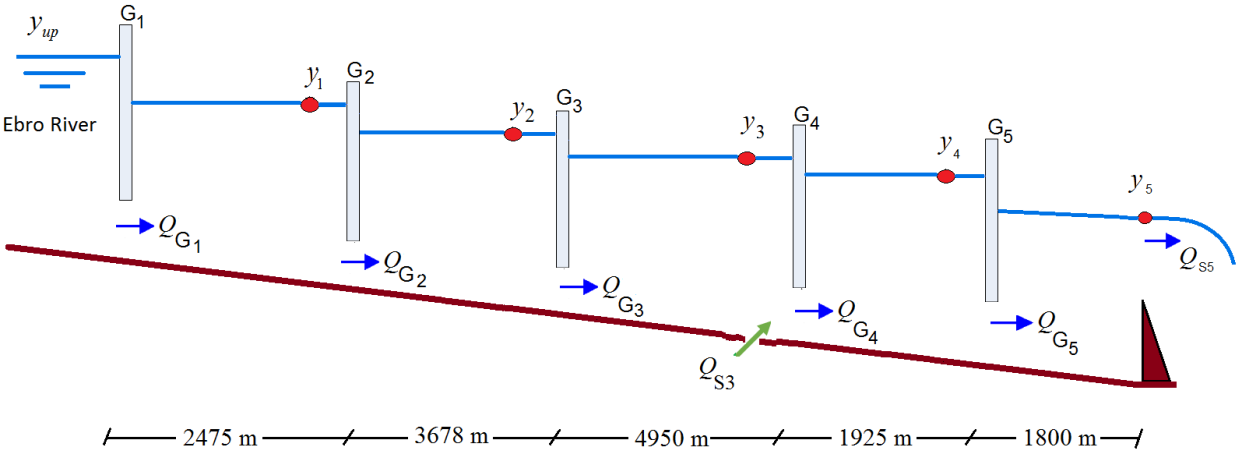

Figure 6.28. Sketch of the scenario 5

In this scenario, the open-loop control leads to steady state errors of y_2 and y_3 greater than 5 cm, as it is illustrated in Figure 6.29. Meanwhile, the supervisor in the SDPC control considers the value of the disturbance Qs_3 to reshape the constraints as described in (6.2). The final steady state errors for all water levels under SDPC control are lower than 5 cm, as it is shown in Figure 6.30.

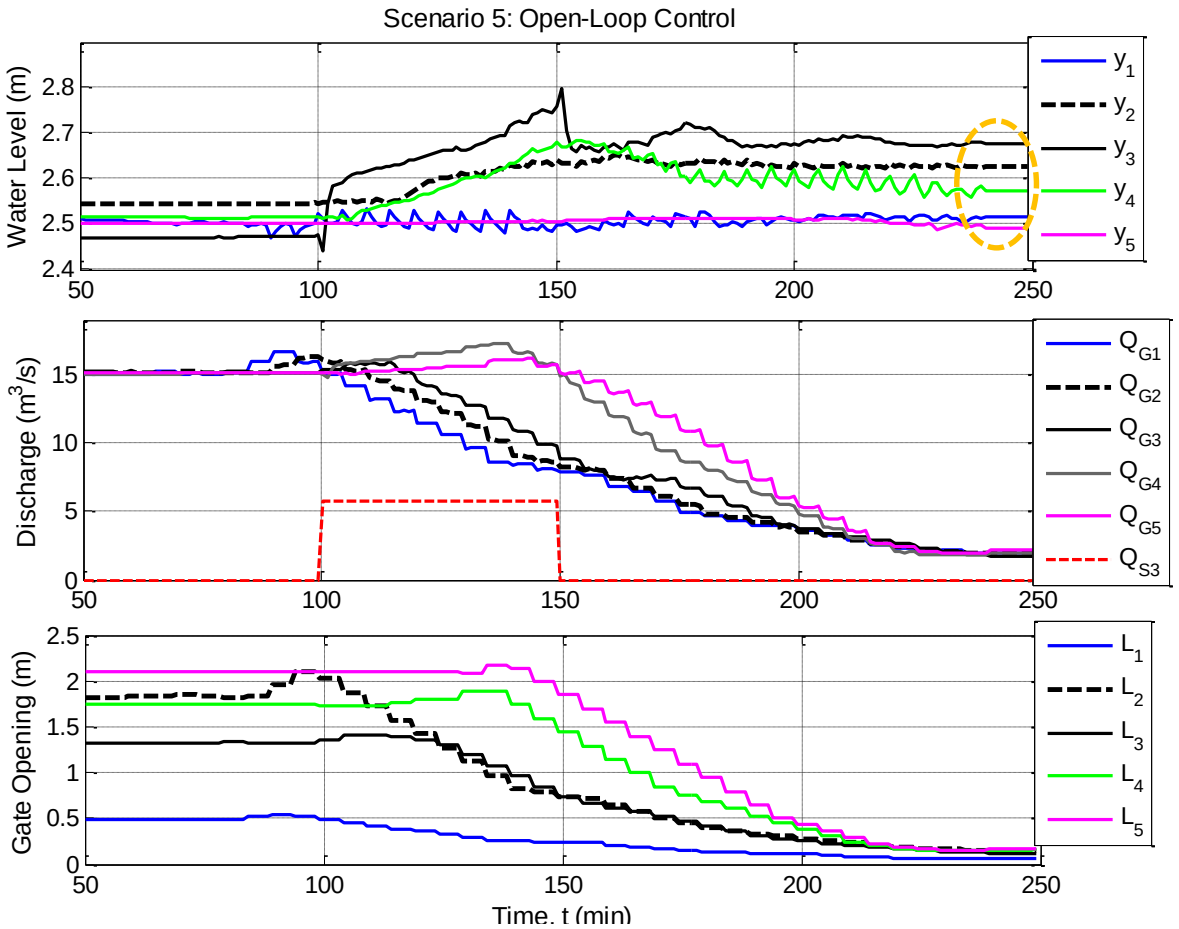

Figure 6.29 Simulation results of closure operation of ERLB canal under open-loop control in scenario 5

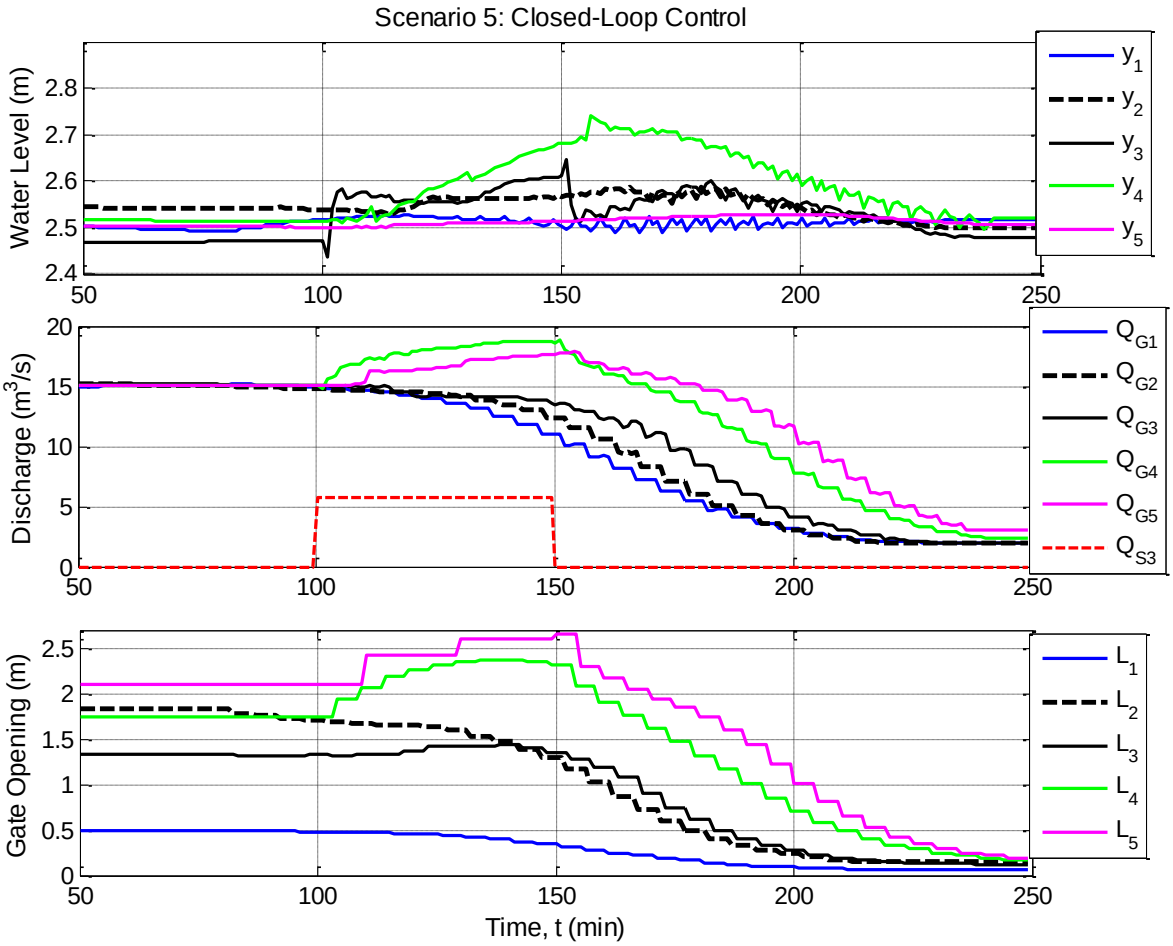

Figure 6.30. Simulation results of closure operation of ERLB canal under SDPC in Scenario 5

- ***Scenario 6***: Partial closure from 15 m^3/s to 2 m^3/s with a lateral offtake of Qs_1 of -4.3 m^3/s, for $100 \leq t \leq 250$ min. For $0 \leq t < 100$ min, Qs_1 is equal to zero.

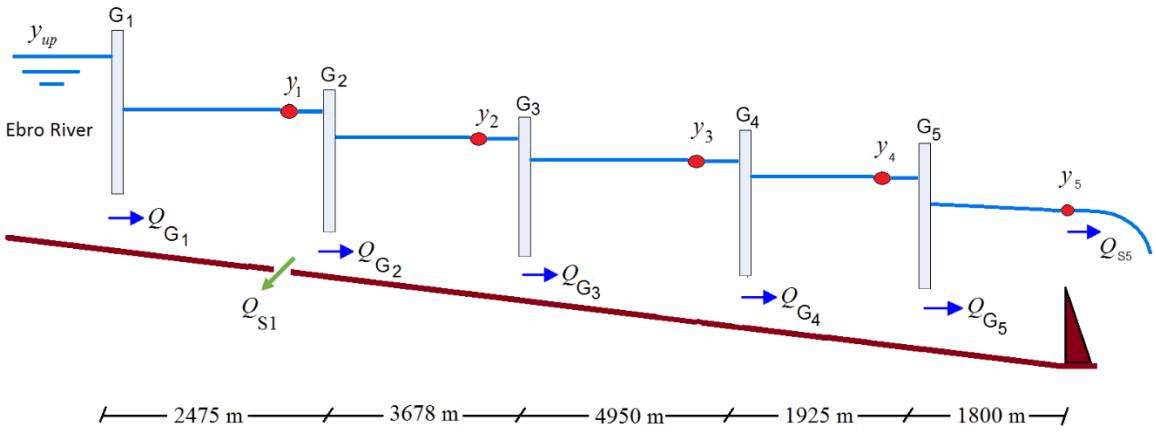

Figure 6.31. Sketch of the Scenario 6

The implementation of a negative disturbance at node 7 in SIC is shown in Figure 6.32. A lateral offtake (*discharge as function of elevation*) has been selected as a *boundary condition at downstream devices* in the SIC window.

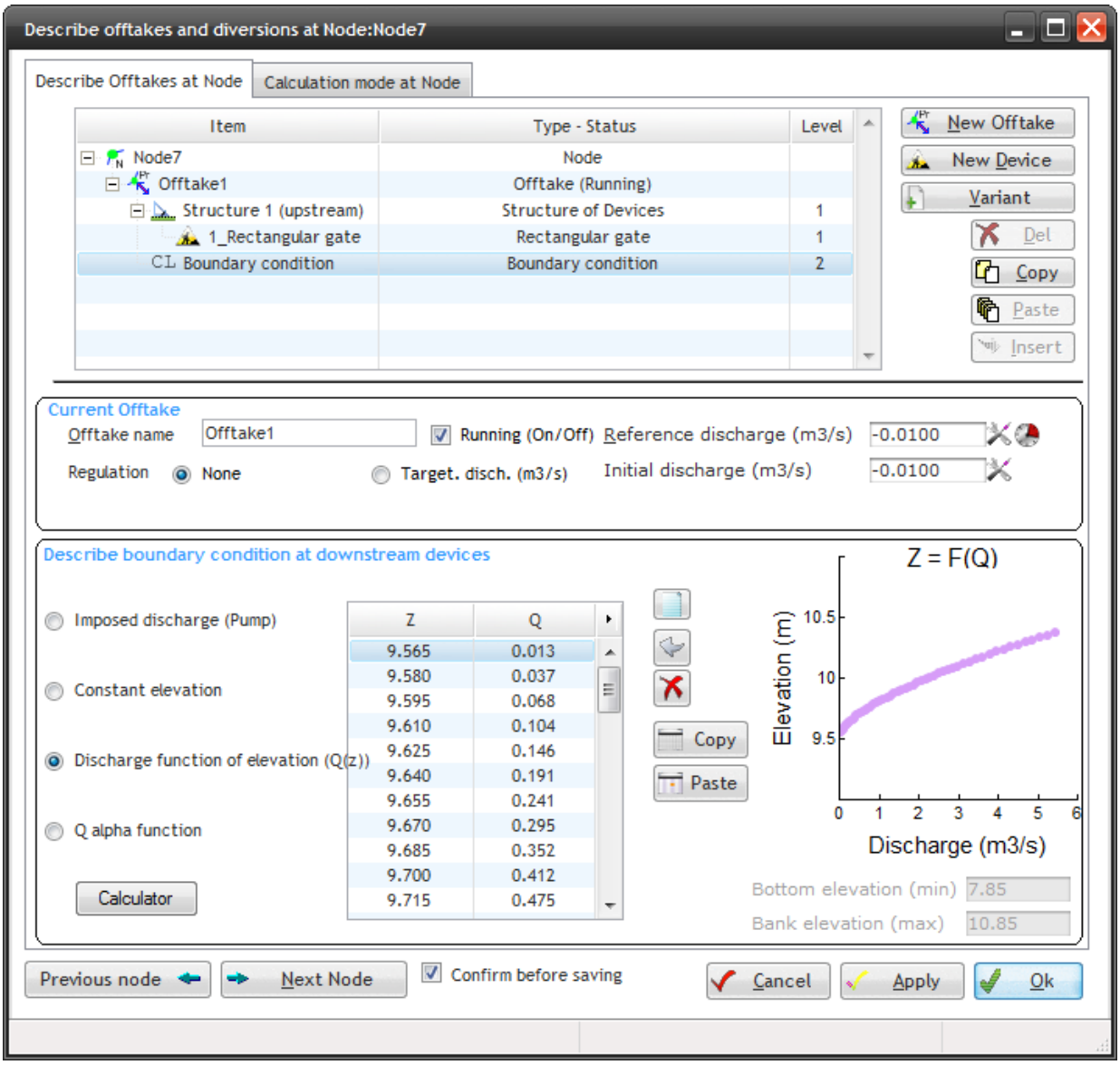

Figure 6.32 Simulation of lateral offtake in SIC

In this scenario, the final value of water level y_1 is determined by the lateral weir height. However a suitable control strategy must allow the rest of the water levels remain around the setpoint of 2.5 m. The setpoint tracking is affected in the open-loop control performance because the water level y_2 is around 2.4 m at the end of the simulation, as it is illustrated in Figure 6.33. The performance of the closed-loop control is better than the open-loop control partly because the SDPC control makes the closure of the downstream pools quicker than the first pool (upstream pool). Finally, the use of dynamic constraints allows gradually decrease the discharge of each pool keeping the setpoints water levels of y_2, y_3, y_4 and y_5 around 2.5 m, as it is illustrated in Figure 6.34.

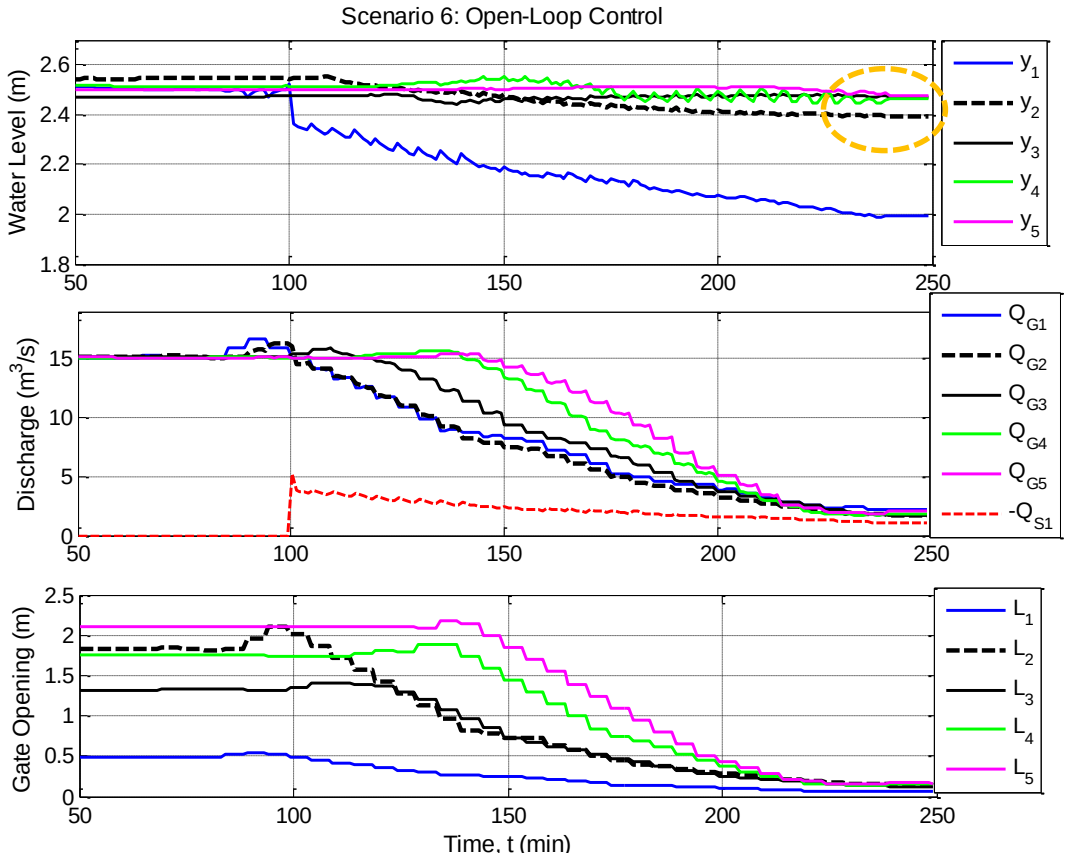

Figure 6.33. Simulation results of automatic closure of ERLB canal under open-loop control in scenario 6

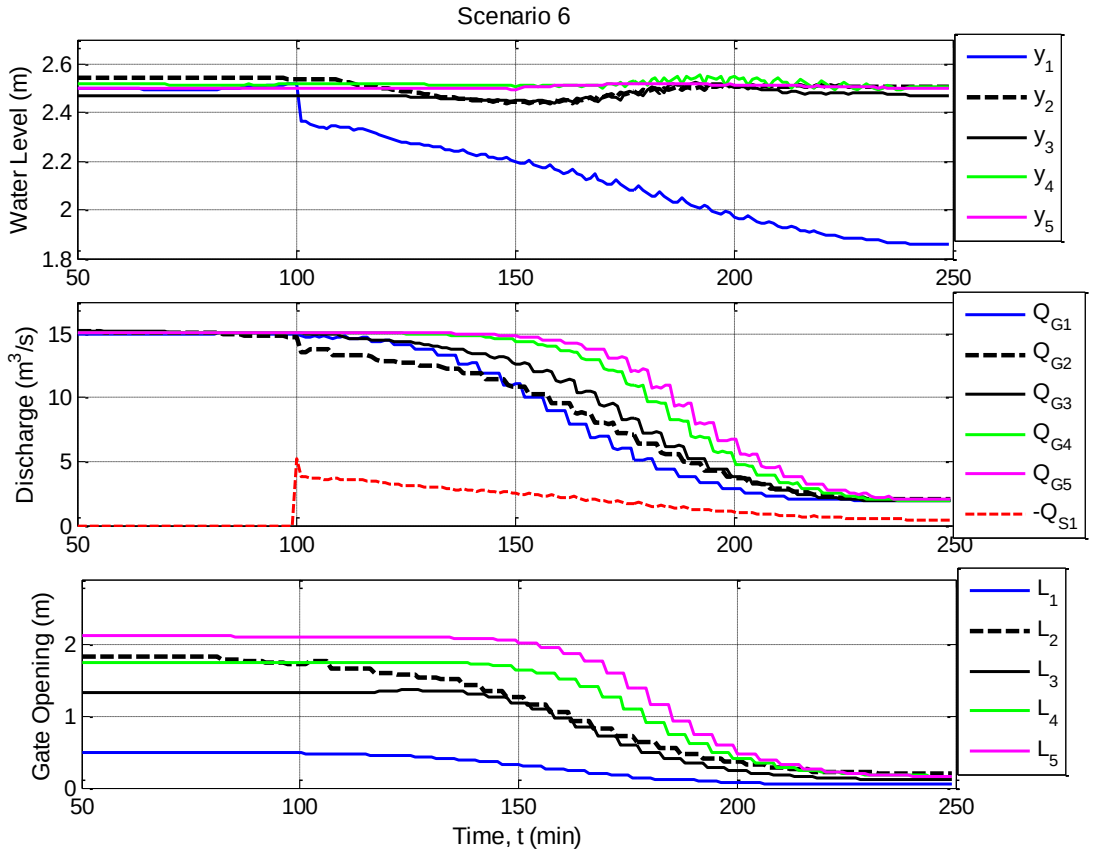

Figure 6.34 Simulation results of closure operation of ERLB canal under closed-loop control in scenario 6

- ***Scenario 7***: Partial closure from 15 m^3/s to 2 m^3/s with two disturbances, and lateral offtake of Qs_1 of -4.3 m^3/s at $100 \leq t \leq 250$ min and another Qs_3 of -3.8 m^3/s at $110 \leq t \leq 250$ min. For the remaining time, $0 \leq t < 100$ min, Qs_1 and Qs_3 being equal to *0* m^3/s.

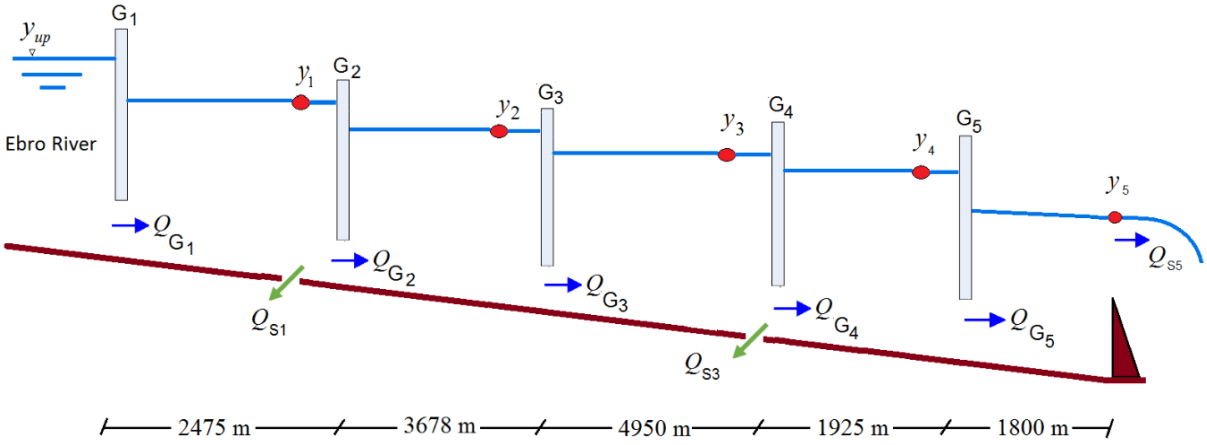

Figure 6.35. Sketch of the Scenario 7

Similar to the Scenario 6, the final values of water levels y_1 and y_3 of Scenario 7 are determined by their respective spillway heights. The automatic closure in this scenario under open-loop control leads to values of SSE of 18.96 cm for y_2 and 12.44 cm for y_4. Namely, both water levels y_2 and y_4 are lower than 2.4 m in the open loop control operation, as it is illustrated in Figure 6.37. Meanwhile, the SDPC control is able to tackle the problem of partial closure with two disturbances, allowing to improve the performance indexes for the closure operation, as it is indicated in Table 6-9, for instance, the steady state errors are 0.88 cm for y_2 and 0.44 cm for y_4. Simulation results of closure operation of ERLB canal under open-loop control in Scenario 7 are illustrated in Figure 6.38.

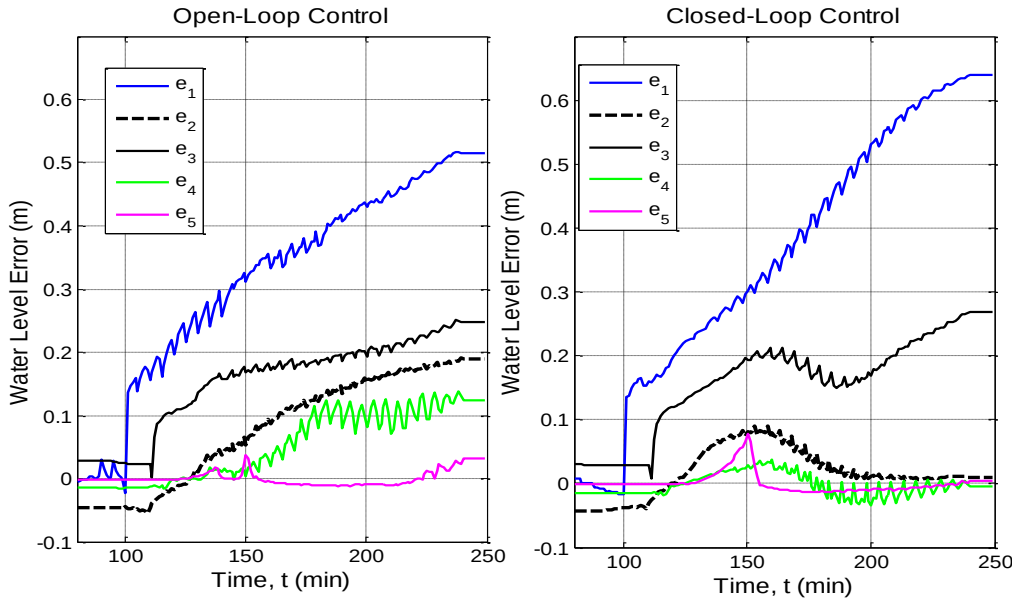

Figure 6.36 Water level error during the closure process in Scenario 7 (open loop vs. closed loop control)

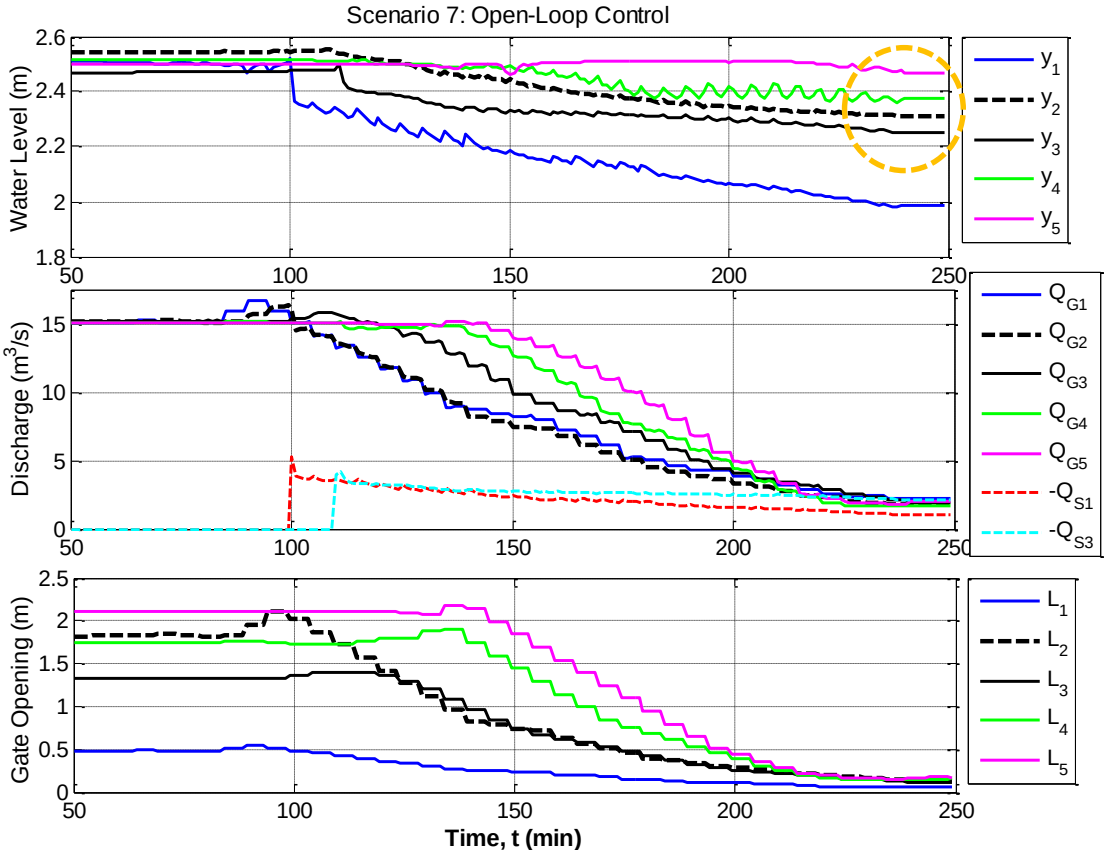

Figure 6.37 Simulation results of closure operation of ERLB canal under open-loop control in Scenario 7

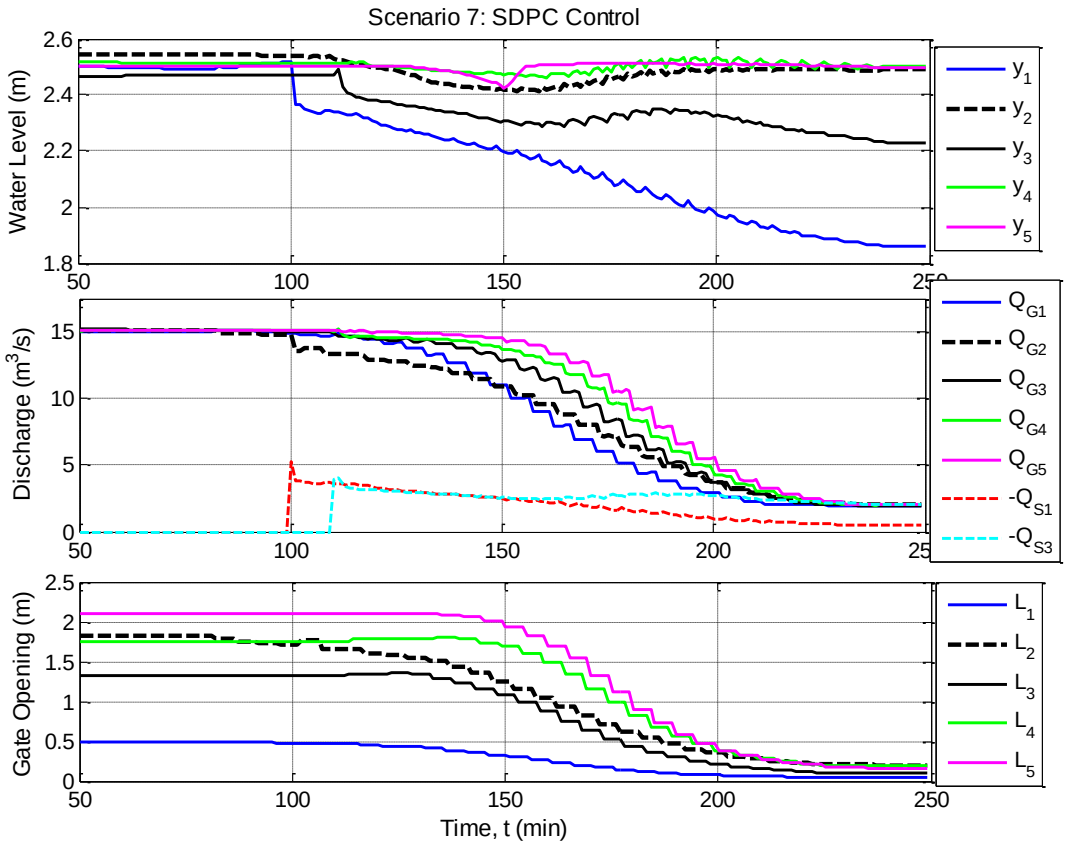

Figure 6.38 Simulation results of closure of ERLB canal under closed-loop control in Scenario 7

Pool	Control	RMSE [m]	MAPE [%]	ISE [m]	IAE [m]	MAO [m]	SSE [m]
Pool 1	OL	0.35538	12.76	21.47	54.23	2.5223	0.5157
	CL	0.41255	14.362	28.934	61.04	2.5172	0.6404
Pool 2	OL	0.11821	4.0452	2.3757	17.192	2.5547	0.1896
	CL	0.04122	1.308	0.2888	5.5589	2.5436	0.0088
Pool 3	OL	0.172	6.2239	5.0293	26.452	2.4981	0.248
	CL	0.17565	6.3564	5.2448	27.015	2.493	0.2692
Pool 4	OL	0.07617	2.3528	0.98632	9.999	2.5157	0.1244
	CL	0.01739	0.5918	0.05144	2.5154	2.5344	-0.0044
Pool 5	OL	0.0119	0.3333	0.02415	1.4167	2.5116	0.0312
	CL	0.0158	0.3712	0.0425	1.5778	2.5142	0.0041

Table 6-9 Performance indexes of Scenario 7 (OL = Open-Loop, CL = Closed-loop)

So far, the study scenarios were all examples of partial closure to show the advantages of closed-loop control over the open-loop control. The two remaining scenarios, which are related to the total closure operation and total opening operation, are tested only under the SDPC control.

- ***Scenario 8***: Total closure from 15 m^3/s to 0 m^3/s with predictive control without considering disturbances. In this scenario, all spillway's thresholds are above water levels, namely, the spillway heights being at its maximum of 3 m and discharge is only over spillway 5, at the end of the canal.

The automatic closure operation under SDPC control exhibits a satisfactory behaviour based on the performance indexes given in Table 6-10. The total closure operation is executed in less than 3 hours, as it is depicted in Figure 6.39. After a series of tests on this scenario, it was determined that the minimum time to closure the canal is 110 min without disturbances. The closure operation with the minimum closing time is illustrated in Figure 6.40. Effectuating the closure operation quicker, results into higher rates of gate opening and higher values of MAO in all pools.

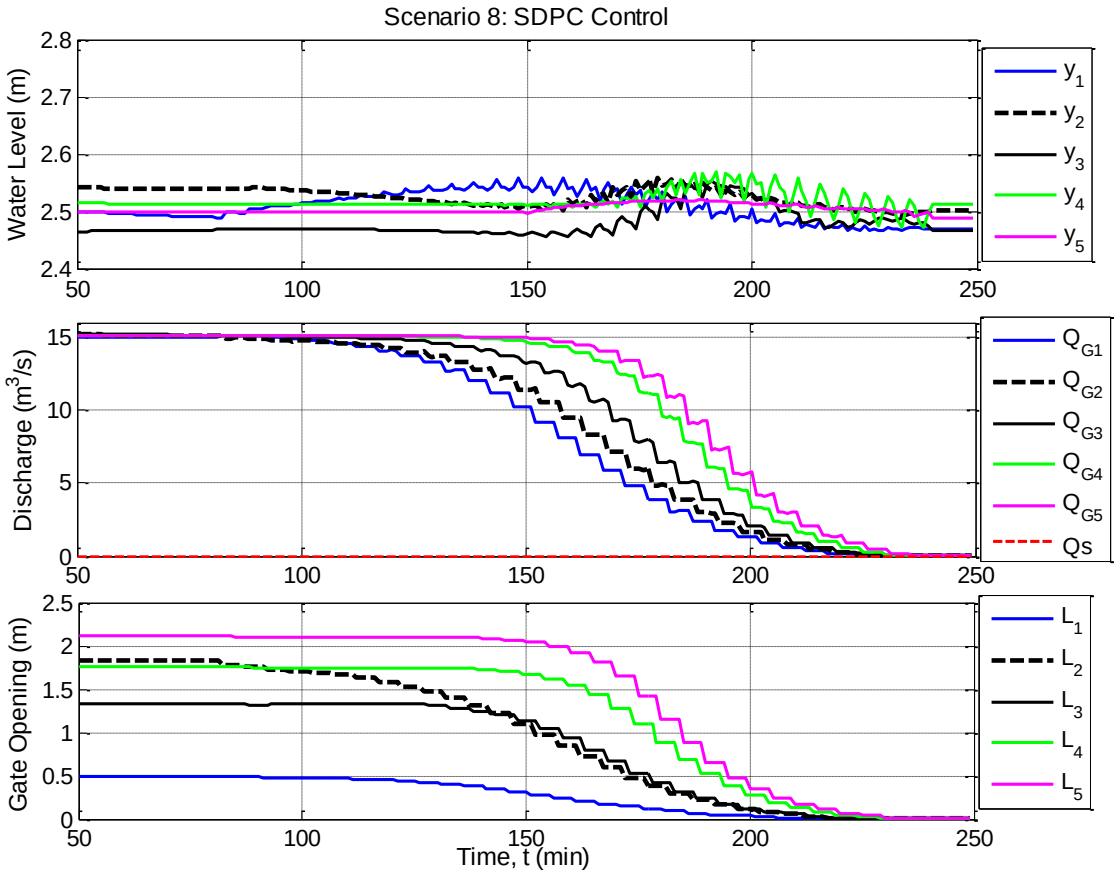

Figure 6.39 Simulation results of total closure operation

Pool	Control	RMSE [m]	MAPE [%]	ISE [m]	IAE [m]	MAO [m]	SSE [m]
Pool 1	CL	0.03024	1.0675	0.1554	4.5368	2.561	0.0282
Pool 2	**CL**	0.02878	0.9614	0.1408	4.0863	2.5602	-0.002
Pool 3	CL	0.02941	1.0995	0.1470	4.6729	2.5543	0.03
Pool 4	**CL**	0.02708	0.881	0.1247	3.7445	2.5726	-0.014
Pool 5	**CL**	0.01067	0.3114	0.0193	1.3235	2.5223	0.0

Table 6-10 Performance indexes of scenario 8 (CL = Closed-loop control).

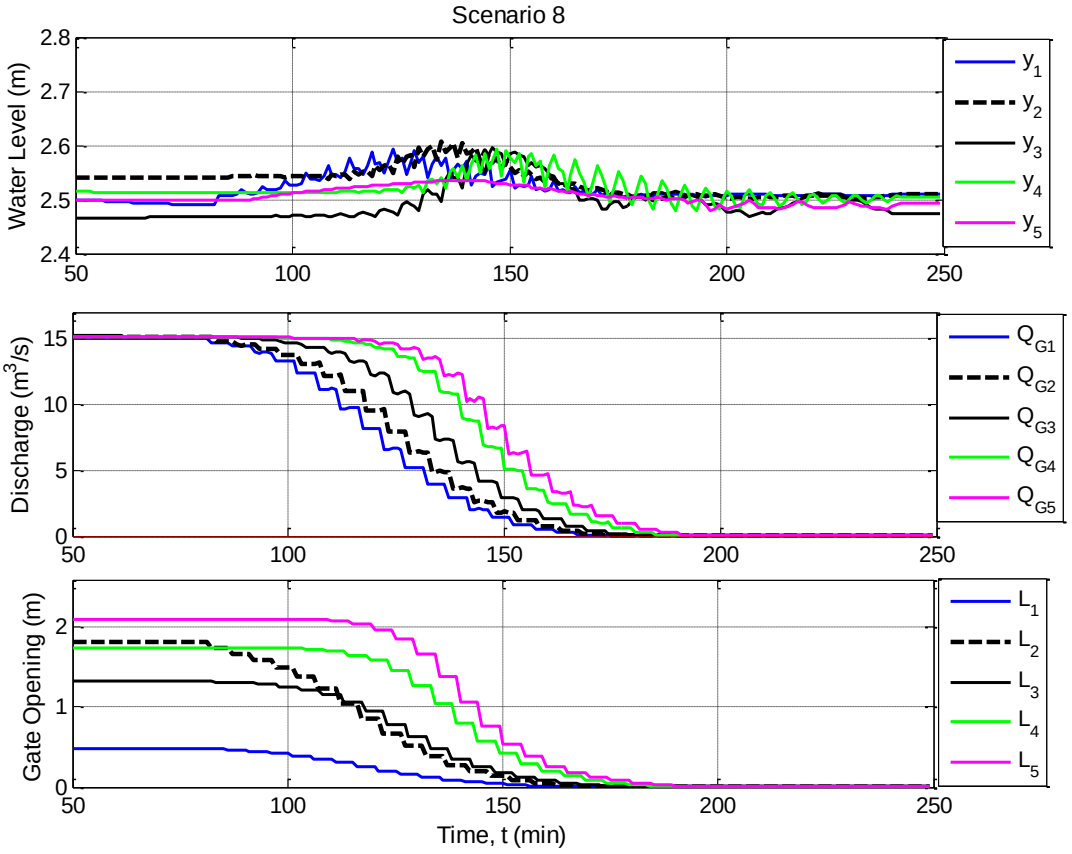

Figure 6.40. Simulation results of total closure operation in 110 min.

- ***Scenario 9***: Total opening operation from 0 m^3/s to 15 m^3/s without disturbances along the opening operation.

The automatic opening operation under the SDPC control is achieved in 130 minutes approximately. The chosen tuning parameters of the controller are detailed in Table 6-11. It is noteworthy that the slope of all sigmoidal functions have increase in comparison with the same parameters in the closing Scenario 1. In general, the automatic opening operation under SDPC control exhibits a satisfactory behaviour based on the indexes given in Table 6-12.

Pool	λ	***Rw***	***a*** *[x10^{-3}]*	***c*** [min]	ΔU_{max} [m^3/s]	ΔU_{min} [m^3/s]
Pool 1	15	1	1.6	90	0.5	0.5
Pool 2	21	1	2	91	0.5	0.5
Pool 3	23	1	2.1	100	0.5	0.5
Pool 4	12	1	2.1	113	0.5	0.5
Pool 5	9	1	2	119	0.5	0.5

Table 6-11 Parameters for each controlled pool for the opening operation

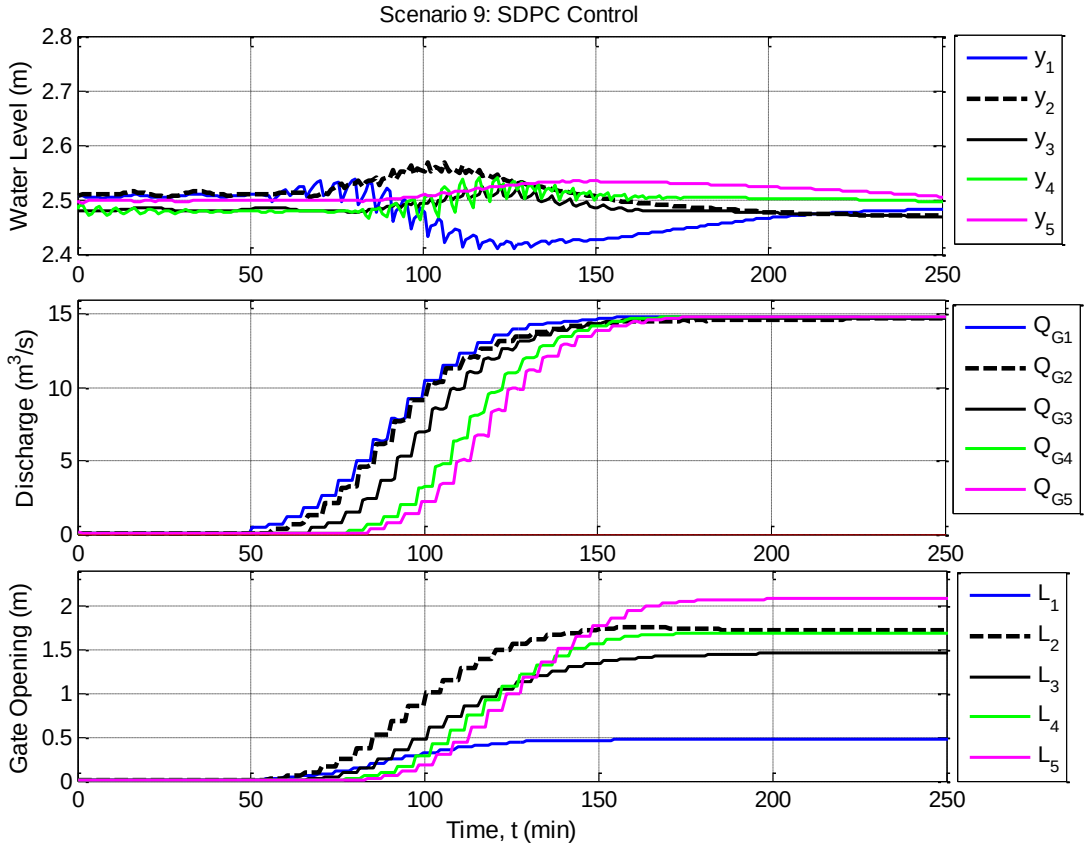

Figure 6.41 Simulation results of opening operation at ERLB canal

Pool	Control	RMSE [m]	MAPE [%]	ISE [m]	IAE [m]	MAO [m]	SSE [m]
Pool 1	CL	0.04054	1.2936	0.44549	8.7641	2.5391	0.01
Pool 2	**CL**	0.02697	0.9124	0.19723	6.1815	2.5698	0.027
Pool 3	CL	0.01897	0.6977	0.09752	4.7269	2.5282	0.03
Pool 4	**CL**	0.01569	0.5034	0.06677	3.4105	2.5433	0.0067
Pool 5	**CL**	0.02034	0.6120	0.11219	4.1466	2.5365	0.0275

Table 6-12 Performance indexes of opening operation at ERLB canal (CL = Closed-loop control)

6.4.4 Discussion of the results

Most of the figures demonstrate that the supervised decentralized predictive control with dynamic constraints is a convenient strategy for closure and opening of irrigation canals automatically. With the simulation results of automatic closure of the ERLB canal, without any presence of disturbances, both open-loop and closed-loop control present a positive performance with small

oscillations (less than 10 cm). However, if during the closure operation, a large disturbance (intake or offtake) is presented along the canal, then the disturbance rejection is better tackled by the closed-loop control than the open-loop control. Indeed, the performance of open loop control presents undesirable large overshoots that lead to overtopping in two scenarios. In general, the steady state errors are lower for the closed-loop than the open-loop control.

The sluice gates movement along the closure operation leads to the occurrence of oscillations of small amplitude that limits both the precision of the setpoint tracking performance and the minimum closing time. It has been established numerically that the minimum time to closure the canal without constraints is 110 min., as it is illustrated in the Scenario 8. However, this period of time increases to 165 min. in the presence of a positive disturbance Qs_1 of 6.8 m^3/s, as it is illustrated in the simulation results of Scenario 3.

An important contribution of this dissertation is the development of a strategy for automatic canal operations involving abrupt changes in operating conditions, which is even able to tackle strong disturbances when the operating point is changing. It is widely agreed that to control a five pool configuration canal, such as the ERLB canal, is more complicated that a three-pool configuration canal, such as the canal PAC-UPC. The SDPC control designed in this dissertation has demonstrated a satisfactory behaviour in both case studies.

In summary, adding dynamic constraints to the predictive control, makes it feasible to tackle the canal closure problem involving a wide change in the operating condition while the water levels are keeping as close as possible to the setpoints. Based on the knowledge of canal system operation, it is possible to generate sigmoidal functions that allow the predictive controller drive the canal from an operating point to another with the occurrence of water level oscillations of small amplitude. In the presence of large disturbances, the controller requires a time shift of the sigmoidal functions that determines the maximum discharge in the downstream pools and consequently the performance indexes of the opening process will improve. The tradeoff of the time shifted operation is that the closure operation takes longer time in comparison with the closure operation without disturbances.

6.5 Real-time implementation of supervised decentralized predictive control on the laboratory canal

This section is devoted to present the experimental results of automated closure and opening operations on the canal PAC-UPC, using the SDPC strategy presented in Chapter 5. The experiments have been done on a three pool configuration of the canal (see Figure 6.2). This section also includes some aspects related to the real-time implementation.

6.5.1 Real-time control

A new supervisory control and data acquisition (SCADA) system for the laboratory canal facility has been built as part of the development of this thesis. It is based on the original one designed by (Sepúlveda, 2008) and illustrated in Figure 6.42. A considerable number of changes in the SCADA software have been implemented to enable imposing abrupt changes in operating conditions.

The SCADA system enables the water master collecting data from the hydraulic variables in field and to send control commands to the motorized gates. The SCADA includes the human-machine interface depicted in Figure 6.43. The operator interface functions as the operator window into the canal. The SCADA is based on a computer which functions as the master terminal unit (MTU). The MTU, located in the master station, is the system controller which may supervise and control the canal operation in real-time. The MTU contains blocks of supervisory level, water predictive control, and gate discharge control (see the control system architecture described in Section 2.2.1).

The control philosophy used in the canal PAC-UPC is a cascade control which contains a set of control loops placed one inside another, as it is illustrated in Figure 6.42. Every pool has a gate position controller (block labeled as *GPC* in Figure 6.43) which is a feedback control that converts the required gate openings (*SPI*) into gate movements. The gate discharge controller (blocks labeled as *GDC* in Figure 6.43) converts the requested discharge under gate (*SPq*) into required gate openings (*SPI*) by inverting the Ferro's flow formulas (Ferro & Ansar, 2001). In the outer loop, the water level control can be fulfilled with several control schemes, for instance the constrained predictive control developed in this dissertation.

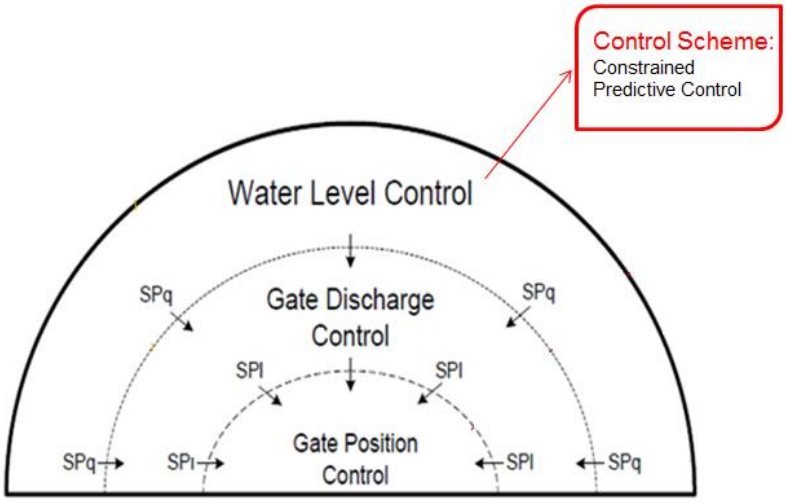

Figure 6.42 Canal Control philosophy used in the PAC-UPC canal (taken from (Sepúlveda, 2008))

The SCADA system has been implemented in Matlab/Simulink® environment. The real-time control is executed by a Matlab's tool so-called Real-Time Windows Target (RTWT). The RTWT toolbox enables to run Simulink models on the MTU that interacts in real-time with the remote devices. The canal control algorithms have been developed in Embedded Matlab language, the

script is inside the block labeled as "*Predictive_control"* in the lower left part of Figure 6.43. In the canal instrumentation, the MTU requests an update from remote site devices every 0.1 s. Meanwhile, the predictive control updates the control variable every 10 s. In the Simulink model, *RateTransition* (RT) blocks have been used in order to transfer data between ports operating at different rates. The 11 water level sensor signals are collected with a DAQ card installed in the MTU. The raw signals are filtered digitally using a low pass filter (block labeled as LPF in Figure 6.44) in order to minimize the random deviation of the sensor signal. After the filtering, signals are modified using calibration curves in order to obtain accurate measurements within the specification limits.

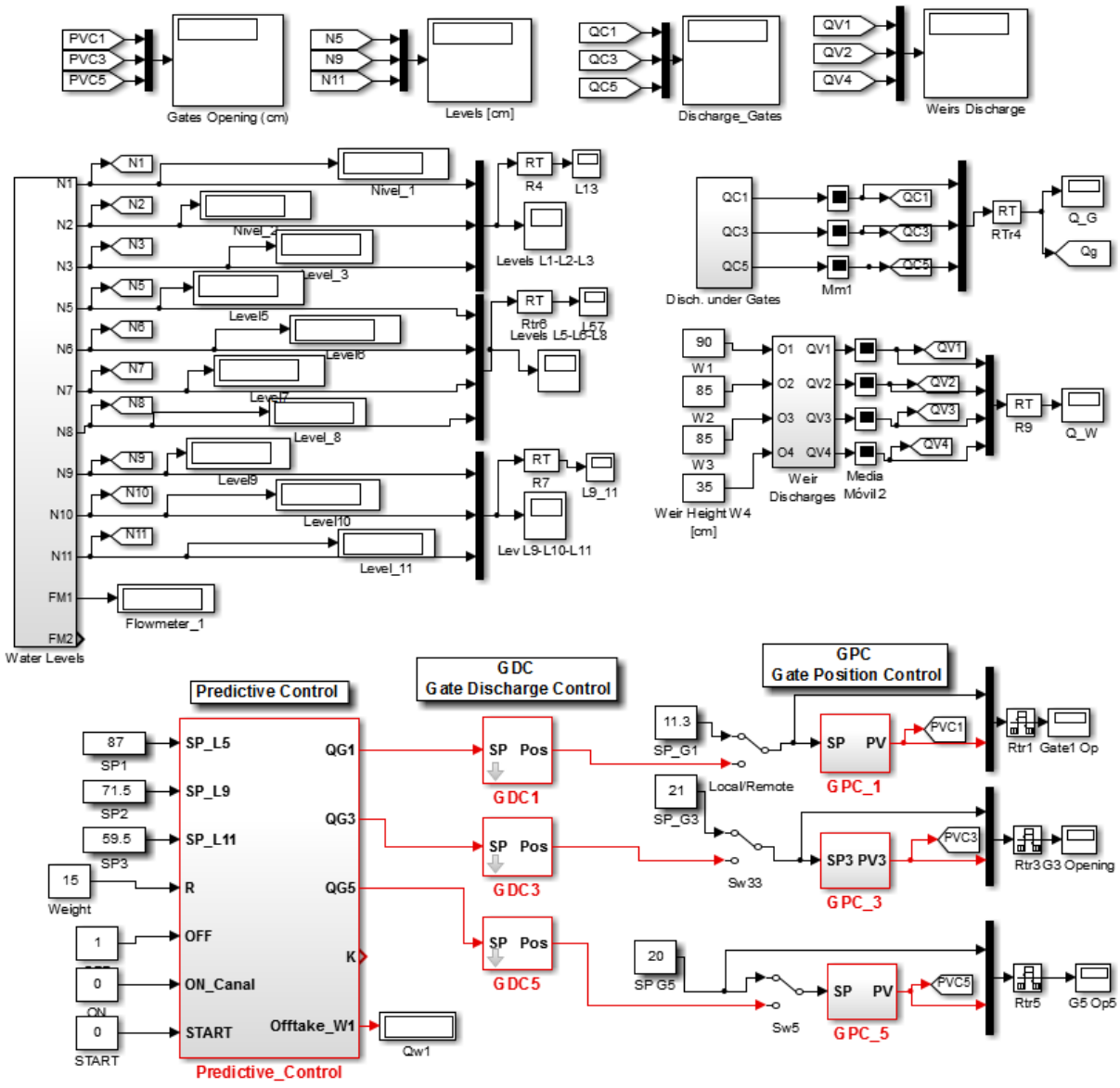

Figure 6.43 Operator Interface in the SCADA system

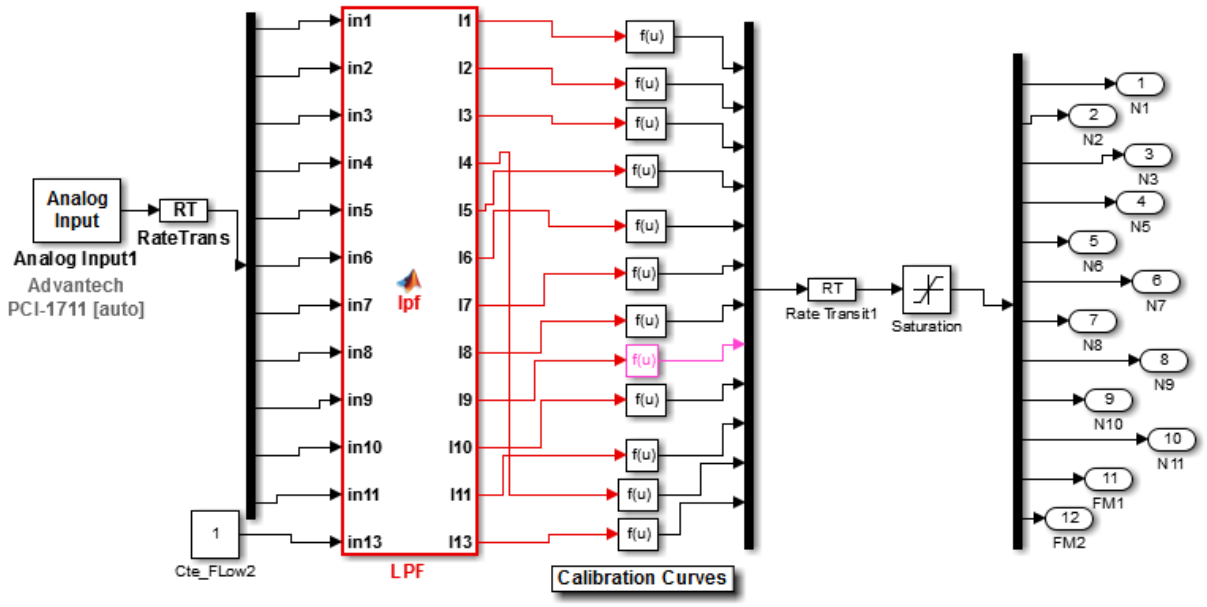

Figure 6.44 Acquisition of water level signals in the SCADA system

The accuracy of the measurements of the SCADA system is affected by both physical and instrumentation constraints in the canal. For instance, the accepted gate position error is 2 mm, owing to the fact that it is not possible to move the motorized gate less than a minimum distance. There are level sensors located upstream and downstream of each gate and at every rectangular weir in order to measure discharge based on these water level measures. The accepted water level error is around 1 cm and the minimum control variable incremental flow variation is around 6 l/s.

The canal has three vertical sluice gates hoisted by three-phase servomotors located on top of the gates. Each servomotor has a position measuring gear embedded in the motor chassis. At the time when the experiments where fulfilled, the gate velocities were 3.125 mm/s for G_1, 1.524 mm/s for G_2 and 3.125 mm/s for G_3. On the other hand, to achieve an operating discharge equal to zero is not allowed in the actual laboratory canal owing to the fact that the minimum gate openings are 3, 5 and 5 mm for gates G_1, G_2 and G_3 respectively. A discharge value around 5% of the operating flow had chosen as minimum discharge in the experiments.

Finally, the watermaster may manipulate the canal-related data in the HMI. The operator may decide when to start a closure/opening operation. The operator may also adjust other parameters such as setpoint along a normal canal operation, penalization over setpoint variation, closing time, opening time, prediction horizon and manual/automatic operation.

6.5.2 Water level control at canal PAC-UPC

6.5.2.1 Control objective and operating scenarios

The general objective of the SDPC controller is to keep the water levels as close as possible to the setpoint, while the operating discharge changes in a wide range. The regulating task is evaluated

by both setpoint tracking and disturbance rejection. The specific requirements to bear in mind for the proposed experimental tests are:

- Canal freeboard of 8 cm.
- Manage the canal to execute a closure operation with an 8 min-settling time (as long as there are no lateral offtakes).
- The accepted steady state error (SSE) is 3 cm for controlled water levels.
- The maximum absolute overshoot must be less than 5% of the setpoint for every controlled water level. It is expected less than 92 cm for the first pool, which means a percentage overshoot lower than 8% of the top of canal lining.

A series of experiments were conducted to test the hypothesis of the dissertation, namely that the supervised decentralized dynamically-constrained predictive control is a convenient strategy for closure and opening of irrigation canals automatically. In the laboratory canal PAC-UPC, the proposed scenarios are:

- Scenario 1: Automatic closure with no disturbances. The initial operating flow is 100 l/s.
- Scenario 2: Automatic canal opening from 5 l/s to 90 l/s with no disturbances. The opening time must be less than 12 minutes.
- Scenario 3: Automatic closure in the presence of a disturbance $\boldsymbol{Qw_1}$ of 36 l/s during $0 \leq t \leq 2.4$ min, and after on the disturbance changes suddenly to 0 l/s.

6.5.2.2 Experimental results

- *Scenario1*: This test is devoted to analyze the closure operation without changes in the lateral offtakes. The initial operating flow is 100 l/s.

This scenario starts from the steady state detailed in Table 6-13. The lateral weirs, W_1 and W_2 are settled to the maximum height of 90 cm and the height of the final weir (W_4) is 35 cm. For this closure operation, levels y_1 and y_2 are the controlled variables. For the new steady state obtained after the closure operation, level y_3 is determined by final weir height at the end of the canal. Setpoint for levels y_1 and y_2 are 0.88 and 0.72 m respectively.

Qop **[l/s]**	$\mathbf{y_1}$ **[cm]**	$\mathbf{y_2}$ **[cm]**	$\mathbf{y_3}$ **[cm]**	$\mathbf{L_1}$ **[cm]**	$\mathbf{L_2}$ **[cm]**	$\mathbf{L_3}$ **[cm]**	$\mathbf{W_1}$ **[cm]**	$\mathbf{Q_{W1}}$ **[l/s]**	$\mathbf{W_2}$ **[cm]**	$\mathbf{Q_{W2}}$ **[l/s]**	$\mathbf{W_4}$ **[cm]**
100	88	72	59	11.2	20	20	90	0	90	0	35

Table 6-13 Initial Steady State for scenario 1

The automated closure operation using SDPC is depicted in Figure 6.45. The controlled system exhibits a satisfactory behaviour based on performance requirements given in Subsection 6.5.2.1. As it can be observed, after 6 minutes the closure operation is completed with the flow reaching a close to zero value, while the water levels are maintained all the time inside the permitted safety

band. The maximum absolute overshoots are 89.53 cm and 72.78 cm for y_1 and y_2 respectively (lower than 1.8 % of the setpoint for both cases). The steady state errors for y_1 and y_2 are 0.1 and 0.8 cm respectively. These SSE values represent magnitudes lower than 1.3 % of the setpoint for both cases.

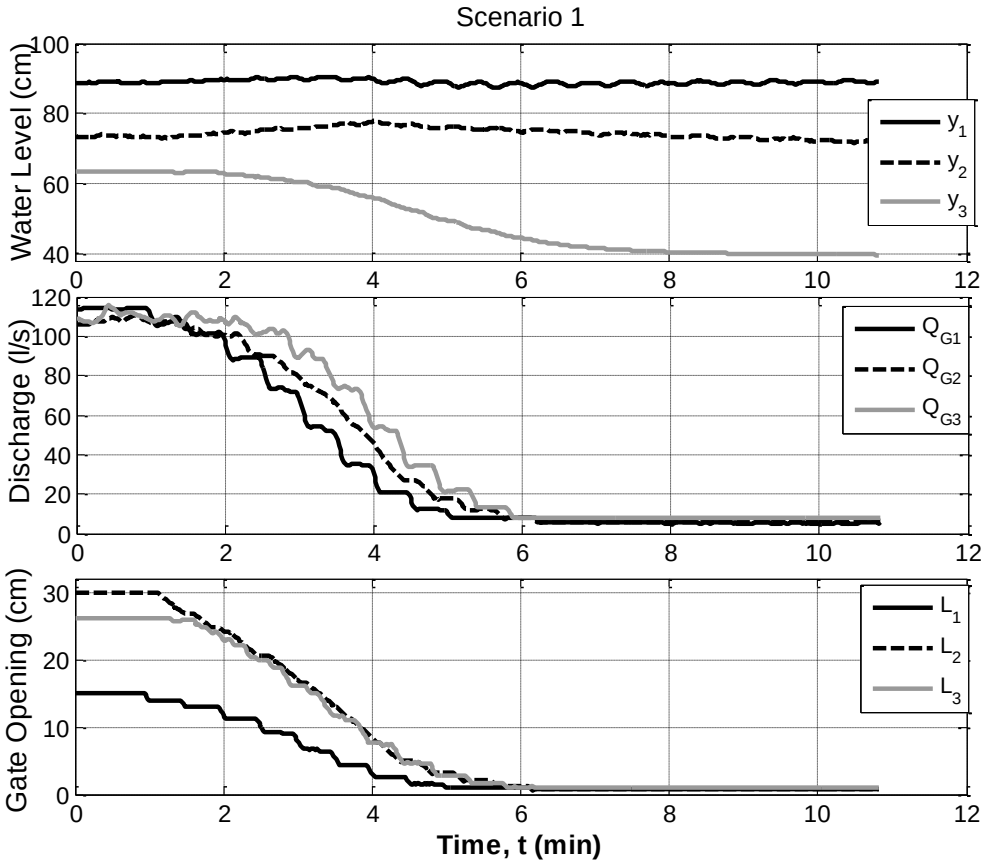

Figure 6.45. Experimental results of automatic closure of canal PAC-UPC under SDPC

- *Scenario 2*: This experiment is devoted to analyze the automatic canal opening from 6.5 l/s to 91 l/s without changes in the lateral offtakes.

This scenario starts from the steady state detailed in Table 6-14. For this opening operation, the three downstream levels are the controlled variables. The setpoints are $SP_1 = 90$ cm, $SP_2 = 72.5$ and $SP_3 = 57$ cm. The experimental results of the automated opening operation under SDPC control are depicted in Figure 6.46.

Qop **[l/s]**	y_1 **[cm]**	y_2 **[cm]**	y_3 **[cm]**	L_1 **[cm]**	L_2 **[cm]**	L_3 **[cm]**	W_1 **[cm]**	Q_{W1} **[l/s]**	W_2 **[cm]**	Q_{W2} **[l/s]**	W_4 **[cm]**
6.5	90	72.5	40	0.9	0.67	0.73	90	0	90	0	35

Table 6-14 Initial Steady State for Scenario 2

The experimental results of the automatic opening under SDPC exhibits a positive performance. For instance, the time taken to achieve a steady state condition for the opening operation is 12 minutes approximately. The maximum level errors are 0.2 cm (lower than 0.5 %) for y_1 and 3.6 cm (lower than 5 % of the setpoint value) for y_2. The steady state errors are 0.2 cm (lower than 0.5%) for y_1 and 0.6 cm (around 0.9 % of the setpoint value) for y_2. The water level y_2 is affected directly by the increase of volume at the end of the canal where there is a rectangular weir, the U-shape of y_2 is modulated by the increase of volume at pool 3. The opening operation duration is longer than the closure operation since the system has to fill up the downstream pool with a volume of 325 m^3 approximately.

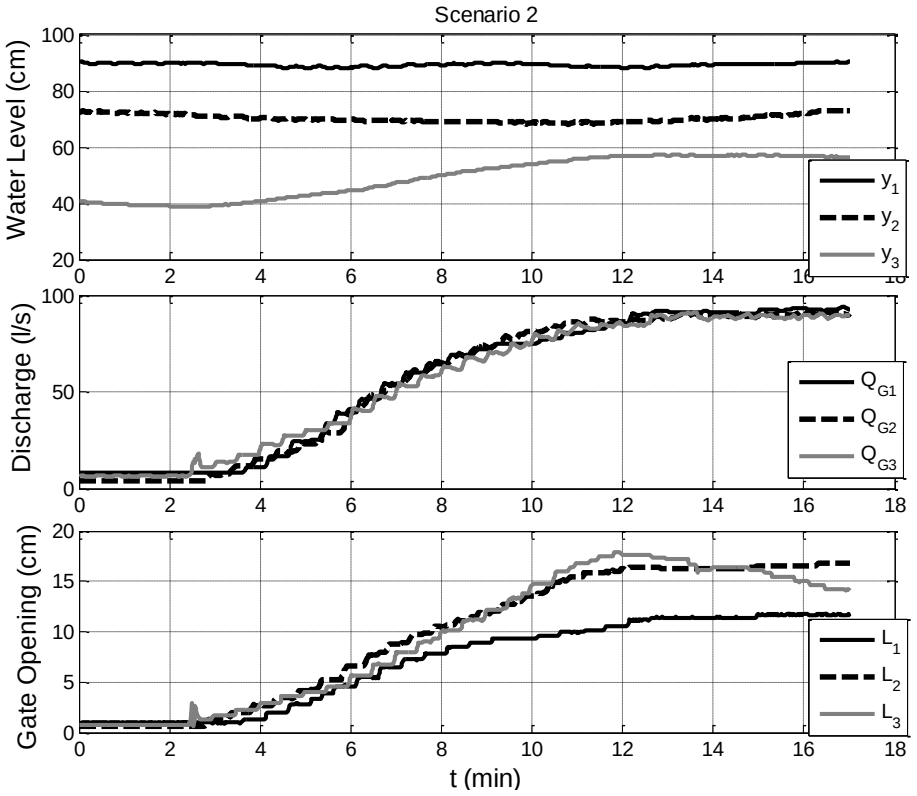

Figure 6.46 Experimental results of automatic opening of canal PAC-UPC under SDPC.

- *Scenario 3*: This scenario is devoted to analyze the automatic closure in the presence of a disturbance. The lateral offtake ***Qw1*** of 36 l/s is present along 2.4 min, and after on the disturbance changes suddenly to 0 l/s.

The initial operating flow in the first pool is 138 l/s. The 36 l/s are equivalent to 26% of the operating discharge in the first pool of the canal. In this closing scenario only water levels y_1 and y_2 are the controlled variables. The setpoints for levels y_1 and y_2 are 84 and 70 cm respectively.

Qop **[l/s]**	y_1 **[cm]**	y_2 **[cm]**	y_3 **[cm]**	L_1 **[cm]**	L_2 **[cm]**	L_3 **[cm]**	W_1 **[cm]**	Q_{W1} **[l/s]**	W_2 **[cm]**	Q_{W2} **[l/s]**	W_4 **[cm]**
138	84	70	59.6	17.8	29.4	21.8	65	36	90	0	35

Table 6-15 Initial Steady State for Scenario 3

The closed-loop automatic control exhibits a satisfactory behaviour even in presence of disturbance along the closure operation. For instance, the maximum absolute overshoots for both water levels are lower than 6%, namely, the MAO of $y_1$is 88.7 cm, which is equivalent to 5.6% of SP_1 and the MAO of $y_2$is 72.7 cm, which is equivalent to 3.85% of SP_2. Meanwhile, the steady state errors for y_1 and y_2 are 2 and 3 cm respectively. These SSEs represent values lower than 5 % of the setpoint for both cases. Experimental results of the automated closure operation under SDPC are depicted in Figure 6.47

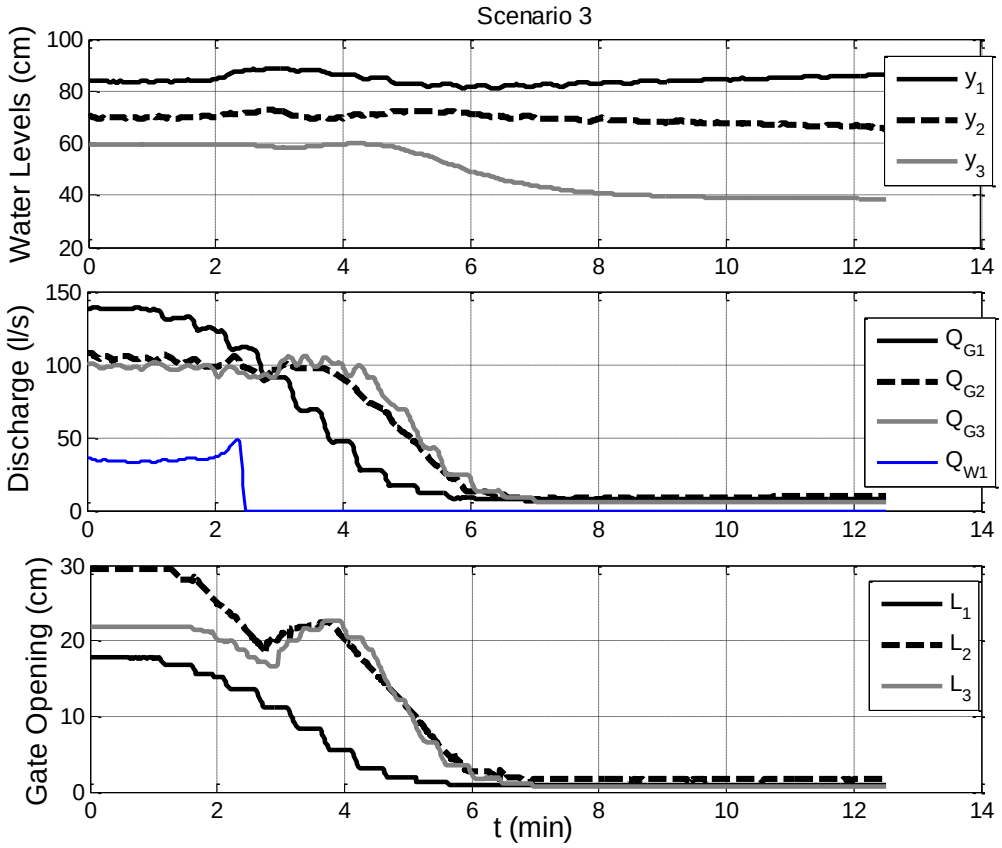

Figure 6.47 Experimental results of closure operation with disturbance rejection at canal PAC-UPC

6.5.2.3 Discussion of the experimental results

In all the experimental scenarios, the controlled water levels in every pool remain inside the safety band along both transient and steady response. In real-time implementation, the gates are moved sequentially from upstream to downstream (with at least 10 seconds delay between them) as driven by the supervisor. The dynamic constraints that determine the maximum discharge of predictive control are defined by the sigmoidal function described in (6.2). The controlled variables converge to the reference with a small acceptable error. As it can be noted in Figures 6.45, 6.46 and 6.47, no overtopping is produced in the automatic operations involving abrupt changes in operating conditions.

The Embedded Matlab® code for real-time control that allows the implementation of the on-line optimization-based control approach has been implemented with a sampling time of 10 sec. The matrices E_i, G_i, P_i and G_0 involved in the predictive control formulation (see Subsection 5.3.1) are calculated offline for the controller algorithm. So, once the SCADA system starts up, a file with the matrices is loaded just one time. The controller tuning parameters used in the real-time implementation are the same used in simulation (see Table 6-1).

The experimental results reveal that the success of the automatic control strategy for closure and opening operations proposed in this dissertation depends highly on the degree of accuracy of the gate position control and the proper calibration of the water level sensors. Therefore, a regular preventive maintenance of the canal instrumentation is highly recommended. Devices that require more technical attention include water level sensors, flowmeters, and motorized check gates. In actual canal irrigation system, control equipment hardware must resist the canal bank environment and function for long continuous periods without failure. The actual implementation in field requires a two-way radio system in order to communicate the headquarter (supervisory controller) with the decentralized control units.

Chapter 7

Conclusions

7.1 Summary and general conclusions

This dissertation has been motivated by the interest for developing automatic control strategies to manage closing and opening operations in irrigation canals that are composed by several pools connected by controllable gates. Such types of operations are challenging and scarcely studied within the literature related to irrigation canals and, in particular, within the state of the art covering the applications of automatic control systems. Main difficulties with closing (and similarly opening) operations are related to the following factors:

- They involve large changes in water discharges, and are sensitive to the couplings between the different pools and to the presence of unknown disturbances.
- They require a critical command of the gate trajectories, with a compromise between producing feasible smooth excursions and completing the canal closing within a specifically needed short time, while keeping the water levels within prescribed bounds.

To contribute towards the solution of the problem, this work has combined knowledge of two wide and different areas: control engineering and hydraulic engineering. From the last side, the thesis has addressed two benchmark case study problems: a laboratory canal available at the Technical University of Catalonia (PAC-UPC) and a main canal of the left bank of the river Ebro in Spain (ERLB). Both have been numerically simulated via a state of art computational code, while the canal PAC-UPC has been additionally used for real-time implementations.

Following a constructive approach, the core of thesis has been initiated by studying the problem of closing and opening these benchmark canals, checking different manual operations. The outcome of this study (in Chapter 4) has been twofold: (1) learning significant issues and difficulties that arise when check structures are required to get completely closed; and (2) getting practical inputs for the automatic control design.

Numerical simulation results have highlighted problems, such as overtopping, that arise when the closure canal operations are not managed properly. These problems motivate the need for automatic control. Five scenarios, depending on the gate velocities, have been designed to check the transient response after closing gates of cases studies under manual local control.

The quality of the closure operation in canals is determined by aspects such as closing velocity, water levels inside the minimum/maximum safety margins required on the canal, and to keep the water levels as close as possible to the setpoint. Wave phenomenon occurs regardless which are the initial conditions or which are the velocities of motorized gates. A canal system to be closed is affected by upstream and downstream disturbances. Therefore, the control system to manage closure and opening operations must avoid the risk of exceeding the safety levels required on the canal to avoid problems such as overtopping and cracking. The closure/opening operations must be done as soon and quick as possible to make feasible the closure in management practices such as, night closure to save water. The minimum allowed time to complete the operation is determined by the geometry of the canal, the flow conditions, the velocity of the check structures and the final objective pursued with the closure. The operational requirements of the closure operation are almost impossible to achieve using local manual control methods. The simulation and real-time experiments in Chapter 4 have demonstrated that closing the gates sequentially from upstream to downstream in a smooth manner may reduce the overtopping risk.

From the control engineering side, the outcome of the thesis (Chapter 5) has been a control strategy for automatic closure and opening of irrigation canals, which has been developed in a two-level architecture: (i) individual decentralized downstream water level predictive controllers formulated via an optimal control problem under dynamic constraints and implemented by upstream local gates; and (ii) a supervising scheme to achieve the compromise of fast execution with smooth gate trajectories and water level regulation, even in the presence of disturbances.

The aim of the supervisor is being responsible for allowing the cyclic sequential movement of each motorized gate of the entire canal system. In the presence of an unexpectedly large disturbance, the supervisor detects the location where a sudden raise of water level has occurred and then command the next controller to operate during the closure operation. Each decentralized control is a local automatic water level controller, which requires the current state of its controlled pool and information of neighbor pools. For the practical implementation, the proposed control system requires a remote terminal unit (RTU). The RTU monitors the water levels and equipment status, and transmits these data to the supervisor.

The final supervised decentralized predictive control (SDPC) strategy has been evaluated (in Chapter 6) by means of numerical simulation on the two cases of study in a variety of operating scenarios. This includes comparisons of the performance with respect to the use of optimal

predictive open-loop control of gate trajectories. In addition, it has been experimentally validated through real-time implementation in the laboratory canal PAC-UPC.

Most of the simulation results show that the closed loop predictive control with dynamic constraints is a convenient strategy for automatic closure and opening operation of canals. In all the simulation scenarios, water levels in each controlled pool remain inside the safety band along both transient and steady response. Nine scenarios have been designed to check the performance of the predictive control in the ERLB canal. Three scenarios have been simulated to check the controller performance in the canal PAC-UPC. Overtopping is avoided in both closure and opening operations. The closure operation performance under SDPC has improved comparing to open-loop closure operations. In the simulation results of closure operation in the ERLB canal, without any presence of disturbances, both open-loop and closed-loop control present a positive performance with small oscillations (less than 10 cm). However, if during the closure operation, a large disturbance (intake or offtake) is present along the canal, then the disturbance rejection is better tackled by the closed-loop control than by the open-loop control. The performance of open-loop control presents undesirable large overshoots that lead to overtopping in two scenarios. In general, the steady state errors are lower for the closed-loop than for the open-loop control.

In all the experimental closure and opening scenarios fulfilled in the canal PAC-UPC, the controlled water levels in every pool remain within the safety margins along both transient and steady response. In the real-time implementation, the gates are moved sequentially from upstream to downstream. The experimental results reveal that the success of the automatic control strategy for closure and opening operations proposed in this dissertation depends highly on the degree of accuracy of the gate position control and the proper calibration of the water level sensors. Therefore, a regular preventive maintenance of the canal instrumentation is highly recommended. Devices that require more technical attention include water level sensors, flowmeters and motorized check gates. In actual canal irrigation systems, control equipment hardware must resist the canal bank environment and function for long continuous periods without failure.

The results presented in Chapter 6, in summary, conclude the efficiency of the control strategy proposed in this thesis to face the problem of closing/opening irrigation canals.

7.2 Contributions of this thesis

The main contribution of this dissertation is the development of a strategy for automatic canal operations involving abrupt changes and disturbances in operating conditions, which has been called *supervised decentralized predictive control with dynamic constraints* (SDPC).

Another contribution is related to how to tackle a predictive control problem that cannot be solved by optimizing the typical linear quadratic cost function with time-invariant constraints when two conflicting control objectives are stated in the control problem. A sigmoidal function, acting as a dynamic constraint, has been proposed in the control design, which contributes to generate the

controlled gate movements in a smooth way. In the presence of disturbances, a supervisor reshapes systematically the sigmoidal function through the relaxation of constraints as soon as a raise of water is detected.

It has been the first time that real-time predictive control *with constraints* has been implemented in the canal PAC UPC facility. The Hildreth's quadratic programming algorithm has been used in this work to obtain the on-line numerical solution of the constrained optimization problem. A new supervisory control and data acquisition (SCADA) system for the laboratory canal facility has been built as part of the development of this thesis. The SCADA system is an extension of the original one designed by (Sepúlveda, 2008).

7.3 Future research

For further research and applications, some ideas could be considered:

- To extend the validations of the supervised decentralized predictive control with dynamic constraints by simulating the implementation in the two ASCE test canals in closing/opening scenarios.

- The transient wave phenomenon originated when the gates are suddenly closed along the canal presents higher peaks in pools which length are shorter than the upstream neighbor one. Therefore the maximum absolute overshoot values are lower in the upstream pool in comparison with the downstream pool. In this way, to compare the performance by means of simulation in another canals is a challenge to extend the results achieved in this dissertation.

- To validate the SDPC control methodology by means of closure/opening operations in a real field irrigation canal. Indeed, field testings would give significant lessons on the different components of the overall system, regarding both the methodologies and the supervision and control practical units.

- To test the SDPC control methodology using gate opening directly as control action variable instead of discharge such as it is proposed in the work (Horváth et al., 2014b). It may be interesting to make a comparison between the two schemes in terms of formulation and performance.

- To propose new scenarios under abrupt change conditions to validate the SDPC strategy. For instance, a scenario where some of the canal gates broke down along the closure operation. Another example could be testing an on demand partial closure involving abrupt change in the operating condition in less time than the total closure operation.

7.4 Publications derived from this thesis

Galvis, E., Mantecón, J., Horváth, K., Gómez, M., & Rodellar, J. (2014). An automatic control strategy for closure and opening of irrigation canals. In *USCID Water Management Conference*. Phoenix, USA.

Horváth, K., Galvis, E., Gómez, M., & Rodellar, J. (2015). New offset-free method for model predictive control of open channels. *Control Engineering Practice*, *41*, 13–25. doi:10.1016/j.conengprac.2015.04.002

Horváth, K., Galvis, E., Gómez, M., & Rodellar, J. (2014a). Experimental comparison of canal models for control purposes using simulation and laboratory experiments. *Journal of Hydroinformatics*, *16*(6), 1390–1408. doi:10.2166/hydro.2014.110

Horváth, K., Galvis, E., Gómez, M., & Rodellar, J. (2014b). Is it better to use gate opening as control variable than discharge to control irrigation canals? *Journal of Irrigation and Drainage Engineering*, *141*(3), 04014054. doi:10.1061/(ASCE)IR.1943-4774.0000798

Galvis, E., Mantecon, J., Horváth, K., Gómez, M., & Rodellar, J. (2014b). Predictive control based on multiple models for canals that require large change in operating conditions. In *Congress on Industrial and Agricultural Canals* (pp. 378–380). Lleida, Spain.

Gómez, M., Galvis, E., Horváth, K., & Rodellar, J. (2014). Canal PAC-UPC: una instalación experimental para el ensayo de algoritmos de control automático de canales. In J. Porta (Ed.), *Congress on Industrial and Agricultural Canals* (pp. 401–404). Lleida, Spain: Universitat de Lleida.

Galvis, E., Mantecon, J., Horváth, K., Gómez, M., & Rodellar, J. (2014). Cierre automático en tiempo real de canales de regadío: estudio en un canal de laboratorio. In Seminario Red de Laboratorios de Hidráulica de España (pp. 33–35). Madrid: RLHE.

Aguilar, J., Langarita, P., Linares, L., Galvis, E., Horváth, K., Rodellar, J., & Gómez, M. (2011). Control automático de niveles en un canal experimental de tres tramos. In *II Jornadas del Ingeniería del agua, Modelos numéricos en dinámica fluvial*. Barcelona.

Horváth, K., Galvis, E., Gómez, M., & Rodellar, J. (2012). Comparison of two control algorithms based on different canal models using numerical simulation and experiments on a laboratory canal. In *10th International Conference On Hydroinformatics.* Hamburg, Germany: IAHR/IWA.

Horváth, K., Galvis, E., Gómez, M., & Rodellar, J. (2011a). Control automático en canales de riego experiencias en el canal de laboratorio UPC-PAC. In *IV Seminario sobre las Líneas Prioritarias de Investigación de la Red de Laboratorios de Hidráulica de España* (pp. 20–21). Madrid: RLHE.

Galvis, E., Horvath, K., Gómez, M., & Rodellar, J. (2011). Simplified modeling of a laboratory irrigation canal for control purposes. In *IV Seminar on Advanced Industrial Control Applications. SAICA 2011*. Barcelona.

Horváth, K., Galvis, E., Gómez, M., & Rodellar, J. (2011b). Pruebas de algoritmos de control automático en un canal de laboratorio y un canal simulado. In *II Jornadas del Ingeniería del agua, Modelos numéricos en dinámica fluvial*. Barcelona.

References

Abbott, M. (1966). An Introduction to the method of characteristics. *Journal of Applied Mathematics and Mechanics*, *47*(5), 347–348. doi:10.1002/zamm.19670470519

Aguilar, J., Langarita, P., Linares, L., & Rodellar, J. (2009). Automatic control of flows and levels in an irrigation canal. *IEEE Transactions on Industry Applications*, *45*(6), 2198–2208. doi:10.1109/TIA.2009.2031941

Aguilar, J., Langarita, P., Linares, L., Rodellar, J., & Soler, J. (2012). Adaptive predictive expert control of levels in large canals for irrigation water distribution. *International Journal of Adaptive Control and Signal Processing*. doi:10.1002/acs.2272

Akouz, K., Benhammou, A., Malaterre, P. O., Dahhou, B., & Roux, G. (1998). Predictive control applied to ASCE canal 2. In *IEEE International Conference on Systems, Man, and Cybernetics* (Vol. 4, pp. 3920–3924). IEEE. doi:10.1109/ICSMC.1998.726700

Allgower, F., Findeisen, R., & Nagy, Z. (2004). Nonlinear model predictive control: From theory to application. *Journal of the Chinese Institute of Chemical Engineers*, *35*(3), 299–315. Retrieved from http://www.cheric.org/research/tech/periodicals/view.php?seq=1018687

Alvarado, I., Limon, D., Muñoz de la Peña, D., Maestre, J. M., Ridao, M., Scheu, H., … Espinosa, J. (2011). A comparative analysis of distributed MPC techniques applied to the HD-MPC four-tank benchmark. *Journal of Process Control*, *21*(5), 800–815. doi:10.1016/j.jprocont.2011.03.003

Álvarez, A., Ridao, M., Ramirez, D., & Sánchez, L. (2013). Constrained predictive control of an irrigation canal. *Journal of Irrigation and Drainage Engineering*, *139*(10), 841–854. doi:10.1061/(ASCE)IR.1943-4774.0000619.

Arnold, E., Linke, H., & Puta, H. (1999). Nonlinear model predictive control for operational management of a canal system. In *IEEE European Control Conference* (pp. 4876–4880). Karlsruhe.

Bastin, G., Bayen, A., Piccoli, B., Litrico, X., & D'Apice, C. (2009). Open problems and research perspective for irrigation channels. *Networks and Heterogeneous Media*, *4*(2). doi:10.3934/nhm.2009.4.2i

Begovich, O., Martinez, E., & Ruiz, V. (2007). Decentralized fuzzy gain scheduling control for an open irrigation canal prototype. In *4th International Conference on Electrical and Electronics Engineering* (pp. 262–265). Mexico: IEEE. doi:10.1109/ICEEE.2007.4345018

Begovich, O., Ruiz, V. ., Besançon, G., Aldana, C., & Georges, D. (2007). Predictive control with constraints of a multi-pool irrigation canal prototype. *Latin American Applied Research*, *37*(3), 177–185.

Begovich, O., Ruiz, V., Georges, D., & Besançon, G. (2005, January 1). Real-time application of a fuzzy gain scheduling control scheme to a multi-pool open irrigation canal prototype. *Journal of Intelligent & Fuzzy Systems*. IOS Press. Retrieved from http://content.iospress.com/articles/journal-of-intelligent-and-fuzzy-systems/ifs00260

Bemporad, A., & Muñoz de la Peña, D. (2009). Multiobjective model predictive control. *Automatica*, *45*(12), 2823–2830. doi:10.1016/j.automatica.2009.09.032

Bolea, Y., Puig, V., & Blesa, J. (2014). Linear parameter varying modeling and identification for real-time control of open-flow irrigation canals. *Environmental Modelling & Software*, *53*, 87–97. doi:10.1016/j.envsoft.2013.10.028

Buyalski, C., Ehler, D., Falvey, H., Rogers, D., & Serfozo, E. (1991). *Canal Systems Automation Manual*. Denver, USA.: Bureau of Reclamation.

Camacho, E., & Bordons, C. (2004). *Model Predictive Control* (2nd ed.). London: Springer-Verlag.

Camacho, E., & Bordons, C. (2010, October 1). Control predictivo: Pasado, presente y futuro. *RIAII*. Retrieved from http://recyt.fecyt.es/index.php/RIAII/article/view/10587

Cantoni, M., Weyer, E., Li, Y., Ooi, S., Mareels, I., & Ryan, M. (2007). Control of large-scale irrigation networks. *Proceedings of the IEEE*, *95*(1), 75–91. doi:10.1109/JPROC.2006.887289

Cardona, J., Gómez, M., & Rodellar, J. (1997). A decentralized adaptive predictive controller for irrigation canals. In *International Workshop on the Regulation of Irrigation Canals: State of the Art of Research and Applications* (pp. 215–219). Marrakech, Morocco.

Charbonnaud, P., Duviella, E., & Carrillo, F. J. (2011). A supervised robust predictive multi-controller for large operating conditions of an open-channel system. In *Proceedings of the 18th IFAC World Congress* (pp. 4620–4625). Milano, Italy: IFAC.

Chow, V. (1988). *Open-channels Hydraulics*. New York: Mc Graw-Hill.

Christofides, P., Scattolini, R., Muñoz, D., & Liu, J. (2013). Distributed model predictive control: A tutorial review and future research directions. *Computers & Chemical Engineering*, *51*, 21–41. doi:10.1016/j.compchemeng.2012.05.011

Clarke, D. W., Mohtadi, C., & Tuffs, P. S. (1987). Generalized predictive control. Part I. The basic algorithm. *Automatica*, *2*(23), 137–148.

Clemmens, A. (2014). Automatic canal controllers. In *USCID Water Management Conference* (pp. 15–27). Phoenix, Arizona.: USCID.

Clemmens, A., Kacerek, T., Grawitz, B., & Schuurmans, W. (1998). Test cases for canal control algorithms. *Journal of Irrigation and Drainage Engineering*, *124*(1), 23–30. doi:10.1061/(ASCE)0733-9437(1998)124:1(23)

Clemmens, A., Strand, R., & Bautista, E. (2005). Field testing of Sacman automated canal control system. In *Irrigation and Drainage Conference. USCID.* (pp. 199–209). San Luis Obispo, California.

Darby, M. L., & Nikolaou, M. (2012). MPC: Current practice and challenges. *Control Engineering Practice*, *20*(4), 328–342. doi:10.1016/j.conengprac.2011.12.004

De Bievre, B., Alvarado, A., Timbe, L., Célleri, R., & Feyen, J. (2003). Night irrigation reduction for water saving in medium-sized systems. *Irrigation Drainage Engineering*, *129*(April), 108–116. doi:10.1061/(ASCE)0733-9437(2003)129:2(108)

Delgoda, D., Saleem, S., Halgamuge, M., & Malano, H. (2012). Multiple model predictive flood control in regulated river systems with uncertain inflows. *Water Resources Management*, *27*(3), 765–790. doi:10.1007/s11269-012-0214-y

Dunbar, W. B. (2007). Distributed receding horizon control of dynamically coupled nonlinear systems. *IEEE Transactions on Automatic Control*, *52*(7), 1249–1263. doi:10.1109/TAC.2007.900828

Durdu, F. Ö. (2005). Control of transient flow in irrigation canals using Lyapunov fuzzy filter-based Gaussian regulator. *International Journal for Numerical Methods in Fluids*, *50*(4), 491–509. doi:10.1002/fld.1075

Duviella, E., Puig, V., Charbonnaud, P., Escobet, T., Carrillo, F., & Quevedo, J. (2010). Supervised gain-scheduling multimodel versus linear linear parameter varying internal model control of open-channel systems for large operating conditions. *Journal of Irrigation and Drainage Engineering*, *138*(8), 543–552.

Ferro, V., & Ansar, M. (2001). Simultaneous flow over and under a gate. *Journal of Irrigation and Drainage Engineering*. Retrieved from http://ascelibrary.org/doi/abs/10.1061/(ASCE)0733-9437(2001)127%3A5(325)

Fletcher, R. (2013). *Practical Methods of Optimization*. John Wiley & Sons. Retrieved from https://books.google.com/books?hl=en&lr=&id=_WuAvIx0EE4C&pgis=1

Galvis, E., Mantecon, J., Horváth, K., Gómez, M., & Rodellar, J. (2014). Predictive control based on multiple models for canals that require large change in operating conditions. In *Congress on Industrial and Agricultural Canals* (pp. 378–380). Lleida, Spain.

Galvis, E., Mantecón, J., Horváth, K., Gómez, M., & Rodellar, J. (2011). Simplified modeling of a laboratory irrigation canal for control purposes. In *Seminar on Advanced Industrial Control Applications* (pp. 83–88). Barcelona.

Galvis, E., Mantecón, J., Horváth, K., Gómez, M., & Rodellar, J. (2014). An automatic control strategy for closure and opening of irrigation canals. In *USCID Water Management Conference*. Phoenix, USA.

Garnier, H., Wang, L., & Young, P. (2008). Direct Identification of Continuous-time Models from Sampled Data: Issues, Basic Solutions and Relevance. In H. Garnier & L. Wang (Eds.), *Identification of Continuous-time Models from Sampled Data* (pp. 1–29). London: Springer London. doi:10.1007/978-1-84800-161-9

Georges, D. (2009). Infinite-dimensional nonlinear predictive control design for open-channel hydraulic systems. *Networks and Heterogeneous Media*, *4*(2), 267–285. doi:doi:10.3934/nhm.2009.4.267

Ghumman, A., Khan, Z., & Turral, H. (2009). Study of feasibility of night-closure of irrigation canals for water saving. *Agricultural Water Management*, *96*(3), 457–464. doi:10.1016/j.agwat.2008.09.009

Gómez, M., Rodellar, J., & Mantecón, J. (2002). Predictive control method for decentralized operation of irrigation canals. *Applied Mathematical Modelling*, *26*(11), 1039–1056.

Gopakumar, R., & Mujumdar, P. (2009). A fuzzy logic based dynamic wave model inversion algorithm. *Hydrological Processes*. doi:10.1002/hyp.7308

Goussard, J.-J. (1993). *Automation of canal irrigation systems*. (I. C. on I. and Drainage, Ed.). New Delhi.

Henson, M. A. (1998). Nonlinear model predictive control: current status and future directions. *Computers & Chemical Engineering*, *23*(2), 187–202. doi:10.1016/S0098-1354(98)00260-9

Herschy, R. (1995). General purpose flow measurement equations for flumes and thin plate weirs. *Flow Measurement and Instrumentation*, *6*(4), 283–293. doi:10.1016/0955-5986(95)00016-X

Hervé, P. (2002). *How Design, Management and Policy Affect the Performance of Irrigation Projects*. Bangkok: FAO.

Horváth, K. (2013). *Model Predicitve Control of Resonane Sensitive Irrigation Canals*. PhD Dissertation. Technical University of Catalonia, Barcelona, Spain.

Horváth, K., Galvis, E., Gómez, M., & Rodellar, J. (2014a). Experimental comparison of canal models for control purposes using simulation and laboratory experiments. *Journal of Hydroinformatics*, *16*(6), 1390–1408. doi:10.2166/hydro.2014.110

Horváth, K., Galvis, E., Gómez, M., & Rodellar, J. (2014b). Is it better to use gate opening as control variable than discharge to control irrigation canals? *Journal of Irrigation and Drainage Engineering*, *141*(3), 04014054. doi:10.1061/(ASCE)IR.1943-4774.0000798

Horváth, K., Galvis, E., Gómez, M., & Rodellar, J. (2015). New offset-free method for model predictive control of open channels. *Control Engineering Practice*, *41*, 13–25. doi:10.1016/j.conengprac.2015.04.002

Igreja, J., & Lemos, J. (2009). Nonlinear model predictive control of a water distribution canal pool. In L. Magni, D. M. Raimondo, & F. Allgöwer (Eds.), *Nonlinear Model Predictive Control* (Vol. 384, pp. 521–529). Berlin, Heidelberg: Springer Berlin Heidelberg. doi:10.1007/978-3-642-01094-1

Khan, M. Z., & Ghumman, A. R. (2008). Hydrodynamic modelling for water-saving strategies in irrigation canals. *Irrigation and Drainage*, *57*(4), 400–410. doi:10.1002/ird.375

Kuure-kinsey, M., & Bequette, B. W. (2010). Multiple model predictive control strategy for disturbance rejection. *Industrial & Engineering Chemistry Research*, *49*(17), 7983–7989. doi:10.1021/ie100093c

Lemos, J., Pinto, L., Rato, L. M., & Rijo, M. (2013). Multivariable and distributed LQG control of a water delivery canal. *Journal of Irrigation and Drainage Engineering*, *130*(10), 855–863.

Lemos, J., Rato, L., Machado, F., Nogueira, N., Salgueiro, P., & Neves-Silva, R. (2009). Adaptive and non-adaptive model predictive control of an irrigation channel. In *Networks and heterogeneous media* (pp. 303–324). doi:doi:10.3934/nhm.2009.4.303

Litrico, X., & Fromion, V. (2004a). Analytical approximation of open-channel flow for controller design. *Applied Mathematical Modelling*, *28*(7), 677–695. doi:10.1016/j.apm.2003.10.014

Litrico, X., & Fromion, V. (2004b). Simplified modeling of irrigation canals for controller design. *Journal of Irrigation and Drainage Engineering*, *130*(5), 373–383. doi:10.1061/(ASCE)0733-9437(2004)130:5(373)

Litrico, X., & Fromion, V. (2006). H/sub /spl infin// control of an irrigation canal pool with a mixed control politics. *IEEE Transactions on Control Systems Technology*, *14*(1), 99–111. doi:10.1109/TCST.2005.860526

Litrico, X., Fromion, V., Baume, J., Arranja, C., & Rijo, M. (2005). Experimental validation of a methodology to control irrigation canals based on Saint-Venant equations. *Control Engineering Practice*, *13*(11), 1425–1437. doi:10.1016/j.conengprac.2004.12.010

Litrico, X., & Georges, D. (1999). Robust continuous-time and discrete-time flow control of a dam–river system. (I) Modelling. *Applied Mathematical Modelling*, *23*(11), 809–827. doi:10.1016/S0307-904X(99)00014-1

Litrico, X., Malaterre, P.-O., Baume, J.-P., & Ribot-Bruno, J. (2008). Conversion from discharge to gate opening for the control of irrigation canals. *Journal of Irrigation and Drainage Engineering*, *134*(3), 305–314. doi:10.1061/(ASCE)0733-9437(2008)134:3(305)

Lobbrecht, A. H., Dibike, Y. B., & Solomatine, D. P. (2005). Neural networks and fuzzy systems in model based control of the overwaard polder. *Journal of Water Resources Planning and Management*, *131*(2), 135–145. doi:10.1061/(ASCE)0733-9496(2005)131:2(135)

Luenberger, D. G. (1969). *Optimization by Vector Space Methods*. New York: John Wiley and Sons.

Maciejowski, J. M. (2002). *Predictive Control with Constraints*. London: Prentice Hall PTR. Retrieved from http://www.booksites.net/maciejowski/

Maestre, J. M., Muñoz de la Peña, D., & Camacho, E. F. (2011). Distributed model predictive control based on a cooperative game. *Optimal Control Applications and Methods*, *32*(2), 153–176. doi:10.1002/oca.940

Malaterre, P. (2008). PILOTE: linear quadratic optimal controller for irrigation canals. *Journal of Irrigation and Drainage Engineering*, *124*(4), 187–194. Retrieved from http://cedb.asce.org/cgi/WWWdisplay.cgi?112889

Malaterre, P. (2011). Canari - www database on irrigation canals.

Malaterre, P. (2012). SIC 5.32 Simulation of irrigation canals. Retrieved April 26, 2015, from http://sic.g-eau.net/?lang=en

Malaterre, P., Rogers, D., & Schuurmans, J. (1998). Classification of Canal Control Algorithms. *Journal of Irrigation and Drainage Engineering*, *124*(1), 3–10. doi:10.1061/(ASCE)0733-9437(1998)124:1(3)

Mantecon, J., Gomez, M., & Rodellar, J. (2010). Teaching control of irrigation canals to non system engineers. *International Journal of Engineering Education*, *26*(6), 1405–1413.

Mareels, I., E.Weyer, Ooi, S. K., Cantoni, M., Li, Y., & Nair, G. (2005). Systems engineering for irrigation systems: Successes and challenges. *Annual Reviews in Control*, *29*, 191–204.

Martín Sánchez, J., & Rodellar, J. (1996). *Adaptive Predictive Control: From the Concepts to Plant Optimization*. Prentice Hall PTR.

Martín-Sánchez, J. M., Lemos, J. M., & Rodellar, J. (2012). Survey of industrial optimized adaptive control. *International Journal of Adaptive Control and Signal Processing*, *26*(10), 881–918. doi:10.1002/acs.2313

Mathworks. (2008). Matlab. Retrieved from http://www.mathworks.com/products/matlab/

Mayne, D. (2014). Model predictive control: Recent developments and future promise. *Automatica*, *50*(12), 2967–2986. doi:10.1016/j.automatica.2014.10.128

Mayne, D., Rawlings, J., Rao, C., & Scokaert, P. (2000). Constrained model predictive control : Stability and optimality. *Automatica*, *36*(6), 789–814.

Montazar, A., Van Overloop, P. J., & Brouwer, R. (2005). Centralized controller for the Narmada main canal. *Irrigation and Drainage*, *54*(1), 79–89. doi:10.1002/ird.155

Morari, M., & Barić, M. (2006). Recent developments in the control of constrained hybrid systems. *Computers & Chemical Engineering*, *30*(10-12), 1619–1631. doi:10.1016/j.compchemeng.2006.05.041

Morari, M., & Lee, J. (1999). Model predictive control: past, present and future. *Computers & Chemical Engineering*, *23*(4), 667–682.

Moreno, F. (1986). El auto-dren: una nueva protección para los revestimientos de canales. *Informes de La Construcción CSIC*. Retrieved from http://informesdelaconstruccion.revistas.csic.es/index.php/informesdelaconstruccion

Murray-Smith, R., & Johansen, T. (1997). *Multiple Model Approaches to Nonlinear Modelling And Control*. London: Taylor & Francis Group.

Negenborn, R., van Overloop, P., Keviczky, T., & De Schutter, B. (2009). Distributed model predictive control of irrigation canals. *Networks and Heterogeneous Media*, *4*(2), 359–380. doi:10.3934/nhm.2009.4.359

Pages, J. C., Compas, J. M., & San, J. (1998). MIMO predictive control with constraints by using an embedded knowledge based model [hydraulic structures]. In *IEEE International Conference on Systems, Man, and Cybernetics* (Vol. 4, pp. 3902–3907). IEEE. doi:10.1109/ICSMC.1998.726697

Portal de CHEbro. (2015). Retrieved June 18, 2015, from http://www.chebro.es/contenido.visualizar.do?idContenido=2341&idMenu=2227

Preissmann, A. (1961). Propagation des intumescences dans les canaux et les rivières. In *Premier congrès de l'Association Française de Calcul.*

Qin, S. J., & Badgwell, T. a. (2003). A survey of industrial model predictive control technology. *Control Engineering Practice*, *11*(7), 733–764. doi:10.1016/S0967-0661(02)00186-7

Ratinho, T., Figueiredo, J., & Rijo, M. (2002). Modelling, control and field tests on an experimental irrigation canal. In *Proc. of 10th IEEE Mediterranean Conference on Control and Automation* (pp. 53–62). Lisbon.

Rijo, M., & Arranja, C. (2010). Supervision and water depth automatic control of an irrigation canal. *Journal of Irrigation and Drainage Engineering*, *136*(1), 3–10. doi:10.1061/(ASCE)IR.1943-4774.0000118

Rivas Pérez, R., Feliu, V., Castillo, F., & Linares, A. (2008). System identification for control of a main irrigation canal pool. In *IFAC World Congress* (Vol. 17, pp. 9649–9654). Coex, Korea.

Rivas, R., Feliu, V., & Sanchez, L. (2007). Robust system identification of an irrigation main canal. *Advances in Water Resources*, *30*(8), 1785–1796. doi:10.1016/j.advwatres.2007.02.002

Rodellar, J., Gómez, M., & Bonet, L. (1993). Control method for on-demand operation of open-channel flow. *Journal of Irrigation and Drainage Engineering*, *119*(2), 225–241. doi:DOI: 10.1061/(ASCE)0733-9437(1993)119:2(225)

Rodellar, J., Gómez, M., & Vide, J. (1989). Stable predictive control of open channel flow. *Journal of Irrigation and Drainage Engineering*, *115*(4), 701–713. doi:10.1061/(ASCE)0733-9437(1989)115:4(701)

Rogers, D. C., & Goussard, J. (1998). Canal control algorithms currently in use. *Journal of Irrigation and Drainage Engineering*, *124*(1), 11–15. doi:10.1061/(ASCE)0733-9437(1998)124:1(11)

Ruiz, C., & Ramirez, L. (1998). Predictive control in irrigation canal operation. In *SMC'98 Conference Proceedings. 1998 IEEE International Conference on Systems, Man, and Cybernetics* (Vol. 4, pp. 3897–3901). San Diego, USA: IEEE. doi:10.1109/ICSMC.1998.726696

Sawadogo, S., Faye, R. M., Benhammou, A., & Akouz, K. (2000). Decentralized adaptive predictive control of multi-reach irrigation canal. In *IEEE International Conference on Systems, Man and Cybernetics. "Cybernetics Evolving to Systems, Humans, Organizations, and their Complex Interactions"* (Vol. 5, pp. 3437–3442). IEEE. doi:10.1109/ICSMC.2000.886540

Sawadogo, S., Faye, R. M., Malaterre, P. O., & Mora-Camino, F. (1998). Decentralized predictive controller for delivery canals. In *IEEE International Conference on Systems, Man, and Cybernetics* (Vol. 4, pp. 3880–3884). IEEE. doi:10.1109/ICSMC.1998.726693

Sawadogo, S., Malaterre, P., & Kosuth, P. (1995). Multivariate optimal control for on-demand operation of irrigation canals. *International Journal of Systems Science*, *26*(1), 161–178. doi:10.1080/00207729508929029

Schuurmans, J., Hof, A., Dijkstra, S., Bosgra, O. H., & Brouwer, R. (1999). Simple water level controller for irrigation and drainage canals. *Journal of Irrigation and Drainage Engineering*, *125*(4), 189–195. Retrieved from http://cedb.asce.org/cgi/WWWdisplay.cgi?118346

Sepúlveda, C. (2008). *Instrumentation, Model Identification and Control of an Experimental Irrigation Canal*. PhD Dissertation. Technical University of Catalonia, Barcelona, Spain.

Soderstrom, T., & Stoica, P. (1989). *System Identification*. New Jersey: Prentice-Hall.

Soler, J., Gómez, M., & Rodellar, J. . (2010). Estudio hidráulico para el plan de emergencia del canal de la Margen Izquierda del Delta del Ebro. *Ingeniería Del Agua*, *17*(2), 171–186.

Soler, J., Gómez, M., Rodellar, J., & Gamazo, P. (2014). Application of the GoRoSo feedforward algorithm to compute the gate trajectories for a quick canal closing in the case of an emergency. *Journal of Irrigation and Drainage Engineering*, *139*(12), 1028–1036.

UN. (2006). *2nd United Nations World Water Development Report*. Retrieved from http://www.unesco.org/water/wwap/

Van den Bosch, B., Hoeveneaars, J., & Brower, C. (1992). *Irrigation Water Management. Training Manual No. 7*. (FAO, Ed.). Rome.

Van Overloop, P. (2006). *Model Predictive Control on Open Water Systems*. PhD Dissertation. Delft University of Technology, Delft, The Netherlands.

Van Overloop, P., Clemmens, A., Strand, R., Wagemaker, R., & Bautista, E. (2010). Real-time implementation of model predictive control on Maricopa-Stanfield Irrigation and Drainage

District ’ s. *Irrigation and Drainage Engineering*, *136*(11), 747–756. doi:10.1061/ASCEIR.1943-4774.0000256

Van Overloop, P., Horváth, K., & Aydin, B. (2014). Model predictive control based on an integrator resonance model applied to an open water channel. *Control Engineering Practice*, *27*, 54–60. doi:10.1016/j.conengprac.2014.03.001

Van Overloop, P., Schuurmans, J., Brouwer, R., & Burt, C. (2005). Multiple-model optimization of proportional integral controllers on canals. *Journal of Irrigation and Drainage Engineering*, *131*(2), 190–196.

Van Overloop, P., Weijs, S., & Dijkstra, S. (2008). Multiple Model Predictive Control on a drainage canal system. *Control Engineering Practice*, *16*(5), 531–540. doi:10.1016/j.conengprac.2007.06.002

Wahlin, B. T. (2004). Performance of model predictive control on ASCE test canal 1. *Journal of Irrigation and Drainage Engineering*, *130*(3), 227–238. doi:10.1061/(ASCE)0733-9437(2004)130:3(227)

Wang, L. (2009). *Model Predictive Control System Design Implementation Using Matlab*. London: Springer.

Weyer, E. (2001). System identification of an open water channel. *Control Engineering Practice*, *9*(12), 1289–1299. doi:10.1016/S0967-0661(01)00099-5

Weyer, E. (2003). LQ control of an irrigation channel. In *42nd IEEE International Conference on Decision and Control (IEEE Cat. No.03CH37475)* (Vol. 1, pp. 750–755). IEEE. doi:10.1109/CDC.2003.1272655

Weyer, E. (2006). Multivariable LQ control of an irrigation channel: Experimental results and robustness analysis. In *Proceedings of the 45th IEEE Conference on Decision and Control* (pp. 6642–6647). IEEE. doi:10.1109/CDC.2006.377437

Wismer, D., & Chattergy, R. (1978). *Introduction to Nonlinear Optimization: A Problem Solving Approach*. (E. Science, Ed.).

Xi, Y.-G., Li, D.-W., & Lin, S. (2013). Model predictive control — status and challenges. *Acta Automatica Sinica*, *39*(3), 222–236. doi:10.1016/S1874-1029(13)60024-5

Xu, M., Negenborn, R. R., van Overloop, P. J., & van de Giesen, N. C. (2012). De Saint-Venant equations-based model assessment in model predictive control of open channel flow. *Advances in Water Resources*, *49*, 37–45. doi:10.1016/j.advwatres.2012.07.004

Zafra-Cabeza, A., Maestre, J., Ridao, M., Camacho, E., & Sánchez, L. (2011). A hierarchical distributed model predictive control approach to irrigation canals: A risk mitigation perspective. *Journal of Process Control*, *21*(5), 787–799. doi:10.1016/j.jprocont.2010.12.012

Appendix A

Quadratic programming using Hildret's Procedure

```
%filaname: QPhild.m
%Quadratic programming using Hildret's Procedure as it is described in
% Wang, L. (2009). Model Predictive Control system design implementation
%using Matlab. Springer. Pag. 67
%The program finds the global optimal solution and checks if all the
constraints are satisfied. If so, the program returns the optimal solution.
%If not, the program then begins to calculate the dual variable lambda.

function [eta]=QPhild(H,f,A_cons,b)
                    % M=A_cons; % gamma=b;
                    % eta =u
[n1,m1]=size(A_cons);
eta=-H\f;           %global optimal solution without constraints
kk=0;
for i=1:n1
    if (A_cons(i,:)*eta>b(i)) kk=kk+1;
    else
        kk=kk+0;
    end
end

if (kk==0)
    return;
end
```

```
% Note that in the quadratic programming procedure, the ith Lagrange
%multiplier  Lambda_i becomes zero if the corresponding constraint is not
%active. Otherwise  it is positive. We need to calculate the Lagrange %
multipliers iteratively.
% We will first set-up the matrices of the dual quadratic programming,
% followed by the computation of the Lagrange multipliers.

P=A_cons*(H\A_cons');
d=(A_cons*(H\f)+b);
[n,m]=size(d);
x_ini=zeros(n,m);
lambda=x_ini;
al=10;

for km=1:38
    %find the elements in the solution vector one by one
    % km could be larger if the Lagranger multiplier has a slow
    % convergence rate.
    lambda_p=lambda;
        for i=1:n
            w= P(i,:)*lambda-P(i,i)*lambda(i,1);
            w=w+d(i,1);
            la=-w/P(i,i);
            lambda(i,1)=max(0,la);
        end
    al=(lambda-lambda_p)'*(lambda-lambda_p);
    if (al<10e-8);
        break;
    end
end

eta=-H\f -H\A_cons'*lambda;
```